UNIVERSITÉ DE GRENOBLE

THÈSE

Pour obtenir le grade de

DOCTEUR DE L'UNIVERSITÉ DE GRENOBLE

Spécialité : **Science de la Terre et Univers, Environnement**

Arrêté ministériel : 7 août 2006

Présentée par

Guillaume PITON

Thèse dirigée par **Alain RECKING**

préparée au sein du **Irstea Grenoble - Equipe ETNA: Erosion Torrentielle, Neige et Avalanches**
dans l'Ecole Doctorale **Terre Univers Environnement**

Sediment transport control by check dams and open check dams in Alpine torrents

Thèse soutenue publiquement le **8 Juin 2016**,
devant le jury composé de :

Prof. Eric BARTHELEMY
Professor, Grenoble Alpes University (INPG-LEGI), FR., Président

Prof. Dieter RICKENMANN
Professor, Swiss Federal Institute for Forest, Snow and Landscape Research (WSL), CH. , Rapporteur

Prof. Anton J. SCHLEISS
Professor, Lausanne Swiss Federal Institute of Technology (EPFL-LCH), CH., Rapporteur

Prof. Vincenzo D'AGOSTINO
Associate Professor, University of Padova (TESAF), IT., Examinateur

Dr. Olivier MARCO
Chef du Département Risques Naturels, National Forest Office (ONF), FR., Examinateur

Dr. Alain RECKING
Researcher, HDR, Grenoble Alpes University (IRSTEA-ETNA), FR., Directeur de thèse

"there was only one liftime.
So much universe, and so little time..."

T. Pratchett (1948-2015), *The Last Hero*

A mon père,

qui, innocemment, m'a mis sur la voie du génie de l'eau; et qui,
tout aussi innocemment, m'a donné sa passion pour le travail bien fait,
pour le meilleur comme pour le pire.

Acknowledgements

This manuscript results from a collaborative work. It bears the print of numerous people, more or less explicitly.

Most of all, my thesis supervisor and mentor for three years, Alain RECKING, has guided me. He encouraged my enthusiasm and tried to control my chronic excesses, a tricky equilibrium. He continues to keep an outstanding patience with me, explaining his numerous ideas again and again, as long as necessary, so that I understand (or at least, feel to). He taught me the special academic writing, to clarify my thoughts, to be (a bit more) concise. He destroyed a part of my engineer way of thinking, to rebuild a young researcher with more doubts and a better informed curiosity. I would like to thank Alain for all the time and natural goodness he had and has for me. I hope to continue our collaboration, for a long time.

Professors Anton SCHLEISS, Dieter RICKENMANN, Eric BARTHELEMY and Vicenzo D'AGOSTINO and the ONF natural hazard department-deputy director, and thus head of the RTM service (Restauration et conservation des Terrains de Montagne, French torrent control service), Olivier MARCO have accepted to judge my work for the defence. To benefit from the views of such a panel of experts is a great honour for me. I am profoundly grateful that they accepted to spend time and interest for my work. Each of them has influenced this manuscript by his past works.

In particular, Eric BARTHELEMY has terrible responsibility in the chain of events that results in this manuscript writing. At the engineer school, he taught me free surface hydraulics and sediment transport. He later recommended me to contact IRSTEA when I spoke him about my project to join a research team. Last year, he accepted my collaboration as a teaching assistant. I finally replaced him shortly during his sabbatical (poor students...). This work, and the pleasure I had to prepare it, owes much to Eric. Thank you Eric, for everything.

At the engineer school too, I had the chance to follow the lectures in "torrential hydraulics" taught by Vincent KOULINSKI. The way Vincent presented this subject greatly attracted my curiosity, it was a milestone in the events that drove me to specifically join IRSTEA and start this work. Vincent subsequently accepted to provide some advices and feedbacks during the three last years. I would like to thank him for the initial stimulus and for the more recent exchanges.

We had extremely interesting discussions and feedbacks with some RTM-service officers. Gilles CHARVET, Christian DEYMIER, Damien KUSS, Yann QUEFFELEAN and Didier WASAK showed great motivation to speak about their experience and case-studies, or to explain and present the technical challenges they are facing, at a daily frequency. Contrarily to researchers that can usually answer to questions with other (eventually more interesting) questions, the RTM officers do their best to provide answers to questions, this in a fuzzy and complex environment. They deserve our respect for carrying out the job and my gratitude for their numerous explanations.

For three years, I met skilled researchers and engineers who provided key advices or simple but essential remarks. I would like to thank them for these sharing: *e.g.*, John PITLICK for his views of the "sketchy" Wolman pebble counts and for our discussions about hydrology; Bernard LEFEBVRE for the what-happen-if-I-am-wrong approach and feedback about racks in slit dams; Joshua ROERING for discussions around the flume and for attracting my attention toward the literature on complexity in geomorphology; Alain DELALUNE for the downstream-bridge-width-

minus-fifty-centimetres design criteria; Mike CHURCH for pointing out our surprising results of check dams that do not reduce slopes, for several discussions about the geomorphic effects of check dams and for a complete review of our historical paper (I can testify that Mike deserves his reputation of tremendous precision); Laurent ASTRADE for our surveys of torrent activity and for monitoring the check dams of the Lampe torrent for nearly 10 years, and finally, Fransesco COMITI for a contradictory debate about long term equilibrium profile and armour breaking in torrents: I actually owe my comprehension of the check dam slope reduction effect to a coffee break with Fransesco at Benediktbeuern, another proof that coffee induces scientific progress.

The IRSTEA-ETNA team has been a wonderful place to work. I would like to thank specifically Frédéric LIEBAULT, Dominique LAIGLE, Jean Marc TACNET, Philippe FREY, Guillaume CHAMBON, Mohamed NAAÏM and Didier RICHARD for our numerous coffee discussions and hallway chats. The ETNA lab. team also owes a special tribute: they have always been of great help and bear with laughs and smiles my regular "*pitonnades*", i.e., enthusiastic but bloody stupid initiatives. I thus want to thank Hervé BELLOT, Firmin FONTAINE, Frédéric OUSSET, Xavier RAVANAT and Christian EYMOND GRIS for their assistance and company.

The other PhD students, and assimilated workers, participated to make our breaks more pleasant. Two of them have a special place: Coraline et Simon. Coraline BEL, my office mate, shared with me her greater experience of the strange world of academia and bear me with a permanent smile. Thank you for your company Coraline. Simon CARLADOUS is an experienced RTM engineer. We had the same weird idea to come back to the student status for a short period. Our coffee discussions and fruitful exchanges are always a real pleasure. The first chapter of this manuscript is clearly our combine work, under the blessing and control of our supervisors.

I want to thank the effort of my trainees. Three master students have been enslaved during long months to calibrate measurement devises and shovel tones of gravels. Jules LE GUERN, Costanza CARBONARI and Ségolène MEJEAN also bore my supervision without complain. Thank you for your help.

My first mentor, as a young engineer, had been Jean Claude CARRE. He transformed a messy student in a more methodological one, while maintaining my curiosity and natural inclination towards perfectionism. This transformation had been difficult and noisy (I would bet that the office walls still remind our debates), but I definitively would not have been the same engineer without these months with him. I am grateful to Jean Claude for his effort in teaching me to become a better engineer. My second mentor had been Céline MARTINET. She taught me to write engineering reports with acceptable amounts of grammatical mistakes. Her patience had also been greatly strained. I learnt a lot during this first job experience, also with support of the all ARTELIA fellows.

My friends continue to bear me despite my lack of availability, which is of great importance for me. David GATEUILLE and Aloïs RICHARD were of particular assistance. They lived the adventure of the PhD just before I joined it. Their recent experiences and numerous advices made mine easier.

My family and particularly my mother Thessy, my two brothers Gabin et Gaël, and my two sisters Olivia and Milena, have also been of great support and immovable patience. I hope to come back in our mountains much more often in the future, I miss it and I miss you.

Finally, I want to thank Cyrielle for every day, and much, much more.

Résumé

Les cours d'eau de montagne constituent une importante source d'alimentation en sédiments des rivières ; toutefois lors d'épisodes de crues, ils peuvent aussi être responsables de dégâts importants en déposant des masses considérables de sédiments dans les vallées. Dans le but de contrôler l'érosion des sols des torrents - et donc ces transferts de masses de sédiments - des travaux de grande ampleur ont été entrepris depuis le XIXème siècle (principalement par reboisement, génie végétal et construction de barrages et seuils de correction torrentielle). Plus récemment, les barrages de correction torrentielle localisés dans les hauts bassins ont été complétés par la création de plages de dépôt équipés de barrages filtrants, ouvrages visant à piéger les apports sédimentaires plus bas dans les vallées. Les gestionnaires de ces ouvrages ont pour mission de réduire les risques d'inondations et d'érosions, mais doivent désormais aussi minimiser les impacts environnementaux liés aux ouvrages de protection; tout en maintenant et adaptant ces derniers à un contexte changeant (climat, démographie). Ceci nécessite une meilleure compréhension des effets des barrages de corrections torrentielles et des plages de dépôts sur le transport sédimentaire des torrents.

Cette thèse s'inscrit dans cet objectif et se décompose en deux parties. Une première partie sur l'état de l'art présente: (i) les différents effets des barrages de correction torrentielle sur la production et le transfert sédimentaire; (ii) la description des processus hydrauliques et sédimentaires ayant lieu dans les plages de dépôts; et (iii) la description des processus liés à la production et au transfert de bois d'embâcle. Une nouvelle méthode de quantification de la production sédimentaire des torrents complète cet état de l'art.

La seconde partie de cette thèse présente le travail réalisé en banc d'essai expérimental. Une première série d'expérience a permis de mettre en évidence un transport par charriage plus régulier lorsque des barrages de correction torrentielle sont ajoutés à un bief alluvial. Une seconde série d'essais a été réalisée sur un modèle générique de plage de dépôt dans l'objectif d'en caractériser les écoulements. Pour cela, une nouvelle procédure de mesure et de reconstruction par approche inverse a été développée. Cette procédure fait appel aux techniques de photogrammétrie et d'une variante grande échelle de vélocimétrie par image de particule (LS-PIV). Il en résulte une description des caractéristiques d'un écoulement proche du régime critique, ainsi que des mécanismes de rétrocontrôle entre morphologie et hydraulique pendant la phase de dépôt.

Une conclusion générale et quelques perspectives sont finalement données.

Mots clés: Torrents, Transport Sédimentaire, Risques Torrentiels, Protection Contre Les Inondations Et L'Erosion, Modélisation Physique

Abstract

Mountain streams are a major sediment source for some rivers; however, they can also be responsible for substantial damage, particularly during sediment-laden floods. Torrents, i.e. very active mountain streams, have been subject to extensive erosion control operations since the 19^{th} century (mainly reforestation, bioengineering, and check dams). More recently, check dams in headwaters have been completed using open check dams that aimed at trapping sediment lower in the valleys. Stream managers must mitigate flood hazards, but now also minimize the environmental impacts of the protection structures, while maintaining and adapting them to a changing context (climate, demography). This requires improved knowledge of the effects of check dams and open check dams on the sediment transport of torrents, and this thesis forms a contribution towards this end.

The section on the current state of research reviews i) the diverse effects of check dams on sediment production and transfer; ii) descriptions of the hydraulics and sedimentation processes occurring in open check dams; and iii) woody debris production and trapping processes. This state of the art is completed with proposition of new bedload transport estimation methods, specifically developed for paved streams experiencing external supply or armour breaking.

Experimental results are then provided. Firstly, flume experiments highlight the emergence of a more regular bedload transport when check dams are built in alluvial reaches. In a second stage, experiments were performed on a generic Froude scale model of an open check dam basin in order to capture the features of laterally-unconstrained, highly mobile flows. A new flow measurement and inverse-reconstruction procedure has been developed, using photogrammetry and large scale particle image velocimetry (LS-PIV). A preliminary analysis of the results describes flows that tend toward a critical regime and the occurrence of feedback mechanisms between geomorphology and hydraulics during massive bedload deposition.

A general conclusion and some perspectives are then presented.

Keywords: Steep Slope Streams, Sediment Transport, Torrential Hazards, Flood Hazard Mitigation and Erosion Control, Small Scale Modelling.

Contents

"Car il ne faut point douter que nous ne cognoissons mieux les mouvements des Planetes, et le cours des Etoiles, que nous ne cognoissons le mouvement des Rivieres et de la Mer."

Benedetto Castelli, (1628) "*Della misura dell'acque correnti*" (1867's old French translation).

Introduction

MOUNTAIN streams transfer water, sediment, and woody debris from headwaters and hillslopes down to valleys and lowland fluvial systems (Wohl, 2006). These streams erratically experience intense torrential floods and massive sediment transport. Their particularly steep slopes provide them with the energy to erode and destabilize vegetated banks, transport sediment, and later spread it onto fans, and into mountain rivers (*e.g.*, Fig. 0.1a).

This natural process of erratic sediment transfer has been fought for centuries by mountain dwellers (Hughes and Thirgood, 1982). During the 19^{th} century, torrent control works tended to become organized at the regional scale, and engineers were specifically trained for such duties (Duile, 1826; Surell, 1841; Demontzey, 1882; Thiéry, 1891). Under their supervision, thousands of torrent control operations were implemented. Their designers tried and tested, probably all the available techniques that could possibly help to stabilize hillslopes and stream beds; from the smallest and simplest bioengineering (Evette et al., 2009), to heavy civil engineering structures (tunnels, retaining walls, dikes, bank protection, check dams; Hübl and Fiebiger, 2005). Check dams were the most numerous of these built structures (*e.g.*, $\approx$ 100,000 in France; Messines du Sourbier, 1964). More recently, since the advent of earth-moving machinery and reinforced concrete, alternatives such as sediment traps with open check dams are increasing in number (Zollinger, 1985; Armanini et al., 1991).

Mountain stream managers now have the complex task of maintaining and adapting these hazard mitigation structures. This is an endless mission; the number of elements at risk has usually shown a consistent increase since the 19th century (compare Fig. 0.1a and b). The task is complicated because there are generally several alternative protection solutions, which include the stabilization of headwaters and gorges (*e.g.*, with check dams), or sediment trapping closer to the elements at risk (*e.g.*, with open check dams).The effectiveness of each alternative varies, and is complicated to assess.

Mountains are highly diversified and fundamentally complex systems. We therefore cannot hope for a definitive and absolute answer to the dilemma over the choice between check dams and open check dams. As stated by Gras (1857), any valley with elements at risk deserves a specific study to discriminate the suitable solutions between headwater/gorge operations, direct protections, and

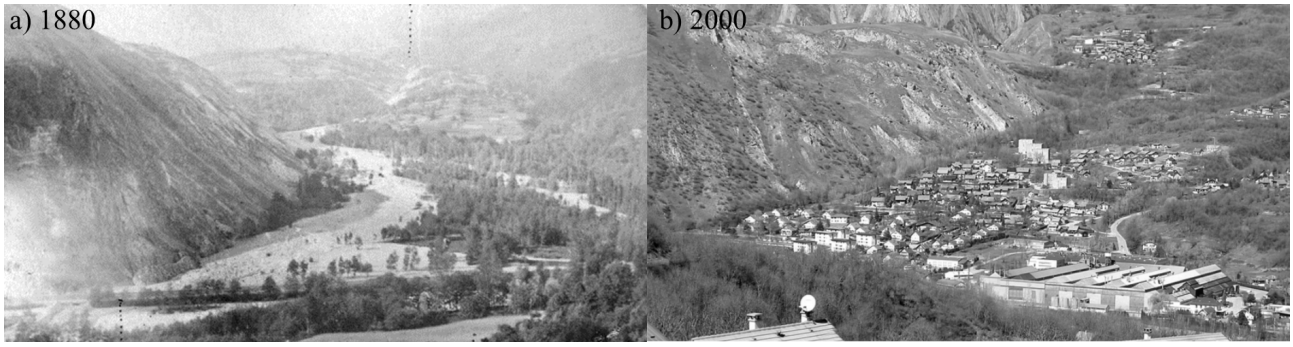

Figure 0.1 – St Michel de Maurienne and the Grollaz torrent fan: a) in 1880 before torrent control works were implemented in the headwater; b) the same location in 2000: buildings are located in the former wandering bed. The torrent definitely seems less active and less prone to massive sediment transport, which has resulted in extensive urbanization in a safer area, providing that torrent control measures are maintained and effective (pictures from the RTM73 archives and from Damien KUSS)

abandonment (or a combination of these measures). Such studies must consider the feedback effects of structures on sediment transport and related hazards; an insufficiently understood topic.

At a broader scale, mountain streams constitute major sediment sources of numerous piedmont rivers. Modern river management policies account for the dramatic consequences of sediment cascade perturbations (Liébault et al., 2010b; Rinaldi et al., 2011; Comiti, 2012). The European Water Framework Directive, for example, explicitly specifies that a high ecological status must be achieved in European rivers, and that this status is partially driven by a suitable continuity in the sediment cascade (EU, 2000, p. 40). However, the necessary torrent control work management policy adaptions must result in better sediment continuity, without detriment to natural hazard mitigation. These objectives appear somewhat contradictory; defining the optimum balance between them therefore requires a precise comprehension of the sediment transport dynamics in streams equipped with torrent control works.

This dilemma between erosion control and sediment continuity is a regular subject of research, well exemplified by the projects that funded this work:

- We participated in the RISBA project[1] , the focus of which was the hazards affecting dam reservoirs, in our case more specifically, to provide insights on the capacity of torrent control works to protect mountain water reservoirs from torrential hazards, and thus to better understand the hazard mitigation capacities of torrent control structures;
- The SedAlp project[2] focused on the integrated management of sediment transport in Alpine basins. We participated in the development and overview of best practices in torrent control and design of innovative structures, aiming to adjust the impact of structures on the sediment continuity.

The effect of torrent control works on sediment production and transfer is therefore a topic that is still worthy of investigation for the resolution of environmental and hazard-related issues. This thesis is a small contribution to the question of sediment transport control by check dams and open

[1]Granted by the Alcotra European Fund, project website: *http://www.regione.piemonte.it/difesasuolo/risba/*
[2]Granted by the AlpineSpace European Fund; project website: *http://www.sedalp.eu*

check dams. It is composed of seven chapters and a conclusion. The first three chapters review the vast existing literature:

- The possible geomorphic effects of check dams have attracted the attention of skilled engineers and researchers for at least 150 years. Chapter 1 reviews archive works, particularly French ones, and seeks to provide a general perspective on the numerous and subtle influences of check dams on their environment. It highlights some poorly known topics, some of which are the subject of more attention later in this thesis.
- Open check dams are sometimes built downstream of a series of check dams. They are possibly the most complicated structure to design in torrent control works, as they must cope with processes that are out-of-equilibrium, fast, violent, diverse, rarely observed and globally poorly understood. At the same time, the structure design can strongly influence its effectiveness. The yet published Chapters 2 and 3 review the available knowledge on the hydraulic design of open check dams (Piton and Recking, 2016a; 2016b). Chapter 2 reviews works describing the hydraulics, sediment depositions, and sediment transfers that occur in sediment traps.
- Complementary to this, Chapter 3 addresses the question of woody debris production and its interaction with check dam openings; floating material causes substantial problems, and the eventual influences of it on structures must be considered by designers.

This literature review highlights subjects deserving more attention:

- The sediment production and transport capacity of mountain streams is a key parameter of torrent control works design. Recking et al. (2016) recently proposed recommendations in sediment transport computation strategy. In their continuity, Chapter 4 used the "*travelling bedload*" concept of Yu et al. (2009) to developed a simple computation procedure adapted to paved streams. It seeks to bridge the gap between the geomorphic description of the sediment supply and the way to compute the stream transport capacity. A formula is also proposed for extreme events involving armor breaking.
- Once the upstream sediment supply defined, the next question is whether or not check dams series modify the dynamics of the sediment transfer. Gras (1857) conceptualized a possible sediment transport regulation by check dams, with a buffering effect resulting from streambed level fluctuations. Long lasting, small scale model experiments were undertaken to explore this phenomena in a simplified case. The paper presented in Chapter 5 (Piton and Recking, 2016c) reports preliminary results confirming a possible influence of the presence of check dams on sediment storage and release dynamics.
- Sediment enters open check dam basins after being transferred in the streambed, including possible buffering by check dams. The literature review of Chapter 2 highlights the fact that the current knowledge on the deposition and spreading of bedload in a basin is relatively limited. A second series of experiments were conducted to acquire data describing massive bedload deposition in laterally unconfined contexts. Chapter 6 describes a new measurement procedure combining photogrammetry with large scale particle image velocimetry (LSPIV - Fujita et al., 1998). This makes it possible to reconstruct a surface repartition of flow and bed features (elevation, slope, roughness, depth, and velocity).

- Chapter 7 reports on a preliminary analysis of the measured flow conditions and geomorphic processes involved in bedload trapping. It highlights a noticeable feedback mechanism between hydraulics and deposition patterns, with interesting similarities with fan and delta constructions, though at a much smaller scale. In this analysis some fluctuations again emerged in the sediment transport processes. In addition to the geomorphic analysis, this chapter contains preliminary descriptions of the flow features and tests a method to compute the sediment deposition slope.

A general conclusion and some perspectives are finally given.

Fig. 0.2 is a visual abstract describing the general organization of the manuscript. A symbolic torrential catchment, equipped with torrent control works, is split into four geomorphic units:

- The natural upstream headwaters, eventually with gullies and landslides;
- The headwaters and gorge channels equipped with check dams;
- The open check dam and its basin;
- The fan trained channel.

Conceptual descriptions of check dams (Chap. 1) and open check dams (Chap. 2-3) are initially given.
Quantitative methods of open check dam functioning are also reviewed in Chapters 2 and 3.
Chapters 3 and 4 provide information on the natural supply of water, sediment and woody debris.
Chapter 5 addresses the question of the transfer of sediment through a series of check dams.
Finally, Chapters 6 and 7 present new results on flows in open check dam basins.

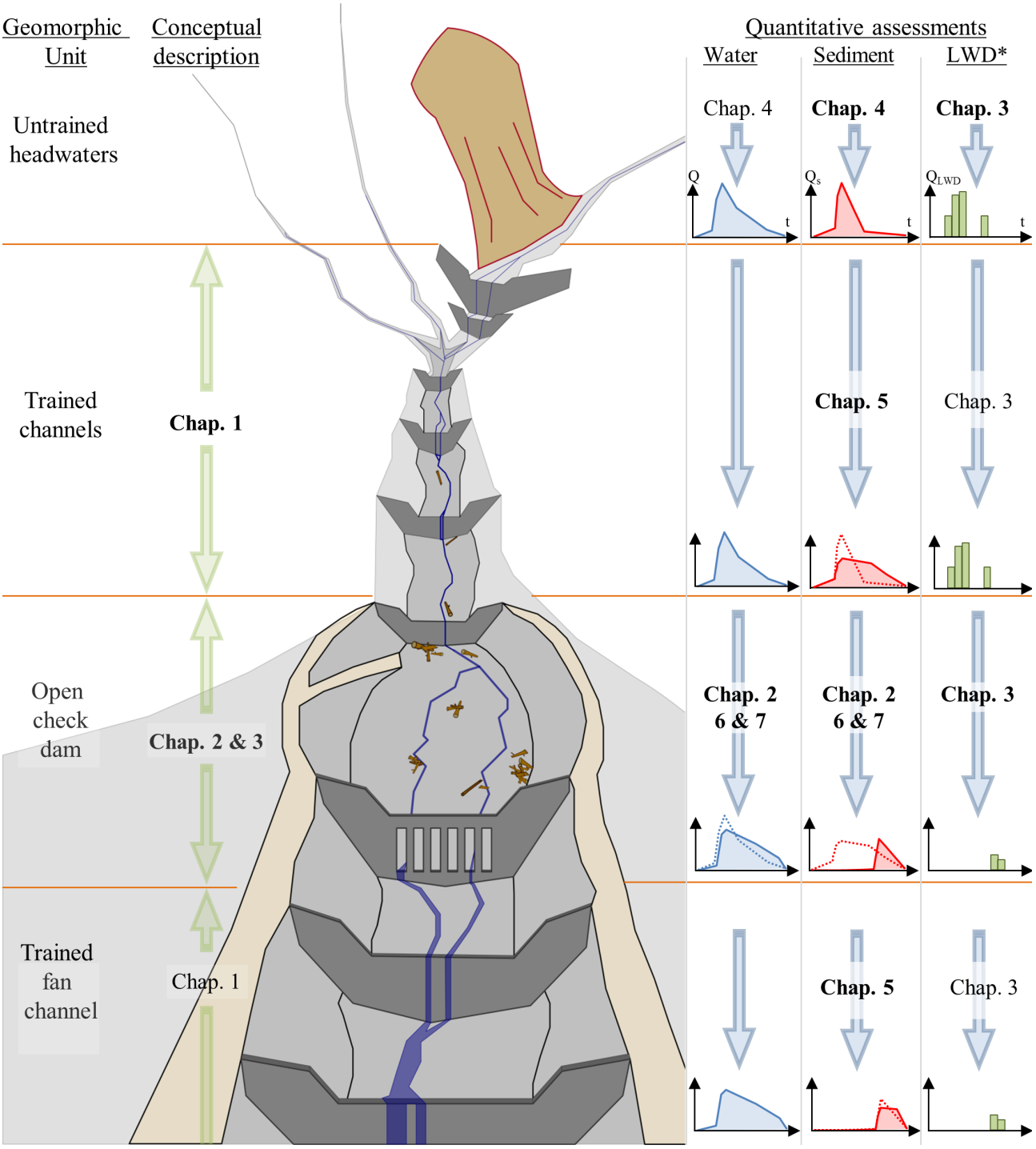

Figure 0.2 – Visual abstract of the manuscript: a symbolic torrential catchment is split into 4 geomorphic units, the effects of check dams and open check dams are conceptually described in Chapters 1, 2 and 3; quantitative methods being provided in Chapters 2–7. Main chapter topics are highlighted in bold, secondary considerations not, although they are also addressed (*LWD = large woody debris)

"Different questions connected with the establishment of barrages, or barriers, for the retention of gravel, have been raised and discussed. But, notwithstanding all that has been done, it appears to me that ideas in regard to what results are to be expected from these barrages are still vague, varied, and undetermined."

Translation of Breton (1867) in Brown (1876, p. 82).

A synthesis of outstanding pioneering works, in the light of more than 150 years of efforts in understanding mountain stream dynamics.

CHAPTER 1

Why do we build check dams in Alpine streams? An historical perspective from the French experience

Guillaume PITON[a], Simon CARLADOUS[a,b,c], Alain RECKING[a], Jean Marc TACNET[a], Frédéric LIEBAULT[a], Damien KUSS[d], Yann QUEFFELEAN[e], Olivier MARCO[e]

[a] Université Grenoble Alpes, Irstea, UR ETGR, St-Martin-d'Hères, France.

[b] AgroParisTech, Paris Institute of Technology for Life, Food and Environmental Sciences, Paris, France.

[c] Ecole Nationale Supérieure des Mines, Saint-Etienne, France.

[d] Office National des Forêts, service Restauration des Terrains de Montagne de l'Isère, Grenoble, France.

[e] Office National des Forêts, Département Risques Naturels, Grenoble, France

This chapter constitutes a combined state-of-the-art synthesis of what is known as possibly been the effects of check dams on Alpine stream systems, with an historical perspective on the emergence of these concepts. Owing to acute questions from Stuart LANE, Fransesco COMITI, and an anonymous reviewer[1], the chapter is now completed with a discussion on the future research works to undertake toward the development of a rigorous and comprehensive analysis of check dams' efficiency, and more generally of any torrent control works' efficiency, in torrential hazard mitigation.

[1]The chapter is in press: Piton et al. *Earth Surface Processes and Landforms*, DOI:10.1002/esp.3967

Abstract

For more than 150 years, humans have tried to limit the geomorphic activity of mountain streams, and the related damages, using torrent control works. Check dams are likely the most emblematic civil engineering structures used in soil conservation programs. Modern mountain societies have inherited thousands of these structures built in upland gullies and streams. To help define their effectiveness and decisions concerning their maintenance or new project designs, a clear understanding of potential effects of check dams on river systems, i.e., their functions, is first needed. The next steps concern quantitative assessments of each function on the flood features and combination of all effects. The present understanding of these sometimes old structures' functions can be complicated because the societal and environmental contexts in which the original structures were built may have changed. To bridge this gap, this paper traces the purposes for which check dams were built, through a detailed analysis of French archives. We first analyse chronologically how each function was theorized and applied in the field. In the nineteenth century, engineers developed a thorough empirical and conceptual knowledge of mountain soil erosion, torrential geomorphology, and sediment transport processes, as well as, check dam interactions with these natural processes. The second part of this paper synthesizes conceptual descriptions of the check dams' functions, in the light of more than 150 years of experience, with their implication on the features of the structures. The French experience is compared to other countries' pioneering works. Finally, the next steps and remaining research challenges toward a comprehensive analysis of check dams' efficiency in torrential hazard mitigation are discussed. This analysis is proposed to remind how, conceptually, check dams may influence geomorphic systems, bearing in mind the knowledge represented in pioneer guidelines and recent works on the subject.

Author key words: *Torrent control works, torrent hazard mitigation, historical analysis, Mountain streams, grade control structures*

1.1. Introduction

Mountains are important sediment sources for piedmont fluvial systems (Wohl, 2006). Rivers and streams play a key role within the sediment cascade by transferring and buffering fluxes between active hillslopes and downstream alluvial environments (Fryirs, 2013). In mountain streams, sediment transport mainly occurs during floods that regularly have dramatic and expensive consequences on exposed elements (Meunier, 1991): reducing capacity of hydro-electric dams, cutting networks, damaging housing, industrial, and agricultural areas, and generating causalities. Human interventions in mountainous watersheds thus often aim to reduce negative consequences of sediment releases from torrents.

The word "torrent" is widely used in Europe and derives from the Latin adjective "*torrens*", meaning rushing, violent, fast-flowing as well as ephemeral (Gaffiot, 1934), and refers to a watercourse showing particular high geomorphic activity compared to more calmer streams or brooks (Fabre, 1797; Surell, 1841). This activity is strongly related to i) the quick hydrological responses typical of upland environments; in conjunction with ii) the sediment availability. The existence of a torrent is thus mainly related to the activity of the sediment sources, defined as discrete, *e.g.*, landslides, debris avalanches; or diffuse, *e.g.*, gul-

lying, soil creep (Reid and Dunne, 2003). Their sediment production naturally fluctuates in time (Fryirs, 2013), depending on various factors such as climate and land-use changes (Gomez et al., 2003; Liébault et al., 2005; Comiti et al., 2012), particularly concerning vegetation cover (Phillips et al., 2013).

The stabilizing role of vegetation on soil erosion has been known since the Antiquity (Van Andel et al., 1986), leading to some regulations specifically concerning erosion prevention at least since the Medieval period (Fesquet, 1997 p. 114; JSA, 2003; Okamoto, 2007; Evette et al., 2009; JSA, 2012). In erosion prone areas, hillslope interventions such as reforestation, soil bioengineering and terracing have sometimes been implemented in combination with gully system control, torrent control, fan channel regulation and, finally, river training. Civil structural measures such as check dams, embankments, and bank protection can thus be found from headwaters streams down to fan channels. Scientific debates have existed between supporters of civil engineering and of soil bioengineering for ages (Fesquet, 1997 p. 520; Hall, 2005 p. 72; Bischetti et al., 2014); but it is now widely accepted that each technique is adapted to a different context and that all are complementary (Combes, 1989; deWolfe et al., 2008). Among all civil engineering structures, check dams are probably the most emblematic of torrent control works.

Throughout this paper, 'check dams' designates transversal structures built across stream beds and gullies in torrential watersheds. They can be made of logs, gabions, dry stones, masonry or/and reinforced concrete. Quite similar structures have been called check-dams, consolidation dams (D'Agostino, 2013b), solid body dams (Wehrmann et al., 2006), SABO dams (Chanson, 2004), crib barriers (Garcia, 2008), bed sills (Gaudio et al., 2000), weirs (Rinaldi and Simon, 1998), thresholds (Blinkov et al., 2013) or grade control structures (USACE, 1994). In agricultural contexts that are out of the scope of this paper, "check dams" may also refer to small water reservoirs for irrigation purposes (Agoramoorthy and Hsu, 2008) or dams dedicated to trap silts and to form agricultural areas (Xu et al., 2013). Conversely small structures used in gully control are also called check dams (Heede, 1967) and may be considered as smaller forerunners of large modern structures, facing similar processes at different scales, erosional systems being intrinsically scale self-similar (Paola et al., 2009).

Small dams fixing the position of fords and protecting agricultural areas were probably regularly used since Antiquity (McCorriston and Oches, 2001; Doolittle, 2013), however the aggressive environment of mountain streams likely has destroyed most of the more ancient structures if they have not been upgraded. In torrential contexts, Armanini et al. (1991); Jaeggi and Pellandini (1997); Okamoto (2007) and Koutsoyiannis et al. (2008) cite examples of check dam constructions long before the eighteenth century, but it seems that such high dams (more than several meters high) were local and relatively rare initiatives taken after a disaster or as a last resort. At that time, the lack of a general understanding of the geomorphic processes and good design standards made it difficult to implement suitable and sufficiently strong mitigation measures in the most active streams.

Modern hydraulics partially developed in the Italian scientific community under the stimulus of Leonardo Da Vinci (1452-1519) and Benedetto Castelli (1577-1643). Pioneering works were implemented, particularly in the Po and Arno river basins (Castelli, 1628; Frisi, 1770; Hall, 2005; Comiti et al., 2012; Bischetti et al., 2014). Their works influenced engineers of other countries in Europe, notably in France (Marsh, 1864, p. 386), and possibly as far as China (Koenig 2014). Some engineers focused on mountains and stressed consistently, though likely independently (Marsh, 1864, p. 205), the features of steep rivers and streams (Frisi, 1770; von Zallinger, 1779; Fabre, 1797).

In the late 19^{th} century, intense development of economy and infrastructures (road, railway, and fluvial transport networks) required protection from sediment carried by mountain streams in Europe and Japan (Napoléon III, 1960, p. 161; Kamibayashi, 2009). This has motivated an important development of torrent control works in headwaters to limit undesirable sediment transfers to the downstream fluvial systems. Soil erosion control plans through reforestation and engineering structures thus became a subject of interest and were locally implemented in mountains. This was supported by national laws dedicated to erosion control in mountains, adopted in numerous countries generally following a period of severe floods and large damages (Eisbacher, 1982): for instance, in France in 1860, in Switzerland in 1876, in Italy in 1877, in Austria in 1884, and in Japan in 1897.

As a result, present-day torrent managers have inherited thousands of protective structures that require costly maintenance operations (Mazzorana et al., 2014). In France, for instance, 92,873 check dams, 10 tunnels, 736 km of drainage networks and 74 km of avalanche barriers and fencing were recorded in 1964 (Messines du Sourbier, 1964). However, only 14,000 check dams are currently regularly maintained by the government through the French torrent control service (RTM) in the public mountain forests of 11 departments in the Pyrenees and the Alps (Carladous et al., 2016a).

Current decision-makers question the relevance of maintaining such old and hard-to-access structures. Within a given watershed, decision-makers must decide between several alternatives: intentionally destroying existing structures, merely stopping their maintenance, maintaining them or investing to build new structures. To help decision makers, the current baseline risk and the residual risk for each alternative must be estimated (Carladous et al., 2014b), taking into account existing structures and their effects (Margreth and Romang, 2010). These studies typically comprise several steps: i) establishing requirements for and objectives of protection, ii) determining check dams' functions, i.e. what is their qualitative role to help achieving the objectives, iii) estimating the expected quantitative effect of structures on morphodynamics: the structures' capacities, iv) propagating the hazard changes through the complete protection system paying attention to uncertainties and structure dependability, v) replicating all steps for each alternative and comparing alternatives with the preliminary defined protection objectives. Determining rigorously all the check dams' functions is thus the key second step that will guide which geomorphic processes are later studied (Carladous et al., 2014b).

From our experience, it is sometimes not straightforward to practically specify these functions, notably because watershed morphodynamics may have changed since the construction period. Moreover, the function must be specified between several potential ones, and the corresponding clear list is not easily available for French practitioners (Carladous et al., 2014a). To close these gaps, the following archive analysis helps to specify (i) what objectives engineers aimed to achieve when building the check dams, and (ii) how the understanding of torrent morphodynamics, and consequently the expected works' effects, has evolved since the pioneers' works. It demonstrates that a structure as simple as a check dam may be built for quite various purposes and has specific expected functions and effects depending on its location and design features. It also shows that torrent control engineers developed a detailed understanding of functions and effects of protective structures on morphodynamics of torrents by conceptual thinking, field observations, and feedback from their tests and trials.

The archive analysis principally focuses on the French example, which is interesting for several reasons: i) despite probably not being the first to theorize the concept (see discussion), France was first to experiment with national scale implementation of torrent control works after the 1860

laws; ii) the French experience later influenced numerous countries in the beginning of their torrent control management, *e.g.*, in Austria (Patek, 2008), Balkans (Kostadinov, 2007; Blinkov et al., 2013) and Japan (JSA, 2003, p. 18; Nishimoto, 2014); and iii) the large scale of French mountain land restoration programs in a comparatively varied environment of three mountain chains (Alps, Massif Central and Pyrenees) forced the French engineers to address extremely varied subjects dealing with torrent control, generally with regionally specific solutions (Kalaora and Savoye, 1986; Fesquet, 1997). A similar analysis could be done, and worth doing, in several other mountainous countries. It would probably help the scientific community to better understand the current approaches and issues of other countries, each of them being partially inherited from their histories.

The first part of the paper traces the evolution of the French good practices through a chronological framework, relating pioneering works and theory evolution, especially during the first torrent control implementations. We secondly review check dam functions in the light of more than 150 years of practical research and field observations. Some elements of torrent control history from abroad are then discussed, as well as the next steps toward a comprehensive analysis of check dam efficiency in torrent hazard mitigation; namely, effect quantification, effectiveness and dependability assessment and, finally, risk analysis and efficiency assessments.

1.2. Historical development of torrent control works in France

1.2.1. Early 19^{th} century: The 'Forester' lobby

In France, during the early nineteenth century, numerous mountain areas were impacted by the pressure of the largest population in their history and forest-management deregulation following the 1789 Revolution (Surell, 1841; Blanchard, 1944; Fourchy, 1966; Fesquet, 1997). The deforestation rate of mountain areas was at its maximum, resulting in increasing soil erosion problems. In reaction, a lobby of 'foresters' comprising officers, scientists, and major landowners promoted reforestation of mountain areas (Kalaora and Savoye, 1986). Their works were diffused abroad (Marsh, 1864, p. 205; Brown, 1876; Woeikof, 1901).

Several civil engineers, *e.g.*, Jean Antoine Fabre (1748–1834) and Alexandre Surell (1813–1887), worked on mountain stream morphodynamics and published pioneering books in French (Fabre, 1797; Surell, 1841). They both recommended to immediately stop deforestation operations on hillslopes prone to erosion and to launch an authoritarian reforestation of mountain areas supervised and supported by the French state. Their analysis of the current mitigation techniques, mainly embankments on fan channels, highlighted the incapacity of dikes to cope with massive sediment supply (see next section). They thus recommended curtailing sediment production at the sources, i.e. in the deforested headwaters, with erosion control work (reforestation and bioengineering); a long task but the only sustainable option.

1.2.2. Mid-19th century: Pioneering works on check dams

Scipion Gras (1806–1873), Philippe Breton (1811-1892) and Michel Costa De Bastelica (1817-?), three civil engineers, wrote books focusing on the design and function of check dams (Gras, 1850; Gras, 1857; Breton, 1867; Costa de Bastelica, 1874). These authors paid great attention to putting the processes of geomorphic hazards at the center of the mitigation measures design, stressing the necessity to adjust protections to the catchment features. They completed the geomorphic study of Surell by first developing the physics of sediment transport. They particularly highlighted that torrent hazards are mainly related to sediment transport excess, rather than to a mere water discharge excess as is generally the case in lowland rivers. They stated that solid material deposition and the related hazards occur when sediment supply exceeds the solid transport capacity of reaches, capacity that was strongly correlated to the slope. Based on these considerations, they fully explained why embankment works of torrents generally show disappointing results. They worked in the Grenoble region where numerous valleys kept traces of former glacial lakes, i.e. large valley bottoms and numerous fans that were disconnected from the downstream (sometimes trained) river systems. They detailed the problem emerging in weakly coupled fan-mainstem systems: nearly total deposit at the fan toe and regular channel backfilling. As a consequence, Gras (1850; 1857) and Breton (1867) recommended not just building embankments on these fan channels, which consequence is a mere transfer further downstream of the sediment excess problem. The downstream fluvial system, lacking sufficient slope to transport the sediment supply, would, with or without dikes, aggrade to achieve equilibrium, although it would be faster and thus more dangerous to cope between dikes. These authors thus considered that the only solution was to act on the sediment sources.

They conceded that reforestation works may be efficient, although sometimes not sufficient: (i) since it would take decades to truly stabilize torrents with a single reforestation plan, check dams could be useful to obtain short-term mitigation effects, and (ii) in highly unstable watersheds, reforestation works would not be sufficient and must be completed with check dams.

They expected that incision would occur on the fans, due to sediment starvation downstream of check-dams, which could be exploited to increase the fan-channel transfer capacity. After check dams filled, the downstream sediment transfer would be restored and these wider and deeper channels would more be able to absorb floods, giving time to enhance the protection system, *e.g.*, by adding new check dams and thus increasing the system trapping capacity. Their books describe three check dam functions: retention, consolidation, and sediment transport regulation.

A. Retention check dams

In disconnected fan-mainstem systems, any sediment supply would generate geomorphic instability. In such cases, a nearly total and definitive trapping of sediment must be sought, hereafter refer to as a retention function. The gorges or the bottom part of the headwaters were suitable locations to maximize the trapping volume for a given structure height (Gras, 1857; Breton, 1867). When seeking this function, the authors recommended the construction of check dam series in an appropriate site rather than spreading the structures through the watershed (Fig. 1.1).

B. Hillslope consolidation dams

Cliff collapses and other hillslope instabilities are strongly driven by toe erosion. To slow down their activity, Gras (1850) and Costa de Bastelica (1874) proposed artificially elevating the valley floor to fill the void created by torrent incision and to protect the cliff and hillslope toe. This filling would be created and durably fixed by a

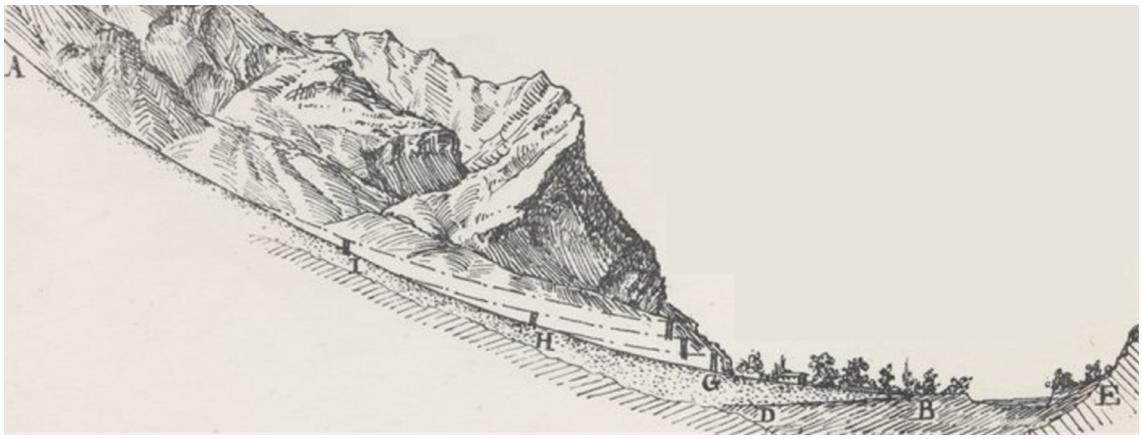

Figure 1.1 – Retention check dam optimal location (at point G) to promote retention in gorges (after Breton, 1867)

structure built downstream of the unstable toe and beyond its influence in term of pressure and mass movement: a consolidation check dam.

C. Sediment transport regulation

Despite a sufficient coupling state with their downstream fluvial mainstem, some torrents experience significant deposition on the fans during debris-flow events. Gras (1857) suggested that the natural tendency of the bed level to fluctuate could be used to regulate high sediment discharge between check dams. He recommended forcing the channel to widen using large, flat-crested check dams. Flowing over these artificially wide places, debris flows would preferentially deposit and partially fill torrent beds between dams; subsequent floods, carrying only bed-load due to the recent upstream sediment flushing, would re-erode the debris flow deposits, leaving in place only boulders that could be re-used to reinforce the structures.

Gras (1857) and Costa de Bastelica (1874) theorized that open check dams, called "retention labyrinths" consisting of dams with slots in their bodies, would have an equivalent regulating effect, anticipating modern sediment traps (see discussion).

Gras (1857) recommended building check dam series in the bottom part of the headwaters and in the gorges to regulate sediment transport. If their dosing effect was not sufficient to curtail torrent hazard on the fans, a retention labyrinth could be added downstream of the series, near the fan apex.

Finally, Gras (1857) conceded that check dam series could also be used on fans for regulation purposes. In this case they should be built as ground sills, i.e., at the bed level, and not above the bed level: heavy uncontrolled deposit on the fan on a high structure would increase avulsion and damage probability on the fan (see discussion).

1.2.3. 1860-1882: Toward mountain area restoration

The authoritarian Second Empire of Napoleon III, established in 1852, promoted major infrastructure works (Lilin, 1986), and decided to launch mountain area reforestation in 1860 (Fourchy, 1966). The more than 50-years old forester lobbying activity (Fabre, 1797; Surell, 1841; Jouyne, 1850; Champion, 1856) along with the hydrological crisis of the mid-nineteenth century (major floods in most large French river systems, Coeur, 2003; Cœur and Lang, 2008) led to an ambitious reforestation program within the 1860 Law (Brugnot, 2002). The role of forests in limiting run-off and protecting cities in lowlands played a key role

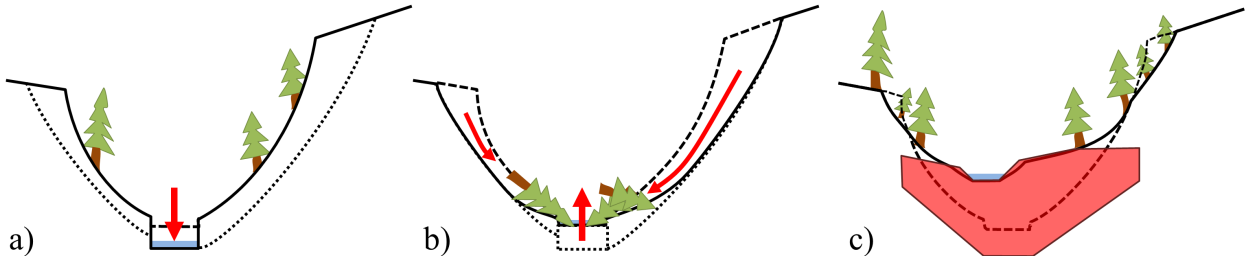

Figure 1.2 – Sketches of a torrent section showing longitudinal and vertical erosion: a) armor breaking and vertical incision leading to b) lateral instability; both effects being stabilized by c) constructing a suitable check-dam: higher than the initial bed level, thus creating a wider thalweg, preventing the incision and bank destabilization and displacing the bed axis from the most erosion-sensitive-bank

in this decision (Andréassian, 2004), though being supported by strong debates in France and elsewhere (Marsh, 1864, chap. 3; Vischer, 2003 p. 17). Too ambitious, this first law was rejected by pastoralists and even led to local armed revolts (Fourchy, 1966). Consequently, a second law dedicated to grass seeding was voted in 1864, aiming at reconciling pastoral activities and soil protection using the grass stabilizing effect (Brugnot, 2002).

The first tests and trials were immediately launched after 1860 by the forestry administration: the "Eaux et Forêts" administration. It did not take place in a specific region: works were undertaken wherever the administration managed to own the perimeters to reforest (Mougin, 1931).

After the fall of the Second Empire in 1870, and following complaints from mountain populations, the law on the conservation and restoration of mountain areas (Conservation et Restauration des Terrains de Montagne, hereafter denoted as RTM) was proclaimed in 1882 (Tétreau, 1883). Concerned with the rural population, the new Republican Assembly voted a law that reduced reforestation ambitions: the torrent control work effort would be concentrated in areas of active erosion, i.e., mainly torrent beds, gully systems, avalanche paths, and landslides, thus more using civil engineering and less extensive reforestation operations (Brugnot, 2002).

1.2.4. Late-19th century: General guidelines

Prosper Demontzey (forestry engineer, 1831-1898) published the first French complete erosion and torrent control technical guideline in 1882 (Demontzey, 1882). He first detailed the geomorphic processes related to torrents and proposed a classification of streams: (i) torrents with gully systems, (ii) torrents with cliffs as sediment production areas, impossible to reforest, and (iii) torrents with glaciers and moraines in their headwaters, too high in altitude to be reforested. The mitigation measures must be partially adapted to each torrent type, although their fan and gorge parts are similar.

Demontzey secondly provided complete RTM techniques. From his forester point of view, torrent beds should be stabilized specifically to facilitate forestry works on hillslopes and on banks. Check dams were thus built as a necessity to stabilize the beds, diminish the slopes, and widen the beds to prevent incision and the related bank destabilization (Fig. 1.2). In this strategy, some structures could be abandoned as soon as the stabilizing function of forests would be achieved.

For torrents with overhead cliffs, glaciers, and moraines in their headwaters, the retention check dam techniques were recommended, completed by stabilization dams preventing incision in the downstream alluvial parts. Subsequently, Edmond Thiéry (forestry engineer, 1841–1918) introduced dam stability and hydraulic calcula-

tions to the empirical descriptions of Demontzey (Thiéry, 1891).

The impressive details, volume of work, and pedagogy showed by Demontzey (1882) and Thiéry (1891) were immediately translated and used abroad (Woeikof, 1901; Kostadinov, 2007; Kostadinov and Dragović, 2013; Bischetti et al., 2014). Interestingly, several details on check dam design and the effects on sediment transport developed in the aforementioned works of Gras and Breton are not mentioned in their guidelines, *e.g.*, the ability of dams to regulate sediment transport. Demontzey and Thiéry re-centered the check dam functions on their ability to facilitate reforestation to "extinguish" all torrents (Fesquet, 1997).

Figure 1.3 – Headwater-moraine-retention-dams in the Ravin des Arandellys (74 – FRA.) (Eaux et Forêts, 1911a)

1.2.5. Early 20^{th} century: RTM engineer second generation

Paul Mougin (1866–1939), Charles Kuss (1857 –1940), and Claude Bernard (1872–1927), three forestry engineers, are some of the key figures of the second generation of torrent control engineers. They had the opportunity to undertake the first assessments of nearly 50 years of torrent control (Eaux et Forêts, 1911b; 1911a; 1911c) and to develop alternative check dam designs in cases where the basic high arched check dam policies did not yield satisfactory results (Messines du Sourbier, 1939b).

The glacial lake outburst flood that resulted in the Saint Gervais disaster (175 fatalities, 1892) demonstrated that high-elevation moraines are dangerous sources of debris flows. Kuss (1900b) detailed it in a book and explained how retention check dams are constructed aiming on the long term to trap these sediment accumulations in the headwaters (*e.g.*Fig. 1.3). The harsh climate and avalanches make other measures (reforestation & drainage) poorly adapted to these contexts.

In addition to glacial torrents, a substantial number of large, debris flow-prone torrents are supplied by landslides and rock avalanches. In this case, the classic reforestation techniques were inefficient and replaced by diversion techniques, such as a landslide-toe bypass using tunnels (*e.g.*, Mougin, 1900) or more generally by using the aforementioned consolidation check dams. Kuss (1900a) provided a thorough description of the interaction between torrents and landslides or rock avalanches and described feedback from several sites where consolidation dams had been tested.

1.2.6. Synthesis of actions implemented until WWI

The period between 1882 and the beginning of World War I (WWI) in 1914 has sometimes been called "the golden age" of the RTM (Brugnot, 2002). During this period of intense activity, torrent control works were undertaken in the French Alps in 1,062 torrents out of 1,891 torrents identified. There is no such detailed inventory for the Pyrenees, the Massif Central, or the Cevennes, where only *ca.* 100 torrents have been identified, which is a doubtful number (Mougin, 1931; Poncet, 1968). Approximately 100 landslides and an equivalent number of avalanche sites were also managed (Requillard et al., 1997).

The RTM lessons of Bernard (1927) synthesized the knowledge acquired since the Demontzey and Thiéry works. The role that check dams play in torrent control plans were more detailed, taking into account the observed sediment transport regulation effects and the usefulness of consolidation dams for landslide treatments.

1.2.7. Post-WWI strategies

The number of new projects declined significantly after WWI (de Crécy, 1983), particularly due to rural depopulation that resulted in decreases in potential damage and in affordable work force availability (Van Effenterre, 1982). In addition, funding to maintain structures tended to decrease and few new structures were built in the headwaters (Requillard et al., 1997; Brugnot, 2002).

Reinforced concrete techniques were increasingly used from the 1940s (Poncet, 1995), allowing to design and build cantilever dams, more affordable for high structures, from *ca.* 1955 (Bordes, 2010). While some conservatively designed reinforced-concrete check dams are still in good condition (Fig. 1.4), attempts to optimize dam thickness sometimes showed disappointing results: regular dam failures resulted from the lack of design and building standards. Consequently, reinforcements could be needed later and were realized under updated civil engineering standards (BAEL, 1980).

Reinforced concrete also allowed building new structure types such as open check dams. After the first tests of the 1950s and the 1960s (Reneuve, 1955; Clauzel and Poncet, 1963), the number of open structures exploded in France during the 1970s and 1980s (Deymier et al., 1995; Poncet, 1995; Gruffaz, 1996) but also in other countries. The development of these open structures did not take place specifically in France (Piton and Recking, 2016a; 2016b).

Figure 1.4 – The 34-m-high 'Fèvre' check dam in the Bonrieu branch of the Saint Martin torrent (73 - FRA.); 4-m-thick at the crest, 7.6-m-thick at the toe, construction: 1939-1942, just upstream of the huge lateral Bon Rieu landslide (Messines du Sourbier, 1939a). The downstream gorge is currently filled by the landslide movement, stabilizing it. The dam is still in good condition, almost completely buried by the landslide, and it fulfills its function perfectly: decrease the energy and erosive power of debris flows upstream of a reach whose incision has catastrophic consequences (photo Apr. 1955 by L. Anchierri courtesy of RTM73).

1.3. Synthesis of check dam functions

Authors working in torrent control works have reported lists of check dam functions for decades (Zollinger, 1985; Ikeya, 1989; Armanini et al., 1991; Poncet, 1995; Hübl and Suda, 2008), although generally less detailed than in this work. The following list describes, in greater detail, our definitions of the different aforementioned functions. They are conceptually distributed within a symbolic catchment in Figure 1.5. Table 1.1 gathers the features (shapes and location) of check dams designed to maximize each different function. These definitions are not consistent with some locally used technical jargons, which, to our experience, remain sometimes quite fuzzy.

Identifying the specific function of a series of check dams can be complicated because some structures clearly have several functions at the same time; they are not mutually exclusive and concern all aspects of mountain geomorphology. It needs a multidisciplinary approach gathering experts in hydraulics, geology, geomechanics and forestry (Hübl et al., 2005). While some structures were built in specific locations with a specific role to play, other structures were built as a series, aiming to achieve several functions (Zeng et al., 2009), *e.g.*, bed stabilization and decreasing slope. Side effects then emerged, *e.g.*, solid transport regulation or downstream consolidation (*e.g.*, Fig. 1.4).

1.3.1. Bed stabilization

Depending on geological bed features, torrential flows eventually induce material removal by longitudinal incision or/and lateral bank erosion (Fig. 1.2). On fans, they can induce damage by lateral scouring of natural banks or protective structures such as dikes and bank protection, or create new flow paths after avulsion. Bed stabilization is the main check dam function. It can be divided into two sub-functions.

- *Longitudinal stabilization* aims at preventing incision by creating fixed points in the longitudinal profile through a check dam series. They stabilize materials which, without structure, would be recruited by the stream, resulting in incision and its secondary effect of bank destabilizations (Fig. 1.2).

- *Planimetric stabilization* aims at limiting channel wandering. For this purpose, the structure crest spillway guides the flows in a chosen direction (Deymier et al., 1995; Jaeggi and Pellandini, 1997). In curves, a few oblique check dams can force the flow toward the center of the downstream bed rather than toward the banks (Fig. 1.6), preventing bank erosion or avulsion that would result from an inadequate structure axis (Tacnet and Degoutte, 2013). Some structures are built specifically for this planimetric stabilization. An equivalent effect is achieved using groynes, but they are less used in steep slope streams because too sensitive to toe scouring (Fabre, 1797).

Check dam crests are generally not set vertically at the initially existing bed altitude, but a few meters above (Fig. 1.2c) because digging several-meter-deep excavations in gullies or torrent beds to build a dam and its foundations could generate lateral and longitudinal destabilization (Jaeggi and Pellandini, 1997). Consequently, side effects of slope-decrease and better bank stabilization are generally observed (see slope reduction function). On the contrary, check dams used to fix degrading beds on fans must not be built over the bed profiles in these alluvial formations but rather at the initial bed level and are consequently called bed sills (see solid transport regulation function).

The bed stabilization function was often coupled, in France particularly, with bank and later hillslope reforestation and grass-seeding operations. In addition to artificial operations, sponta-

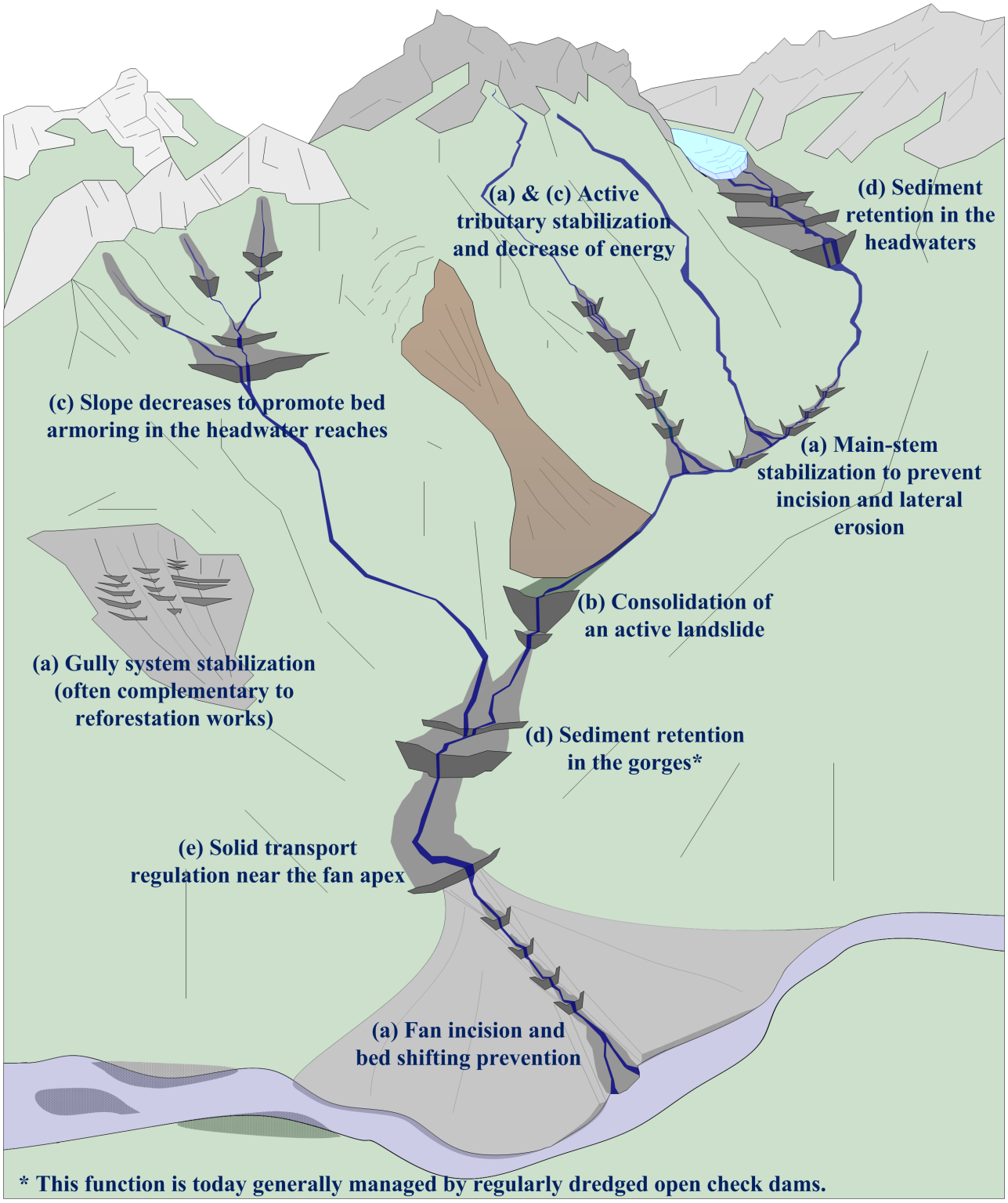

Figure 1.5 – Examples of typical check dam configurations and structure main functions: (a) stabilization, (b) consolidation, (c) slope-decrease, (d) retention and (e) solid-transport regulation; complementary measures (reforestation, drainage networks, artificial bed paving, embankments and open check dams) as well as check dam secondary functions and side effects are not mentioned for the sake of clarity

Table 1.1 – Check dam shape features and location depending on their main function

Function	Characteristic dam feature and shape	Dam position compared with other dams	Location within the watershed
Channel stabilization	Dam crest spillway width ≈ natural channel width	Close enough to allow a continuity in the longitudinal bed control and in the flow centering	Anywhere incision and lateral channel shifting must be prevented
Hillslope consolidation	Dam or dam series significantly higher than the initial bed level		Directly downstream of important hillslope instabilities: landslides, gullies, or cliffs
Channel slope decrease			Where slopes are steeper than the alluvial equilibrium and anywhere aggradation is not a problem so that the structure will create a milder slope that will decrease flow energy and ability to transport boulders
Sediment retention*	High dam or dam series to maximize sediment trapped volume	One or few dams close to each other downstream of an extended backfilling area	Where long-term sediment storage is possible: in the headwaters or in the gorges† (and considering the actual situation, where downstream sediment starving is not a problem).
Solid discharge regulation	Wide crest spillway to promote flow spreading	Distanced structures to maximize upstream deposition surface areas.	Where the slope is mild enough and the available area is large enough to temporarily store sediment

* In modern torrent works this function is more generally achieved using open check dams maintained by regular dredging with earth-moving machinery.

† Old retention check dams earth-filled up to the crest currently often constitute advantageous solid discharge regulation structures.

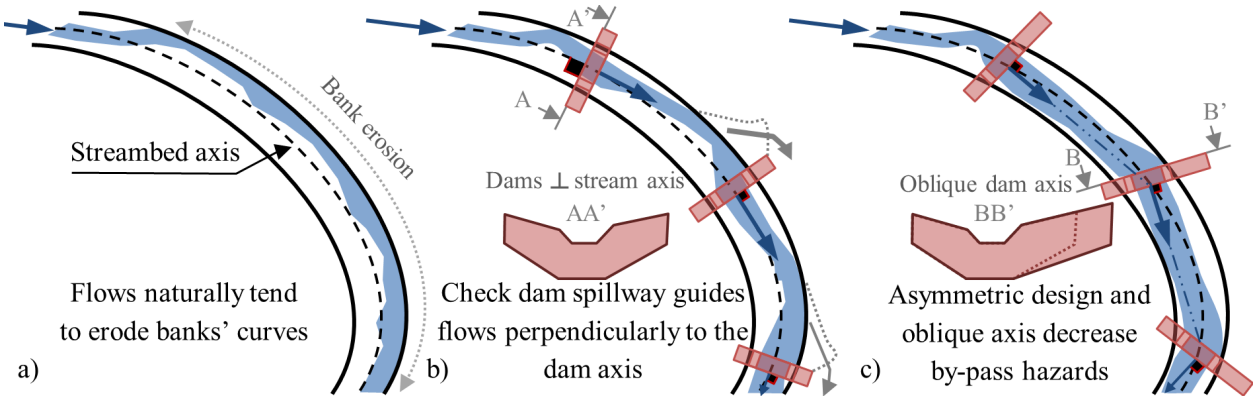

Figure 1.6 – Planimetric stabilization of check dam: a) without structures, curves' banks are preferential eroded areas. Check dams guide flows in a given direction either: b) toward the downstream structure wings and banks promoting lateral erosion (unsuitable implantations – perpendicular to the stream axis); or c) toward the downstream structure spillway, promoting centered flows and decreasing by-pass threat (suitable implantations that are counter-intuitively oblique compare to the stream axis).

neous revegetation is reported as a side effect of stream bed stabilization by check dams (Bombino et al., 2009; Zeng et al., 2009; García-Ruiz et al., 2013). Zeng et al. (2009) compared two similar torrential watersheds (*ca.* 14 km^2, Yunnan Province, Southwestern China), one left natural and the other one with check dams built at the beginning of observations in the 1960s (117 small structures, all destroyed in 1974, then 44 new check dams, 3-6-m high). After 25 years, they reported "*many mature trees, grass and brushes living in the bank slopes above the channels protected by check-dams*" and described the coupling process of bed channel stabilization and bank revegetation: gully down cutting regularly used to triggered shallow landslides, preventing any durable vegetation fixation; after check dam alluviation, no intense incision could occur, which resulted in bank toe stabilization, bank slope decreases and, incidentally, more stable slopes, more prone to vegetation settling.

To conclude, this function aims at stabilizing quite diffuse sediment sources. When built in areas were revegetation is not possible or not adapted, they merely aim to durably stabilize stream beds, preventing incision, and thus curtailing sediment production. Within an area where revegetation is naturally or artificially possible, another long term stabilization of sediment production emerges. The vegetation growth is enhanced by more stable thalwegs and fewer shallow landslides and hillslope gullying. Check dams thus sometimes aim at temporary or durably stabilizing slopes during the vegetation settling.

1.3.2. Hillslope consolidation

While some streams experience excessive sediment transport due to active diffuse soil erosion in their headwaters, others may be entirely vegetated but a few located sediment sources erratically generate sediment-laden floods. The erosion rate of the hillslope and the activation of hillslope instabilities are significantly controlled by their bottom boundary, i.e., by the incision of valley thalwegs (Sklar and Dietrich, 2008; Egholm et al., 2013). More specifically, landslide reactivation following a torrent incision is the nightmare of all torrent control work engineers because it generally strongly increase debris flows activity (Gras, 1848; Messines du Sourbier, 1939a; Zeng et al., 2009; Wang, 2013). Re-filling of the valley and consolidation of the hillslope instability toe is often an effective measure to decrease the activity of the key sediment sources that are landslides and debris avalanches (Kuss, 1900a; Eisbacher, 1982; Kronfellner-Kraus, 1983). This can be achieved by consolidation check dams (Fig. 1.5b), which seek to significantly elevate the bed level and consolidate the lateral hillslope, whose sediment supply sometimes completely fills the former thalweg (Fig. 1.7).

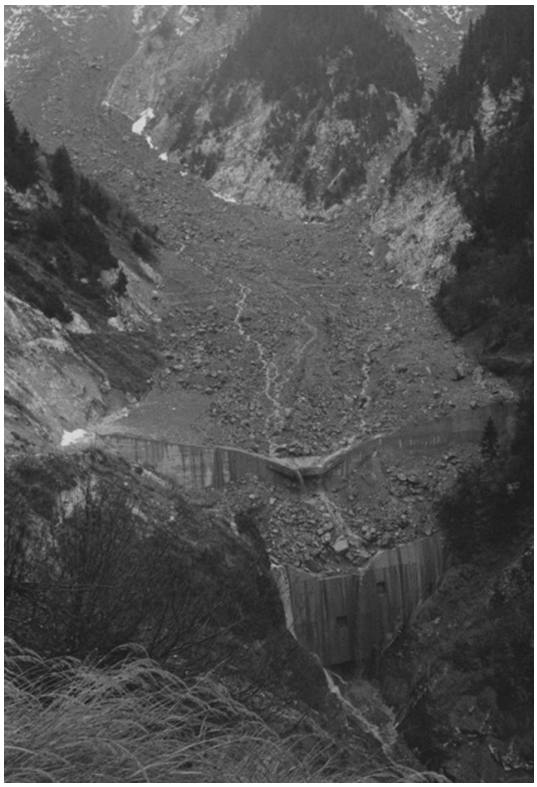

Figure 1.7 – Bon Attrait deepseated landslide and its double consolidation dam ($\approx 100m$ wide, from left to right bank wings), Ravoire de Pontamafrey torrent (73) Fr., construction: 1968-1970 (photo Nov. 1979 by JL. Boisset courtesy of ONF-service RTM 73)

By creating a wider valley floor, sometimes with a milder slope, massive deposits occur and

flows increasingly tend to shift laterally and erode banks, thereby requiring new planar stabilization structures or dredging operations on the consolidation dam backfilling area (Delsigne et al., 2001). Therefore strong elevation of a torrent profile, and these undesirable secondary effects, must be justified by a clear limitation of key sediment sources' activation; otherwise, simple stabilizations are easier to maintain (see regulation function for the problem of excessively high check dams).

Elevating a stream bed may however have strong geomorphic effects. They may propagate on the upstream fluvial network by backfilling, while the related sediment trapping usually generates a transient downstream sediment starving (Heede 1986). In addition, depending on the geological availability of stable locations suitable for high structures' building, and on the spatial extension of the unstable hillslopes, consolidation may be achieved by a few high structures (Fig. 1.7), or by check dam series that gradually elevate the profile and look like stabilization check dam series (Fig. 1.8). Bed stabilization and hillslope consolidation are very similar and thus regularly confused. The authors propose the following distinction: even if they could be built at the level of the existing torrent beds to achieve their main stabilizing function, stabilization check dams are generally built *slightly* (few meters) above the torrent beds for multiple reasons: construction ease, seeking of secondary effects of bank consolidation and decrease in slope; but overall the bed is fixed at its current position. On the contrary, consolidation dams are built *specifically* to elevate the bed profile (up to dozens of meter, *e.g.*, 50-m for the Illgraben landslide consolidation dam, Wallis, CHE - Eisbacher, 1982, or 33 m in the Riou Bourdoux case, Fig. 1.8), in order to re-fill the incised valley and slow down the activity of a *nearby important* sediment source.

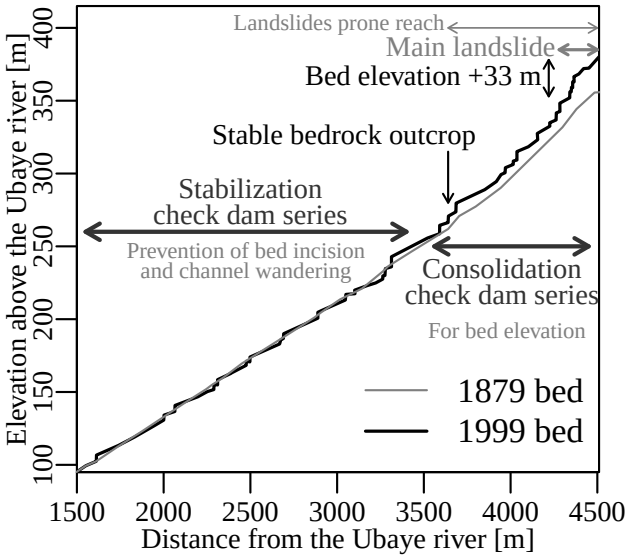

Figure 1.8 – Longitudinal profiles of the Riou Bourdoux torrent (Barcelonette, FRA.) in 1879 before check dam series construction, and in 1999 with check dams: in the downstream part, the check dams series stabilize the bed at its former location, on the contrary the upstream part, prone to landslides, is equipped with a consolidation check dam series, which gradually elevate the bed up to 33 m above the initial bed at the toe of the most active landslide (adapted from Demontzey 1882 and Delsigne et al. 2001)

1.3.3. Decreasing slope

Check dams can often reduce the slope of the upstream reach. In most torrents, the initial slope is not a graded alluvial slope (*sensu*, Lane, 1955). It is most of the time caused by an armoring made of coarse elements brought by colluvial processes such as avalanches, rock falls, and landslides or even by bedrock channel erosion. This bed, often paved by boulders seldom moved by the torrent activity (Recking et al., 2012a), is generally steeper than the alluvial equilibrium (Gras, 1850). Given that most check dams are built above the initial bed level, their upstream reaches are subsequently sediment-filled by flood transported material, *creating an alluvial section in a colluvially influenced environment* (Piton and Recking, 2016c). This newly formed alluvial section develops a slope that is necessarily milder than (or at least equal to) the initial non-alluvial slope (Fig. 1.9). This feature interests torrent control works because a lower slope generates lower energy flows, diminishing (i) flow velocities (decrease of Froude numbers and problems related to hydraulic jumps, highly erosive phenomena), (ii) bank erosions, (iii) armor breaking, (iv) sediment transport, and (v) displacement of very large boulders prone to break the structures, to jam in a narrow section and likely to aggravate the downward erosion by destabilizing the bed armor. This outcome is emblematically illustrated by large boulders, originally recruited in the channel or from the hillslope and finally not transferred down to the fan, that are found at rest on check dam crests (Fig. 1.10).

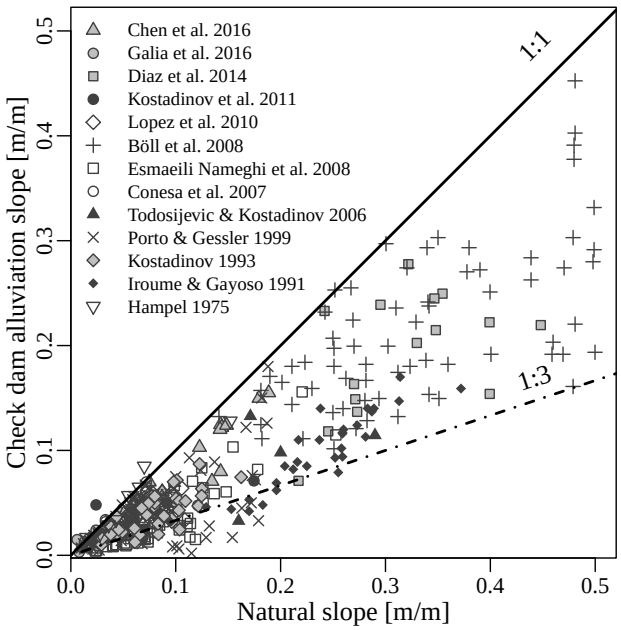

Figure 1.9 – Comparison between initial natural channel slope and alluvial slope measured upstream of check dams illustrating the general trend to decrease in a field dataset (428 data, after Hampel, 1975; Iroume and Gayoso, 1991; Kostadinov, 1993; Porto and Gessler, 1999; Todosijević and Kostadinov, 2006; Garcìa et al., 2008; Böll et al., 2008; Esmaeili Nameghi et al., 2008; López et al., 2010a; Kostadinov et al., 2011; Dìaz et al., 2014; Chen et al., 2016; Galia et al., 2016)

Figure 1.10 – Huge boulder stopped on the check dam series of the St. Antoine torrent upper basin (73 – FRA.) – 2014 (photo courtesy of S. Carladous)

1.3.4. Retention

The filling of the upstream reach durably traps sediments (Fig. 1.3 & 1.5d). This function is a side function of all check dams whose spillway crest is set above the initial bed. Nevertheless, some structures, called retention check dams, are built specifically to trap a maximum amount of sediment in their backfilling reach (Fig. 1.1).

This long-term trapping creates sediment starvation downstream of the dam with multiple consequences (Brandt, 2000). Once the structure has been filled up to the crest, additional check dams are eventually built near the main structure crest to continue the filling of the upstream thalwegs. Structures specifically dedicated to the retention function have preferentially been built in areas where a limited bed elevation would trap a maximum sediment volume. Perfectly aware that this solution was not sustainable (Wang and Kondolf, 2014), the original designers Breton (1867) stressed that complementary solutions designed to stabilize the sources were necessary in addition to this last-resort and short-term, although highly efficient, counter-measure. The advent of earth-moving machinery has made it possible to dredge the structures after each strong flood (Dodge, 1948; Van Effenterre, 1982), making new high-retention check dams quite rare. This concept of total trapping is far from the current concept of promoting sediment continuity, but it can explain the existence of old high check dams in some Alpine valleys.

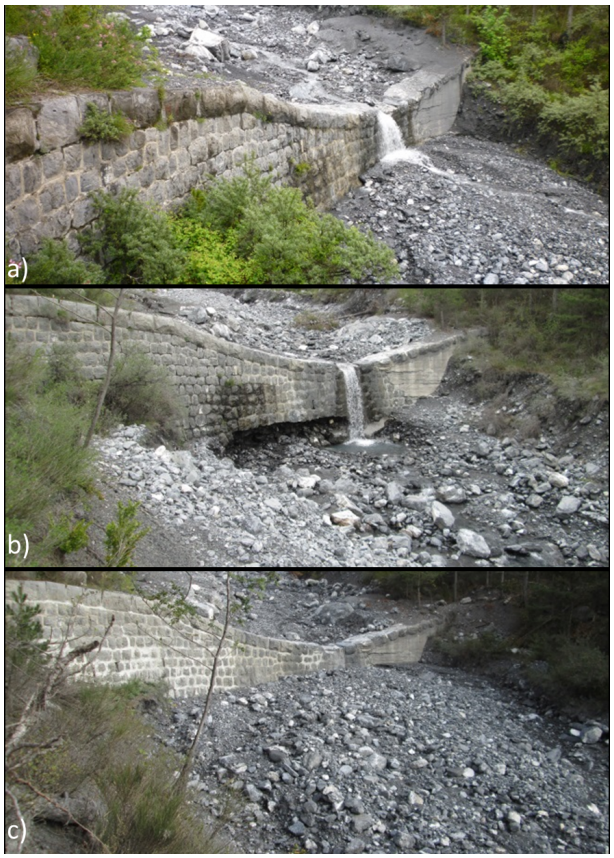

Figure 1.11 – Observations of sediment buffering downstream of a 5-m-high check dam in the Bourdous torrent (06 – FRA.): a) May 2013; b) May 2014 and; September 2014 (photos courtesy of K. Royer - ONF-service RTM 06).

1.3.5. Sediment transport regulation

Check dams regulate sediment transport (Fig. 1.11). Torrent beds show natural fluctuations in grain size distribution, lateral location, and level, i.e., in sediment storage (Church and Ferguson, 2015). Field observations of sediment stock fluctuations at check dam toes are numerous (Fabre, 1797; Jaeggi, 1992; Poncet, 1995; Glassey, 2010; Astrade et al., 2011; Theule et al., 2012; 2015). These fluctuations are natural in the sediment cascade (Fryirs, 2013) and may be influenced by the hydrology, the sediment (dis)connectivity, sediment grain sizes, and sediment-transport-autogenic fluctuations (Jerolmack and Paola, 2010). The creation of fixed points in the longitudinal profile of torrents makes the upstream part of the torrent independent of the fluctuations of the downstream part (no more headward propagating erosion). These independent compartments store and release sediment, creating buffer areas between dams (Jaeggi, 1992). Inter-check-dam reaches store sediments during sediment-laden flows and release them subsequently during clearer flows. Check dams thus change the dynamics of sediment storages and release related to the continuous exchanges between the flow and the bed (Recking, 2014). This trend led Poncet (1995, p. 713) to think that check dams are useful in torrent hazard protection because "*they release in small doses what the torrent would abruptly transport in a single massive dose.*" This buffer effect has been demonstrated experimentally by Piton and Recking (2016c).

Even if this effect can probably be observed on all structures, it is often considered a side ef-

fect. However some check dams are specifically designed to maximize it (Fig. 1.5e), *e.g.*, the three first modern torrent control check dams built in France were designed by Scipion Gras in 1851 in the Roize torrent (Voreppe), specifically to promote sediment transport regulation a short distance upstream of the fan apex (Gras, 1857; Culman, 1865). Open check dams with a "dosing" objective play a similar role but are much more sensitive to floating material influences than check dam series (Piton and Recking, 2016b).

Gras (1857) conceded that sediment transport regulation also occurs in fan channels equipped with check dams. Precaution must be taken in these contexts. A fan channel should be as deep as possible to absorb and efficiently transfer floods and sediment supply to the downstream channel network. Transversal structures seeking to stabilize the bed thus must not be built over, but at the bed level, thus more being "bed-sills" or "chute structures" rather than check dams (Dodge, 1948). Moreover, their crest spillways should not be too wide (*e.g.*, compare Fig. 1.5(a) and (e)) because flow spreading promotes deposition and, incidentally bed shifting, which overall would dramatically increase avulsion hazards and uncontrolled fan flooding. Not taking this into account lead some check dams, that were built above the bed on fan channels, to be subsequently voluntarily destroyed (Boscdon torrent, Les Crots 05, FRA.: one check dam taken off in 2004; Piezan torrent, Cons St Colombe 74, FRA.: one check dam taken off in 2014; La Salle torrent, La Salle Les Alpes 05, FRA.: three check dams taken off in 2016), costly experiences that we must keep in mind.

1.4. Discussion

1.4.1. Torrent control in other countries

Damage and casualties related to mountain streams and debris flow prone torrents occur on all continents and have generated human interventions to limit their related damage for ages (Skermer and VanDine, 2005). The next paragraphs do not seek to be exhaustive; the topic would worth complete books. However, having a look on the history of other countries where modern torrent control experienced its pioneering period is interesting because it helps to understand some cultural similarities and differences in the varied ways to approach torrent control. Additionally, such syntheses are usually available in local country languages but seldom available in English for an international readership.

A. Italy

Deforestation consequences on soil erosion and lack of woody material, have been reported since the Roman period in Italy (Hughes and Thirgood, 1982; Comiti, 2012). The theory underlying torrent control (stabilization of sediment sources, stream erosion limitation, and solid transport diminution) was developed, at least from the late 17th century in an already very active Italian scientific community. The 1877 law on reforestation was considered exemplary in its restoration approach (Hall, 2005, p. 40), although it was not followed by as many works as expected (Fesquet, 1997 p. 315, Hall, 2005 p. 51 & 74). Italy and France share the southwest of the Alps. The lag time between Italian and French public investment in torrent control likely had a combined historical and political origin: heavy land use management is older in Italy than in France. It was the rapidity of the degradation, making it more obvious and worrying, which made the French engineers and policy makers more prone to take ambitious decisions (Marsh, 1864, p. 237). Additionally, country-scale laws were more easily taken in the French authoritarian and unified regime than in the Italian fragmented political powers and technical services (Marsh, 1864, p. 217; Fesquet, 1997 p. 177) before the 1861 Italian unification.

However, some regions, notably the western Italian Alps close to the French border, concentrated large torrent control works (reforestation

and check dams) since 1869 (Hall, 2005, Chap. 2). Torrent control works were also implemented in Tyrol as early as 1841 (Marchi and Cavalli, 2007), as well as in Slovenia (Logar et al., 2005), i.e. in regions, at that time, under the control of the Austro-Hungarian Empire, thus fields of Austrian engineers.

B. Austria

The ideas of the aforementioned French authors had previously emerged in Austria (and also possibly elsewhere) within the works of von Zallinger (1779), von Aretin (1808) and Duile (1826; 1841). Austrian decision makers did not immediately seem to take into account at the Austrian scale their pioneer recommendations. It was only after the 1882 dramatic flood events that torrent control implementation at the Austrian scale was decided, partially based on the French model (Zollinger, 1984a; Patek, 2008). Austrians rapidly became experts in torrent control and spread their knowledge in Europe and farther, for instance as far as Japan under the influence of Amerigo Hofman (Zollinger, 1984a; Luzian et al., 2002; Okamoto, 2007).

C. Switzerland

Retention basins dedicated to trap sediments were created as early as the late 1840s to protect railways in Switzerland (Vischer, 2003). They inspired Demontzey and were used, for instance, on the Palles and Merdaret torrents (Chantelouve 38, FRA. – Bernard, 1927). The first check dam series built in an accurately defined torrent control system in Switzerland was due to the aforementioned Austrian engineer Josef Duile (1776-1863), who designed the Rüfirunse correction in Mollis (Duile, 1841). Several other operations were implemented following this example (Vischer, 2003, Chap. 12). The Culman report 1865 was a country-scale assessment of the need for torrent control works. Its author stressed the necessity to complete check dam constructions with complementary works (hillslope stabilization and reforestation) to seek a complete correction of watersheds. A great number of works were performed following the 1876 law on torrent control (Vischer, 2003, Chap. 15) and contributed to making Switzerland a leading country in mountain hydraulics.

D. Japan

Sediment transport-related hazards are a huge problem in Japan (JSA, 2003). The country has thus an ancient culture of torrent and erosion control with regulation on deforestation at least since the 7th century, river training since the 16th century and "SABO" operations, i.e. coping with sediment related problem, since the 17th century (JSA, 2003). Some check dams built *ca.* 1700 A.D. in the former Fukuyama domain (Hiroshima prefecture) are, for instance, still in good state (Okamoto, 2007). Collaboration with European and American civil engineers began during the late 19^{th} century (Okamoto, 2007; Kamibayashi, 2009). It continued in the early 20^{th} century, for instance with the Austrian expert Amerigo Hofman, while Japanese engineers came to Austria, *e.g.*, Shitaro Kawai in 1871 and Otokichi Watanabe 1877 or Moroto Kitaro in the early 20^{th} century (J. Hübl and A. Nishimoto, *pers. com.* 2015), and France (Nishimoto, 2014) to be trained in hydraulics and forestry engineer schools and visit torrent control works, bringing back European techniques that partially inspired some works in Japan (Wang, 1901, p. 474; JSA, 2003, p. 16). The Japanese developed their own specific mitigation measures adapted to higher magnitude events due to heavier rainfall (typhoons), the influence of volcanic geology (modifying the debris flow rheology; lahars) and more regular occurrence of landslide dam outburst floods (Schuster, 2000; JSA, 2003; 2012). Japanese later went, and continue to go, to other countries to help torrent hazard mitigation implementation (JSA, 2003, p. 106; Skermer and VanDine, 2005; Lin et al., 2010) while their scientific researches continue to be very active.

E. North America

European techniques of restoration and torrent control were brought back to America by authors such as George Perkins Marsh (1801-1882), who confessed that German, Italian and especially French theories of mountain land restoration strongly influenced him (Marsh, 1864, p. 217; Hall, 2005, p. 41). North American experiences of erosion control more generally have focused on soil bioengineering than on large scale civil engineering (Hall, 2005, Chap. 3; deWolfe et al., 2008). Gully system stabilization has used small check dams made of wood and cobbles (Heede, 1960; 1978; 1982). Some high structures intended to stabilize stream beds and retention check dams were used in the mid-20^{th} century in California, the American debris flow hotspot (Skermer and VanDine, 2005). Both mechanically dredged debris basins and definitive retention check dams were built (Dodge, 1948; Ferrell and Barr, 1965). However, the former are much more used than the latter (VanDine, 1996; M. Church, *pers. com.* 2015; O. Hungr, *pers. com.* 2016).

1.4.2. Toward a comprehensive analysis of torrent control work effects

After the functions' definition, the next steps toward a comprehensive analysis of the effects of check dams, and torrent control works more generally, on mountain stream hazards are briefly reviewed in the next section(Fig. 1.12): namely, effect quantification, effectiveness and dependability assessment and, finally, risk analysis and efficiency assessment, and of their respective research challenges.

A. Quantifying each functional effect on torrent hazards

Natural hazard assessments are determined through multidisciplinary studies basically determining (Mazzorana et al., 2012) i) which kinds of phenomena eventually occur in the catchment, ii) at what magnitudes and frequencies and, iii) to what extent (hazard mapping). Within a given catchment, protective actions such as check dams aim to modify hazard from its baseline, i.e., hazard in a natural structureless catchment. This hazard modification should be quantified through the modification of the probability of some phenomena to occur with a given magnitude (*e.g.*, volume released, solid discharge, transported boulder size). Consequently, for each identified function, some methods to determine how much the structure modifies the flood phenomena should be used. It is usually referred to as a structure functional capacity estimation: its measurable ability related to a function (Tacnet et al., 2012).

The literature contains some methods for evaluating check dam effects on slopes (Kostadinov, 1993; Porto and Gessler, 1999; Ferro and Porto, 2011; Kostadinov and Dragović, 2013), as well as preliminary results concerning landslide - check dam interactions (Nicot et al., 2001) or solid transport regulation (Remaître et al., 2008; Astrade et al., 2011; Remaître and Malet, 2013; Piton and Recking, 2016c). However these topics need complementary researches in order to correctly estimate the structures capacities.

The stabilization and retention capacities of structures are strongly related to the stream bed topography (longitudinal profile and valley width) in conjunction with: i) the potential erodibility (Hungr et al., 1984) and general bed incision trends (Hungr, 2005; Takahashi, 2014) in the reaches influenced by the structure for stabilization capacity assessment and; ii) general catchment sediment production for the time duration of retention capacity assessment (Recking, 2012; SedAlp, 2015a). These two subjects present some technical issues (Liebault et al., 2013).

A general review of the available methods to use in functional capacity assessment is worth doing (deWolfe et al., 2008) with a fair look at scale change from the structure to the watershed,

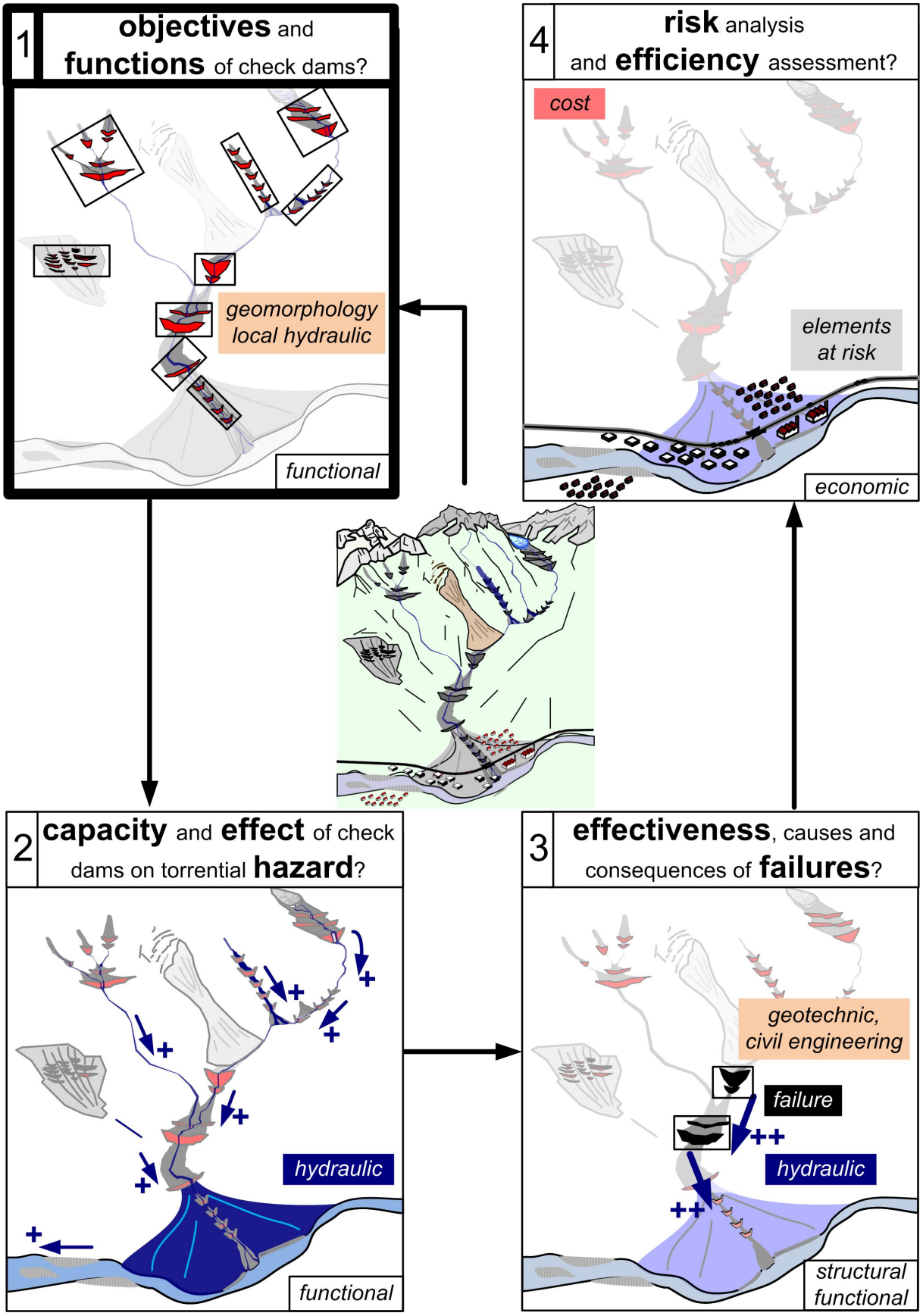

Figure 1.12 – the next steps to address for completion of a comprehensive and integrative analysis of torrent control works effects on mountain stream hazards and to help maintenance decisions taking into account functional, structural and economic aspects

applicability of methods and uncertainties in the results.

B. Effectiveness analysis and potential failure consequences

Torrential hazards generally occurring within the sediment cascade, capacity assessment methods must be able to take into account the effect of the whole check dam series on the hazard modification (*e.g.*, Remaître et al., 2008). Namely, a potentially complicated exercise of data synthesis must be done once i) the complete catchment study has been performed, ii) the structures' functions have been identified, iii) their respective expected effects on hazards (capacities) determined, and iv) their structural and functional potential failures identified. This work will conclude to the check dams' functional effectiveness, i.e., to an estimation of the beneficial effects of the structures, compared to what could be technically expected from them (reaching the level of an objective, AFNOR, 2001).

Effectiveness assessment must also consider potential structure failures. It is worth stressing that check dam failures are most of the time not considered as heavily aggravating hazards, even after cascade failure of a complete check dam series (Jaeggi and Pellandini, 1997; Wang, 2013; Chen et al., 2015). However the 1996 Aras disaster near Biescas (Central Pyrenees, SPA.), where eighty seven people died on a campsite, is an important counterexample of dramatic consequences related to the failure of 35 check dams of a 40-dam series (Garcìa-Ruiz et al., 1996; Benito et al., 1998). The lack of correct maintenance of some structures is increasingly pointed to as a potential source of additional hazards (Sodnik et al., 2014) and other equivalent situations are likely to be expected.

Field feedbacks, notably from specific disasters that are meaningful case studies (*e.g.*, Aras 1996) or from the existing structure management database (Dell'Agnese et al., 2013; Carladous et al., 2014a), can help to analyze failure modes (Vuillet, 2012), their related effects, and later proposing possible preventive actions. For instance, a retention check dam does not retain (function) the expected volume of sediments (capacity) because it is laterally by-passed (functional failure mode) or because it is ruined (structural failure mode) (Tacnet et al., 2012; Carladous et al., 2016b). These failure modes have been studied in various works (*e.g.*, Rudolf-Miklau and Suda, 2011; 2013; Comiti et al., 2013) that would also be worth a comprehensive review, which in a second step will help to provide recommendations in structure design (*e.g.*, Bergmeister et al., 2009; Suda et al., 2010; Rudolf-Miklau and Suda, 2013).

In sum, further works are still needed to propose complete methods aiming to combine the information on the capacities and potential failures of structures, to a structural and functional point of view, in order to provide catchment scale effectiveness assessments.

C. Risk analysis and efficiency assessment

The fourth step for quantifying the potential effects of check dams would likely be to estimate the structures' efficiency (AFNOR, 2001), i.e., to compare their effect on hazards and associated risk with the resources used (*e.g.*, maintenance cost) to help decision makers in land use and structure management. Implementing complete hazard and risk analysis with structures needs to take into account their expected functional effect, but also potential negative effects such as sediment cascade disconnectivity (Fryirs, 2013) and consequences of structure failures. Moreover risk evaluation (Tacnet et al., 2014b) must integrate excessive decrease in risk perception after check dam implementation (Eisbacher, 1982; White et al., 1997). Comparing several alternatives to choose which one is the more relevant to implement is a complicated decision problem.

Decision-aid methods such as Cost-Benefit Analysis (CBA - more adapted to compare investments), Cost-Effectiveness Analysis (CEA - more adapted to compare maintenance scenarios), Multi-Criteria Decision Analysis (MCDA – able to take into account damages on domains hardly monetarized, such as environment and health) have been applied to natural hazards since the 1990s (Gamper et al., 2006; Carladous, 2013). They aim to compare alternatives through aggregation of several criteria (Schärlig, 1985). CBA application tools have been notably developed in Switzerland (Greminger, 2005; Bründl et al., 2009) and in Austria (BLFUW, 2009). In France, CBA was first tested on the Saint-Antoine torrent (Modane, 73 - Verrier, 1980) and then on the Manival torrent (St Nazaire les Eymes, 38 - Brochot et al., 2003), demonstrating dramatic lack of sufficient data for correct application in torrent hazard contexts, a general problem in torrent hazard studies (Poncet, 1975). Conversely, it is used in lowland river flood problems (Erdlenbruch et al., 2008) which are less complex.

To make the decision problem on maintenance of existing structures even more complicated, the decision context has changed over time since the 19^{th} century (Carladous et al., 2016c): i) Exposed elements have evolved from a native permanent population to a touristic temporary one (de Crécy, 1983; Brugnot, 2002; Comiti, 2012); ii) torrent activity and catchment morphodynamics have changed due to spontaneous or planned reforestation or to the implementation of check dams which fundamentally impact upon the geomorphic functioning of landscapes; iii) new alternatives to old torrent control techniques emerged with the advent of earth-moving machinery (*e.g.*, direct torrent bed mechanical dredging) and open check dams (Piton and Recking, 2016a; 2016b); and finally iv) the importance of the sediment cascade and continuity within the river system is now better understood and is taken into account in various policies, *e.g.*, within the European Water Framework Directive (EU, 2000).

Consequently mountain stream morphodynamics continue to be worthy of investigation, at least in order to provide the necessary data for the implementation of decision aid methods in changing climatic, biological, technical and societal environments.

1.5. Conclusion

Thousands of alpine torrents are equipped with check dam series. As their maintenance is very expensive, one can question their effectiveness to reduce risk and could be tempted to abandon old structures. This is also often discussed as a solution to reactivate sediment stocks trapped and stabilized by torrent control works (Bravard, 1991; Liébault et al., 2008; Pont et al., 2009; Rinaldi et al., 2011). However, to decide maintenance strategies, it is of utmost importance to be aware of their effect on morphological processes. These effects are assessed conceptually through their functions, and quantitatively through their capacity, this, at the structure and the catchment scales. Comparing their effects with given objectives helps to assess their effectiveness, whereas their costs aid assessing their efficiency.

In some cases, abandonment may be justified because the original risk (related to morphological process and exposed elements) that the structure was intended to remedy no longer exists: *e.g.*, structures used to be built to protect agricultural areas or villages that are now abandoned. In other cases, the removal of such a structure could be catastrophic in terms of risk mitigation, because it has been so effective over time that we have simply forgotten their function, i.e. why the structure was built in the first place. Our present expectation of the structure's functions can also be complicated by changes in the socioeconomic and environmental contexts (Dufour and Piégay, 2009; Carladous et al., 2016c): for instance, our understanding of sediment continuity processes has evolved, and many watersheds have been sponta-

neously or artificially reforested since the structures' construction.

The review and historical analysis of French developments presented in this paper should be helpful for closing this gap. The main check dam design and functions are recalled and summarized in Table 1.1 and Figure 1.5. This summary may not be exhaustive and we must keep in mind that most of structures may play several functions, sometimes through complex secondary effects (*e.g.*, Fig. 1.4). However, the authors believe that it offers a useful framework to define the potential effects of a given structure considered in the current environment and with regard to the recent catchment history.

In a complementary section, the next steps toward a comprehensive analysis of torrential hazard and check dam efficiency have been discussed. Several research topics worthy of further investigation have thus been stressed throughout this paper.

From a broader geomorphic point of view, modern and future river system management must take into account sediment transport dynamics (EU, 2000), which requires sufficient comprehension of the watershed sediment cascade (Church and Ferguson, 2015). The description of the latter must take into account the multiple human impacts on mountain streams (Wohl, 2006), and especially the sediment cascade "*barriers*" and "*blankets*" (*sensu.* Fryirs, 2013) created by check dams and their side effects. The present review will hopefully help geomorphologists to determine how the structures may influence catchment dynamics, to extend their approaches correctly to take into account this influence; and to determine to what data and proxies they must pay attention to correctly grasp the subtle and multiple geomorphic roles played by check dams.

Acknowledgments

This study was funded by Irstea, the French Agricultural and Forest Ministry, the French Environment Ministry, the INTEREG ALCOTRA European RISBA project and the ALPINE SPACE European SEDALP project. The authors would like to thank Stuart LANE for his helpful comments on several previous versions of this manuscript; Sebastian SCHWINDT for his help with German works; Johannes HÜBL, Mike CHURCH, Stefano CREMA, Oldrich HUNGR and Haruo NISHIMOTO who provided information on torrent control in Austria, North America Italy and Japan; Mike CHURCH for an additional thoughtful and precise review; as well as the constructive comments of the AE Fiona KIRKBY, of Francesco COMITI and of an anonymous reviewer.

"If I have seen further, it is by standing on the shoulders of giants."

Bernard de Chartres, 12th century.

Here are synthesis of giants' works.

CHAPTER 2

Design of Sediment Traps with Open Check Dams. I: Hydraulic and Deposition Processes

Guillaume PITON[a], Alain RECKING[a]

[a] Université Grenoble Alpes, Irstea, UR ETGR, St-Martin-d'Hères, France.

This chapter is the first part of two yet published companion papers[1].

It aims at summarizing the state of knowledge concerning hydraulic and sediment transport processes that occur in open check dam basins. This constitutes the foundation of the subsequent researches presented in this thesis. Chap. 3, its companion paper, addresses the same question but for woody debris. The scientific gaps that remains are stressed, and three of them have been addressed in subsequent works treated in Chap. 4, Chap. 6 & Chap. 7.

NOTA: The additional notes brought to this chapter since its journal publication are highlighted in grey.

[1]Piton, G. and A. Recking, **(2016)**. "Design of Sediment Traps with Open Check Dams. I: Hydraulic and Deposition Processes", *J. Hydraul. Eng.* ASCE, Vol. 142, no. 2, 23 pp., DOI:10.1061/(ASCE)HY.1943-7900.0001048

Abstract

Sediment traps with open check dams are widely used structures in flood hazard mitigation. This paper reviews the literature dedicated to their design. First, the general context in which sediment traps are built and their functions are presented. The second part proposes hydraulic design criteria for classical types with details on the opening shapes and dam crest spillway. The third part details sediment deposition dynamics: its initiation, its controls through the trap basin and open check dam shapes, the effect of hydrographs and the control of trap self-cleaning. The methods to determine the deposit slope and height are discussed. To finish, a step-by-step design procedure is proposed and future research challenges are highlighted. Field feedback has shown that driftwood can substantially influence sediment trap behaviour. A companion paper thoroughly covers the production and transfer of driftwood and the interactions with open check dams.

Author key words: *bed-load trap, debris flow basin, torrent hazard mitigation, torrential barrier*

2.1. Introduction

"Sediment trap" is a common term used in very different contexts. Farmers throughout the world have built small sediment traps in erosion-sensitive agricultural areas to protect rivers from suspended load and related pollution (*e.g.*, Zaheer et al., 2003). Suspension and bed load are major threats to the duration of dam reservoirs (Julien, 1998; Morris et al., 2008), some of them are therefore equipped with sediment traps. In lowland gravel bed rivers, natural and anthropogenic discontinuities in sediment transport capacity sometimes make it necessary to trap sediments and dredge them to prevent aggradation and flood hazard aggravation (*e.g.*, Cazaillet et al., 2008). In steep slope streams, this type of facility has become even more crucial when debris flows and hyperconcentrated flows are likely to occur. In this case, retention basins are built on alluvial and colluvial fans (Zollinger, 1983) or even upstream in steep slope mountain channels to break the energy and erosive power of debris flow surges (*e.g.*, Mizuyama et al., 1996; Rudolf-Miklau and Suda, 2013).

This paper investigates the hydraulic design of sediment traps that aim to trap bed-load transport (pebbles, cobbles and occasional boulders), possible debris flow surges and driftwood in mild and steep slope streams. The characteristic components of these traps are illustrated in Fig. 2.1. A sediment trap comprises a basin and an outlet structure hereafter called an open check dam. Depending on the site configuration, designers add lateral dykes and an inlet structure, often a grade control structure, hereafter referred to as a solid body dam.

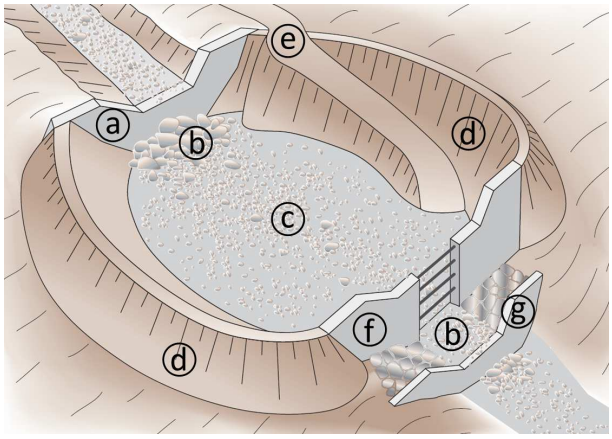

Figure 2.1 – Characteristic components of a sediment trap with an open check dam: a) inlet structure: solid body dam, b) scour protection, c) basin, d) lateral dykes, e) maintenance access, f) open check dam, g) counter-dam (adapted from Zollinger 1983, with permission)

Human structures placed on fans are morphologically threatened over the short and long terms, especially where watersheds and channels continue to be morphologically active (Schumm and Harvey, 2008). In steep slope areas, where morphological changes are characteristically short and abrupt, torrential hazard mitigation is still an important issue and new protection methods are constantly being developed (Mizuyama, 2008).

Various methods and techniques have been used in torrent mitigation projects (Van Effenterre, 1982; Heumader, 2000; Chanson, 2004; IRASMOS, 2008). For instance in France, torrent hazard mitigation began during the second part of the 19^{th} century with forestry engineers who theorised and managed watershed-scale projects. They undertook large headwater reforestation plans aiming to curtail sediment production in active gullying areas and stream-bed stabilisation operation using series of solid body dams (Surell, 1841; Gras, 1857). Older structures have been reported in the literature but remain rare, *e.g.*, in 1537, a dam was built upstream of Trento, Italy (Armanini et al., 1991), as was a dam series around 1697 in the Fukuyama domain, Japan (Okamoto, 2007). Vischer (2003) reported that the first Swiss deposition basins aiming to trap sediment were built in the 1840s, nearly at the same time as the first check dams, hereafter referred as solid body dams (Fig. 2.2*i*). At that time, a filled sediment trap had to be dredged manually or abandoned. Such facilities were used only in specific cases and as a last resort. Upstream bed stabilisation works or reforestation were preferred (Van Effenterre, 1982). Nowadays, earthmoving machinery can easily dredge filled traps, while it has become complicated and expensive to maintain difficult-to-access structures or to undertake extensive reforestation programs.

After first tests and trials during the 1950s and the 1960s, (Reneuve, 1955; Clauzel and Poncet, 1963), or even before in California (Dodge, 1948), sediment traps with open check dams grew in number during the 1980s and the 1990s. For instance in France, the number of traps managed by the French Torrent Control service increased from 21 in 1970 to 176 in 1996 (Gruffaz, 1996). This great increase in the number of works triggered a need for design criteria (though some quite detailed guidelines were ever due to Dodge, 1948). During the 1980s, various researchers published articles on open check dams, including general papers presenting this kind of structure (Van Effenterre, 1982; Johnson and McCuen, 1989) and basic design criteria specifying the dimensions necessary for outlet openings (Watanabe et al., 1980; Senoo and Mizuyama, 1984; Mizuyama, 1984; Ikeya, 1985; Mizuyama et al., 1988; Ikeya, 1989). In his pioneering work, Zollinger (1983; 1984b; 1985) proposed descriptions of trap filling based on Froude-scale analogue models and descriptions of the existing wide variety of different outlet structures in Europe. During the 1990s, authors continued to stress the advantages of open check dam sediment traps. Papers were published concerning the structures' objectives and complementary design criteria (*e.g.*, Armanini et al., 1991; Chatwin et al., 1994; Poncet, 1995; Deymier et al., 1995; VanDine, 1996; Mizuyama et al., 1996). Since 2000, authors have detailed what can be expected from open check dams in watershed-scale hazard mitigation plans. These plans have to be adapted to each site with its own specificities (Leitgeb, 2002; Hübl and Suda, 2008); therefore, a single universal relevant structure shape does not exist. In addition, feedback from the field has brought out the need to pay particular attention to the effect of driftwood. Complementary approaches designed for this problem have been developed (Kasai et al., 1996; SABO Division, 2000; D'Agostino et al., 2000; Bezzola et al., 2004; Lange and Bezzola, 2006; Koulinski and Richard, 2008). Complementary to field and small-scale models, numerical approaches have been and are being developed to model sediment and driftwood deposition processes (*e.g.*, Busnelli et al., 2001; López et al., 2010b; Shrestha et al., 2012; Campisano et al., 2014). More recently, some authors and government entities have at-

tempted to propose design standards[1] (Ono et al., 2004; ONR24803, 2008; ONR24800, 2009; Suda et al., 2010; ONR24802, 2010; ONR24801, 2013; Osanai et al., 2010; Rudolf-Miklau and Suda, 2013), but they mainly have focused on civil engineering aspects rather than hydraulics and sediment transport.

Torrential hazard mitigation converges at the border of very different technical and scientific domains such as applied geomorphology and geology, fluid dynamics, forestry and structural engineering. More than a century of empirical approaches made it possible for practitioners to adjust management technics of steep slope streams (Hübl et al., 2005; Fiebiger, 2008). Nonetheless scientific knowledge remains incomplete. This paper has gathered and compared the results of empirical approaches, feedback from the field and applications of open check dam hydraulic design. These studies have often been undertaken by joint teams of practitioners and researchers and have sometimes not yet been published in English.

This paper primarily reports a classification aiming to standardise the varied vocabulary used to describe structures, presents their objectives and describe their management. In the second part, the general hydraulic functioning of these structures is detailed, stressing the importance of each structural part. The processes leading to sediment deposition are then described. The existing design criteria are reported and a step-by-step design procedure is proposed. To finish the remaining gaps in today's knowledge are highlighted.

[1]Since the pioneering work of Dodge (1948) in the Los Angeles region, updated versions of debris basin design standards are regularly published (L.A. County, 1979; 2006). These "Californian Debris Basins" look like earth dams or urban rainfall retention basins, from which they are closer than from Japanese and European open check dams. They however constitute a tried and tested alternative. They sometimes have to cope with debris flows, especially after forest wild fires. In this case, adaptations to the L.A. County guidelines have been proposed by Prochaska et al. (2008).

Disaster feedback indicates that in addition to massive sediment releases, numerous flood problems occurring in steep slope streams are related to driftwood. In open check dams, driftwood management is often considered a key point (Bezzola et al., 2004; Lange and Bezzola, 2006). This subject required a detailed literature review and is treated in a companion paper.

2.2. General design considerations

2.2.1. Design input data

Prior to any mitigation measure design, a morphodynamic study is needed to better understand the catchment's behaviour (Mériaux et al., 2013). Details on the methods to use in this study are not within the scope of this paper. The following list is not exhaustive but reviews the main necessary data: types of solid transport processes likely to occur (bed-load, debris floods, debris flows, driftwood presence, etc.); the hydrology of the river and the related uncertainty (peak flows for different return periods, flood volumes and durations, etc.); catchment sediment production (grain size distributions, solid discharges and transported volumes); and downstream channel features and hydraulic capacity (IRASMOS, 2008).

The general design will be undertaken for a flood with a given probability, hereafter referred to as design-event (see Rudolf-Miklau and Suda, 2013, for details). A stronger flood, hereafter called the extreme-event, is generally used to design the spillway capacity (see below). The statistical return period of the design and extreme events are often set between 100 and 200 years and between 500 and 1000 years, respectively (VanDine, 1996; Böll et al., 2008; Rudolf-Miklau and Suda, 2013; CFBR, 2013). However, the probabilities of these events must be adapted to the local regulations and to the potential damage in the area to protect.

2.2.2. Denomination and classification

No universal name exists for sediment traps. In the literature, similar structures have been called debris / detention / deposition / sedimentation / retention / sediment retarding basins, sediment traps, open / slit check dams, SABO dams, torrential barriers, debris flow breakers. Any structure designed to manage bed-load / debris floods / debris flows and/or driftwood, made up of a transversal dam with an opening, is hereafter called a sediment trap in this paper.

Given that multiple shapes of open check dams have been tested by designers throughout the world, it is worth clarifying the main type of structures. Wehrmann et al. (2006) proposed a classification of structures depending on crest shape and opening dimensions (Fig. 2.2) that will be used throughout this paper and its companion. Other common names proposed in the literature will only be reviewed when first mentioned.

2.2.3. Objectives and functions

Consistency can be found between authors on the main functions of open check dams (Zollinger, 1985; Armanini et al., 1991; Fiebiger, 1997; Hübl et al., 2005). Open check dams can have the same function as solid body dams (Bernard, 1927): (i) *stabilization*: Fixation of the longitudinal profile of a torrent bed at a distinct elevation to stop incision and/or lateral erosion; (ii) *consolidation* : elevation of the longitudinal profile for the same purpose and to stabilise upstream hillslopes; (iii) *upstream slope reduction*: in order to reduce the flow erosive power and ability to transport boulders; (iv) *retention*: storage of water and/or deposition of sediment during an event aiming to reduce total transferred volume.

Complementary function are possible with the openings: (v) *sorting or sizing*: filtration and storage of undesirable components during an event (bed-load sizing and/or wood grading); (vi) *dosing*: peak flow modulation by temporarily retaining water/sediment, an effect obtained with a lower slope in the trap basin and/or the open check dam shape; (vii) *debris flow breaking*: reducing the high-energy level of a debris flow to a lower level (energy dissipation).

2.2.4. Location

Sediment traps are generally built near the fan apexes, where enough allowable surface exists close to human settlements and areas needing protection. Feedback from the field has shown that, downstream of the sediment trap, flows often consist of clear water with high erosive power. If the downstream channel is not naturally armoured or equipped with bank protection and ground sills, lateral erosion and incision will occur, reloading the watercourse with sediment (Breton, 1867; Brandt, 2000). The channel downstream of the trap has to be as short as possible to prevent this problem so that new protection structures will be less necessary.

Nonetheless, some open check dams, often referred to as debris flow breakers or torrential barriers, are built upstream in gorges or other adapted sites if accessibility and land use allow. Their purpose is principally to break debris flows energy. Debris flow tend to have a huge erosive and scouring effect, and to grow in volume and discharge during their propagation along the channel (Remaître et al., 2008; Remaître and Malet, 2013). Sometimes it can be more relevant to break their energy in the upper part of the catchment. An open check dam can be designed far from the fan, close to the reaches where debris flows initiate for this purpose.

The maintenance access to the basin is a key point in sediment trap management (Dodge, 1948; VanDine, 1996; Garcìa et al., 2008) because a lack of maintenance inducing lower mitigation efficiency often results from difficult access. Dodge (1948) also stressed the importance to choose a sediment trap location close to a suitable stor-

Shape parameters:
Dam height h_d
Opening height h_0
Opening width w_0
Solid part width w_S
Open structure total width $W_{os} = \Sigma(w_0+w_S)$
Narrow side of the opening $n_0 = \min(h_0;w_0)$
Long side of the opening $l_0 = \max(h_0;w_0)$

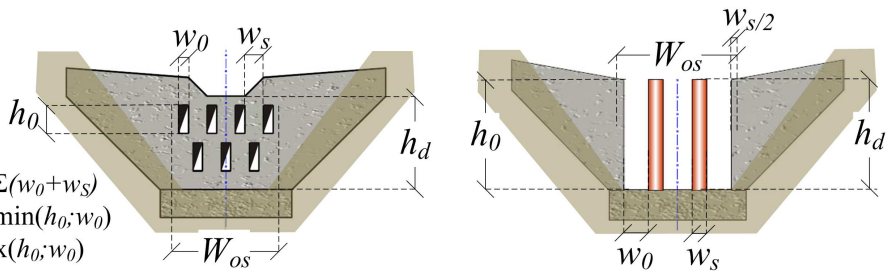

Structure class	Shape criteria	Shape examples	Subclasses (not exhaustive)
a) Solid body dam	No openings	i) Solid body dam	Single / Arched / Multiple Solid Body Dams
b) Compound dams	$h_0<h_d/2$	ii) Gap crested compound dam with triple slits; iii) Sectional compound dam with double fins	Depend on superior part type
c) Sectional dams	$\Sigma w_s < \Sigma w_0$ Several fins or piles	iv) Sectional dam with double piles; v) Sectional dam with double inclined fins	Inclined / Vertical – Open / Rake / Beam / Grill Dams with *n* Fins / Piles
d) Lattice dams	Built of bars	vi) Vertical rake dam; vii) Frame dam	Inclined / Vertical – Beam / Rake / Grill Dams – Frame Dams
e) Net Dams	Net is a functional part	viii) Net dam	
f) Slot Dams	$l_0<2n_0$	ix) Multiple small slot dam; x) Double large slot dam	Large / Small – Open / Rake / Beam / Grill Slot Dams
g) Slit Dams	$l_0>2n_0$	xi) Double horizontal slit dam; xii) Gap crested single slit dam	Gap crested / continuous crest – Single / Multiple – Horizontal / Vertical – Open / Rake / Beam / Grill Slit Dams

Note: If there are several openings in the dam body, the opening with the maximum height (h_0), width (w_0) or long side (l_0) is relevant for selecting the suitable dam classification. Further detail can be found in Wehrmann et al. 2006

Figure 2.2 – Wehrmann et al. (2006) classification with definition of shape parameters, main classes and sub classes of structures, shape criteria and examples (adapted from Hübl et al. 2005, with permission)

age area, *i.e.*, with a sufficient capacity to store the mechanically excavated material. Evacuating poor quality materials far from confined traps make their maintenance cost exploding.

In addition, whenever possible, direct access to check dam openings for earth moving machinery are necessary. This access is well worth the investment so that driftwood and boulders jams can be cleared from the open check dam to initiate the structure's self-cleaning (see below).

2.2.5. Basin shape

Observation of existing sediment traps shows that the basin shapes are mainly determined by local topographic constraints to limit levelling costs and the number of retaining walls to build. As a consequence, secondary currents sometimes result from basin curvature, influencing deposition patterns and driftwood accumulations (*e.g.*, Itoh et al., 2013).

If the allowable area is long and narrow, the creation of a sediment trap series is a good option (*e.g.*, Kaitna et al., 2011). Basins regularly adopted a pear shape (Zollinger, 1983; VanDine, 1996). A large inlet side with a narrow outlet side tends to maximise sedimentation. On the contrary, a narrow inlet side with a large outlet side promotes self-cleaning (Zollinger, 1985).

For structures with an expected self-cleaning trend, Mizuyama and Fujita (2000) suggested that deposit areas be prepared not only upstream but also downstream of the open check dam.

2.2.6. Bottom outlet

To limit mechanical excavation and maintenance costs, it can sometimes be advantageous to design structures able to transfer, with a minimum trapping effect, low floods unlikely to threaten downstream areas. Within this objective some sediment traps have an open bottom outlet (Figure 2.3a & b).

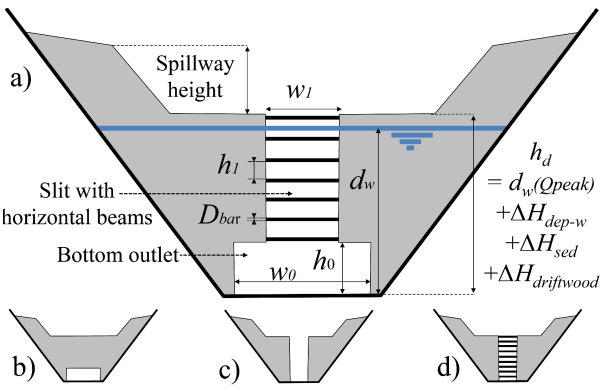

Figure 2.3 – Definition of shape parameters for water stage-discharge equation; example of a) a slit dam with horizontal beams and a slot as the bottom outlet, b) a slot dam, c) a slit dam and d) a slit dam with horizontal beams (adapted from Zollinger, 1983, with permission)

Its hydraulic capacity must be adapted to each site's specificities and to potential damage for all flood magnitudes. For instance, in their case-studies, Rimböck (2004) and Jordan et al. (2004) both proposed bottom outlets able to transfer the 20-year-return-period flood with minor influences.

This structural part must be carefully studied; otherwise it can have unexpected consequences. See, for instance, Bezzola et al. (2004) for a case study reporting dramatic consequences related to a problem with the bottom outlet.

2.3. Hydraulics of open check dams

2.3.1. Hydraulic vs mechanical control

Two complementary approaches are generally considered in the design of open check dams: hydraulic and mechanical controls of deposits (Figure 2.4 - Armanini et al., 1991; Deymier et al., 1995; D'Agostino, 2006):

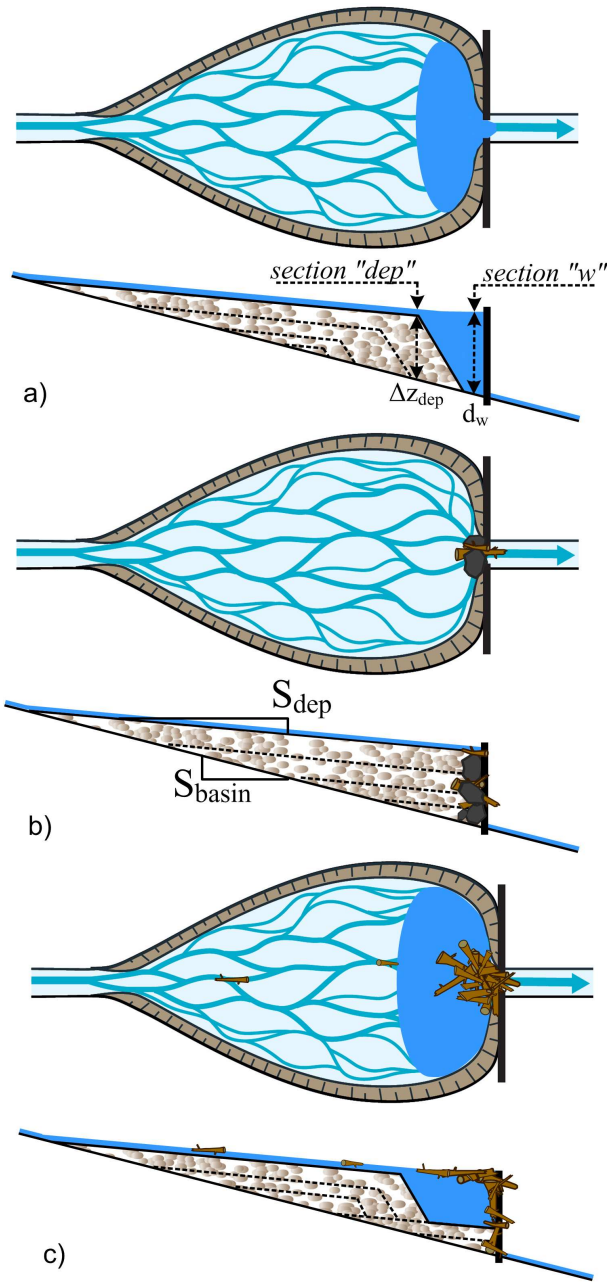

Figure 2.4 – Plan and longitudinal schemes of a) hydraulic control of the deposits: shear stresses collapse in tranquil water, b) mechanically controlled deposits: boulders and driftwood jamming leading to open check dam clogging, and c) mixed controlled deposits: mechanically blocked driftwood generates a calm water area and thus a hydraulically controlled deposit of sediments (adapted from Lange et and Bezzola 2006, with permission)

A. Hydraulically controlled deposits

Hydraulically controlled deposits are related to a decrease in shear stresses. This decrease often results from a head-loss induced by an obstacle to the flow (narrower dam openings when compared to the natural channel section or driftwood jam - Fig. 2.4a & c). The thus created calm water area, shows higher water depths and a lower energy-slope likely to induce a drop in flow velocities and shear stresses. As soon as these values fall under the threshold transport value, sediments tend to deposit. In a fixed section, the head loss is correlated to water discharge and is maximum at the flood peak, as is the trapping effect.This kind of control more generally concerns gravel and sand transport. Open check dams with large slits and slots characteristically use this control.

Such structures are almost completely transparent to small floods. Nonetheless, disaster feedback shows that, during extreme events, debris flows are sometimes able to clog several-metre-wide slits with a few large boulders (Fig. 2.5) or to create dense wood jams that can be higher than the dam structure (Masuko et al., 1996).

B. Mechanically controlled deposits

Mechanically controlled deposits are related to direct clogging of small openings when compared to coarse transported materials (Fig. 2.4b & 2.5). This trapping process mainly concern debris flow boulders and driftwood. The outlet capacity decreases and deposits grow in correlation with the clogging ratio. The flood magnitude, and more precisely the supply of coarse materials, control the trapping efficiency. Sectional, lattices, frame or net open check dams (Fig. 2.2*iii-viii*) use mechanical control design criteria (SABO Division, 2000).

D'Agostino (2006) and Takahashi (2014, p.451) considered that the mechanical collisions between boulders approaching the open check dam also have a significant effect in addition to the direct mechanical blockage of the openings.

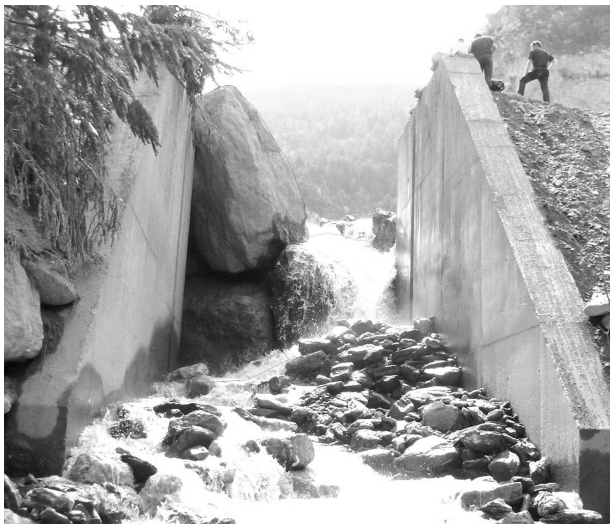

Figure 2.5 – Downstream view of the St Antoine sediment trap after the 31 July 2014 debris flows: mechanical blockage of the 5-m-wide, 8-m-high slit dam by three boulders 3-4 m in diameter (image by Guillaume Piton)

C. Mixed control

Hydraulic control and mechanical control do not necessarily occur alone and may occur together (Fig. 2.4c). In bed-load and driftwood-laden flows, mechanically controlled driftwood jams at the open check dam can generate upstream hydraulically controlled sediment deposition (Lange and Bezzola, 2006; Comiti et al., 2012). Dams with vertical openings (*e.g.*, Fig. 2.2*vii*) tend to be rapidely clog in case of massive driftwood supply while dams equiped with inclined structures (*e.g.*, Fig. 2.2*v*) tend to maintain a partial sediment transfer capacity (see companion paper). In traps where mixed controls is possible, designers must pay attention to a possible upstream channel backfilling (Zollinger, 1983; Jordan et al., 2003; Kaitna et al., 2011) that can promote dyke over-topping and open check dam bypassing (*e.g.*, Böll et al., 2008, p.34). The sensitivity of open check dam shapes related to driftwood are presented in the companion paper. To summarise, once the basin features and structure shape have been chosen, designers will first estimate the probability that boulders will clog the structure following the mechanical control criteria presented below. In the second step, they will compute the hydraulic capacity of the open check dam and the induced hydraulically controlled trapping (criteria detailed further). To finish, possible driftwood influences will be controlled: (i) using a mechanical approach for logs to estimate the accumulation probability and (ii) using a formula to estimate the related accumulation head loss (see companion paper). If the theoretical trap behaviour is not satisfactory, the open check dam type or shape has to be adapted.

2.3.2. Design of mechanically controlled structures

A. Opening dimensions

The probability of clogging is estimated with the relative opening, which is the ratio between n_0 the shorter dimension of the opening (Fig. 2.2) and the relevant material dimension, which is D_{max}, the maximum sediment diameter in the case of boulders. An equivalent criterion exists for driftwood; see companion paper for details. D'Agostino (2013b) proposed retaining $D_{max} \approx D_{75}$ to D_{84} of the armoured bed surface.

$$\textbf{Relative Opening} = \frac{Opening\ size}{Material\ size} = \frac{n_0}{D_{MAX}} \tag{2.1}$$

Table 2.1 shows the usual values reported in the literature and the related sediment clogging probability. To summarise, it is generally accepted that relative openings of 3 and 1.5 are unlikely and likely, respectively, to be clogged by boulders (Tacnet and Degoutte, 2013).

Takahashi (2014, p.454) analysed small scale models results of grid check dams (horizontal, vertical, both of them and frame configurations). Using sediment mixtures with *Relative openings* = 0.5 − 0.6, complete structure clogging was systematically observed, except in horizontal bars configurations, the sediment accumulation then partially self-cleaned. For small-boulders' transportation, consistently with Zollinger (1984b), he

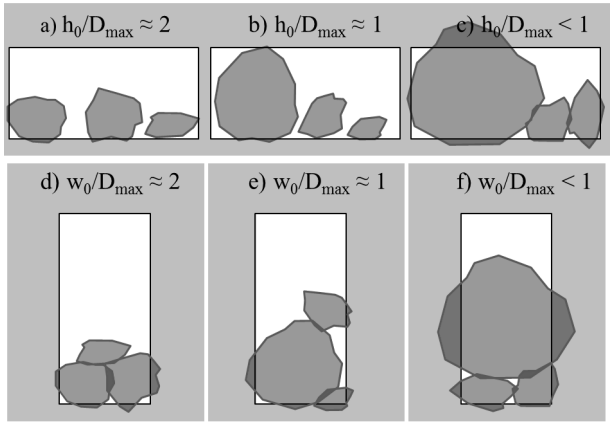

Figure 2.6 – Sketch of boulder jamming process depending on the verticality or the horizontality of equivalent *Relative Opening* slots: a) $h_0/D_{MAX} \approx 2$ jamming weakly probable; b) $h_0/D_{MAX} \approx 1$, jamming probable; c) $h_0/D_{MAX} < 1$, certain jamming; d) $w_0/D_{MAX} \approx 2$, quite probable jamming, e) $w_0/D_{MAX} \approx 1$, even more probable jamming; and f) $w_0/D_{MAX} < 1$, certain jamming.

concluded that "*the vertical bars play the major role in checking the large particles in the forefront of the debris flow and the addition of horizontal bars enhances the engaging between particles that stabilize the deposited sediment*".

In structures subjected to debris flows with meters-scale boulders, if trapping is sought for the front boulders but not for the subsequent debris flow tails (constituted of hyperconcentrated flows), large slits and slots with $n_0 = w_0 \approx 1.5 - 2D_{MAX}$ seems an interesting design (*e.g.*, Fig. 2.5). Slots with a relatively small height $n_0 = h_0 \approx D_{MAX}$, but a large width $w_0 \gg h_0$ will have an even more changing behaviour: transferring most of the bedload and even possibly small debris flows, they will however be suddenly obstructed in presence of large boulders and / or large woody debris (*e.g.*, Vogl et al., 2016). If, on the contrary, the debris flow tails must also be trapped, $w_0 \approx D_{MAX}$ seems better, since even $\approx D_{MAX}/2$-boulders will likely jam (Fig. 2.6). Obviously smaller openings will have even better trapping efficiencies, although it will also make the structure more prone to be jammed by woody debris, even for not extreme floods (see later).

It remains difficult to estimate the maximum probable size of large materials. To take this uncertainty into account, Osanai et al. (2010) recommended a relative opening of 1 as the design criterion, even if they assumed that a value of 2 would be sufficient to clog the openings if D_{MAX} was accurately determined.

To ensure clogging even for smaller transported diameters, a lower relative opening was also conservatively recommended by Ono et al. (2004) and Itoh et al. (2011). During the basin filling process, a grain size sorting effect in the deposits is regularly reported (López et al., 2010a; Itoh et al., 2011). A decrease in the frame's upper opening sizes has to be adopted if the designer wishes to trap the fine tail of the flood hydrograph (Mizuyama et al., 1996; Itoh et al., 2011). Driftwood can have an equivalent effect by clogging the upper part of the openings.

B. Decrease in instantaneous debris flow discharge

Debris flows can induce catastrophic erosion which, in addition to bank / hill-slope destabilisation and structure failures, leads to a general increase in the debris flow volume along the channel (Hungr et al., 2014; Remaître et al., 2008; Remaître and Malet, 2013). The debris flow can be more complicated to trap and store if it has the time and space to fully develop. Sectional and lattice dams can be used to trap debris flow surges in the upper part of the watershed, especially their coarse granular front. They must however be located on reaches where the debris flow front are ever developer (Takahashi, 2014, p.463), if built too upstream, debris flow main body may reform downstream of the structure.

Such structures are basically designed using Eq. (2.1). Using small-scale models and sometimes numerical reanalysis, some authors have attempted to estimate the trapped volume or decrease in sediment discharge induced by this type of structure. Equations can be found for slit

Table 2.1 – Relative opening clogging probability

Opening*	Relative opening†	Clogging probability	Sources
w_0	1.5	100%	Watanabe et al. (1980)
-	2	0%	-
w_0	1.6	High	Zollinger (1983)
h_0	1.2	High	-
w_0	1.5	High	Ikeya (1989)
w_0	1.5	100%	Frey and Tannou (2000)
-	2	33%	-
h_0	1.5	100%	-
-	2	0%	-
n_0	1‡ (2)	100%	Ono et al. (2004), Osanai et al. (2010), Itoh et al. (2011)
w_0	1.18	89%±7% [75%-95%]⋆	Silva et al., 2016
w_0	1.37	78%±12% [60%-95%]⋆	-
w_0	1.49	52%±31% [0%-90%]⋆	-
w_0	1.77	37%±15% [27%-54%]⋆	-

* w_0, h_0 and n_0, the horizontal and vertical and minimum size of the opening, respectively (Fig. 2.2)

† $Opening\ dimension/_{Material\ dimenson} = \frac{w_0\ or\ h_0}{D_{MAX}}$

‡ see comments in the text.

⋆ ratio $\frac{debris\ flow\ trapped\ volume}{supplied\ volume}$: mean value ± standard deviation [minimum value-maximum value]

dams in Watanabe et al. (1980); for frame dams in Mizuyama et al. (1996), Wu and Chang (2003), Ishikawa et al. (2004) and Takahashi (2014, p.454); and for sectional dams with multiple fins (narrow side charged walls - Fig. 2.2 *v*) in Lien (2003), Choi et al. (2014) and Silva et al. (2016). We recommend using these formulas carefully, because their results likely depend a great deal on experimental features such as the grain size distribution, flume characteristics, the initial bed state, etc. In addition, all these results address the decrease induced on a singular debris flow surge; the effect of multiple surges is generally not considered. As stated by D'Agostino (2013b), these data give a preliminary rough analysis of the structure effect.

2.3.3. Hydraulic capacity of check dam openings

In hydraulically controlled structures, Δz_{dep}, the deposit heigh (Fig. 2.4a), is directly related to the backwater effect induced by the open check dam. The backwater effect is computed using water stage-discharge equations that can be analytically deduced from formulas found in the literature for the simplest shapes (Zollinger, 1983).

In orifices, free surface and pressured flows are not computed with the same equations: In free surface flow conditions, *i.e.*, if $d_w < h_0$, Eqs. (2.3) or (2.5) are used. A pressure flow occurs once the top of the orifice is reached, *i.e.*, for $d_w > h_0$, then Eq. (2.2) is used.

When the inertia term linked to the approaching velocity is not negligible, d_w has to be replaced with $d_w + v_w^2/2g \approx d_w + Q^2/2gW^2d_w^2$, with v_w the approaching velocity (m.s^{-1}) and W the basin width (m) (Lencastre, 1983). Neglecting the inertia term in steep slope contexts may result in dramatic deviation from the actual flow configuration (*e.g.*, Le Boursicaud et al., 2016).

Theoretical hydraulic laws concerning more complicated slit shapes allowing linear water stage-discharge or constant velocity in the slit, are reported in Ferro (2013). All the studies related to stage-discharge formulas presented below provide

few details on errors and accuracies. As regularly done for water sreservoir dam spillways , small-scale experiments are appropriate tools to confirm theoretical results (Lefebvre and Demmerle, 2004; CFBR, 2013).

A. Grand Orifice formula (Fig. 2.3b dam type)

To compute the hydraulic capacity of slot and continuous crested slit check dams (Fig. 2.2*ix* to *xi*), Zollinger (1983), Mizuyama et al. (1988) and Sasahara et al. (2002) retained the Grand Orifice formula:

$$Q = \mu_0 w_0 \frac{2}{3}\sqrt{2g}(d_w^{3/2} - (d_w - h_0)^{3/2}) \qquad (2.2)$$

where Q is the water discharge ($m^3.s^{-1}$), w_0 and h_0 are the slot width and height (m), respectively, g the gravitational acceleration ($m.s^{-2}$), d_w the water depth over the slot bottom (m) (Fig. 2.3a) and μ_0 is the slot coefficient (-), taken as 0.65 (Zollinger, 1983; or 0.68: Mejean, 2015; Piton et al., 2016a).

B. Slit formula (Fig. 2.3c & d dam types)

Zollinger (1983) proposed an adaptation of Eq. (2.2) for gap crested slit dams:

$$Q = \mu w_0 \frac{2}{3}\sqrt{2g} d_w^{3/2} \qquad (2.3)$$

μ_0 is the slit coefficient (-), also taken as 0.65 (Zollinger, 1983; Mejean, 2015; Piton et al., 2016a). When horizontal beams are added (*e.g.*, Fig. 2.3a & d), a correction factor of μ has to be taken into account. The authors used the original graphs of Zollinger (1983) to estimate values of μ for different bar spaces[1] (Table 2.2).

Table 2.2 – Horizontal beam influence on slit coefficients

h_1 [m]*	$\psi = \frac{h_1}{h_1+D_{bar}}$ †	μ‡	$\beta^\circ = \mu/\mu_0$
No beam	1	0.65	1
2	0.91	0.60	0.92
1	0.83	0.53	0.82
0.5	0.71	0.45	0.69
0.2	0.5	0.31	0.47

* Space between beams [m]: see Figure 2.3

† Grill void ratio, D_{bar} = 0.2m in Zollinger (1983)

‡ Slit coefficient in Eq. (2.3)

° Equivalent contraction coefficient = μ/μ_0

Armanini and Larcher (2001) retained a critical water depth condition hypothesis in their analysis of single slit dams (Fig. 2.3*c*). If the contraction effect is strong enough, a subcritical regime is forced in the basin upstream of the open check dam. The slit flow is therefore generally critical and the water stage-discharge equation directly upstream of the open check dam (section w in Fig. 2.4) can be expressed by:

$$d_w + \frac{Q^2}{2gW^2 d_w^2} = \frac{3}{2}\sqrt[3]{\frac{Q^2}{w_0^2 g}} \qquad (2.4)$$

If the basin is wide enough, the upstream inertia term becomes negligible and the equation can be rearranged as follows:

$$Q = w_0 \left(\frac{2}{3}\right)^{1.5} \sqrt{g d_w^3} \qquad (2.5)$$

Other versions of Eq. (2.4) can be used for debris flows and muddy flows (see Larcher and Armanini, 2000; Armanini et al., 2006 for details).

Equation (2.5) provides an 11% lower discharge capacity when compared to Eq. (2.3), or in other words is equivalent to Eq. (2.3) with a slit coefficient $\mu = 0.58$. The pure-water-measurements of Mejean (2015), presented in Piton et al. (2016a), let the authors think that Eq. (2.3) is more appropriate to use than Eq. (2.5) in bed-load and

[1] A detailed back analysis of these μ values showed that the original author considered the water stage - discharge capacity of a grill to be the sum of the capacity of the spaces between beams, considered as orifices (Eq. 2.2) plus, for the uppermost flooded space of the slit, the capacity of a slit (Eq. 2.3) taken from the last submerged beam.

debris flood traps with relatively thin dams (*i.e.*, with dam-thickness/$d_w \in [0.05; 0.47]$).

C. Sectional and rack formula (Fig. 2.2 iii-vi dam types)

Vertical and inclined rack or fin outlets are commonly used in Austrian open check dams (Rudolf-Miklau and Hübl, 2010; Rudolf-Miklau and Suda, 2011; Moser and Jäger, 2014). They can be composed of beams or fins sometimes with an inclination. Di Stefano and Ferro (2013; 2014), and Vatankhah (2014) analysed water stage-discharge equations in small-scale experiments on these structures and proposed the following equation:

$$\frac{d_w}{W_{OS}} = c_0 \psi^{c_1} \frac{\sqrt[3]{Q^2/W_{OS}^2 g}}{W_{OS}} \tag{2.6}$$

with the open structure total width $W_{OS} = \sum_n (w_0 + w_s)$ with n the number of spaces in the structure (see Fig. 2.2), w_s the solid part width: the rack bar diameter or fin width (m), w_0 the open space between solid components (m), ψ the void ratio $= \frac{w_0}{w_0+w_s}$ and two coefficients depending on the rake angle with horizontal α (°): $c_0 = 0.957 + (sin\,\alpha)^{1.833}$ and $c_1 = 0.9 - 1.5(sin\,\alpha)^{0.11}$. The equation was calibrated in the following range of dimensionless parameters $\psi \in [0.16; 0.74]$, $d_w/W_{OS} \in [0.09; 0.71]$, $\sqrt[3]{\frac{Q^2}{gW_{OS}^2}}/W_{OS} \in [0.05;\ 0.17]$, $\alpha \in [45°; 90°]$ and without sediment or driftwood. Rearranging their equation gives the following hydraulic capacity:

$$Q = W_{OS} \sqrt{\frac{g}{c_0^3 \psi^{3c_1}}} d_w^{3/2} \tag{2.7}$$

Di Stefano and Ferro (2013) reviewed the hydraulic capacity of bottom rack structures with floor grills, often used as water intake and called Tyrolean weirs. Complementary details on the use of Tyrolean weirs in torrent control works can be found in Clauzel and Poncet (1963), Okubo et al. (1997), Lefebvre and Demmerle (2004), Mizuyama (2008), Kim et al. (2012) and Brunkal and Santi (2016)

D. Compound shapes

If the open check dam has multiple openings (*e.g.*, Fig. 2.2*ii*, *ix-xi*), the hydraulic capacity of each opening, computed with Eq. (2.2), (2.3) or (2.5), must be summed to take into account the total flow section for a given water depth (SOGREAH, 1994). In case of a slit over a slot structure (*e.g.*, Fig. 2.3a), the discharge is computed by adding the hydraulic capacities of the bottom slot and of a slit starting on the top of the slot (Zollinger, 1983). For sectional and rake dams, Eq. (2.7) integrates the total flow section through the parameters W_{OS} and ψ.

Theoretically, all the formulas presented above should depend the basin to open check dam contraction, *i.e.*, on $\sum w_0/W$. The authors can simply report that, for an equivalent W_{OS}, the contraction effect increases with the number of slits. For example, Hasegawa et al. (2004) observed that a singular slit dam tended to store less sediments and to have a better self-cleaning behaviour than a double slit dam with an equivalent total width. Equations (2.3), (2.5) compare to (2.7) highlight this phenomenon when used on a site with an equivalent total width opening.

E. Complementary head loss

In addition to the head losses directly related to the openings, some authors stressed the necessity to take into account upstream additional head losses. Armanini and Larcher (2001) recommend taking into account ΔH_{dep-w}, the equivalent Borda head loss, related to the energy dissipation at the transition between the *dep* and w sections in Fig. 2.4 (Borda, 1769):

$$\Delta H_{dep-w} = \frac{Q^2}{2gW^2 d_{dep}^2} \left(1 - \frac{d_{dep}}{d_w}\right)^2 \tag{2.8}$$

The above simple hydraulic equations probably remain valid as long as the sediment deposit

does not disturb the outlet flow. An additional increase in the water level was detected in various experiments once the sediment deposit front had reached the outlet and bed-load transfer had begun. Uchiogi et al. (1996) and Frey et al. (1999) proposed estimating the additional head loss related to sediment transport through the outlet using:

$$\Delta H_{sed} = 1 \text{ to } 1.5 D_{Max} \quad (2.9)$$

with D_{max} the maximum sediment diameter. This detected increase in the water depth is likely to be the sum of (i) the volume taken by the transported sediment layer below the water and (ii) the additional energy losses induced by sediment transport (*e.g.*, Recking et al., 2008b).

h_d, the overflow dam height (Fig. 2.3a), is the sum of all the different head losses:

$$h_d = d_w + \Delta H_{dep-w} + \Delta H_{sed} + \Delta H_{LWD} \quad (2.10)$$

with ΔH_{LWD}, the additional head losses related to driftwood accumulation (see companion paper).

2.3.4. Dam crest spill flow capacity

Hydraulics and hydrology of torrents still present a large stochastic element. Phenomena such as driftwood clogging and debris flows remain partially unpredictable. By-pass flows caused by uncontrolled dam over-topping are a major threat and must be prevented (Chatwin et al., 1994; Hübl et al., 2005; López et al., 2010a). Taking into account the probability of complete clogging of the openings, the open check dam crest is generally designed as a trapezoid spillway able to transfer the extreme event's instantaneous peak discharge (Deymier et al., 1995; VanDine, 1996; Ono et al., 2004; Rudolf-Miklau and Suda, 2013; CFBR, 2013), alternatively, the structure must be reinforced to resist to a general over-topping.

The lateral dyke crest level is deduced including a reasonable freeboard adapted to the deposition slope (Dodge, 1948) and to the torrent's hydraulic uncertainties and high velocities (see Hunzinger, 2014 for a freeboard computation method).

2.4. Open check dams and sediment transport

Sediment trap filling processes are clearly non-equilibrium events. Since stream floods are rapid and unpredictable, no direct observations of sediment trap filling have yet been reported in the literature. The processes described hereafter were generally observed in small-scale models or through field analysis of deposit shapes after floods.

2.4.1. Deposition initiation

Four different effects lead to sediment deposition in sediment traps (Zollinger, 1983):

1. a decrease in transport capacity due to a milder energy slope in the basin,
2. a decrease in transport efficiency due to flow spreading in a basin wider than the upstream channel,
3. a drop in the shear stresses related to the tranquil calm water area formation (hydraulic control), and
4. a mechanical blockage against the open check dam (mechanical control).

Depending on the basin shape (narrow / wide, steep / mild slope) and on the flood features (bed-load / debris floods / debris flows / driftwood), each effect can contribute to initiating and developing the deposition. The two first effects, related only to the basin shape, must not be underestimated. They can induce a significant trapping if used efficiently (*e.g.*, Kaitna et al., 2011). At

a larger scale, they are responsible for all debris and alluvial fan creations.

A. Basin width influence

Deposition initiation first depends on the trap basin width. In a wide basin without lateral flow confinement, significant deposition takes place at the inlet structure's toe (Dodge, 1948; Zollinger, 1983; Le Guern, 2014; Takahashi, 2014, p.447). If the basin bottom slope is milder than the deposition slope, deposits in the basin's upper part must be expected. Backwater effects and mechanical blockage thus influence deposition processes only once the basin's upper part has been completely filled and the deposit front has reached the calm water area or the open check dam.

In a narrow, steep and totally flooded basin, deposition is mainly initiated by the structure's control type. (i) In a mechanically controlled sediment trap, the deposition directly depends on the opening clogging rate. The boulder or driftwood jams constitute a fixed point from which basin backfilling propagates backward (Fig. 2.4b). (ii) In a hydraulically controlled structure, small-scale experiments demonstrate that the deposit is generally initiated when sediments enter the calm water area (Fig. 2.4a & c). In supercritical flows, deposition initiation occurs immediately downstream of the hydraulic jump between channel flow and the check dam backwater-influenced-area (Hunzinger and Zarn, 1996). This deposition tends to propagate downstream like a delta and upstream through a backfilling process. The hydraulic jump is prone to disappear due to a reduction of the upstream Froude number related to the new milder slope (Armanini and Larcher, 2001; Busnelli et al., 2001).

B. Similarities with deltas

Dodge (1948), Zollinger (1983), Frey et al. (1999), Jordan et al. (2003; 2004) and Le Guern (2014) report clear similarities between sediment trap filling and delta formations.

The deposit longitudinal profiles present the characteristic two slopes of a delta profile (Fig. 2.4a & c). An underwater steep slope progrades in the calm water area. A milder slope of "dry" deposits, hereafter called S_{dep}, is found above the water surface. Like an alluvial equilibrium slope, S_{dep} is reported to increase with the supply's solid concentration (Frey et al., 1999; Le Guern, 2014). Constituting the border between the two domains, a fixed point called a *fulcrum* is found near the water's surface (Van Dijk et al., 2009).

The literature dedicated to fan and delta geomorphology contains interesting descriptions. They can help to better understand the geomorphic phenomena occurring in sediment traps at a significantly shorter time scale (see Parker et al., 1998; Van Dijk et al., 2009; Van Dijk et al., 2012; Reitz and Jerolmack, 2012).

2.4.2. Hydrograph recession and self-cleaning effect

In his review on coupling effects between fans and fluvial systems, Harvey (2012) stressed that fan and delta morphologies are highly sensitive to downstream boundary conditions, such as changes in the water level or fan toe cutting.

The self-cleaning trends showed by some open check dams, have similarities with fan and delta toe cutting phenomena. All authors agree that the hydrograph recession and the subsequent erosion are clearly not the symmetric effect of basin filling (Compare Fig. 2.4 and Fig. 2.7). In a hydraulically controlled basin, the calm water level decreases with the instantaneous water discharge during hydrograph recession. The former underwater steep slope becomes exposed to direct flow erosion. Small-scale modelling, as well as field observations, report the creation of a deep singular channel (Fig. 2.7a & Zollinger, 1983; Armanini and Larcher, 2001; Busnelli et al., 2001; Catella et al., 2005). This phenomenon is similar to water dam reservoir flushing, which gen-

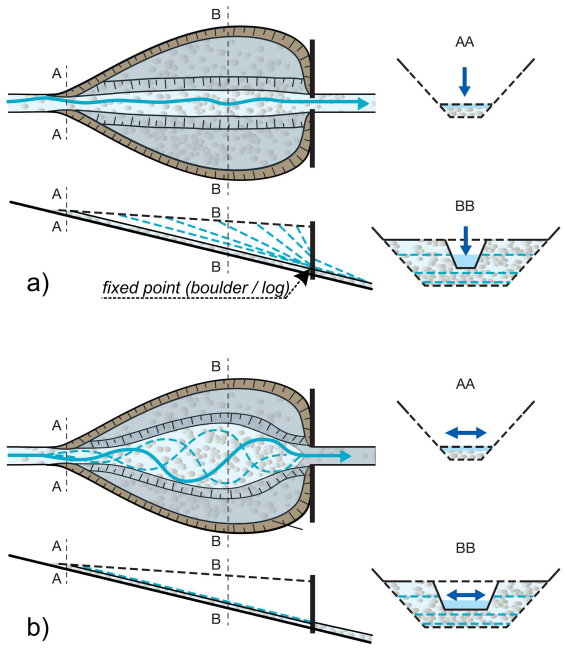

Figure 2.7 – Self-cleaning main steps: a) backward channel incision, b) channel widening (adapted from Zollinger 1983, with permission)

erally results in a channel formation in the deposit (Morris et al., 2008). Once the incision reaches a fixed point (basin bottom or mechanically blocked material in the open check dam), bank erosion and collapses tend to widen the channel (Fig. 2.7b). If a clear water flow lasts long enough, a substantial part of the basin can be cleaned. This self-cleaning process is generally sought for hydraulically controlled structures. Clogging of the openings, for instance related to large woody debris, is the worst enemy of this interesting behaviour. The use of inclined structures limits driftwood clogging (see companion paper). Dodge (1948) alternatively reported successful experiments of post-flood boulder and log jam removing, thus initiating an economical partial self cleaning of the traps. In addition, this partial restoration of the sediment continuity help limiting the undesirable incision trends nearly systematically observed downstream of sediment traps. Mechanically controlled structures generally show no or weak natural self-cleaning trends (IRASMOS, 2008).

2.4.3. Deposition slope

A. General considerations

If the sediment trap and the upstream channel widths are similar, the deposition slope in the trap is likely to be comparable to the alluviation slope above solid body check dams. Field measurements above existing check dams or bedrock outcrops are probably the most accurate method to determine S_{dep} (Deymier et al., 1995). Field measurements must take into account former patterns of torrential activity (Kaitna and Hübl, 2013) and be completed with historical analysis (D'Agostino, 2013a).

In laterally unconstrained areas, the estimation of deposition slopes remains complex and, until now, insufficiently known. In sediment traps, mechanical dredging generally levelled the basin bottom and no stable and predetermined channel exists. During trap filling, aggradation is fast and flow paths highly unstable. When trapping bed-load, cycles of sheet flows (thin layer of water spreading on a large width of the deposit, Parker et al., 1998) and channelisation are likely to occur, resulting in high morphological instability. Grain size sorting plays a key role in these instabilities and fluctuations (Le Guern, 2014).

The flow spreads when entering a wider area, which tends to produce shallower water depths and lower shear stresses. This results in equilibrium slopes that are steeper in alluvial wide reaches than in narrow reaches, *i.e.*, upstream of solid body dams (Thiéry, 1891; Hunzinger, 2004). Koulinski (1993), Lala Rakotoson (1994), Frey et al. (1999) and Le Guern (2014) all highlighted decreases in sediment transport capacity when flows in narrow constrained channels enter a wider area.

B. Existing equations

Rough formulas[1] developed for solid body dams can be used to determine deposition slopes (Osti and Egashira, 2013; D'Agostino, 2013b):

$$S_{dep} \approx 1/2 \; S_{init} \tag{2.11a}$$

$$S_{dep} \approx 2/3 \; S_{init} \tag{2.11b}$$

with S_{init} the natural initial slope of the upstream reach before construction of solid body dams. Equation (2.11a) is often used for low flows and afters several small floods, thus for initial conditions prior to a disaster. Equation (2.11b) is proposed for deposition occurring during extreme floods with higher solid concentrations (SABO Division, 2000). These differences in slopes, depending on sediment supply and hydrology, illustrate that slope values fluctuate over time, resulting in a small dosing effect through a sediment buffering effect (Gras, 1857; Jaeggi, 1992; López et al., 2010a).

Some authors have attempted to apply classical sediment transport formulas to small-scale models of sediment trap filling. Jordan et al. (2003) and Kaitna et al. (2011) reported that the Smart and Jaeggi (1983) equation provides good estimations of their results. Frey and Tannou (2000) reported that the Rickenmann (1991) and Couvert et al. (1991) formulas provided a good estimation of the deposit slope in the upstream channel but only the lower value of the slope range in the basin. Le Guern (2014) also observed that these three formulas, although calibrated for torrential flows, underestimate S_{dep} in laterally unconstrained flows.

More recent approaches had been tested on numerical models. Osti and Egashira (2008) and Osti and Egashira (2013) presented an application of their debris flow propagation model on a case study of check dam design in Venezuela.

Armanini (2014) recently proposed constitutive relations for sediment-laden flows, without clay in the interstitial fluid that would change its rheology. The equations describe debris flow to bed-load transition but still need to be validated on other field and laboratory datasets. The use of these approaches remains difficult in self-formed channels, where the active width is unknown. New formula taking into account the channel width adjustment are needed. Similar problem exist in braided rivers (Ashmore et al., 2011; Ashmore, 2013).

For sediment-laden flows with a substantial clay concentration in the interstitial fluid, *i.e.*, muddy debris flows, deposit slopes in the sediment trap can be very low due to changes in rheology and constitutive equations (*e.g.*, muddy debris flows of the Saint Antoine stream, July, 31^{th} 2014 Modane, FRA., $S_{dep} \approx 3\%$, Tacnet et al., 2014a).

To summarise, the methods to estimate the maximum value of the deposits' slope have not yet been sufficiently validated in the field. The detailed methods presented above still lack field confirmation. This is particularly true in laterally unconstrained areas and under low excess shear stresses, even though such conditions often seem to take place in steep slope streams and gravel bed rivers during floods (*e.g.*, Recking et al., 2012a; Pitlick et al., 2013). Observations of large fluctuations of deposition slopes, even if reported from field observations over a long period of time (*e.g.*, Fabre, 1797; Thiéry, 1891; Jaeggi, 1992), have only recently begun to be studied in detail and this is still an active field of research (*e.g.*, Recking, 2013a; Bacchi et al., 2014). The potential expression of these phenomena in laterally unconstrained channels needs to be addressed in the future.

[1] This subject is discussed further in details in §2.7, p. 55 within a Closure paper and a synthesis of the related Discussion paper.

2.4.4. Deposit height

A. Mechanically controlled deposits

In mechanically controlled structures, the deposit level is controlled by the level of the coarse materials jammed against the structure. If the sediment supply is comparable to the sediment trap volume, the basins are generally filled up to the crest level:

$$\Delta z_{dep} = h_d \tag{2.12}$$

with h_d dam height between the outlet bottom and crest levels (Fig. 2.2).

B. Laterally unconstrained flows and hydraulic controlled deposits

The deposit height Δz_{dep} has to be estimated once the water stage-discharge formula directly upstream of the open check dam has been determined, taking into account additional head loss induced by bed-load and driftwood (Fig. 2.3 and 2.4). In a basin large enough to allow a non-constraint flow, Jordan et al. (2003) reported that Δz_{dep} was comparable to the mean value of the water depth in the basin during the flood, and not to the dam height or to the maximum water depth. Δz_{dep} can thus be estimated by computing the mean value of $d_{w,tot} = d_w + \Delta H_{dep-w} + \Delta H_{sed} + \Delta H_{LWD}$, the total water depth during the flood:

$$\Delta z_{dep} = \frac{1}{T_{flood}} \int_{T_{flood}} d_{w,tot}(t)\, dt \tag{2.13}$$

with T_{flood} the duration of the flood. This highlights the importance of the water stage-discharge capacity of the outlet and the sensitivity to the hydrograph when assessing the trap's theoretical behaviour for a given event.

C. Laterally constrained flows and hydraulic controlled deposits

Armanini and Larcher (2001) theorised and experimented single slit check dams installed in a relatively narrow basin such that the flow covers its entire width. Their approach is more likely to concern sediment traps built directly in the channel or in gorges and without widened basins. If the sediment supply is high enough, experiments have shown that the deposition process looks like nearly steady states of transport over a topset equilibrium slope. Assuming that the Froude number in the calm area is subcritical, a preliminary approximation of the deposit height for slit check dams can be estimated using:

$$\Delta z_{dep} \approx d_{dep} \left(\frac{W - \Sigma\, w_0}{\Sigma\, w_0} \right) \tag{2.14}$$

Equation that may be rearranged to depend only on open check dam hydraulics and shape in:

$$\Delta z_{dep} \approx \frac{d_w}{1 + \frac{\Sigma\, w_0}{W - \Sigma\, w_0}} \tag{2.15}$$

with d_{dep} the water depth above the deposit at section *dep* of Fig. 2.4, W the basin width upstream of the open check dam and $\Sigma\, w_0$ the sum of the opening widths (Fig. 2.2). D'Agostino (2013b) also suggested using use Eq. (2.15) but recommended using it only for slit dams with $\Sigma w_0 < 0.4W$. Armanini and Larcher (2001) proposed abacuses giving the percentage errors when using this simplified formula compared to the more precise equation described below. A more precise estimation of the deposit height Δz_{dep} depending on d_{dep} the flow depth over the deposit, can be computed if Fr_{dep} the flow Froude number on the deposit, is known $\approx \frac{v_{dep}}{\sqrt{g d_{dep}}}$, with v_{dep} flow velocity on the deposits (m/s):

$$\frac{\Delta z_{dep}}{d_{dep}} = \frac{3}{2} \left(Fr_{dep}.\frac{W}{w_0} \right)^{2/3} - 1 - \frac{Fr_{dep}^2}{2} \left(1 - \left[1 - \frac{2}{3} \left(Fr_{dep}.\frac{W}{w_0} \right)^{-2/3} \right]^2 \right) \tag{2.16}$$

The drawback of this approach is that it requires prior knowledge of the relevant friction law and solid transport formula on massive deposits oc-

curring in sediment traps, which have not yet been determined. The accurate estimation of the Froude number and the water depth remains difficult.

The deposit formation behaves more like a delta prograding in the basin if the sediment supply is low, i.e the dimensionless dam trapping parameter $M = V_{sed,supply}/V_{sed} << 1$, with $V_{sed,supply}$ the volume of sediment supplied by the flood to the trap and V_{sed} the maximum volume of sediment trapped in the open check dam basin (Armanini and Larcher, 2001). It this case, Eq. (2.16) cannot be applied to assess the deposit height directly upstream of the open check dam.

In specific conditions with a sufficiently wide slit, the basin flow could remain supercritical, including directly upstream of the slit. In this case, Eq. (2.16) is no longer valid and alternative equations were proposed by Armanini and Larcher (2001). In mudflows and debris flows, the framework of Armanini and Larcher (2001) was tested in small-scale models and additional formulas were proposed to take into account the complementary head loss induced by dead and recirculation zones (Larcher and Armanini, 2000; Armanini et al., 2006).

Busnelli et al. (2001), Campisano et al. (2013) and Campisano et al. (2014) accurately numerically modelled Armanini and Larcher's (2001) small-scale experiments after a recalibration of the Meyer-Peter and Müller (1948) transport equation. For a given hydrograph, numerical simulations showed that Δz_{dep} is slightly overestimated by Eq. (2.16) at the peak flow. In addition, during the falling part of the hydrograph, significant self-cleaning of the basin was modelled, resulting in thin remaining deposit heights (Campisano et al., 2014). During post-flood field investigationss Catella et al. (2005) also observed that deposition heights in four slit dams were slightly less than expected with Eq. (2.16). These results could be explained by non-saturated solid transport conditions, partial self-cleaning processes, different processes related to the wide basin width and laterally unconstrained flows or the quasi-steady assumptions used by Armanini and Larcher (2001) can fall in defect. In summary, Eq. (2.16) can be considered as the envelope of the maximum potential deposit height before self-cleaning.

2.4.5. Basin maintenance slope and low flow channel

Using various basin longitudinal profiles in a small-scale models, Ishikawa et al. (1996) and Frey et al. (1999) showed that the final deposit shape does not depends on the initial basin topography. The latter plays a role in the total storage capacity and low-flow transfer but not on the final volume deposit shape. The basin bottom topography of a sediment trap is generally only representative of the last dredging campaign and/or past partial filling by previous floods.

As a minimum value, SOGREAH (1992) recommend not to dredge basin slopes gentler than the fan slope. A recommendation that makes sense wherever a partial sediment transport continuity is sought. A very low basin slope is a suitable choice only for total retention structures. Designers have sometimes been tempted to adopt a low basin longitudinal slope to increase the total storage capacity for a given open check dam height. This type of design curtails nearly all the transport capacity of low-floods. Strong problems of incision often appear downstream of this kind of structures (SOGREAH, 1992). Costs related to regular dredging and downstream-channel-protection-structures curtailing sediment starvation effects (Brandt, 2000; López et al., 2010a) must be taken into account in long-term project costs.

After dozens of years using sediment traps, French dams managers now seek to minimise trapping effects on floods that do not threaten downstream areas (*e.g.*, Koulinski, 2010).

An alternative solution to increase trap volume while keeping slight influences on low-flows

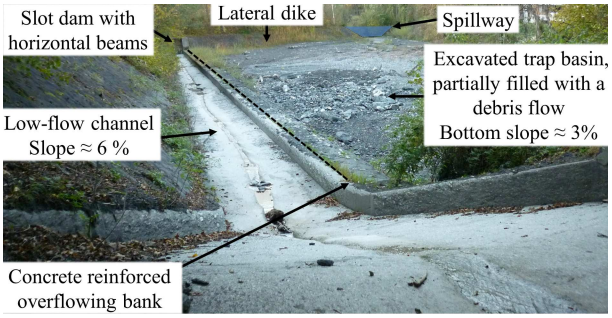

Figure 2.8 – Upstream view of the Reninge stream parallel sediment trap with its low-flow channel and excavated trap basin with a trapping capacity of 5,000m^3 (Haute Savoie, French Alps - image by Guillaume Piton)

is to build a steep relatively narrow channel in or on the side of the trap (Fig. 2.8 & De Montmollin and Neumann, 2014). Such structures are called parallel sediment trap, in contrast to traps in series, directly built transversally to the channel (SOGREAH, 1992 , Lefort, 1996). The basin is sometimes dug lower than the low-flow-channel (Fig. 2.8 & *e.g.*, Ghilardi et al., 2012). When significant floods occur, they overflow the channel and spread in the basin where massive deposition occurs. The cost of the reinforced channel increases the initial cost of the trap, but over the long term, it can significantly decrease maintenance costs, especially in watercourses with regular but rarely dangerous sediment production. As stressed by IRASMOS (2008), cost-benefit analysis must be undertaken to highlight the short and the long-term relevance of the various possible solutions adapted to each site.

2.4.6. Scour and erosion protection

Erosive stream power at the toe of check dams can be extremely high and is a major threat for structures (Deymier et al., 1995; Hübl et al., 2005; Comiti et al., 2013). Downstream of a sediment trap, it can become even stronger because the flow is often constituted of clear water: in addition to local scouring due to energy dissipation, sediment starvation can lead to a general incision and check

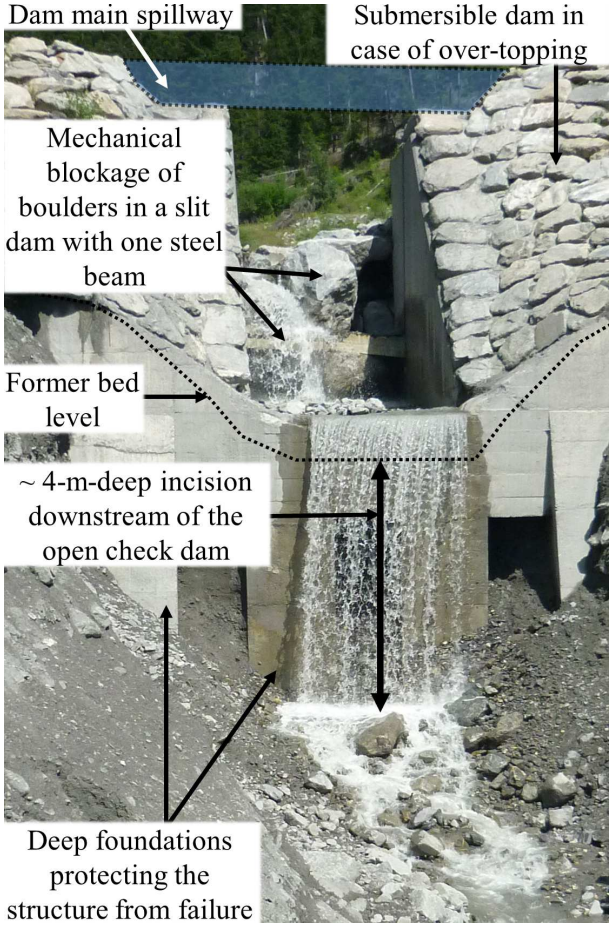

Figure 2.9 – Downstream view of the slit dam with horizontal beams of the Ravoire de Pontamafrey stream (Maurienne, French Alps), 3 to 4-m incision following two subsequent debris flows (Jul. 27 & 30, 2014), deep foundations protect the structure from failure; partial mechanical blockage of large boulders in the slit (image by Guillaume Piton)

dam toe destabilisation (*e.g.*, Fig. 2.9). Like for solid body dams, open check dams must be protected. Ground sill or counter-dams are often built downstream of the main structure (Fig. 2.1). Formulas calibrated to estimate scour depths can be found in Comiti et al. (2013) and D'Agostino (2013b). The inlet structure must also be protected even if its toe generally shows deposition trends. Its failure would induce dramatic consequences such as upstream channel destabilisation.

In addition to vertical erosion on hydraulic falls, steep slope streams generally show a strong tendency to lateral erosion and channel shifting. In sediment traps, strong deposition takes place

at the centre of the basin and flows regularly split into multiple channels often following the basin sides. Riprap and riprap masonry are often used to protect lateral dykes from erosion. Details on riprap design in the steep slope context can be found in Recking and Pitlick (2013).

2.5. Design procedure steps

In summary, the following steps are recommended in the design of a sediment trap with an open check dam:

1. Determination of torrential hazards on the area to protect through a complete watershed study determining flood features (data input) and stressing, as precisely as possible, the processes leading to potential damage (*e.g.*, driftwood/boulder accumulation in a given section, insufficient channel hydraulic capacity due to deposits, solid transport insufficient capacity, etc;); field investigations (Kaitna and Hübl, 2013) and historical analysis (D'Agostino, 2013a) must be used to complete theoretical and numerical approaches (Zollinger, 1985);
2. Choice of the structure's location;
3. Determination of the structure's objectives (qualitative functions as described above and quantitative objectives such as the expected trapped volume) leading to the choice of the outlet shape;
4. Depending on the available area, design of the basin shape and type (series or parallel);
5. Choice of the basin bottom slope and maintenance practices;
6. Computation of S_{dep} and its uncertainty (Eq. (2.11) and field data);
7. Estimation of the necessary ΔZ_{dep} to reach the volume of the structure, depending on the bottom and deposition slopes and available area;
8. Determination of the opening sizes and $d_{w,tot}$ with the appropriate formula (Eqs. (2.12) to (2.16)) to achieve the targeted value of ΔZ_{dep};
9. Control of the consistency between the functions and the likelihood of the mechanical blockage of coarse sediments with Eq. (2.1) and of driftwood (see companion paper);
10. Control of the consistency between the functions and the possible hydraulic trapping with Eq. (2.2) to (2.7), taking into account the possible influence of additional head losses (Eqs. (2.8) & (2.9) and related to driftwood - see companion paper);
11. Determination of h_d the check dam height with Eq. (2.10);
12. Design of the spillway and lateral dykes with a suitable freeboard;
13. Design of scour and erosion protections.

If the dam height and lateral dyke sizes deduced are excessive, designers must decide whether it is more relevant to (i) increase the available area for the basin and dykes, (ii) design multiple sediment traps in a series or (iii) review and lower the trapping objectives. If a verification demonstrates inconsistencies between the trap's theoretical objectives and the expected behaviour based on expert assessment and design criteria, the open check dam shape must be revised.

2.6. Future research challenges

Much remains unknown in torrent mitigation and more particularly concerning the processes occurring in sediment traps with open check dams.

2.6.1. Sediment production assessment and field survey

A key question, which is not directly addressed in this paper, is the assessment of sediment productivity and transport during disasters and low-floods. These basic parameters are needed by engineers to design sediment traps. Until now, to our knowledge, no simple and accurate method has been developed. The structure must be adapted to local geomorphology, geology, hydrology, land use, etc..

From this point of view, existing traps are useful structures. Trap dredging provides data on sediment production and transfer. Long-term analysis and surveys of sediment traps will improve our knowledge of the natural variability of sediment production over time and between watersheds. Once enough data have been collected, regional methods can be calibrated to give an approximation of sediment production of watersheds (*e.g.*, Peteuil, 2010; Peteuil et al., 2012).

In addition to natural watershed sediment production, the influence of upstream torrent control works, such as solid body dams, on sediment transport has not been sufficiently understood. Numerous design criteria address toe scouring, slope adaptation and the structure design of solid body dams. However, how a series of upstream solid body dams changes sediment transport at the instantaneous or the flood scale is not yet clear. Preliminary results are reported in Remaître et al. (2008) and in Piton and Recking (2014; 2016cc), but more small-scale experiments and confirmation by field surveys are needed. This is important because designers have to be able to take into account upstream torrent works in the design of a sediment trap.

In addition to the basic data concerning sediment volume production, it would be worth surveying trap filling and self-cleaning in greater detail. Grain size sorting, channel shifting, driftwood production and their influences are examples of natural processes taking place when disaster occurs, which has not been properly understood. A large number of the processes discussed in this paper come from small-scale and numerical models. Confirmations of laboratory results by field observations are clearly needed. Extensive field surveys such as those conducted by López et al. (2010a) on the structures built after the Vargas disaster (Dec. 1999, VEN.) are useful.

2.6.2. Hydraulic and deposition processes

Mechanical blockage criteria exist, but remain based on few small scale experiments. The development of Discrete Element Models of debris flows seems promising for numerical simulation able to determine impact forces and detailed granular and mechanical behaviour (*e.g.*, Ishikawa et al., 2014; Albaba et al., 2014). Adding an interstitial fluid with non-Newtonian rheology will probably be the next challenge[1] to address to extend the types of debris flow that can be simulated.

Water stage-discharge equations to determine slot and more exotic shapes exist but, to our knowledge, they generally came from fluvial, low Froude-number and clear-water hydraulic studies. Thorough studies of these simple hydraulic formulas in the torrent context with upstream changing regime flow and massive sediment transport are still lacking.

Better comprehension of sediment transport and torrential hydraulics is clearly needed and must be integrated into numerical models (Egashira, 2007). The effect of lateral confinement absence needs further study. The general comprehension of torrential processes has to address constrained and unconstrained flows in and out of equilib-

[1] Actually, coupled DEM-SPH (Discrete Element Model for coarse grains coupled with Smooth Particle Hydrodynamics for the interstitial fluid) with Non-Newtonian rheology as ever been developed by Canelas et al. (2015) and Silva et al. (2016) who show preliminary results comparing small scale models and numerical simulations of debris flow breakers, a promising tool, though currently heavily costly in computational power.

rium conditions. This general comprehension of the processes will make it possible to develop 1D, 2D and 3D numerical models that are useful tools.

Fan and delta similarities with trap filling processes are clear. The literature generally addresses fluvial processes. Torrential processes with lower excess shear stress and highly pulsatil behaviour compared to low-land alluvial fans and deltas also require further study. Grain size sorting and channel sediment recharge are also subjects of interest. The assessment of precise sediment transport capacity, deposition slope, deposition height and self-cleaning processes are among the many key questions all related to the precise understanding of sediment transport in laterally unconfined deposits.

In addition, the specific effect of hydrographs and related hysteresis in sediment concentration is a point to highlight in order to compute sediment trap filling and self-cleaning with more realistic boundary conditions. Preliminary results coming from small-scale models (*e.g.*, Mao, 2012) have to be verified in the field.

Self-cleaning optimisation and sediment continuity for low flows have been insufficiently addressed. Numerous open check dam shapes have been tested, with often disappointing results (Mizuyama 2008). Solutions can probably be found to prevent downstream sediment starvation related to total trapping, which results in numerous problems and useless maintenance costs. Too conservatively designed structures, *e.g.*, with too low *relative openings*, systematically generate impressive incisions in downstream alluvial reaches. The Ebron sediment trap (Fig. 2.10 - Tréminis, FRA.; capacity $\approx 100,000\ m^3$, 5-m high) exemplifies this situation: a wide slit has been cut in the formerly triple slot dam after few years of operations: several meters deep incision downstream on the fan threatened bank protections and bridges of collapse. The new configuration give satisfactory results, illustrating how conservative was the initial design. The use of channels in the trap basin is likely to be a solution, but research is needed on this point. Further research is required to define structures with only a slight influence on sediment transport for low floods and, at the same time, able to mitigate disasters.

Figure 2.10 – Downstream view of the slit dam on the Ebron torrent (Tréminis (38), FRA), the initially triple small slit dam built in 1990 (see one obstructed slit on the left) has been cut *ca. 1998* to became a large slit dam. This operation having deteriorated the structure strength, a big riprap layer fixed with concrete has been added on the dam upstream side to increase the structural resistance to debris flow impact. (image by Guillaume Piton)

Interactions between torrential flows and structures is another key scientific field in need of attention. A better comprehension of flow details could improve debris flow breakers and similar structures. One can hope that more detailed criteria will be proposed in the future using numerical models, new small-scale experiments and key calibration field surveys.

Acknowledgments

This study was funded by Irstea, the INTEREG ALCOTRA European RISBA project and the ALPINE SPACE European SedAlp project. The authors would like to thank Sebastian Schwindt for his help with the German literature, Thanos Papanicolaou for his editorial works, Gilles Charvet, Christian Deymier, Damien Kuss, Ségolène Mejean, Yann Quéféléan, Didier Waszak and two anonymous reviewers who greatly contributed to this paper by providing helpful reviews of an earlier version of this manuscript. In addition,

the authors acknowledge Johannes Hübl and Fritz Zollinger for their help in improving this work with their past works and their authorization to re-use adapted versions of their meaningful figures.

Notation

The following symbols are used in this paper:

c_0 & c_1 = coefficients of Eq. (2.7) depending on α (-);

D_{bar} = piles, beams or rake bar diameter (m);

D_{Max} = maximum diameter of transported sediments (m);

D_x = diameter such that x% of the grains are finer (m);

d_{cr} = critical flow depth upstream of the open check dam $\approx \sqrt[3]{\frac{Q^2}{gW^2}}$ (m);

d_{dep} = water depth on the deposits (m);

d_w = water depth upstream of the open check dam due to the open check dam water stage-discharge law(m);

$d_{w,tot}$ = water depth upstream of the open check dam, taking into account all head losses $= d_w + \Delta H_{dep-w} + \Delta H_{sed} + \Delta H_{LWD}$ (m);

Fr_{dep} = Froude number of the flows on the deposits = $\frac{v_{dep}}{\sqrt{g d_{dep}}}$ (-);

g = gravitational acceleration (m/s^2);

h_d = dam height from the top edge of the footing up to the overflow level (m);

h_0 = opening height: vertical dimension of the opening (m);

h_1 = distance between beams in a slit dam with horizontal beams (m);

l_0 = long side of the opening = maximum of h_0 and w_0 (m);

M = dimensionless trap capacity $= V_{sed,supply}/V_{sed}$ (-);

n = number of spaces between rack bars or fins in a rake or sectional dam (-);

n_0 = narrow side of the opening = minimum of h_0 and w_0 (m);

Q = water discharge (m^3/s);

S_{dep} = deposition slope (m/m);

S_{init} = initial slope of the upstream stream in a reach not disturbed by anthropogenic structures (m/m);

T_{flood} = flood hydrograph duration (s);

V_{sed} = volume of sediment trapped in the open check dam basin (m^3);

$V_{sed,supply}$ = volume of sediment supplied by the flood to the trap(m^3);

v_{dep} = flow velocity on the deposits (m/s);

v_w = flow velocity upstream the open check dam (m/s);

w_0 = opening width (m);

w_s = width of the dam's solid part between the opening: horizontal dimension of the solid part (m);

W = river or basin width (m);

W_{OS} = open structure total width = $\sum_n (w_0 + w_s)$ (m)(see Fig. 2.2);

α = rake inclination : angle between the rake and the horizontal ($^\circ$);

β = contraction coefficient due to beams presence in slits = $\frac{\mu}{\mu_0}$ (-);

ΔH_{dep-w} = Borda head loss at transition between *dep* and w section in Fig. 2.4 a (m);

ΔH_{LWD} = head loss induced by large woody debris jam upstream of the open check dam (m);

ΔH_{sed} = head loss induced by sediment passing through the open check dam (m);

Δz_{dep} = deposit maximum height (m);

μ_0 = slot coefficient (-);

μ = slit coefficient corrected to take into account beams (-);

ψ = Void ratio = $\frac{h_1}{h_1 + D_{bar}}$ for slits with beams and = $\frac{w_0}{w_0 + w_s}$ for rakes fins (-);

2.7. Discussion and Closure additional papers

Following the publication of Chap. 2 (Piton and Recking, 2016a), Chen et al. submitted a discussion paper, to which we replied by a Closure paper (*in press* in the *J. Hydraul. Eng.*). This short section gathers a synthesis of the remarks of Chen et al. (2016) and a complete version of our Closure.

2.7.1. Synthesis of the Discussion by Chen et al.

Chen et al. (2016) do not fundamentally discuss a particular point of the Chap. 2, but eventually provide complementary results, so far only available in Chinese.

Their works address the question of the deposition slope estimation. They concede that *"there is no reasonable and scientific method of determining the deposition slope upstream of a check dam, and the coefficient range of the natural initial slope is relatively broad and highly random"*. They cite several older analysis also focusing on this problem and often providing analysis of the ratio S_{dep}/S_{init} ranging from 0.5 to 0.95, with the deposition slope upstream of check dams S_{dep} (m/m) and the initial streambed slope, without a structure S_{init} (m/m).

More recently, experimental investigations were undertaken on the same subject in typical gully small scale models. The experimental conditions allowed complementary measurements, concerning, for instance, flow mixture rheology and density. The following equations were then proposed and the results are gathered in Fig. 2.11.

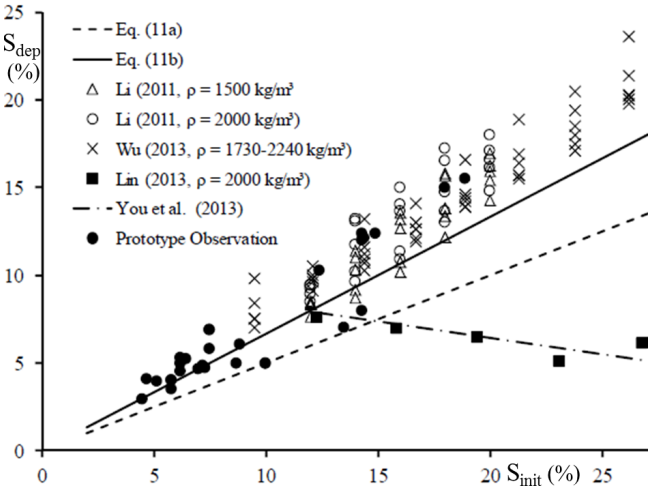

Figure 2.11 – Discussion paper Figure: "Comparison of the experimental data with the empirical formulae" (after Chen et al., 2016, see the original paper for the cited references)

$$S_{dep} = 0.6041\gamma^{0.0526} S_{init}^{0.9470} \qquad (2.17)$$

$$S_{dep} = S_{init} + \frac{\tan\phi - S_{init}}{\tan^2(45 - \phi/2)} \qquad (2.18)$$

with $\gamma = \rho g$, (kN/m^3), ρ being the density of the debris flows, and the internal friction angle of the debris flow ϕ (°).

Equivalent approaches were already available, but raise two problems that made us avoiding their presentation in Chap. 2: i) in our knowledge, no method are available so far to estimate *a priori* the debris-flow rheology, making Eqs. 2.18 & 2.18 hardly usable by a lack of data; and ii) small scale models of gully erosion may present some limits that are summarized in the closure paper.

2.7.2. Closure paper by G. Piton and A. Recking

The authors appreciate the opportunity afforded by the *Journal* to enrich their work with details concerning the point raised by the discussers. The discussers Chen et al. (2016) completed the recent review of Piton and Recking (2016a) by providing additional information on the challenging topic of deposition slope assessment, most particularly two formulas based on small-scale experiments. This question is important because i) it is a key step in the determination of structure volume capacity, and ii) it plays a significant role in protecting the structure from failure: the lateral basin dikes must be designed with a sufficiently steep crest slope to prevent dike overflow, which would eventually result in open check dam by-pass and structure failures (*e.g.*, Böll et al., 2008 p. 53). In response to Chen et al.'s (2016) comments, this note first seeks to clarify the origin of the deposition slope and its comparison with the streambed slope within a geomorphological perspective. This perspective is then tested with a field data set and a number of comments on small-scale model results are reported. Finally, a few words address the question of lateral confinement.

A. Origin of the milder slope upstream of check dams

In most cases the deposition that occurs upstream of check dams has a gentler slope S_{dep} (m/m) than the initial streambed slope, without a structure S_{init} (m/m), which has been known since the first design guidelines of torrent control works (Demontzey, 1882; Thiéry, 1891). Interestingly however, in lowland rivers, this slope reduction upstream of a chute structure is not expected (Malavoi et al., 2011). In the authors' opinion, it should be emphasized that the geomorphic origin of these observations has resulted in misunderstanding and unsuitable structure design (Piton et al., 2016c).

Mountain streams, by definition, are surrounded by hillslopes that eventually supply them with sediment of all sizes, from clay to boulders, through slow (soil creeping, gullying) to fast transport processes (rock avalanches, rock falls, avalanches, debris flows, shallow and deep-seated landslides). In addition, bedrock outcrops or even bedrock channels are quite common in some mountain areas. The initial slopes of mountain streams are consequently not graded alluvial slopes (*sensu.* Lane, 1955), but rather armored beds, paved by seldom moved boulders (Recking et al., 2012a), often steeper than the alluvial equilibrium, and thus supply-limited rather than transport-limited (Montgomery and Buffington, 1997).

Check dams are usually built above the initial bed level for several reasons (Piton et al., 2016c): basically to trap sediment in their backfilled upstream reach, but also to take advantage of the resulting decrease in slope that promotes boulder deposition and less intense sediment transport, and finally for ease of construction (Demontzey, 1882; Jaeggi and Pellandini, 1997). Sediments transported by the stream then deposit upstream of these raised fixed points in the stream's longitudinal profile, resulting in the creation of alluvial sections in an eventually excessively steep environment, influenced by hillslopes or bedrock. The deposition slopes that settle in these sections are graded alluvial slopes, *i.e.*, they depend on water and sediment supplies and sediment grain size. In contrast, the initial stream slope depends strongly on its armoring state related to non-alluvial influences, combined with a classical alluvial influence related to the supply conditions.

There are a few particularly active streams with unlimited sediment supply where strong armoring and stable bed structures, such as step pools, tend to disappear (Recking et al., 2012a). These transport-limited mountain streams more likely have bed slopes entirely in equilibrium with their specifically high-supply conditions, *i.e.*, their initial bed slope is likely an equilibrated deposition bed slope.

To conclude, in mountain streams, the initial bed slope is likely only an upper limit of the deposition slope (Gras, 1850, p. 26). Such steep deposits are observed i) along the entire channel of a few particularly active streams that are supply-unlimited and ii) more generally where non-alluvial influences are weak, *e.g.*, near or on the fans, provided that i) the bed width varies only slightly, *i.e.*, the flow is still laterally confined (see below), and ii) no changes occur in the supply conditions, *i.e.*, in the alluvial influences (*e.g.*, in case of dramatic sediment supply, the stream slope increases, after landslides for instance - Logar et al., 2005; Chen et al., 2015). Where the non-alluvial-pavement influence amplifies, *e.g.*, with increasing boulder supply from hillslopes, the deposition slope should deviate from this upper envelope toward a general decrease. Consistently, in lowland alluvial rivers, the non-alluvial influences are often negligible, explaining that a decreasing slope upstream of weirs and sills, which form mere steps in the river profiles, is not observed.

Dodge (1948) reported from observations in 22 debris basins built near the fans' apexes in the Los Angeles county (CAL.) that:

$$S_{dep} \approx 0.6 S_{init} \tag{2.19}$$

with S_{init} taken as the initial slope of the channel at the basin location. He reported that Eq. (2.19) was reasonably consistent with the observation made during the 1938's major floods. Eq. (2.19) may thus been used to design the debris basin volume capacity, or eventually more conservatively with a coefficient of 0.4-0.5 in place of 0.6 (some concave upward profiles have been observed during the 1938 floods). However, knowing that this deposit slope varies between events and sites, when estimating S_{dep} to design the lateral dike crest and considering that preventing structure bypass is of prime importance, he recommended using:

$$S_{dep} \approx S_{init} \tag{2.20}$$

Eq. (2.20) must be considered for a longitudinal profile taken from the open check dam spillway.

B. Field proof of concept

In order to test the Dodge's (1948) guidelines, the authors gathered data sets of field measurements of S_{init} and S_{dep} upstream of check dams built in gullies and mountain streams (Fig. 2.12; data sets of Hampel, 1975; Iroume and Gayoso, 1991; Liu, 1992; Maita, 1993; Kostadinov, 1993; Porto and Gessler, 1999; Todosijević and Kostadinov, 2006; Conesa-Garcia et al., 2007; Böll et al., 2008; Esmaeili Nameghi et al., 2008; Zeng et al., 2009; López et al., 2010a; León Marín, 2011; Kostadinov et al., 2011; Dìaz et al., 2014; Chen et al., 2016; Galia et al., 2016). This quite large data set (456 data) covers two orders of magnitude of slopes [0.005; 0.5], representing geomorphic contexts from steep gullies and headwater channels down to gentle fan channels.

Consistent with the proposal developed above and with the Dodge (1948) guidelines, it can be noted that the equality line between S_{init} and S_{dep} constitutes a clear upper envelope.

Beneath the equality line envelope, scattering is considerable. The existing equations for the deposition slope mentioned in SABO Division (2000); D'Agostino (2013b), and Osti and Egashira (2013) ($S_{dep} \approx 1/2 S_{init}$ - Eq. 2.11a and $S_{dep} \approx 2/3 S_{init}$ - Eq. 2.11b) provide a good average estimation, although the complete envelope is roughly provided by:

$$S_{dep,MAX} \approx S_{init} \tag{2.21a}$$

$$S_{dep,min} \approx 1/3 \; S_{init} \tag{2.21b}$$

It is important to stress that these data are all measured in laterally confined beds and that, to the authors' knowledge, there is no equiva-

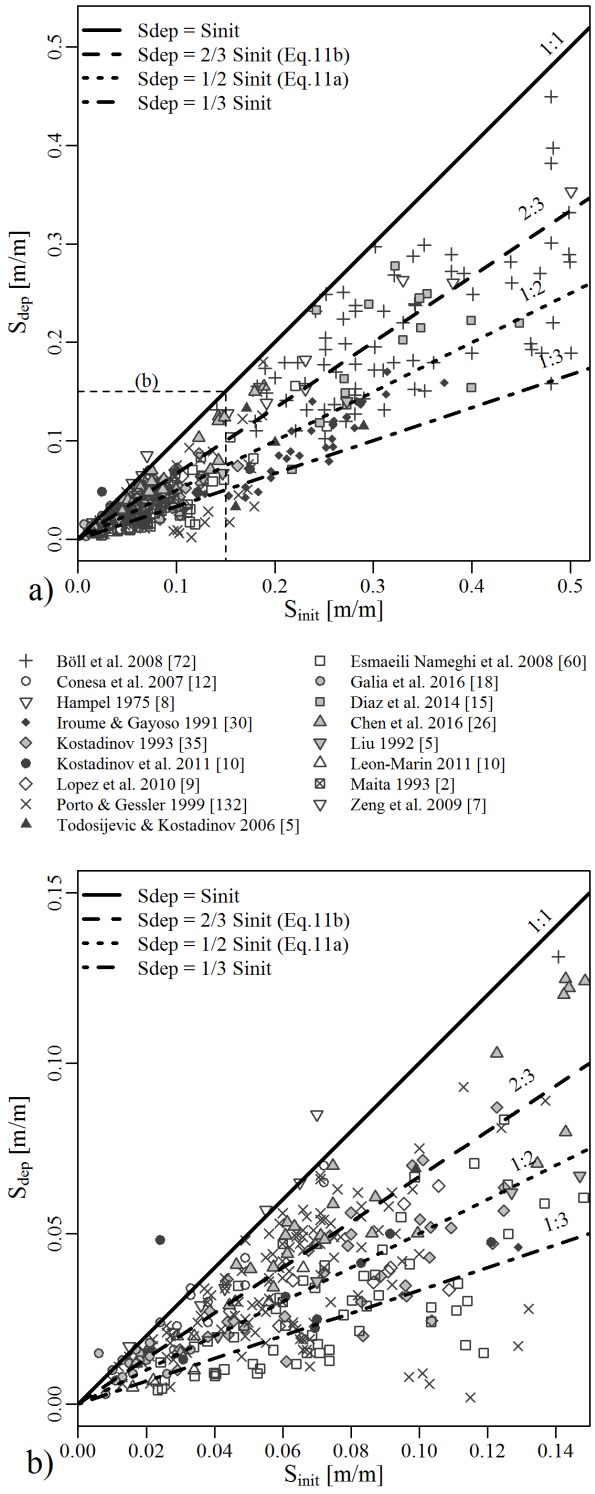

Figure 2.12 – Comparison of the deposition slope and the initial channel slope on a data set with 456 field measurements: a) within the complete range and b) zoom on the slopes < 0.15. Confirmation of the nearly systematic relation $S_{dep} \leq S_{init}$ (Numbers between brackets are the number of data of each reference)

lent data set of slope measurement in artificially widened basins such as upstream of open check dams (see below).

C. Hillslope–channel coupling in small-scale models

Small-scale experiments are useful tools, but they must be used with caution when studying erosion processes. One of the multiple problems emerging in gully laboratory models is that respecting similitude of geomechanics (to correctly represent hillslope dynamics) requires increasing gravity when the scale decreases (Heller, 2011), which is not done in typical hydraulic laboratories. In other words, classic small-scale models represent the channel sediment transport processes fairly well, but poorly represent the actual hillslope stability. The representativeness of the initial slope and its coupling with the hillslope stability, which are known to be key drivers of river longitudinal profiles (Egholm et al., 2013) and thus of S_{init}, are consequently subject to dramatic uncertainties in small-scale models. This is the main reason why the authors did not include laboratory data in the Fig. 2.12 data set: S_{dep} is likely to be reliable but S_{init} is likely to show poor reliability.

In one case of a small-scale model experiment, without hillslope coupling, with rigorously similar supply conditions and sufficient time to wait for the dynamic equilibrium settling, the deposition slope with check dams was observed not to differ from the reference slope without check dams (Piton and Recking, 2016c), *i.e.*, $S_{dep} \approx S_{init}$. On a simple laboratory case, it confirmed that in pure alluvial contexts, check dams do not induce slope reduction. Conversely, although the mean value and dynamics of the initial slope – products of long-term geomorphic adjustments between geology, climate, land use, hydraulics and hillslope, and tributary dynamics – are complicated to model rigorously in the laboratory, it seems more reliable to attempt to determine methods to estimate the deposition slope based

on measurable flow features like the equations proposed by the discussers.

D. Influence of the lateral constraint relaxation

In bed-load transport reaches, the transport capacity and thus the slope equilibrium depend on the river width (Hunzinger, 2004). Böll (1997), for instance, following consideration based on the gravel threshold of motion, proposed :

$$S_{dep} = 0.4 \frac{D_{90}^{9/7}}{(Q_{max}/W)^{6/7}} \qquad (2.22)$$

with Q_{max} the maximum water discharges in the channel (m^{33}/s), W the channel width (m) and D_{90} the sediment diameter such that 90% of the sediment mixture is finer (m). Eq. 2.22 gives similar deposition slopes on both the fan channel and upstream of a check dam, if the discharge, width and sediment sizes are similar. Conversely, the deposition slope should increase if the deposit occurs in an artificially widened basin.

Similarly, but for debris flow deposition, Hungr et al. (1984) reported that deposition slope measurement of debris flows occurring on the Canadian west coast usually settled between 8 and 12°, *i.e.*, $S_{dep} \approx 0.14 - 0.21$ when confined and 10–14°, *i.e.*, $S_{dep} \approx 0.18 - 0.25$ when laterally unconfined.

However, to the authors' knowledge, no clear quantification of this lateral constraint relaxation exists to date. It is not yet clear if Eq. (2.22) can be applied when multi-channel braided patterns appear, as is usually the case in wide reaches. Determining which value of W is relevant to use in the sediment transport formula is a recurrent issue in braided river morphology (Recking et al., 2016). The question of determining the deposition slope upstream of check dams and open check dams is therefore still worthy of investigation.

Notation

The following symbols are used in this section:

D_{90} = sediment diameter such that 90% of the sediment mixture is finer (m).

g = gravitational acceleration (m/s^2);

Q_{max} = maximum water discharge in the channel (m^3 /s);

S_{dep} = deposition slope (m/m);

S_{init} = initial slope of the upstream stream in a reach not disturbed by anthropogenic structures (m/m);

W = river or basin width (m);

γ = dimensional debris flow density = ρg (kN/m^3);

ϕ = internal friction angle of the debris flow (°);

ρ = debris flow density (kg/m^3);

"Sometimes, a picture is worth a thousand words."

Incredible woody debris accumulation, jamming an open check dam on the Trübenbach, Kärnten AUT. (Photo: WLV in Hübl et al., 2003)

CHAPTER 3

Design of Sediment Traps with Open Check Dams. II: Woody Debris

Guillaume PITON[a], Alain RECKING [a]

[a] Université Grenoble Alpes, Irstea, UR ETGR, St-Martin-d'Hères, France.

This chapter is the second part of two yet published, companion papers[1].

As developed in Chap. 1, flood hazards in torrents are strongly related to their capacity to erode and transport massive amounts of sediment. Everywhere vegetation grow, these flood erosions also recruit floating materials as dead-wood pieces and living trees. Experience demonstrates that woody debris sometimes play a key role in the functioning of hydraulic structures, as, for instance, open check dams; generally perturbing the theoretical "pure hydraulics" functioning. As a consequence, it is important to take them into account when designing such structures. This work thus aims at summarizing the state of knowledge concerning woody debris production and their interaction with open check dams.

NOTA: The additional notes brought to this chapter since its journal publication are highlighted in grey.

[1]Piton, G. and A. Recking, **(2016)**. "Design of Sediment Traps with Open Check Dams. II: Woody Debris", *J. Hydraul. Eng.* ASCE, Vol. 142, no. 2, 17 pp., DOI:10.1061/(ASCE)HY.1943-7900.0001049

Abstract

Sediment traps with open check dams are widely used structures in flood hazard mitigation. This paper and its companion review the literature on their design. The companion paper examines hydraulic and deposition processes associated with sediment transport. However, field feedback has shown that open check dam behaviours during floods are dramatically influenced by the presence or absence of driftwood. To better assess large woody debris hazards and influences, this paper first reports the methods available to estimate driftwood production in terms of volume and dimensions. Information is given on their recruitment and transfer in the catchment. The presence of driftwood and the relevance of trapping them strongly influences the choice of the suitable shape and type of the open check dam. The performance of the different open check dam shapes in terms of driftwood management are detailed. Design criteria to estimate clogging probabilities, trapping efficiencies, volume capacities to trap driftwood and hydraulic head losses due to driftwood accumulations are detailed. A step-by-step design procedure is proposed, and finally, suggestions to complete today's knowledge are outlined. **Author key words:** *Driftwood, floating material, wood jam, sediment basin*

3.1. Introduction

In addition to water and sediments, rivers transport floating materials during floods, generally mainly composed of woody debris. In torrents, driftwood likely to cause problems in hydraulic structures, hereafter called large woody debris (LWD), can be defined as being longer than 1 m and greater than 10 cm in diameter (Braudrick et al., 1997). Naturally, this definition must be adapted to the size of the river and the structures studied (Wohl et al., 2010). For instance, in large lowland rivers, bridges and dam spillways are generally designed to be unaffected by logs that are a few metres long. Driftwood can be dead wood, recently uprooted stand trees or logged trees stored by human activities in the flooded area and recruited by floods with an unusually high water level. Anthropogenic floating material such as cars, caravans, gas cisterns and plastic pipes can participate in floating debris accumulations. All these materials are considered to cause similar problems to LWDs.

The stabilising effects of vegetation have been understood for centuries and were emphasised in old documents on torrential hazard mitigation, for instance in Japan, France and Switzerland during the late 17th and the 18th centuries (Fabre, 1797; Vischer, 2003; Okamoto, 2007). Good practice guidelines are currently to maintain riparian forests but prefer vegetation in the coppice state (Poncet, 1995; Rudolf-Miklau and Hübl, 2010). Even if they reinforce banks against flow shear stress, stand trees are sometimes uprooted and conveyed by floods. Narrow sections and under-designed bridges and culverts are then preferential areas for LWD accumulation. They generally aggravate hazards related to water and sediment transport (Ishikawa and Mizuyama, 1988; D'Agostino et al., 2000; SABO Division, 2000; Jaeggi, 2007; Rudolf-Miklau and Hübl, 2010; Schmocker and Hager, 2011; Schmocker and Weitbrecht, 2013) but are seldom taken into account in hazard mapping (Mazzorana et al., 2009). Although the transport of a single log generally does not induce flooding or overflows, when congested, LWD can abruptly accumulate on a structure or a nat-

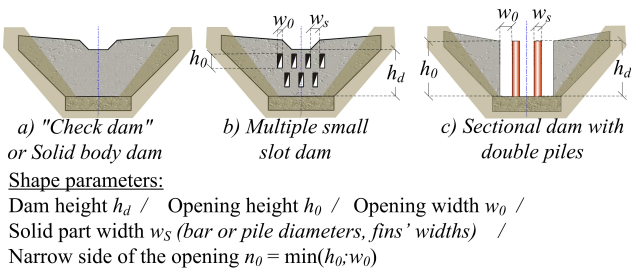

Figure 3.1 – Schematic downstream view of a) a "check dam" or solid body dam, b) a multiple small slot dam and c) a sectional dam with 2 piles (structures' names following the Wehrmann et al. 2006 classification ; reprinted from Hübl et al. 2005, with permission)

ural obstacle and become an unpredictable source of hazard (D'Agostino et al., 2000).

Check dams are transversal structures built in stream beds for torrent control purposes (Fig. 3.1). Structures without openings, hereafter refered as solid body dams, have been built in number since the mid 19^{th} century (Vischer, 2003). Check dams with openings increased in number, since the 1970s, to improve sediments and LWD management structures. The companion paper explores the design of sediment traps with open check dams. It more specifically details hydraulic and deposition processes associated with sediment transport. In sediment traps as well as in all structures built across watercourses, LWD can dramatically influence flow transfer. Since the 1997 floods in Switzerland, greater attention has been paid to LWD and structure interactions (*e.g.*, Bezzola et al., 2004; Lange and Bezzola, 2006; Schmocker and Weitbrecht, 2013; Schmocker and Hager, 2013). Pioneering work was undertaken in Japan during the 1990s (*e.g.*, Uchiogi et al., 1996; Kasai et al., 1996).

A good assessment of the potential influence of LWD in open check dams is crucial and is therefore investigated in this paper, which, in the first part, reviews the literature on LWD production in torrential watersheds, recruitment and transfer by floods. In the second part, the sensitivity to LWDs of the main types of open check dams is reported. Finally, design criteria concerning LWD and open check dams are provided, a step-by-step design procedure is proposed and what remains to be investigated is noted. For similar aspects in larger low-land rivers, see the reviews by Bradley et al. (2005) and Schmocker and Weitbrecht (2013).

3.2. Assessing woody debris volume

3.2.1. Preliminary remarks

As for watershed sediment production, LWD recruitment and transfer remains a largely open question (Comiti et al., 2012). The following section reports formulas and methods to estimate naturally produced LWDs. If significant wood has been logged or has accumulated in the watershed due to human activity, engineers must take this point into consideration when estimating LWD watershed production (Lange and Bezzola, 2006). Historical forest management can also play a role on LWD production (Nowakowski and Wohl, 2008).

When assessing LWD volumes and accumulation, the first variable underreported in the literature is the porosity of the LWD accumulation: $\frac{V_{LWD}-\Sigma V_{log}}{V_{LWD}}$ with V_{LWD} the LWD accumulation volume (m^3) and ΣV_{log}, the sum of the volume of each individual log (m^3). It can significantly change depending on the shapes of the logs and on the hydraulic constraints that led to the accumulation, from 0.5 to 0.8 for dense to loose accumulations (Lange and Bezzola, 2006). Few authors have clarified whether the method gives a sum of the log volumes or an accumulation volume with a given porosity. Actually, taking into account the natural strong stochastic component of the phenomenon, today's methods generally do not target a highly accurate result but seek to give an order of magnitude of potential LWD production.

3.2.2. Woody debris production

LWDs mainly come from three different areas: (i) landslides and hill slopes (avalanches, windfall, etc.), (ii) steep slope tributaries and (iii) banks and vegetated terrace erosion (SABO Division, 2000; Mazzorana et al., 2009; Wohl et al., 2009). In steep small mountainous watersheds, LWD catastrophic production is regularly reported to mainly come from landslides (*e.g.*, Masuko et al., 1996; Comiti et al., 2008). In contrast, large lowland rivers, especially former braider rivers with numerous vegetated terraces, usually mainly recruit LWDs through bank erosion (*e.g.*, Comiti et al., 2012; Bertoldi et al., 2013). Between these two types of torrential watercourses, in mountain valley rivers, the LWD supply tends to be strongly influenced by debris flow-prone tributaries as well as both of the aforementioned production areas depending on sites' features (Wohl et al., 2009; Wohl et al., 2012). Two main types of methods are proposed in the literature to assess LWD production: (i) empirical methods based on flood characteristics and, (ii) map analysis of production areas.

A. Flood characteristic methods

These methods have generally been calibrated in deposition areas where LWDs and sediments were mechanically excavated or in accumulation areas close to a gauging station. The expected LWD volume can be estimated using the following formulas for each flood event:

$$V_{LWD} = 4 \times V_{Wat}^{2/5} \qquad (Rickenmann\ 1997) \tag{3.1}$$

$$V_{LWD} = \beta \times V_{sed,trapped} \qquad (Uchiogi\ et\ al.\ 1996) \tag{3.2}$$

with the LWD, water and sediment volumes (m^3) expressed by V_{LWD}, V_{Wat} and $V_{sed,trapped}$, respectively, and β the LWD to sediment volumes ratio. Uchiogi et al. (1996) retained $\beta = 0.02$.

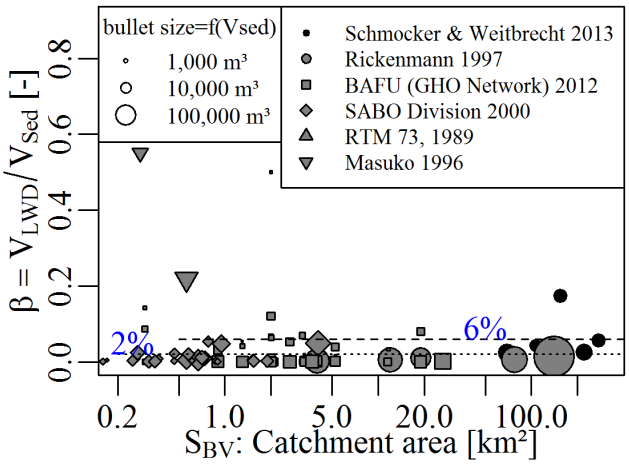

Figure 3.2 – Ratio of $\beta = V_{LWD}/V_{sed,trapped}$ depending on the catchment area for several datasets (Masuko et al., 1996; Rickenmann, 1997b; SABO Division, 2000; BAFU [GHO Network], 2016; Schmocker and Weitbrecht, 2013), $\beta = 0.06$ is about the 90% quantile.

The Japanese *Guideline for Driftwood Countermeasures* shows that this value is the higher limit of scattered values measured during the major disasters that occurred in Japan in the 1980s and 1990s (SABO Division, 2000). A higher ratio than the basic 2% can be expected in small forested watersheds, as observed in Switzerland during the 1997 floods (Bezzola et al., 2004). Actually, the SABO Division (2000) report events when β reached 0.20 to 0.30 in small watersheds with S_{BV} the watershed surface $\lesssim 1km^2$. Even for larger watersheds ($S_{BV} \in [70; 460km^2]$), a post-analysis of the 2005 floods in seven Switzerland streams using Eq. (3.2) showed that β varied between 0.02 and 0.17 (mean value, 0.06; standard deviation, 0.054; Schmocker and Weitbrecht, 2013). Figure 3.2 gathers a few measurements of β from some field data[1], showing that in 90% of the recorded floods, $\beta < 0.06$ and that this approach seems relevant for catchment of quite diverse sizes ($S_{BV} \in$ [0.2;460km^2]).

To date, the data coming from disaster feedback have been too scarce to develop more de-

[1]The RTM 73, 1989 reference corresponds to the Merdaret flood (La Chapelle St Martin-Traize) of 1989, producing 5,000 m^3 of driftwood in a 5.2 km^2 catchment (source: G. Charvet RTM 73, *pers. com.*).

tailed and precise methods taking into account watershed features in addition to flood intensity, as done for normal LWD densities in watercourses (*e.g.*, Nowakowski and Wohl, 2008; Wohl and Goode, 2008; Cadol et al., 2009; Wohl and Jaeger, 2009). The drawback of Eqs. (3.1) and (3.2) is that the water and sediment volumes have to be accurately estimated, a complex task; on the other hand, it relates LWD volume to flood magnitude.

B. Production areas analysis methods

These methods consist in map analysis with various degrees of complexity. Recent work and GIS development have improved their accuracy. Following the 1997 floods in Switzerland, Rickenmann (1997b) proposed three simple empirical formulas:

$$V_{LWD} = 40 \times L_{For}^2 \text{ for } L_{For} < 20 \text{ km} \quad (3.3)$$

$$V_{LWD} = 45 \times S_{BV}^{2/3} \text{ for } S_{BV} < 100 \text{ km}^2 \quad (3.4)$$

$$V_{LWD} = 90 \times S_{BV,For} \quad (3.5)$$

with L_{For} the forested length of the upstream reach (km), S_{BV} the watershed surface and $S_{BV,For}$ its forested part (km^2). Similar to Eq. (3.5), Uchiogi et al. (1996) suggested considering a proportionality between the LWD volume and the forested watershed surface, but only the part steeper than 5°, denoted as $S_{BV,For>5°}$ (km^2):

$$V_{LWD} = \gamma . S_{BV,For>5°} \quad (3.6)$$

Equation (3.6) has been calibrated on watersheds with $S_{BVFor>5°} \lesssim 2km^2$. Depending on whether the forest is evergreen or deciduous, γ belongs to a range of [10; 1000] or [10; 100], respectively. The upper values represent the envelop of the maximum possible production (see SABO Division, 2000 for details). Equations (3.3 - 3.6) do not take into account parameters representing the flood magnitude, these formula evaluate the maximum LWD production based on disaster feedback.

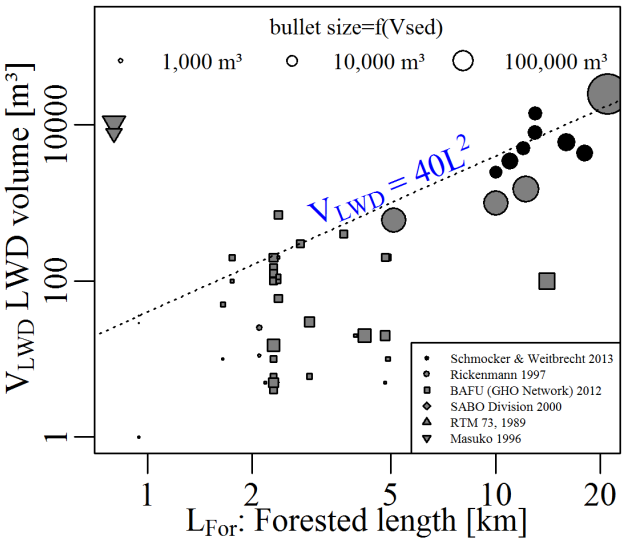

Figure 3.3 – LWD production depending on the forested length of the stream for several datasets (Masuko et al., 1996; Rickenmann, 1997b; SABO Division, 2000; BAFU [GHO Network], 2016; Schmocker and Weitbrecht, 2013), only 6% of the flood data overpass Eq. 3.3.

Observing data from the few available datasets, Figure 3.3 shows that Eq. (3.3) is a reasonable envelope, only 5% of the data are higher if a coefficient 45 is taken rather than 40. Concerning the catchment area-dependent Eqs., Figure 3.4 shows that $\gamma = 100$ m^3/km^2 is about the quantile 85% and only the extreme data of Masuko et al. (1996) (see below) strongly overpass the existing data with $\gamma = 1{,}000$ m^3/km^2. The coefficient of 45 in Eq. 3.4 seems a bit underestimated, the equation would correspond to the 80% and 95% quantiles with coefficients of 100 and 450, respectively.

After the June, 13th 1993 typhoon in Japan, Masuko et al. (1996) reported that in case of substantial windfall and large landslides, V_{LWD} reached six times the volume computed with Eq. (3.2) ($\beta = 0.02$) and nine times the volume computed with Eq. (3.6) in a 0.84-km^2 watershed, highlighting the key role played by landslides in LWD production.

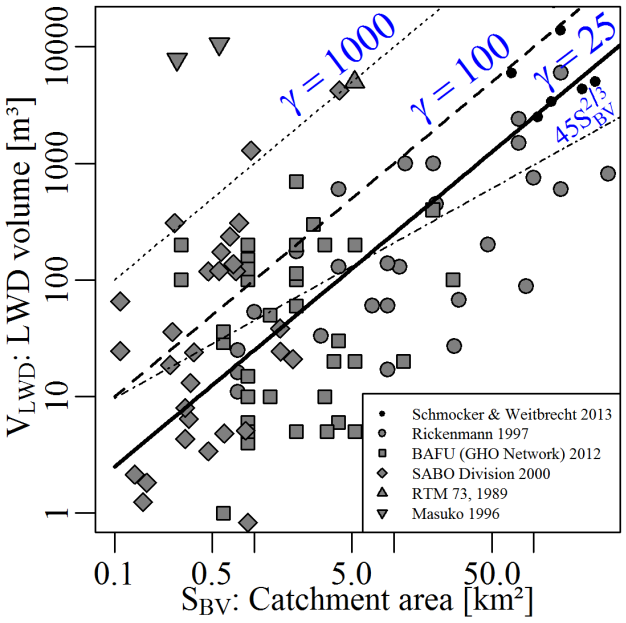

Figure 3.4 – LWD production depending on the catchment size for several datasets (Masuko et al., 1996; Rickenmann, 1997b; SABO Division, 2000; BAFU [GHO Network], 2016; Schmocker and Weitbrecht, 2013), see the comment in text for the Eqs. criticisms.

More recently with the same idea of volume conservation between production area (Fig. 3.5) and deposition sites, a more detailed approach was proposed by Mazzorana et al. (2009). The procedure consists in mapping five different production areas from existing GIS databases (relief, flood hazard, landslide sensitivity, etc.). A recruitment coefficient is adjusted for each type of area depending on forest density. A more detailed procedure was later proposed to take into account flood dynamics, LWD recruitment depending on velocity and water depth and estimation of the clogging probability of existing structures (Mazzorana et al., 2011).

All authors agree that field surveys are absolutely necessary to assess forest erosion, debris flows and landslide sensitivity and to adjust the method's parameters (*e.g.*, dead wood and stand tree density, average log volume, tree height).

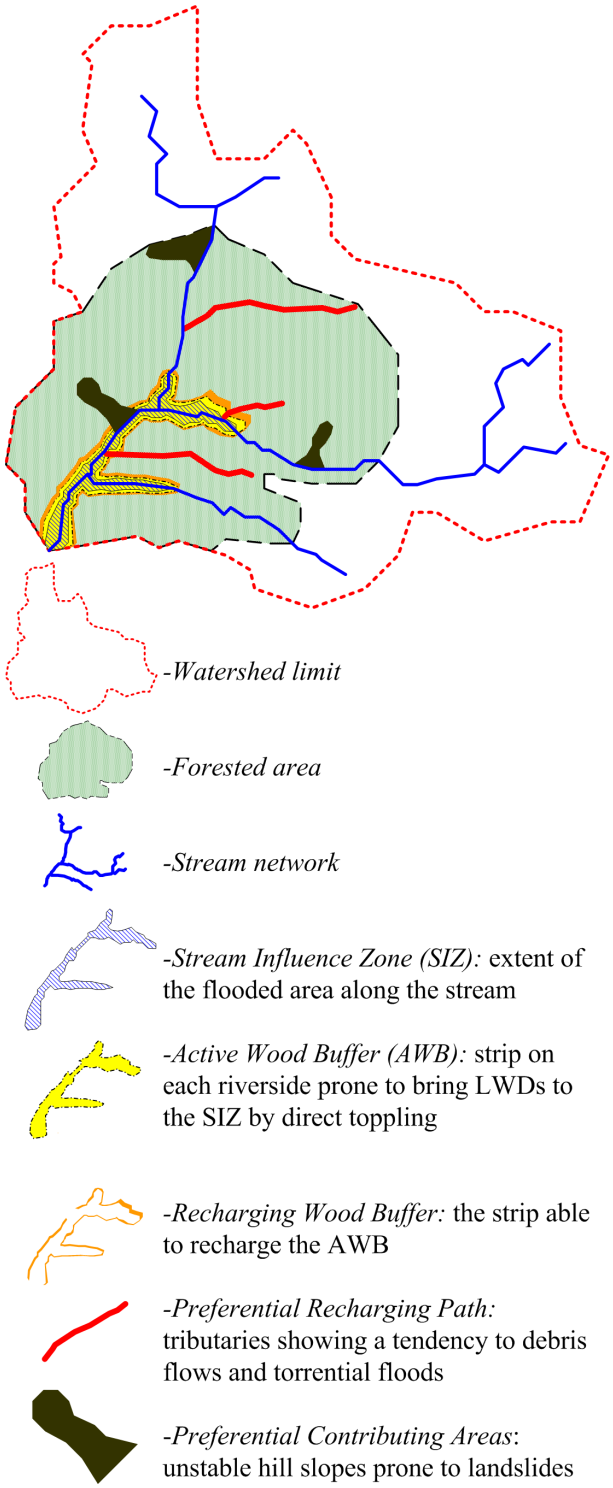

Figure 3.5 – Schematic spatial delimitation of the different woody debris recruitment areas defined in the Mazzorana et al. (2009) method (adapted from Mazzorana et al. 2009, with permission)

3.3. Woody debris recruitment

The different LWD production estimation methods generally take into account the recruitment and transport from production areas to the site studied. Nonetheless, some authors have focused on recruitment and transport problems.

3.3.1. LWD recruitment process

For a given flood, LWD recruitment depends on the past floods' recruitment, which is influenced by the hydrological history, most particularly the time since the last severe flood event. Dead wood density and stand trees on terraces grow with time. When extreme events occur, banks are eroded and flood plains are inundated; standing trees are then uprooted and floating logs captured by the flow. It is generally considered that LWDs appear when the hydrograph rises (Zollinger, 1983), but detailed field surveys are still needed on this point.

At the log scale, the threshold for motion by flotation depends on the water depth, the log diameter, the water and log density and the channel features (see Braudrick et al., 1997; Braudrick and Grant, 2001; Mazzorana et al., 2011 for details). LWDs can be transported in uncongested, semi-congested or congested regimes, *i.e.*, with increasing piece-to-piece contact and influences. Transported logs tend to be trapped by existing LWD accumulations, or simply individual large trunks, especially if they occupy a substantial width of the riverbed (Wohl and Jaeger, 2009; Wohl et al., 2009; Chen and Chao, 2010; Beckman and Wohl, 2014). Once destabilised, their transportation tends to occur in the congested regime (Braudrick et al., 1997). The ratio between L_{LWD} the entire LWD length with the root wad (m), and W stream width (m) play a key role in the transfer. Low-order streams with $W/L_{LWD} \approx 1$ are prone to creating LWD accumulations and thus to undergoing congested transport.

Small-scale experiments have shown that hydraulic jump tends to disaggregate log clusters, giving back a less congested log flow. This property could be used where LWD clogging has to be prevented, since congested transport increases jamming probability (D'Agostino et al., 2000; Degetto and Righetti, 2004). However, sediment deposition often occurs in the vicinity of hydraulic jumps and tends to make them disappear (Hunzinger and Zarn, 1996, see companion paper).

3.3.2. LWD length

When log dimensions and channel width are on the same order of magnitude, stable LWD accumulations can be created and the longest logs are generally not transferred downstream. In gullies with longer L_{LWD} than channel width, LWDs often create stable accumulations and are sometimes considered to stabilise the system (Poncet, 1995; Lancaster et al., 2001).

Uchiogi et al. (1996) and Hasegawa et al. (2010) estimated $L_{max,LWD}$ the maximum transportable log length using $L^*_{Stand\ tree} = {}^{L_{Stand\ tree}}/_{W}$, the dimensionless stand tree length:

$$L_{max,LWD} = L_{Stand\ Trees} \text{ if } L^*_{Stand\ tree} < \eta \tag{3.7a}$$

$$L_{max,LWD} = \eta W \text{ if } L^*_{Stand\ tree} > \eta \tag{3.7b}$$

with η the dimensionless threshold length, $\approx$ 1.3-1.67 based on small scale debris flow experiments. Field surveys of mountain rivers seldom report mobile LWD longer than the channel width, *i.e.*, $\eta \approx 1$ (*e.g.*, Nowakowski and Wohl, 2008; Wohl and Goode, 2008; Wohl et al., 2009).

However, not only $L_{max,LWD}$ must be estimated for structure design but also the $L_{mean,LWD}$ the mean log length (Shibuya et al., 2010; Ishikawa et al., 2014). Field survey and historical analysis are necessary to determine LWD characteristic sizes: $L_{mean,LWD}$, $L_{max,LWD}$ and D_{LWD}.

3.3.3. LWD velocity

The particle tracking velocimetry (PTV) technique used by D'Agostino et al. (2000) and Degetto and Righetti (2004) showed that LWD and mean surface water velocity were nearly equal. The SABO Division (2000) also considers that LWD velocity is equal to the water surface velocity in bed-load reaches ($\approx$ 1.2 mean section velocity) and equal to the mean flow velocity in debris flow reaches. Mizuyama (1984) used video analysis to explain how velocity distribution in debris flow fronts and low LWD density result in LWD accumulation on debris flow fronts. Using PTV, D'Agostino et al. (2000) observed that LWD axes and the flow direction were not parallel in 97% of the logs observed. Degetto and Righetti (2004) showed that LWD transported at the centre of the flow tends to present a more transversal position, compared to the flow direction, than LWD transported near the banks. Finally Shrestha et al. (2012) showed that the mean plane rotation velocity was null on average, but its variability was proportional to the Froude number.

3.4. Woody debris entrapment

A number of different open check dams designs were tested and built (Zollinger, 1985). To encourage consistency in the vocabulary used to refer to all these structures, the Wehrmann et al. (2006) classification is used in this paper and its companion. Even if LWD trapping shows a strong intrinsic stochastic component (D'Agostino et al., 2000), some general trends can be drawn from the literature and field feedback.

3.4.1. LWD accumulation pattern

Schmocker and Hager (2013) described how LWD accumulations tend to develop against a vertical rack (Fig. 3.6). These small-scale experiments seem consistent with feedback from the field for different types of structure (*e.g.*, Lange and Bezzola, 2006). At the beginning, LWD tends either to get trapped against the structure or to pass it if it approaches it with the proper angle and velocity (Fig. 3.6a). As soon as some LWD has been trapped, the structure porosity decreases, the probability of LWD being trapped increases and accumulation begins. LWD being stuck by the approaching velocity, the accumulation first develops against the structure (Fig. 3.6b). The diminishing structure's porosity increases the water head loss, the upstream water depth and thus the upstream Froude number and approaching velocity. Once the water depth has significantly increased, approaching velocities become too low to carry LWD underwater and stuck them against the structure. The LWD then tends to accumulate as a floating carpet and no longer as a dense accumulation against the structure (Fig. 3.6c). The time it takes to fully develop the first step of dense accumulation depends on the total open surface to clog.

In low-slope basins with a sufficient water-depth-to-log-diameter ratio, processes separating sediments and LWDs can occur (Bezzola et al., 2004; Comiti et al., 2012 & Fig. 3.7). Sediments are expected to deposit upstream when entering the backwater-influenced area and LWDs are likely to be transported and clog the open check dams. This phenomenon can also occur if the volume of sediment supplied during a flood is lower than the basin volume. If the basin is filled up to the crest, LWDs have often been released or are stored on the sediment. In addition to the natural accumulation of LWD against structures, sediment deposit tends to store significant amounts of LWD as soon as flow depth becomes comparable to LWD diameter, as in braided rivers (Welber et al., 2013; Bertoldi et al., 2013; 2014).

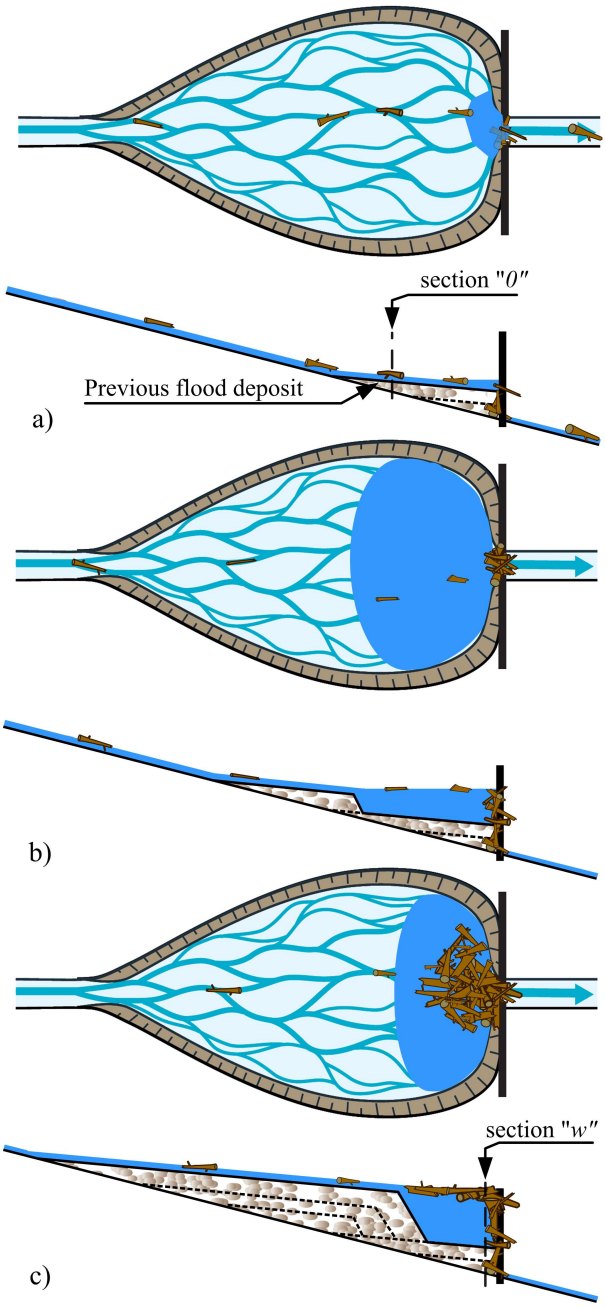

Figure 3.6 – Main steps of a LWD accumulation formation: a) initial trapping of the first pieces, b) LWDs are stuck against the structure by drag forces and sediment loading, they decrease the structure porosity and increase its backwater effect, and c) development of a floating carpet when flow velocities are no longer able to entrain LWDs underwater (adapted from Lange and Bezzola 2006, with permission)

3.4.2. Structure type performances in LWD and sediment trapping

The choice of the structure type and shape is often mainly dictated by the presence and the absence of LWD, and whether or not it must be trapped. Table 3.1 summarises the different structure types' performances in LWD and sediment trapping.

Structure overloading and LWD release induced by structure saturation must be prevented. Rimböck (2004) proposed simple indicators to estimate this overloading state (see Fig. 3.8 for recommendations): he recommended restricting the use of light structures (net and pile sectional dams) to streams with limited V_{LWD}/W, LWD unit accumulation volumes (m^3/m) and limited Q/W, water unit discharges ($m^3/s.m$) with Q the water discharge (m^3/s), V_{LWD} the LWD volume (m^3) . The following sections describe the specificities of the main types of structure cited in Table 3.1.

A. Rope nets

Rope net barriers are light structures (Fig. 3.8b). Depending on their location and the type of stream they equip, they are mainly designed for LWD or debris flows trapping (Rimböck and Strobl, 2002; Volkwein et al., 2011). Net dams can be very effective in trapping sediment due to their backwater effect (Rimböck, 2004; Lange and Bezzola, 2006). Rimböck (2004) proposed limiting the use of this kind of structure to narrow mild-slope streams ($W < 15m$; slope$< 5\%$) with limited sediment accumulation unit volumes ($V_{sed,trapped}/W < 100m^3/m$) in addition to the restrictions illustrated in Fig. 3.8. These structures have to be carefully located to avoid asymmetrical currents and loading (see Rimböck, 2004 for a detailed design procedure). A ground sill must be built under net dams and sectional dams

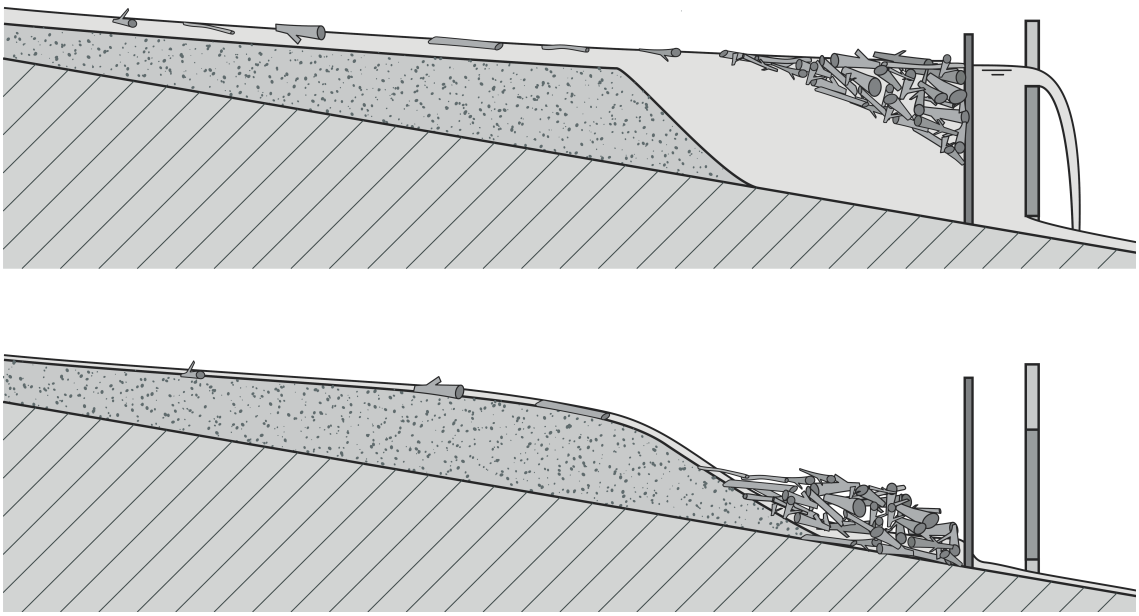

Figure 3.7 – Separation of bed-load and LWDs as a consequence of a provoked backwater (reprinted from Bezzola et al. 2004, with permission)

Table 3.1 – Structure type performances in LWD and sediment trapping

Sediment trapping	Nearly total LWD trapping	Partial LWD trapping	Limited LWD trapping
Nearly total trapping	Net dams Lattice & frame dams "Small"* slot & slit dams	Sectional dams	†
Partial trapping	Inclined rakes and fins dams Slot & slit dams with crest baffle		Solid body dams Chicane dams

Note: "Large"* slot and slit dams present highly changeable behaviour depending on LWD presence, see text.

* "small" and "large" in term of relative opening, see Eq. (3.8) and companion paper Eq. (2.2).

† In torrential context, no structure traps all sediments but no LWD, both are linked, at least partially.

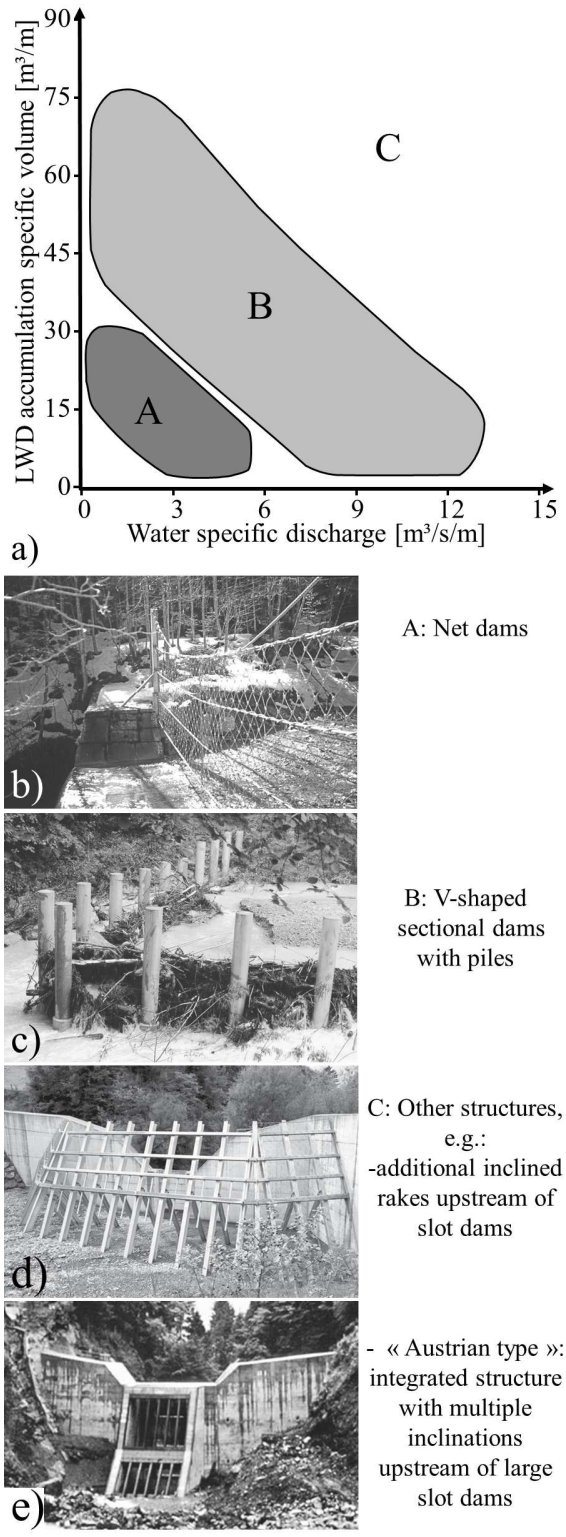

Figure 3.8 – Recommended range of use for different woody debris entrapment constructions: a) graph of adapted structure type depending on specific LWD accumulation volume and specific water discharge at the structure; b) net dams [(a) and (b) reprinted from Rimböck 2004, with permission]; c) V-shaped sectional dams with piles; d) additional inclined rakes upstream of slot dams; and e) Austrian type integrated structures with multiple inclinations upstream of large slot dams [(c), (d), and (e) reprinted from Lange and Bezzola 2006, with permission]

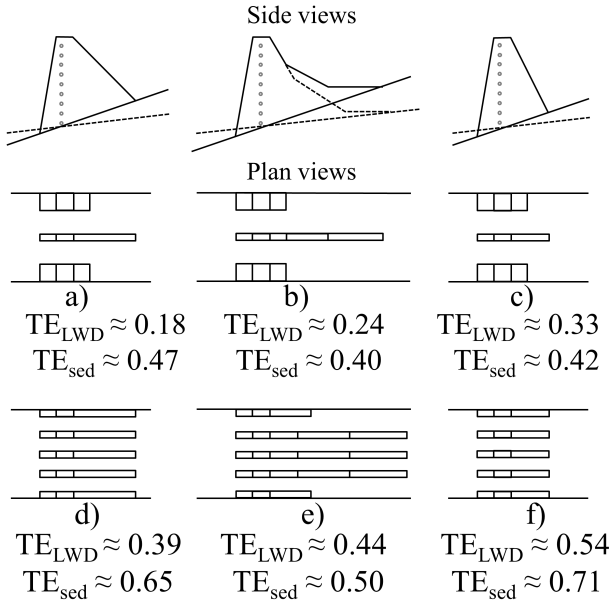

Figure 3.9 – Shape details of Austrian sectional dams tested by Ishikawa and Mizuyama (1988) and their respective TE_x, Trapping Efficiency of LWD and sediment, in their experimental conditions. All shapes were tested with and without a grill; shapes (a)-(f) are classified from the lowest to the highest TE_{LWD} without a grill

to prevent structure failures due to toe scouring and bank erosion (*e.g.*, Fig. 3.8b).

B. Sectional dams: piles or fins

Sectional dams are structures opened over more than half the dam-width and height (Fig. 3.1 *iii*). The structure's centre is generally composed of piles (columnar bodies, *e.g.*, Fig. 3.8c) or fins (narrow side charged walls, *e.g.*, Fig. 3.9).

Sectional dam designers seek a modest influence on low flows and small floods using large openings. Economical maintenance is expected in their use. In presence of LWD during a flood, the accumulation on the sectional dams creates a self-built dam, trapping other LWD and sediments.

Different shapes have been tested: the V-shape, ∧-shape (Fig. 3.10) and straight-shape (Bezzola et al., 2004; Lange and Bezzola, 2006; Koulinski and Richard, 2008). The choice is dictated by the need to increase the dam discharge capacity, which is nearly proportional to the total

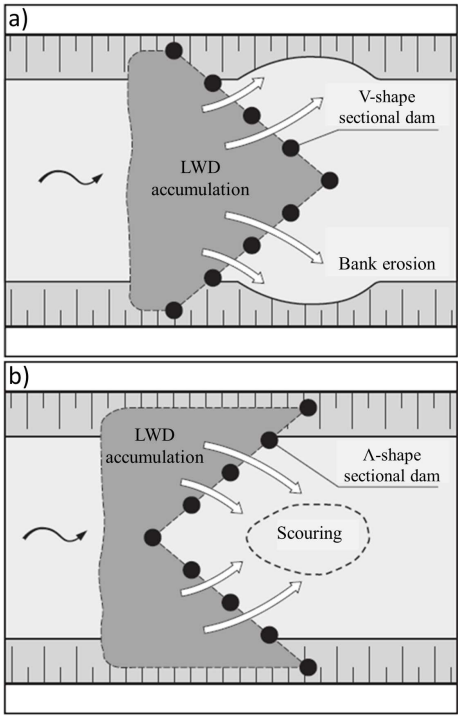

Figure 3.10 – Pile sectional dams: a) V-shape guiding flows toward banks and b) ∧-shape concentrating flows in a central scour hole; bed sill and bank protection are not represented for the sake of clarity (reprinted from Lange and Bezzola 2006, with permission)

structure's length. A V-shape will store LWD in the middle of the channel and guide passing flows toward the banks. In contrast, a ∧-shape will concentrate passing flows in a central scour hole (Lange and Bezzola, 2006 & Fig. 3.10). The straight-shape allows a continuity in flow direction but tends to store higher LWD unit volumes on a narrower structure, thus inducing a greater backwater effect.

If the structure is only built to trap LWDs and limited sediment trapping is sought, the design can be optimised to enhance the effect of secondary currents to store LWDs on one side when the main current still transports bed-load (Oda et al., 2008; Schmocker and Weitbrecht, 2013).

C. Frame dams and lattice dams: grills and racks

Japanese engineers have been developing frame dams and lattice dams made up of rakes and grills since the beginning of the 1970s (Kasai et al., 1996 & Fig. 3.11). Frame and lattice dams trap more LWD and sediments than sectional dams due their to narrower openings. Frame and lattice dam wings must be well designed, taking into account large over-topping and secondary currents in curves (Masuko et al., 1996; Rimböck and Strobl, 2002): designers have to prevent possible dam by-pass leading to significant bank erosion and probable dam failure (Hübl et al., 2005). Whenever possible, frame and lattice dams have to be designed sufficiently high to prevent over-topping; otherwise the check dam tends to store LWDs during the rising part of the hydrograph and can release it abruptly at the peak flows (Ishikawa et al., 2014).

Frames or lattices are sometimes added to a secondary dam (also called a counter-dam) on the foot of another first check dam (Fig. 3.11 a). During the 1967 disaster in Japan, Mizuyama (1984) reported that *"innumerable logs were found between main and secondary check dams"*. Small-scale experiments were undertaken to explore the phenomenon. It was observed that the reverse current taking place at the foot of main dams, upstream of counter-dams, tends to naturally store LWD. Counter-dam rakes are designed to improve this natural tendency.

D. Slit and slot check dams

Slit and slot dams present highly changeable behaviour depending on LWDs. Field feedback emphasises that the natural self-cleaning behaviour of slit check dams is particularly efficient (Mizuyama et al., 1988; Sasahara et al., 2002). Nonetheless, it generally no longer occurs once LWD clogs the opening. For example, in a small-scale model this phenomenon leads to three times more sediment storage with LWD than without (Koulinski et al., 2011). A number of specific structures have been developed to improve the basic behaviour of slit and slot check dams.

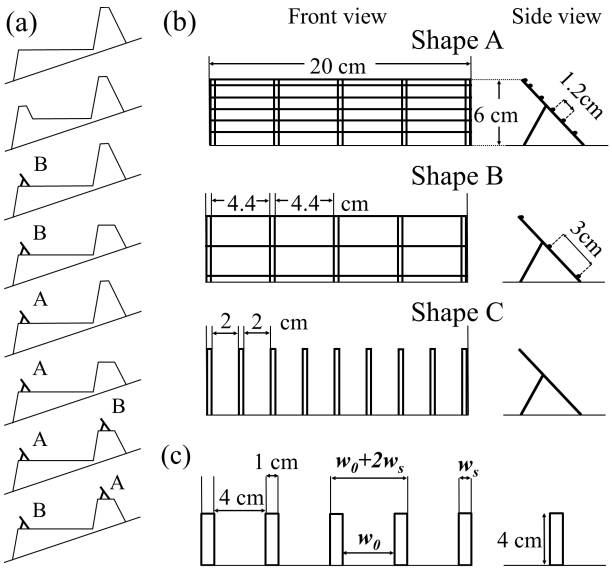

Figure 3.11 – Configurations and shapes of lattice check dams and grills: a) possible implantations of the grills on the check dam or its counter-dam. Configurations classified, from top to bottom, from the least to the most efficient in terms of trapping efficiency (Ishikawa and Mizuyama 1988); b) details of grill shapes tested by Ishikawa and Mizuyama (1988) to calibrate Eqs. (3.10) and (3.11) and c) details of grill shapes tested by Shibuya et al. (2010) to calibrate Eq. (3.12) (Note: shapes B and C were also used directly in a basin outlet configuration in the Eqs. (3.10) and (3.11) calibrations)

D.a. Austrian open check dams

Austrian open check dams are open check dams designed with inclined fins or racks emerging in the basin and forming an obstacle to the complete clogging of the dam slits or slots (Figs. 3.8e and 3.9). These open check dams maintain a sediment transfer capacity even in presence of LWDs (Ishikawa and Mizuyama, 1988; Lange and Bezzola, 2006; Rudolf-Miklau and Hübl, 2010) because the LWD accumulation slides up and down on the inclined structure (D'Agostino et al., 2000). On a vertical open structure, LWD tend not to move, once clogged against the openings, due the flow drag force and sediment loading (SedAlp, 2015b, App. 5.1). This sliding of the LWD accumulation frees the lower part of the inclined outlet allowing bed-load transport under the LWD accumulation. According to practitioners, the longer the bottom part with a low inclination, the better the sediment self cleaning capacity (M. Moser, *pers. com.* 2015). Fig. 3.9 also reports the lower sediment trapping of shapes (b) & (e) compare to other shapes with equivalent opening widths.

Using small-scale models, Ishikawa and Mizuyama 1988 showed that $TE_{sed} = {}^{V_{sed,trapped}}/_{V_{sed,supply}}$ the sediment trapping efficiency of this kind of structure was only 0.40-0.70 depending on the space between fins, the fins' shape and the basin slope (Fig. 3.9). The LWD trapping efficiency, *i.e.*, $V_{LWD}/V_{LWD\ supply}$ was of 0.20-0.60. In these tests, more than half of the LWDs were also transferred downstream because of the large space between the fins compared to D_{LWD} or L_{LWD}. Adding grills to these structures transformed them into rapidly clogged lattice dams with sediment trapping efficiency of almost 0.95 and LWD trapping efficiency of 0.60-0.80.

D.b. Dam crest baffle

Dam crest baffles are reported by Bezzola et al. (2004) in their review of driftwood retention works in Switzerland (Fig. 3.12). Such structures serve much the same purpose as upstream inclined

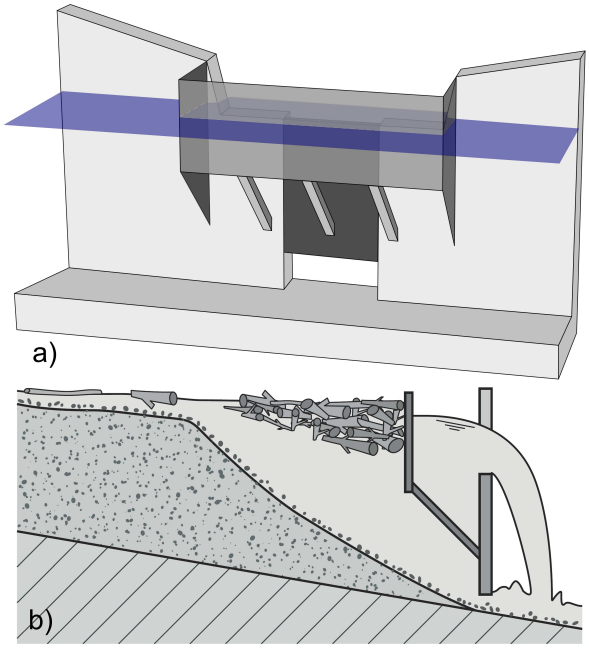

Figure 3.12 – a) Downflow baffle to retain driftwood in a slot dam (adapted from Bezzola et al. 2004, with permission) and b) flow conditions at a bottom slot dam equipped with a baffle (reprinted from Bezzola et al. 2004, with permission)

racks or fins but are lighter (compare Figs. Fig. 3.7 / 3.8d with Fig. 3.12). A baffle fixed upstream of the dam crest prevents floating material from over-topping the dam while bed-load and water can flow under the baffle. The hydraulic criteria of these structures are based on: (i) a minimum water depth, not to disturb bed-load transport; (ii) a maximum approach velocity to prevent an excessively dense log accumulation, and (iii) a maximum transfer velocity under the baffle, to prevent aspiration of logs, which could clog the structure (Bezzola et al., 2004). See Campisano (2009) for dimensionless equations describing floating material entrapment conditions upstream of dam crest baffles.

D.c. Chicane dam

In contrast, sediment sometimes needs to be partially stopped, but not LWD. An original solution was tested by Koulinski and Richard (2008). The structure looks like 25-m-spaced groynes. Since the opening is very large compared to other sediment traps, only a small proportion of the incoming sediment supply can be stored by this kind of structure (*e.g.*, $0.2V_{sed,supply}$ in Koulinski and Richard, 2008). The initially planned slit dam showed an unsatisfactory tendency to be clogged by LWD. The chicane check dam never clogged during experiments but was able to store the targeted sediment volume.

3.5. Design criteria

Once the structure shape is chosen, the sediment trap is designed following the criteria given in the companion paper. If LWDs are expected during floods, the design has to take into account their possible influences on the structure's behaviour. The following section presents methods to assess structure and LWD interactions.

3.5.1. Relative opening

The mechanical LWD clogging of open check dam outlets is clearly similar to boulder clogging, as described in the companion paper. The relative opening, *i.e.*, the ratio between the check dam characteristic opening size and L_{LWD} determines the likelihood of the structure clogging:

$$\textbf{Relative Opening} = \frac{Opening\ dimension}{Material\ dimension} = \frac{w_0}{L_{LWD}} \tag{3.8}$$

For floating materials, w_0, the horizontal width (m), is generally taken as the relevant opening dimension to assess clogging probability. L_{LWD} the LWD length is preferred to LWD trunk or root diameter because LWD tends to accumulate transversally to structures and seldom to flow exactly parallel to the flow direction (D'Agostino et al., 2000). Different authors have proposed various critical values for w_0/L_{LWD} below which clogging is probable (see Table 3.2). In sum, logs two and three times longer than the opening width are, respectively, likely and very likely to be trapped. The method proposed by D'Agostino et al. (2000) and detailed in the next section, can

Table 3.2 – Relative opening below which clogging is highly probable

Flood type*	Relative opening†	Sources
DF	1/3	Mizuyama et al., 1988
DF & BL	1/2-1/3	Uchiogi et al., 1996
DF & BL	1/2	SABO Division, 2000
DF & BL	2/3	Bezzola et al., 2004
BL	1/2-1/3	Wallerstein et al., 2013

* Debris Flow (DF) or Bed load (BL)
† $\frac{Opening\ dimension}{Material\ dimenson} = \frac{w_0}{L_{LWD}}$

also be used to design an open check dam with a given trapping efficiency (*e.g.*, Comiti et al., 2012).

If absolutely all LWD has to be trapped, n_0 the smallest dimension of the openings must be lower than D_{LWD} the LWD diameters (Ishikawa and Mizuyama, 1988). This induces a substantial increase in the clogging frequency. This conservative choice has to be reserved only for highly sensitive sites because traps will need more maintenance work to remove the regularly trapped woody debris.

3.5.2. Trapping efficiency

As for sediment, the more basic index of trapping efficiency is expressed as the ratio between trapped and supplied LWD volumes:

$$TE_{LWD} = V_{LWD}/V_{LWD\ supply} \tag{3.9}$$

with V_{LWD}, the volume of LWDs trapped in the open check dam basin (m^3) and $V_{LWD\ supply}$ the volume of LWDs supplied by the flood to the trap (m^3) estimated, for instance, using Eq. (3.1) to (3.6). $TE_{LWD} = 1$ means that all supply logs were trapped and $TE_{LWD} = 0$ that the structure is transparent to LWDs.

Generally speaking, LWDs tend less to be trapped when the water discharge, the Froude number or the relative opening increase (Ishikawa and Mizuyama, 1988; Campisano, 2009; Schmocker and Hager, 2013; Wallerstein et al., 2013; Ishikawa et al., 2014).

A. In high Froude number context with sediment deposits

Ishikawa and Mizuyama (1988) used small scale models of rake and grid dams to calibrate Eq.(3.10) (see Fig. 3.11a and b for shape and configurations). The authors tested varying relative openings, rake shapes, basin slopes, sediment supply volumes and presence or absence of a counter-dam. As the experiments were conducted in constant water supply, it is not clear if Fr_w and d_w must be computed for the mean flow discharge or the peak flow, with $Fr_w = \frac{v_w}{\sqrt{gd_w}}$ (-), the Froude number of the flow (at section w in Fig. 3.6), d_w the water depth and v_w the mean water velocity. Both might be tested and compared. In torrential conditions ($Fr_w \in [0.9; 3]$), they proposed estimating TE_{LWD} by:

$$TE_{LWD} = 1 \text{ if } \varphi \in [0; 0.8] \tag{3.10a}$$

$$TE_{LWD} = log_{10}\left(\frac{8}{\varphi}\right) \text{ if } \varphi \in [0.8; 8] \tag{3.10b}$$

$$TE_{LWD} = 0 \text{ if } \varphi \in [8; \infty] \tag{3.10c}$$

where φ is estimated with:

$$\varphi = Fr_w \frac{d_w}{D_{LWD}} \left(\frac{w_0}{L_{max,LWD}}\right)^2 \tag{3.11}$$

Shibuya et al. (2010) recently undertook complementary experiments. They confirmed the relevance of using Eq.(3.10) for pile sectional dams in high Froude flows but, paying attention to the influence of the logs' lengths, slightly modified the formulation of φ to increase the method's accuracy:

$$\varphi = Fr_w \frac{d_w}{D_{LWD}} \left(\frac{w_0 + 2w_s}{L_{mean,LWD}} \right)^2 \quad (3.12)$$

with w_s the solid structure width: pile diameter or fin width. They demonstrate that using $L_{mean,LWD}$ rather than $L_{max,LWD}$ in the φ computation give better results (see Fig. 3.11c for rake shape and parameter definitions).

B. In low Froude number context not influenced by sediment deposits

In pure water and subcritical conditions ($Fr \in [0.1; 0.2]$), D'Agostino et al. (2000) suggested expressing TE_{LWD} with parabolic curves adjusted on experimental results for each rake inclination:

$$TE_{LWD} = a_\alpha . \xi_{LWD}^2 + b_\alpha . \xi_{LWD} + c_\alpha \quad (3.13)$$

with ξ the single parameter of flow conditions, estimated with:

$$\xi_{LWD} = \frac{1}{Fr_w^2} . \frac{w_0}{L_{mean,LWD}} \quad (3.14)$$

The values of the curve parameters a_α, b_α and c_α for different inclinations are given in Table 3.3. Using Eqs. (3.13) and (3.14), LWDs tend more to be trapped in higher Froude numbers. The Froude number plays an inverse role when compared to other experiments (*e.g.*, Ishikawa and Mizuyama, 1988; Campisano, 2009; Schmocker and Hager, 2013). This inverse trend is likely to result from narrow range of Froude numbers tested in the experiments used to calibrate these equations. We therefore recommend not using Eqs. (3.13) in conditions with significantly different Froude numbers than those used for the calibration ($Fr \in [0.1; 0.2]$). Since their experiments were performed without sediment and with high LWD submersion d_w/D_{LWD}, LWDs could not be trapped on deposits or on the channel bed.

Table 3.3 – LW Trapping efficiency curve parameters of Eq. (3.13)

Rake angle with horizontal	a_α	b_α	c_α
90°	0.0006	-0.054	1.16
60°	0.0007	-0.068	1.20
45°	0.0015	-0.092	1.23
30°	0.0026	-0.120	1.26
20°	0.0064	-0.190	1.27

Note: Parameters calibrated for Q_{LWD} = 1 log/s, see text for higher Q_{LWD}

Equation (3.13) was fitted on low instantaneous LWD supply (Q_{LWD}= 1 log/s). Other tests done with higher log discharges (50 and 100 log/s) showed 0-20 % higher trapping efficiency; so Eq. (3.13) is conservative with regard to the minimum expected TE_{LWD}. The positive correlation between jamming probability and log discharge was confirmed by Shrestha et al. (2012) in experimental and numerical models.

3.5.3. Maximum trapping volume

The structure maximum trapping volume has to be controlled when a high V_{LWD} is expected to deposit in a small trap basin. An excess of LWD supply can induce undesirable effects as, for instance, abrupt LWD releases or obstruction of the basin upstream part. Japanese guidelines considers that the maximum LWD trapping volume is proportional: to the volume of trapped sediment for debris flow and, to the surface of the trap basin for bed-load transport (see Uchiogi et al., 1996; SABO Division, 2000 & Table 3.4).

Table 3.4 – LWD maximum storage volume depending on transport phenomena and type of structure

Structure type	Debris flows	Bed-load transport
Solid check dams	$0.01V_{sed,trapped}$	$0^{\dagger}$
Open check dams	0.1 to $0.3V_{sed,trapped}$	Trap basin surface$\times D_{LWD}$
† Solid body dams are generally considered not to trap LWD (Maricar and Hashimoto, 2014)		

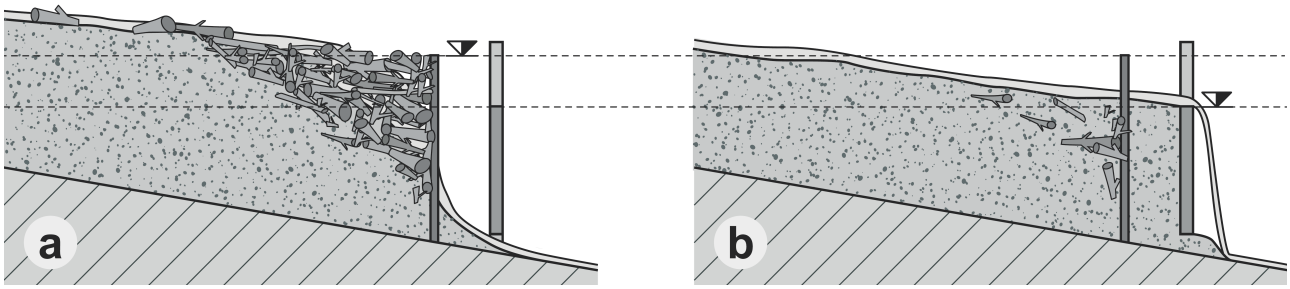

Figure 3.13 – In a slot check dam equipped with a vertical rake, illustration of the probable influence of LWD presence or absence, a) thicker deposit related to LWD accumulation: "hidden reserve" b) thinner deposit without LWD accumulation (reprinted from Bezzola 2004, with permission)

3.5.4. Head loss due to LWD accumulation

A. Conceptual approach

As detailed in the companion paper, general sediment deposit patterns first depend on the water level in the basin (Zollinger, 1984b; Jordan et al., 2003; Kaitna et al., 2011). Hydraulic analysis of outlets and spillways provides a fairly good estimate of the water level, as long as LWD does not accumulate on the structure. LWD accumulations induce hydraulic head losses that designers must assess to better estimate the uncertainty on the deposit level. A thicker deposit in the basin can propagate upstream and potentially threaten the upstream channel with backfilling (Jordan et al., 2003; Kaitna et al., 2011) or generate lateral dyke over-topping and structure failure (Böll et al., 2008, p. 34).

The formulas presented below have generally been calibrated on small-scale models. As for all phenomena related to LWD, a strong natural variability is likely to exist in the field. The head loss formulas give an idea of the magnitude of the influence of LWD on a given structure. However, their results could be significantly influenced by stochastic effects in the LWD accumulation, the presence of small woody debris likely to increase the LWD accumulation density and the related head loss, etc.

The increase of sediment trapping capacity due to LWD jamming is highly probable but hard to guarantee. Unexpected phenomena such as secondary currents, asymmetric accumulations or even upstream jamming freeing the sediment trap of LWD can occur (Rimböck and Strobl, 2002; Rimböck, 2004; Koulinski et al., 2011). As proposed by Bezzola et al. (2004), the additional sediment storage related to LWD jamming has to be taken into account to ensure the safety of the design (freeboard, backfilling, etc.), but it should be considered as a "hidden reserve" in the design procedure (Fig. 3.13).

B. LWD induced head losses

Different formulas exist to assess the head loss due to LWD jamming ΔH_{LWD} for different structure types.

Net dams

Rimböck (2004) proposed a formula calibrated on net dam prototypes:

$$\Delta H_{LWD} = 3.22(V_{LWD}/W)^{\Omega} \quad (3.15)$$

with V_{LWD} the LWD volume (m^3), W the stream width and Ω depending on the upstream slope (Ω=0.2 for S=1%, Ω=0.25 for S=3%, Ω=0.26 for S=5%). Equations (3.15) provides a significantly higher estimation of ΔH_{LWD} compared to the equations presented below that are calibrated for sectional and frame dams. This is likely to be the result of the condition in which Eq. (3.15) was calibrated: rectangular, relatively narrow section and relatively small logs (see Rimböck and Strobl, 2002; Rimböck, 2004).

Frame dams

For frame dams, the SABO Division guidelines (2000) propose:

$$\Delta H_{LWD} = 2 \times D_{LWD} \quad (3.16)$$

The authors recommend using a minimum of 1 m if $2 \times D_{LWD}$ <1 m (Uchiogi et al., 1996).

Rake dams / sectional piles dams

Schmocker and Hager (2013) provide a temporal analysis of headwater loss at a straight vertical rake / sectional dam depending on various parameters (rake bar diameter, LWD size, LWD soaking duration, V_{LWD}, LWD discharge). They demonstrated the key influence of the approaching Froude number for the LWD accumulation density, size and influence on hydraulics. They proposed the following simple formula to assess the headwater loss depending on d_0 the undisturbed approaching water depth at section 0 of Fig. 3.6 ($Fr_0 \in$ [0.5;1.5]).

$$\Delta H_{LWD} = d_0(0.4 + 1.9Fr_0) \quad (3.17)$$

Lange and Bezzola (2006) cite the approach proposed by Knauss (1995) for *V-shape* sectional dams with piles (Fig. 3.8c and 3.10a). The head loss is directly expressed as:

$$\Delta H_{LWD} = \mu\frac{v_0}{2g} \quad (3.18)$$

with v_0 the undisturbed velocity in the reach (m/s), g the gravitational acceleration (m/s^2) and μ the head loss coefficient equal to 1.5 to 2.5 for LWD accumulation with large and small logs, respectively.

C. Total dam height design

These formulas can help designers to determine the open check dam height. If LWD releases have to be prevented, a reasonable freeboard has to be taken in addition to LWD accumulation head losses and hydraulic and sediment transport-related head losses (see companion paper for details).

A spillway must be added above the dam openings to prevent lateral dyke over-topping for floods stronger than the project flood, or in case of unexpectedly severe clogging of the openings. If LWD releases have to be prevented for the project flood, a reasonable freeboard has to be taken between the spillway crest and the flood height = $\Delta H_{sed} + d_w + \Delta H_{LWD}$.

Small-scale models are accurate tools to estimate the influences of LWD accumulations on the hydraulic behaviour of a structure (CFBR, 2013). However, they require an hypothesis on LWD sizes. Field feedback showed that the presence of small woody debris increases the LWD accumulation density and its influence on hydraulics (*e.g.*, Knauss, 1995; Rimböck, 2004). To gain an idea of the maximum possible effect of a LWD accumulation on the structure's behaviour, an exploratory test can be performed with a board completely clogging the structure, representing an extremely dense LWD accumulation (L. Schmocker, *pers. com.* 2014). This test is conservative but will give an idea of the higher limit of the possible influences of driftwood.

3.6. Design procedure

In summary, the following steps are recommended in the design of a sediment trap with an open check dam:

1. Undertake a catchment study aiming to determine sediment and LWD-related hazards and the resulting potential damages. This will include the estimation of: (i) the potential solid transport phenomena that can occur (debris flows, debris floods, bedload), (ii) the sediment and water discharges and volumes for different event probabilities, (iii) LWD potential production (Eqs. (3.1 - 3.6) and the method illustrated in Fig. 3.5), and (iv) LWD characteristic sizes ($L_{max,LWD}$ with Eq. (3.7), $L_{mean,LWD}$ and D_{LWD}). This study must be based on field surveys, historical analysis of past disasters (D'Agostino, 2013a) and expert assessment.

2. Define the best-adapted sediment and LWD management policies depending on potential problems and damage (*e.g.*, under-designed bridges or culverts, deposition and accumulation-prone areas, sediment deposition-prone reaches but with a sufficient hydraulic capacity, etc.).

3. Determine the relevant location of the structure depending on LWD and sediment fluxes along the watercourse (*e.g.*, Schmocker and Weitbrecht, 2013).

4. Define the trap objectives concerning sediment management (see companion paper) and LWD management qualitatively (*e.g.*, maximum trapping, partial trapping, trapping as a side effect, minimum trapping) and quantitatively (*e.g.*, volume, size).

5. Determine the best-adapted structure type and shape to satisfy these objectives and depending on the stream features, LWD and sediment volumes, and water discharges (Table 3.1 and Fig. 3.8).

6. Determine the opening sizes depending on sediment trapping functioning (see companion paper).

7. Check that the trap objectives and opening sizes are consistent (Eq. (3.8) with Table 3.2 and Eqs. (3.13) & (3.14) or (3.10) & (3.12)).

8. Determine the minimum dam height depending on hydraulic and sediment transport criteria (see companion paper);

9. Compute the additional dam height necessary to prevent LWD overflowing related to the additional head loss induce by LWD: Eqs. (3.15) to (3.18).

10. Check that the size of the trap basin, designed depending on sediment deposition and maintenance management (see companion paper), is sufficient to store the targeted LWD volume (Table 3.4).

11. Design the dam crest spillway, dam wings and lateral dykes taking into account the structure clogging probability for an extreme event and a sufficient freeboard (see Hunzinger, 2014 for freeboard computation).

If one or more verifications show inconsistencies between the trap's theoretical objectives and the expected behaviour based on expert assessment and design criteria, the trap design must be revised: trap objectives can lowered / the allowable area and budget can be increased to satisfy the objectives / smaller multiple structures can be built in series with different shapes and specific objectives.

3.7. Incomplete knowledge

In addition to the questions stressed in the companion paper, this literature review stresses the need to continue general research on the subject of LWD production, recruitment, transfer and trapping.

Following disasters, rapid surveys are needed to gather more data on LWD accumulation and production. A few papers have reported feedback from extreme floods in Japan and Europe, but data remain sparse. LWD often accumulates on key facilities and emergency post-flood works remove them, which complicates the evaluation of LWD accumulation volumes. Data must be collected quickly following disasters (*e.g.*, Uchiogi et al., 1996; Rickenmann, 1997b). Sediment and LWD traps are artificial accumulation areas. Dam managers should measure and record the volumes and sizes of the LWD trapped in the structures to extend datasets and adjust their trap design when sufficient feedback is available. To allow comparisons between data sets, common metrics have to be used such as those proposed by Wohl et al. (2010).

Continuous field surveys are also needed to better estimate when LWDs are recruited during the flood (*e.g.*, Kramer and Wohl, 2014). The hysteresis between water, sediment and LWD discharges must be better understood to improve the realism of boundary conditions in models.

Field feedback leads us to believe that in some debris flow torrents, LWDs tend to be crushed by transported boulders and therefore only slightly influence open structure behaviour. To bring small-scale experiment closer to field conditions, research on material resistance mechanics could help to find a relevant material able to respect floating and mechanical resistance similitudes in Froude-scale models. In small-scale debris flow experiments, natural wood mechanical resistance induces bias through the possible over-estimations of the LWD influence on the structure's behaviour.

To extend the work done by Schmocker and Hager (2013) on the influence of LWD accumulation against rakes, similar experiments with sediment transport and for other elementary shapes notably the widely used inclined rakes and fins, would be useful (Fig. 3.9 and 3.11).

Numerical models taking into account LWD have recently shown promising results (*e.g.*, Shrestha et al., 2012; Ishikawa et al., 2014). Continuous efforts in this direction will develop useful tools that can complete field analyses and small scale experiments. The development and calibration of models with coupling effects between fluid, sediments and LWDs, in Newtonian and non-Newtonian rheologies will be a significant challenge for the future.

Today's methods to assess LWD production and trapping remain highly empirical and / or need expert assessment. Nonetheless, the natural variability and the complexity of the coupling effects of extreme phenomena linking fluids, sediments and LWD is so great that expert assessment will always be necessary.

Acknowledgments

This study was funded by Irstea, the INTEREG ALCOTRA European RISBA project and the ALPINE SPACE European SEDALP project. The authors would like to thanks Yoichi Ito, Markus Moser and Sebastian Schwindt for their help with Japanese and German papers, Thanos Papanicolaou for his editorial work, Ségolène Mejean and two anonymous reviewers who contributed to this paper by providing helpful reviews of an earlier version of this manuscript. In addition Johannes Hübl, Bruno Mazzorana, Andreas Rimböck and more especially Daniela Lange-Nussle and Gian Reto Bezzola were of great assistance through their past works and kindly accepted that their meaningful figures be used to illustrate this paper.

Notation

The following symbols are used in this paper:

a_α, b_α and c_α = coefficients of equation (3.13) depending on α (-);

w_s = dam solid part width: piles, beams or rake bar diameter or fins' width(m);

D_{LWD} = LWD diameter (m);

d_w = water depth in the basin directly upstream the open check dam (m);

d_0 = water depth in the basin, considered undisturbed by the open check dam (m);

Fr_x = Froude number of the flow at section x, $Fr_x = \frac{v_x}{\sqrt{g d_x}}$ (-);

g = gravitational acceleration (m/s^2);

h_0 = opening height: vertical dimension of the opening (m);

L_{For} = forested length of the upstream reach (km);

L_{LWD} = large woody debris length (m);

$L_{max,LWD}$ = maximum length of the supplied LWD (m);

$L_{mean,LWD}$ = mean length of the supplied LWD (m);

$L_{standtree}$ = living stand tree length in production areas (m);

$L^*_{Stand\ tree}$ = dimensionless stand tree length= $L_{Stand\ tree}/W$ (-);

n_0 = narrow side of the opening = minimum of h_0 and w_0 (m);

Q = Water discharge (m^3/s);

Q_{LWD} = LWD discharge (m^3/s);

S = River or trap basin slope (m/m);

S_{BV} = watershed surface (km^2);

$S_{BV,For}$ = forested watershed surface (km^2);

$S_{BV,For,>5^\circ}$ = Forested watershed surface, part steeper than 5° (km^2);

TE_x = Structure Trapping Efficiency for x: $= \frac{V_{trapped}}{V_{supplied}}$ (-);

v_w = flow velocity in the basin directly upstream the open check dam (m/s);

v_0 = flow velocity in the reach undisturbed by the open check dam (m/s);

V_{LWD} = volume of an accumulation of LWD taking into account the porosity (m^3);

$V_{LWD\ supply}$ = volume of LWD supplied by the flood to the trap (m^3);

V_{log} = volume of a singular log (m^3);

V_{wat} = volume of water of the hydrograph (m^3);

$V_{sed,trapped}$ = volume of sediment trapped in the open check dam basin (m^3);

$V_{sed,supply}$ = volume of supplied by the flood to the trap (m^3);

W = river or basin width (m);

w_0 = opening width (m);

α = rake inclination : angle between rake and horizontal (°);

β = ratio of volume of LWD to volume of sediment = $\frac{V_{LWD}}{V_{sed,trapped}}$ (-);

γ = unitary production of LWD depending on forest type:evergreen or deciduous (m^3/km^2);

ΔH_{LWD} = energy head loss induced by the LWD accumulation upstream of the open check dam (m);

η = dimensionless LWD threshold length, see Eq. (3.7) (-);

Ω = power coefficient of Eq. 3.15 depending on the upstream slope (-);

μ = head loss coefficient of equation (3.18);

φ = dimensionless parameter of Eq. (3.10), we recommend to use Eq. (3.12) to compute it (-);

ξ = dimensionless parameter of Eq. (3.13) = $\frac{1}{Fr^2} \cdot \frac{w_0}{L_{LWD}}$ (-);

"Ainsi pendant que l'on croit le torrent au repos, il recueille, sans qu'on y prenne garde, les éléments de ses ravages : il fait, si l'on peut parler ainsi, ses approvisionnement."

Scipion Gras (1850, p. 94).

CHAPTER 4

Quantifying sediment supply The concept of "travelling bedload" and its consequences for bedload computation in mountain streams

Guillaume PITON[a], Alain RECKING[a]

[a] Université Grenoble Alpes, Irstea, UR ETGR, St-Martin-d'Hères, France.

Sediment supply quantification is a prerequisite for any rigorous torrent hazard study and open check dam design (Mériaux et al., 2013). At the same time, numerous open check dams yet exist and their dredging provide interesting information about the actual sediment supply. In the continuation of his works on bedload transport computation, Alain RECKING had some ideas, that are used here, on a way to account for armouring and armour breaking in mountain streams. After some preliminary analysis of literature data, we show how to take advantage of an existing open check dam to better understand a catchment sediment transport dynamics, while stressing the difference between background and extreme event-related sediment supplies. Most of all, this chapter seeks to clarify, when using this or that equations, *e.g.*, for design purposes, which underlying assumptions exist concerning the modelled-geomorphic processes.

Abstract

In bedload transport modelling, it is usually presumed that transported material is fed by the bed itself. This may not be true in some mountain streams where the bed can be very coarse and immobile for the majority of common floods, whereas a very different finer material, supplied by bed-external sources, is efficiently transported during floods, with marginal interaction with the bed. This transport mode was introduced in an earlier paper as "travelling bedload". It could be considered as an extension of the washload concept of suspension, applied to bedload transport in high energy streams. Since this fine material is poorly represented in the bed surface, standard surface based approaches are likely to strongly underestimate the true transport in such streams. This paper proposes a method to account for travelling bedload. The method is tested on published datasets and on a typical Alpine stream, the Roize (Voreppe, France). The results, particularly on active streams that experience greater transport than would be expected from the grain sizes of their bed material, reinforce the necessity of accounting for the "travelling bedload concept" in bedload computation. The application of the concept is discussed, as are the methods accounting for the opposite situation of full bed mobility in the case of armor breaking. To conclude, this paper considers the computation strategy for a wide range of situations, ranging from sediment starved cases, to general armor breaking, including the intermediate case of external source supply.

Author key words: *Armouring, Paved Bed, Torrent, Armour Breaking, Sediment Transport Efficiency*

4.1. Introduction

Bedload transported by rivers is a central component of our environment. It conditions the rivers morphology and is the support for the river ecosystems (Wohl, 2013a). The prediction of bedload transport is therefore very important, yet many aspects of this remain very challenging (Parker, 2008). An important question that the research community aims to answer is how to predict sediment transport in mountain streams, as these streams often represent the main sediment input to the downstream fluvial system (Wohl, 2006), and this sediment load aggravates damage during floods (Badoux et al., 2014). From an environmental perspective, a better understanding of input from mountain streams is essential for the preservation and restoration of sediment continuity in alpine stream networks. From a risk mitigation perspective, the design of structures such as sediment traps, still suffers from substantial difficulties in estimating the sediment volumes concerned (Piton and Recking, 2016a; 2016b).

Among the difficulties associated with estimation of bedload transport in mountain streams, recent studies have shown that steep slope streams develop specificities, preventing a direct transfer of standard equations that were initially established for mild slope, alluvial rivers (Rickenmann, 2001). Particular aspects include the changing critical Shields stress with slope (Mueller et al., 2005; Lamb et al., 2008; Recking, 2009; Bunte et al., 2013), transport regulation by grain sorting and rearrangement (Recking et al., 2009; Turowski et al., 2011; Bacchi et al., 2014; Recking, 2014), and form resistance due to poorly mobile large stones (Canovaro and Solari, 2007; Rickenmann and Recking, 2011; Nitsche et al., 2012; Yager et al., 2012b; Yager et al., 2012a; Ghilardi et al., 2014b). There have been several attempts to accommodate these steep slope specificities,

but one aspect that remains less predictable and limits application is sediment availability (Recking et al., 2012a).

Different sediment contexts exist in mountain streams. In lowland streams, hereafter referred to as alluvial streams, the bed is generally composed of loose sediments that are deposited by the stream itself (Church and Ferguson, 2015). The channel geometry and the slope are self-formed in the alluvial material, and the associated morphology in mountain valley rivers is usually braided or plane-beds. Conversely, many mountain streams are not purely alluvial, having bed sediment composed of immobile or poorly mobile large stones (or bedrock). Finally, many streams are semi-alluvial, with alternating alluvial and non-alluvial reaches. In such streams the non-alluvial reaches usually act like 'tubes' efficiently transporting the load imposed by the alluvial section, though with marginal morphological response (Mueller and Pitlick, 2005).

In these streams the prediction of bedload considering only the bed material, as is usually done in alluvial rivers, can be strongly misleading. Indeed, in contrast to lowland rivers, where the bedload of a given section is fed by remobilization of bed material from an upstream section, mountain streams can be locally fed by very active colluvial inputs (Recking et al., 2012a), through event-related processes such as hill-slope / bank collapses (Schuerch et al., 2006; Molnar et al., 2010). These incoming sediments usually have a grain size distribution very different to that of the bed material, eventually extending over a wide range, from clay to boulders. The coarser parts tend to recharge the bed, while the finer sediments may be very efficiently transported downstream (Schuerch et al., 2006). In field surveys, Yu et al. (2009) demonstrated how this incoming fine material can enhance bedload (up to three orders of magnitude) under a given flow condition, in comparison with transport of the bed forming material. They called this transport of fine material "*travelling bedload*", to distinguish it from "*structural bedload*", which is associated with bed remobilization.

The concept of travelling bedload consists of transport of bedload material from an upstream injection point to a downstream deposition zone, with little or no interaction with the bed (no morphological effect). This could be considered an extension of the washload concept (fine suspension not interacting with the bed) to bedload in high energy streams. Structural bedload plays a very important role in terms of geomorphology, since it fixes the channel slope. However, it may sometimes have a secondary influence on transported volumes, influence limited to large and rare flood events. Conversely, travelling bedload has only a limited impact on geomorphology, although in many streams, travelling bedload could be responsible for a non-negligible supply of bedload material to the downstream systems or sediment trapping structures.

This paper aims to investigate methods to account for the travelling bedload concept, and improve computation of bedload estimation for mountain streams. We initially present a methodology based on a distinction between the different sediment populations (the bed and incoming sediments), and their respective roles on friction and transport. In the second step, we test the methodology using some previously published examples, and data from the Roize, a French Alpine mountain stream. Finally, the results are discussed and we conclude that the concept of travelling bedload deserves more attention in mountain streams where the bed is poorly mobile, and where standard approaches strongly underestimate transport rates. In these situations this approach is shown to improve the computation accuracy.

4.2. Travelling versus Structural grain size distributions

In most computation strategies, qualitative and quantitative knowledge of the sediment present in the channel bed is required. This is sufficient for predicting both the hydraulics and the associated transport, with appropriate equations linking the fluid forces to bed surface sediment features (Wilcock and Crowe, 2003). We consider a contrary situation, where transported material is only marginally present at the bed surface, with the surface being strongly paved by poorly mobile elements. The transported material is injected into the channel by floods (bank erosion) or colluvial processes (landslides), and is transferred downstream, with only weak interaction with the bed. In this situation, special attention must be paid to the sediment grain size distributions, which acts at two levels:

i) the bed surface grain size distribution controls the hydraulics, and consequently the shear stress $\tau = \rho g R S$, which can be represented by friction equations usually given in the following form:

$$\frac{U}{u^*} = f\left(\frac{R}{D_{friction}}\right) \tag{4.1}$$

where U is the mean flow velocity (m/s), $u^* = \sqrt{gRS}$ is the shear velocity (m/s), R is the hydraulic radius (m), S is the slope (m/m), and $D_{friction}$ is a characteristic grain size of the bed surface (m);

ii) the travelling bedload grain size distribution controls bedload computation through the dimensionless shear stress defined by the Shields parameter τ^* (Shields, 1936) and the dimensionless sediment discharge defined here by the Einstein parameter Φ (Einstein, 1950):

$$\tau^* = \frac{\tau}{g(\rho_s - \rho)D_{bedload}} \tag{4.2}$$

$$\Phi = \frac{q_{sv}}{\sqrt{g(\rho_s/\rho - 1)D_{bedload}^3}} \tag{4.3}$$

where $D_{bedload}$ is a characteristic diameter representative of the transported material (m), q_{sv} $(m^3/s.m)$ is the volumetric unit solid discharge, ρ_s (kg/m^3) is the sediment density, and ρ (kg/m^3) is the water density.

The standard approach used in most bedload computation strategies consists of assuming a unique grain size distribution, measured at the bed surface, and defining $D_{friction}$ and $D_{bedload}$ as quantiles of the bed surface (*e.g.*, D_{84} for friction and D_{50} for bedload, with D_X diameter such that $X\%$ of the mixture is finer). However, this approach may not always be valid. For example, if the material transported during floods is not the surface material, but remobilized subsurface material, some authors have distinguished two grain size populations, the surface and subsurface, for computation of friction and transport respectively (Parker and Klingeman, 1982).

Similar properties emerge with the study of travelling bedload in mountain streams. In this case the strategy could consist of distinguishing: $D_{friction} = D_{84,BS}$, D_{84} of the bed surface controlling the hydraulics; and for the transported material $D_{bedload} = D_{84,TraBL}$, D_{84} of the travelling bedload material, possibly measured in a downstream deposition area (see below).

Dozens of bedload equations exist, and it is not the objective of this paper to test their ability to compute bedload transport in mountain streams. Instead, we aim to investigate how the above distinction regarding grain size distribution can improve the predictive ability of a given equation that ever proved to perform well for a wide range of river morphologies (Recking, 2013a;

2013b; Recking et al., 2016):

$$\Phi = \frac{14\tau^{*2.5}}{1 + (\frac{\tau^*_m}{\tau^*})^4} \quad (4.4)$$

$$\tau^*_m = 1.5S^{0.75} \quad (4.5)$$

where τ^* (Eq. 4.2) and Φ (Eq. 4.3) must be computed for D_{84}. In the following, two terms will be computed to consider two options: the bed surface $D_{84,BS}$ and the incoming lateral input sediments $D_{84,TraBL}$. The parameter τ^*_m (Eq. 4.5) gives the transition between partial transport and full mobility, and is dependent on morphology (Recking et al., 2016). As discharge rather than depth measurements are usually available, the hydraulics are computed using Eq. 4.6, derived from the flow resistance equation proposed by Rickenmann and Recking (2011) for all flow ranges, including steep-slope streams.

$$d = 0.015 D_{84,BS} \frac{q^{*2p}}{p^{2.5}} \quad (4.6)$$

where $q^* = q/\sqrt{gSD^3_{84,BS}}$ and $p = 0.24$ if $q^* < 100$ and $p = 0.31$ otherwise.

4.3. Method validation

4.3.1. Evidence from published datasets

We illustrate the above scenarios using a selection of six mountain streams described in the literature (Table 4.1): the Egger Creek (King et al., 2004), the Toots Creek (Marion and Weirich, 2003), the Rio Cordon (Billi et al., 1998; D'Agostino and Lenzi, 1999; Lenzi, 2001; Mao and Lenzi, 2007), the Pitzbach (Turowski and Rickenmann, 2009; Turowski et al., 2011), the Diagoa Yu et al. (2009; 2010; 2012), and the Erlenbach (Rickenmann, 1997a; Rickenmann, 2001; Schuerch et al., 2006; Molnar et al., 2010).

The results are shown in Fig. 4.1. Egger creek, Toots Creek, Rio Cordon and Pitzbach are described as alluvial channels, with no particular mention of hillslope influences being made. For these four streams, the computation using the bed surface grain size distribution gives satisfactory results. This is not the case for the Erlenbach and Diaoga streams, where lateral bank erosions were mentioned as major sediment contributors. For both of these, the use of the bed grain size distribution (Erlenbach $D_{90} = 400mm$, Rickenmann, 2001; Diaoga - $D_{84} = 300mm$, Yu et al., 2009) results in a substantial underestimation of transport. Conversely, using the grain size distribution of transported material (Erlenbach $D_{90} = 140mm$; Diagoa $D_{84} = 61mm$ for the coarsest bedload curve) for τ^* and Φ strongly improves the results.

These tests support the hypothesis that in some streams consideration of the traveling bedload concept can considerably improve bedload transport computation. This analysis was therefore extended to a typical torrent: the Roize.

4.3.2. Case study: the Roize

We tested the above concepts in the Roize torrent, which exemplifies a typical situation where managers need to predict bedload transport for reasons of risk mitigation and estimation of sediment trap dredging requirements. A detailed presentation on this study site can be found in Lamand et al. (2015).

A. Catchment presentation

The Roize torrent is a tributary of the Isere River located in the south western part of the Chartreuse massif (FRA. – Fig. 4.2). Its $16.1 - km^2$ catchment is drained by two main-stems: The Upper Roize is the more active in term of sediment transport, although it has half the catchment area of the Roizette.

Limestone cliffs founded on marl layers constitute the main catchment sediment sources (Fig. 4.3a) and extend over a $0.38 - km^2$ area (RTM38,

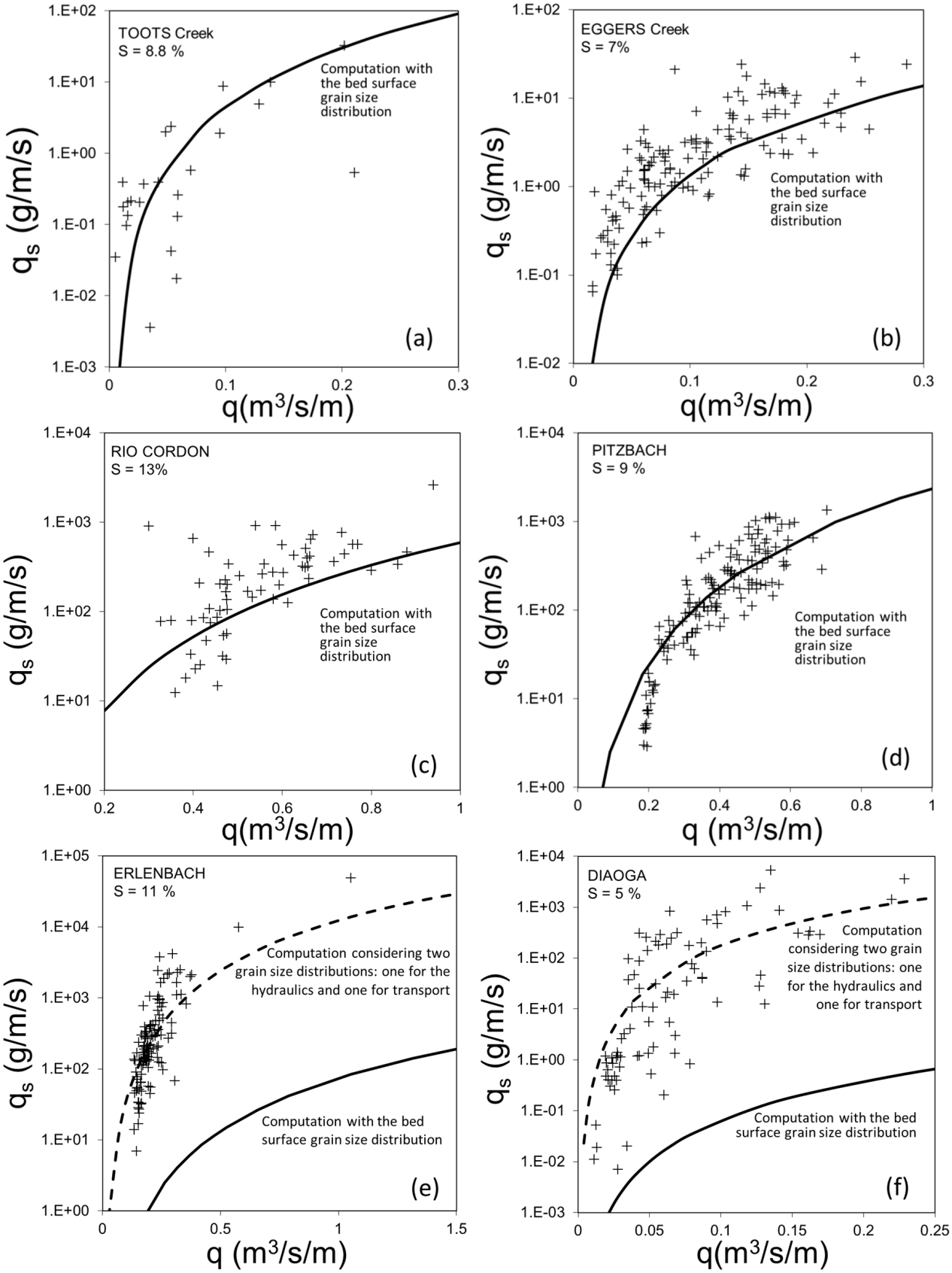

Figure 4.1 – Comparisons of Eq. 4.4 on published datasets, distinguishing between the bed surface and the travelling bedload material

Table 4.1 – Six mountain streams considered from published studies

Catchment	size (km^2)	Slope (m/m)	$D_{84,BS}$ (mm)	Sediment context
Egger Creek	1.29	0.070	100	Relatively fine and loose material
Toots Creek	0.39	0.088	126	Step-pool in alluvial loose material
Rio Cordon	5	0.136	260	Step-pool in alluvial loose material
Pitzbach	27	0.090	150	Step-pool in alluvial loose material
Diaoga	18	0.050	300	Step-pool strongly impacted by human activities, frequent landslides*
Erlenbach	0.74	0.100	400	Step-pool with very active small landslides on hillslopes adjacent to the channel*

* Bedload material is fed by event-related bank collapses (Schuerch et al., 2006; Yu et al., 2009).

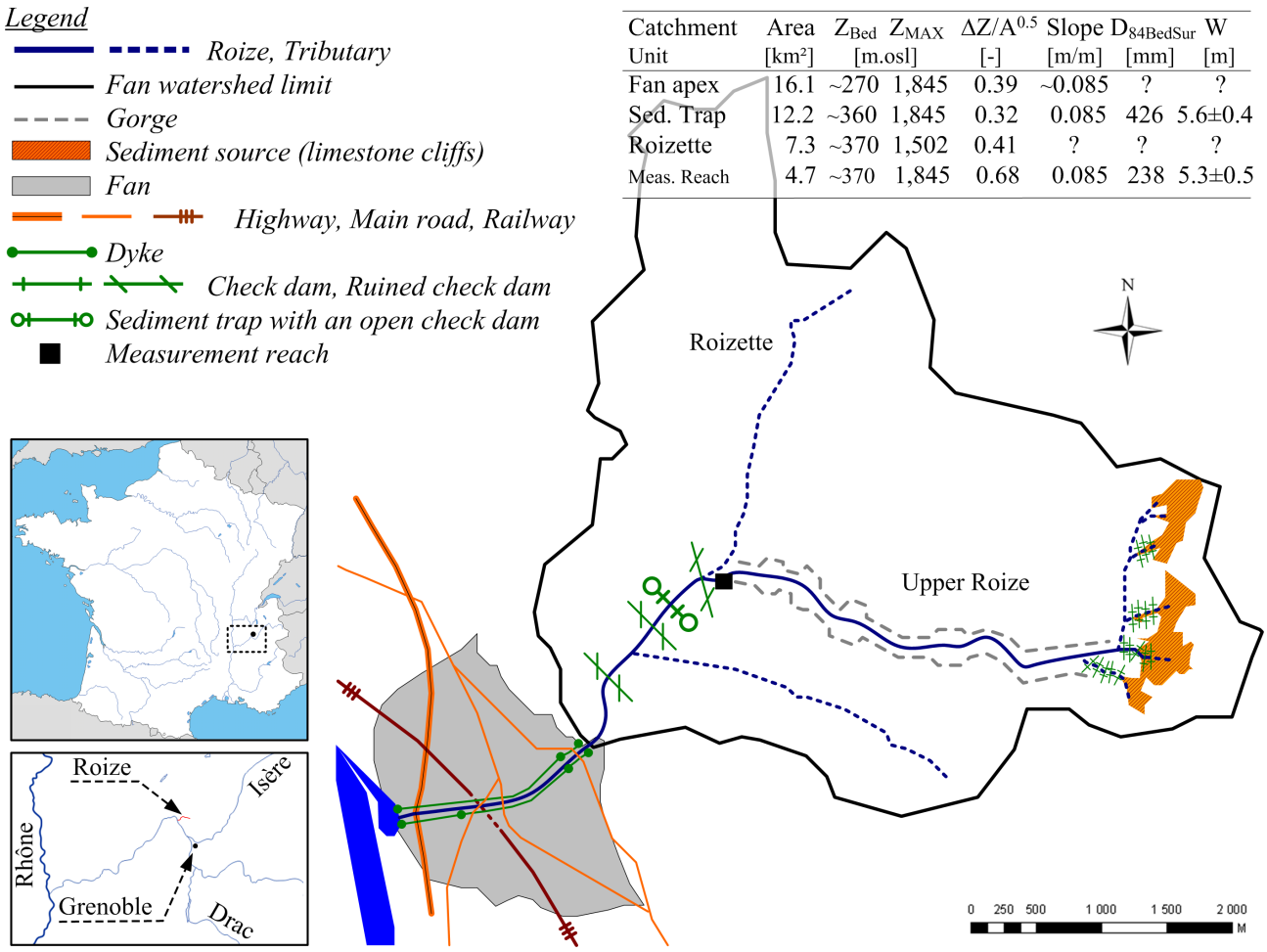

Figure 4.2 – Location of the Roize catchment and main geomorphology and structures, indication of catchment and sub-catchment area, lower and top elevation, roughness index (Melton, 1965), outlet bed slope, bed-surface grain size and channel width

2009). The headwaters experience sediment transport through debris flows that deposit into several wider reaches, distributed along the 3.3-km-long downstream gorge (Fig. 4.2). Consequently, sediment transport shifts from debris flows to bedload, which is the main transport process observed in the final gorge reach and in the sediment trap (Fig. 4.3b & c). The bed morphology changes from bedrock/cascade to step-pools along the gorge (*sensu.* Montgomery and Buffington, 1997). Conversely, the Roizette catchment consists of woodland and fields and presents no clear sediment source. Its bed, which consists of very stable step-pools, is much narrower than in the Roize, and is heavily constrained by stable vegetation. It appears that solid transport is negligible outside of extreme events (Jail and Martin, 1971). The Roize-Roizette confluence is located 200 m upstream of a sediment trap (Fig. 4.2). The water input of the Roizette into the Roize induces an increasing sediment transport capacity, with negligible sediment input. Consequently, the bed is considerably more paved downstream of the confluence. The sediment trap is assumed to nearly totally disrupt bed-load transport, since the morphology changes drastically immediately downstream of the structure (only few pebble patches, vegetation much more present, numerous bedrock outcrops, nearly no evidence of sediment transport, Fig. 4.3d). The apex of the Roize fan is located about 1.3 km downstream of the sediment trap. The Roize fan is well developed and is currently nearly completely urbanized by the town of Voreppe ($\approx 10,000$ inhabitants in 2015).

The historical workings on the Roize catchment are typical of a large French torrent, and include the following features (Lamand et al., 2015; Piton et al., 2016b): i) a fully-trained fan channel (Fig. 4.3d), stabilized with bed-sills and surrounded by cut-stone protected dikes. This protection system dates to the 18^{th} century, and was completed during the 19^{th} century; ii) about 140 small check dams located in the headwaters, built in the late 19^{th} and early 20^{th} centuries; iii) a sediment trap with an open check dam built in 1985. This is located upstream of the fan apex, in the vicinity of the (now-ruined) first modern torrent control check dams built in France, dating from 1851 (Gras, 1857; Piton et al. *sub.*).

Figure 4.3 – Pictures of the Roize catchment: a) headwaters: marl-limestone cliffs drained by check dam-equipped steep channels; b) coarse Roize bed at the measurement reach c) sediment trap and its open check dam and d) trained fan channel experiencing weak sediment transport as demonstrated by the well-developed grass (Photos by Guillaume PITON)

The measurement reach, in which sediment transport computations are performed, is located in the lowest part of the gorge (Fig. 4.2). The slope S is deduced from a linear fit of a longitudinal profile consisting of more than ten elevation measurements along 30–60 m-long profiles, measured using a laser telemeter (Trupulse 300X©). Three transversal geometry profiles have been surveyed within this reach; the slopes and widths for other locations within the catchment are also given (Fig. 4.2).

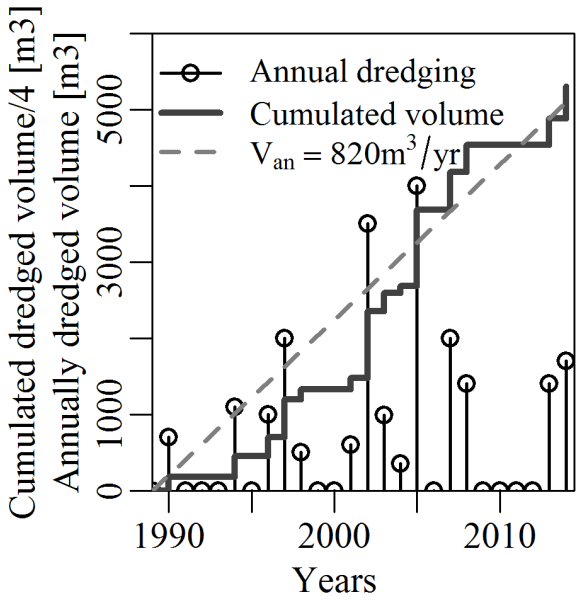

Figure 4.4 – Sediment dredging in the open check dam, a useful proxy for sediment production in the catchment

B. Sediment data

In the last 25 years, an accumulated volume of 21,200 m^3 has been dredged from the Roize sediment trap (Fig. 4.4), *i.e.*, $820 \pm 1000\ m^3/yr$ (*mean* $\pm$ *standard deviation* σ). This dredging shows a strong inter-annual variability, with no dredging or low supply some years (*e.g.*, 350 m^3 in 2004), and a much greater supply in other years (*e.g.*, 4000 m^3 in 2005).

In addition to these measurements, archives report on catastrophic floods in 1971, with an estimated rainfall of between 150 mm and 200 mm in less than 9 hr. The bed width increased by a factor of five in several reaches (Jail and Martin, 1971), specifically downstream of the Roize-Roizette confluence, where the catchment area triples compared to our calculation point. This induced considerable increases in the transport capacity (Piton et al., 2016b). The cumulated sediment transport is very uncertain, but all historical testimony and reports refer to several dozens of thousands of cubic meters (Lamand et al., 2015). In this study the event-related estimated volume will be referred to using only different orders of magnitude.

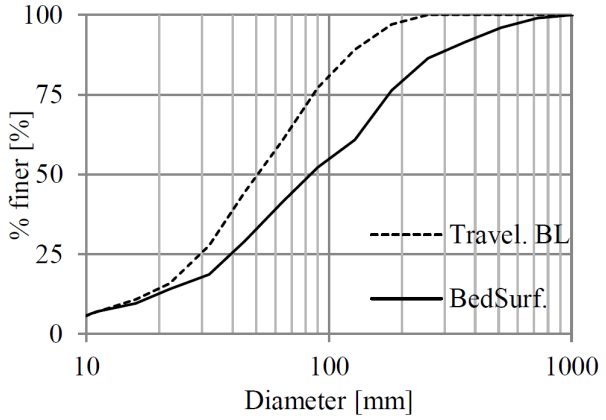

Figure 4.5 – Complete grain size distributions of the travelling bedload measured in the sediment trap, and of the bed surface measured in the step-pool section of the measurement reach

C. Grain size distributions

The bed surface grain size distribution was measured in the main channel of the torrent, within the step-pool morphology (Fig. 3b). The resulting $D_{84,BS}$ was 238 mm. Conversely, the travelling bedload grain size distribution was measured in the sediment trap, where the transported bedload is fully deposited; the corresponding $D_{84,TravBL}$ was 112 mm. Both grain size distributions were measured using the standard Wolman (1954) surface count technique, and are plotted in Fig. 4.5.

D. Hydrology

No gauging station exists in the Roize catchment. The hydrology has therefore been reconstructed using a classical regionalization approach, utilizing stations present in neighboring watersheds. A very brief summary is given here, with more information available in Piton et al. (2016b), and all details being provided in Lamand et al. (2015). Data from discharge stations and rain gauges located in the Chartreuse, Vercors and Bauges massifs, which are mountains located within a quite homogeneous hydrological region (Mathys et al., 2013), were downloaded from the Banque Hydro database (*hydro.eaufrance.fr*) and Meteo France database (*publitheque.meteo.fr*). A preliminary examination of the data resulted in the

exclusion of stations showing excessive karst influence, insufficiently long time series, and excessively large catchments ($> 115km^2$). The flow-duration curves (curve $Q_{X\%}$ vs X; X: non-exceedance frequency; $Q_{X\%}$: quantile of probability X) were determined on the remaining seven small catchment stations ($10 < A < 63km^2$) with a homogeneous rainfall regime. The catchment size influence was de-trended using a simple power law (Mueller and Pitlick, 2005):

$$Q^* = \frac{Q}{S_{BV}^{0.75}} \tag{4.7}$$

with the discharge Q (m^3/s), the station catchment area S_{BV} (km^2) and the pseudo-specific discharge Q^* ($m^3/s.km^{1.5}$). The power coefficient *0.75* has been found as optimal for collapsing the pseudo-specific flow-duration curves of the sample, specifically for high flows that influence sediment transport (non-exceedance frequency$>$ 0.5; Fig. 4.6a). Additionally, this value is consistent with other equivalent works (Mueller and Pitlick 2005), as well as classical flood hydrology methods (Cipriani et al., 2012; Mathys et al., 2013).

The inter-annual variability of the flow-duration curves was estimated using the Vence catchment data, a directly eastern neighbor of the Roize. In addition to the mean flow duration curve, the flow-duration curves for all of the 25 years of the Vence data were computed, *i.e.*, 25 quantile $Q^*_{X\%}$ per non-exceedance frequency X. We defined "Dry" or "Wet" years with a 10-yr return period as the 10% and 90% quantiles of each of these 25-$Q^*_{X\%}$ samples ($[Q^*_{X\%}]_{Y\%}$, with $Y = 10\%$ and 90%; Fig. 4.6b). Interestingly, the dry and wet curves envelop the curves of the Albane and Gresse stations (lower and higher Q^* on Fig. 4.6a), implying that the temporal variability of Q^* in one station is here more pronounced than the inter-station variation in mean Q^*.

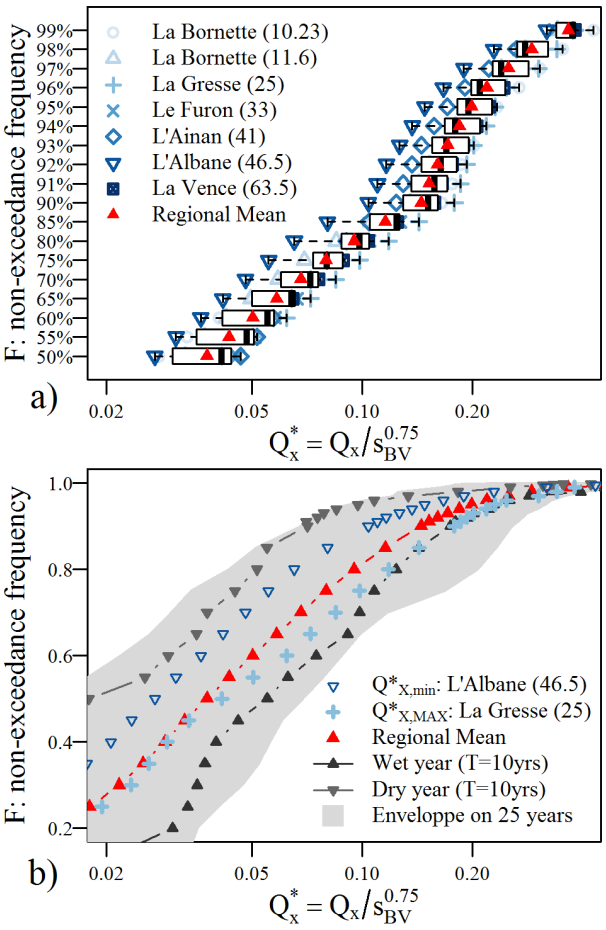

Figure 4.6 – Pseudo-specific flow-duration curves: a) data from the seven small mountain stream stations (numbers between brackets are the station catchment surface areas in km^2) and regional mean value; and b) envelope of the Vence pseudo-specific discharge, regional mean curve, correction for wet and dry years (empirical quantiles $[Q^*_{X\%}]_{Y\%}$, with $Y = 10\%$ and 90%) and pseudo-specific discharge of the Albane and Gresse stations: lower and larger pseudo-specific discharges: the inter-annual variability is higher than the inter-station variability

E. Bedload transport computation

The bedload data in Figure 4.4 are cumulative volumes for a given year. Additionally, as no measurements were available for the Roize hydrology, event related transport evaluation was not sufficiently rigorous to provide a satisfactory validation of the method (reconstruction of flood hydrographs would have been too speculative, and is only addressed in the discussion). Instead, the mean annual transport was computed with the Wolman and Miller (1960) frequency distribution approach, using the above presented flow-duration curves. The computation was performed considering the two different grain size distributions, $D_{84,BS}$ and $D_{84,TraBL}$, and results are plotted in Figure 4.7. Nine estimations were obtained by using three values of stream width (measured at the three transversal profiles located in the measurement reach), and the dry, mean, and wet flow-duration curves, thus taking into account the uncertainty and natural variability in the stream width and annual discharge distribution.

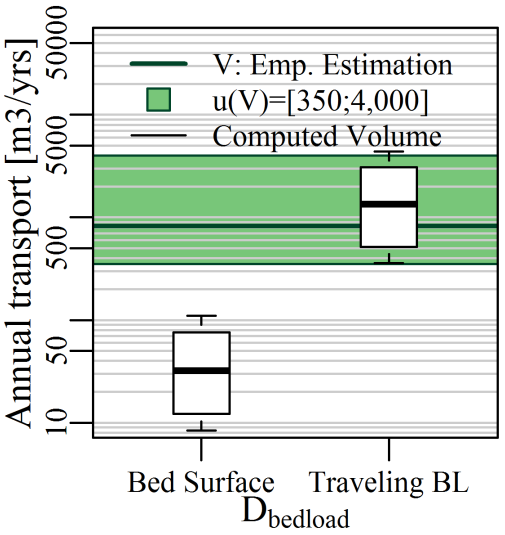

Figure 4.7 – Annual transport computed from Eq. 4.4 using the bed surface grain size and traveling bedload grain size, V: empirical estimation is the mean inter-annual 820 m^3 /yr, *u(V)* being the variability range of years with sediment transport. The mean empirical estimation and the uncertainty *u(V)* envelop are of similar order of magnitude than the computed volumes using the travelling bedload approach. Using the bed surface, coarser grain size results in substantial underestimation

Figure 4.7 indicates that estimations made using the bed $D_{84,BS}$ lead to substantial underestimation (by more than one order of magnitude) of the mean annual transport measured in the sediment trap. Conversely, if the $D_{84,TraBL}$ is used as the reference diameter, the computed volume range is precisely within the range of variability of dredged volumes in years with notable sediment transport ($350 - 4000\ m^3/yr$). This result is obtained without using the data to tune the equation, thus constituting an additional validation of the method and equations.

Furthermore, the variability in results is much more related to variability in the hydrology, than to uncertainty in the width (Piton et al., 2016b). This means that the inter-annual variability in the hydrology, here estimated using dry, mean and wet flow-duration curves, is sufficient to explain the high variability in sediment transport, without consideration of fluctuations in sediment source production. Non linearity will transform small variations in discharge (approximately ±50%) into changes of an order of magnitude in the transported volume. Characterization of variability in the natural hydrology is therefore very important for annual sediment transport computation.

F. Travelling versus Structural bedload

The Roize example suggests that the concept of travelling bedload could help to explain why standard computation strategies sometimes fail to accurately estimate bedload production in mountain streams. The new method, however, still needs to be confirmed with other field observations.

Additionally, travelling bedload should always be considered as part of a more general transport process. Indeed, as explained in the introduction, travelling bedload co-exists with structural bedload, which is bedload associated with bed remobilization. In the case of the Roize tor-

rent, structural bedload should be considered in two situations:

1. When travelling sediments were flushed from the upstream production zones (very low transport). Figure 4.4 indicates years with no sediment trap dredging, and such years are assumed to be related to nearly total inactivity of the headwater sediment sources, *i.e.*, to the absence of travelling bedload production. With such an absence, the Roize becomes a classical paved stream, with marginal primary sediment production. Consequently, it is more likely to be represented by the computations performed using the classical method, with the bed surface as reference (*e.g.*, Pitzbach, Toot Cr., Egger Cr. and Rio Cordon in Figure 4.1). For the Roize torrent, estimations of annual transport using this method are of only a few tens of cubic meters per year, a result which is very consistent with our latest observations (a camera taking daily pictures of the sediment trap basin was installed in 2015, and showed negligible supply in an 11-month period[1]).

2. For extreme floods (very high transport) that remobilize the armor and for which $D_{bedload}$ should take into account the armor material. The only available information for extreme floods is the 1971 event. Unfortunately, in addition to the very uncertain volume, there is no information on the related flood discharge and duration, or on grain size distribution of the bed material preceding this event. It would thus be excessively speculative to compute bedload specifically for this event. However, computing extreme events still remains a challenge and is very important for risk mitigation; a section proposing a way to account for these extreme floods is therefore presented in the discussion.

[1] See pictures in the Perspective section, p. 185

4.4. Discussion

4.4.1. The nature of travelling bedload

Travelling bedload usually concerns materials that are not alluvial bed-forming material, but materials that are event-related, in-channel supply. This supply may be from either material that is stocked temporarily and locally in the watershed before being remobilized, or materials that are injected into the channel from a colluvial process during an event (Fryirs, 2013). Situations leading to travelling bedload are therefore not limited to active hill-slope processes and bank collapses, but also to any situation where the coarse fractions are retained upstream and the finer fractions can freely transfer downstream.

For example, some deposition basins may retain coarse material for risk mitigation, but allow gravel to pass. The presence of such structures can explain the segregation between structural and travelling bedload. This is the situation in the Arve River (a snow-melt regime, cobble and boulder-bed river in Chamonix, supplied by steep periglacial streams; Peiry, 1990), where dredging operations in sediment traps located at the tail of the Houches hydroelectricity reservoir dam (Les Houches, FRA.), suggest transport of up to 60,000 m^3/yr of sand, gravel and small cobbles, whereas computations using standard approaches that consider the unique bed surface grain size indicate no bedload (there is not yet enough information on the travelling material to test the above computation method).

Travelling bedload can also result from kinematic sorting, which is responsible for a natural regulation of fine sediment, successively captured and released by the bed armor (Bacchi et al., 2014). Such a process can explain the alternation of dormant periods without sediment production (bed recharge; Recking, 2014), and pulses of intense transport of fine material (released by the bed). This situation could have been present in

the Roize torrent (unfortunately the difficulty in accessing the upstream part of the Upper Roize gorge did not allow enough evidence of meter-scale bed level fluctuations to be found).

4.4.2. Limitations: transport capacity

The concept of travelling bedload implies that no adjustment exists between transport and bed, and that what is computed is a transport at capacity for the given discharge and slope. In other words, the method computes a maximum capacity for the given morphological slope and discharge. This should correspond to the actual transport each time the event related sediment supply is sufficient. Thus, the computation strategy should be considered with regard to travelling material production within the watershed. This is illustrated in Figure 4.4 where productive years alternate with unproductive years.

4.4.3. Selection of measurement sites for appropriate grain size distributions

In the Roize case study, the non-truncated Wolman count method was applied at the following locations: (i) in the main channel, directly along the stream axis on the step-pool series, to determine $D_{84,BS}$; (ii) on an untouched 1.5-m-thick deposit in the sediment trap to determine $D_{84,TraBL}$; (iii) on gravel patches located aside the main channel within the gorges. The grain size distribution of these gravel patches was generally finer than in the main channel, but only by a factor of 1.5–2 (conversely in the gorges $D_{84,BS}/D_{84,TraBL} \approx 4$ for most of the complementary measurement sites, Lamand et al., 2015). The sediment transport computations using grain size distributions measured on the gorge patches as an estimator of $D_{84,TraBL}$ resulted in equivalent underestimation to using only $D_{84,BS}$, though not as strong (Lamand et al., 2015). A reach with near total bedload trapping must be found to qualify the travelling bedload features. Existing sediment traps are useful structures to facilitate the measurement of $D_{84,TraBL}$, in addition to gathering bulk sediment transport data. Such data should be used to try and test transport approaches, as done here on the Roize and in previous works by Rickenmann (1997a); Rickenmann and Koschni (2010); Peteuil et al. (2012) and Rickenmann et al. (2015).

An alternative would be to directly measure the grain size distribution in an area of deposition as a laterally unconfined reach with pure alluvial equilibrium. Examples include the fan, or if the stream is confined on the fan, in the vicinity of the confluence between the stream and the downstream main-stem.

4.4.4. Accounting for extreme events

The travelling bedload concept can help in estimation of the annual production of a catchment. However, in the event of extreme floods that generate major changes in the bed structure, the influence of structural bedload could drastically increase. The travelling bedload approach, which assumes a fine transport on a somewhat fixed and rough bed structure, may then no longer apply. Its use is a scenario (*sensu.* Mazzorana et al., 2012) requiring further study, with appropriate attention paid to both the sediment source volume and activity.

Sediment also comes from recruitment from the stream bed (Warburton, 1992; Lenzi et al., 2004; Turowski et al., 2009; Molnar et al., 2010). This can be *a priori* computed using Equation 4.4 with the bed material grain size distribution, although this would only give an average transport assuming a constant bed surface texture. From a risk mitigation perspective it is the high magnitude peak solid discharges that must be estimated. These peak solid discharges especially concern short time duration transport, immedi-

ately following possible armor breakup; this is where the transport rate efficiency was shown to be considerably enhanced (Recking et al., 2009; Bacchi et al., 2014). The released fine subsurface then smooths the bed, enhancing transport efficiency and generating a self-reinforcing feedback, since collective grain motions increase the recruitment of bed sediment by the flow (Heyman et al., 2013). Flume experiments have indicated that asymptotic transport equations established for high transport rates, appear adequate for capturing solid discharge associated with armor breaking, when applied to the full range of transport regimes (Recking, 2006, p. 159; Recking et al., 2009).

Such an asymptotic approach was previously used by Meunier (1989), who deduced the following equation from the steep slope, flume data of Smart and Jaeggi (1983):

$$Q_{sv} = \beta Q S^2 \tag{4.8}$$

with β a coefficient equal to 6.3 on average. All Smart and Jaeggi (1983) data, and data later published in Couvert et al. (1991), are nearly comprised in the range $\beta = [3; 10]$ (Meunier, 1989). Equation 4.8 is still used as a rough and easy approximation of event related transport by the French torrent control service. It does, however, have the drawback of not taking into account the grain size of the transported material, which is a key parameter of the stream transport capacity.

Rickenmann and Koschni (2010) also proposed simplified equations for bulk bedload transport estimation that related Q_s to Q, S and D_X. For example, Rickenmann and Koschni (2010) reused the Recking et al. (2008b) asymptotic equation $\Phi = 14\tau^{*2.45}$ (flume-based, determined for high transport stage, *i.e.*, $\tau^*/\tau^*_{cr} \gg 1$). They introduced to it: i) a Chézy friction law (coefficient C), ii) a rectangular channel hypothesis, iii) a sediment density of 2.68, and iv) a pore space hypothesis (30% of the volume). The purpose was to compare the computations with trap dredging data. This resulted in the simplified equation:

$$Q_{sv} = 1.3\frac{5.09}{C}\left(\frac{d}{D_m}\right)^{0.95} Q S^{1.95} \tag{4.9}$$

where D_m is the mean sediment diameter (m). Estimations made using Equation 4.9, and an equivalent form derived from the Meyer-Peter and Müller (1948) equation, were compared to transport volumes measured from flood events in Switzerland in 2005. The parameters C and d/D_m were assumed to vary in the range $4.7 < C < 17.1$ and $5 < d/D_m < 20$. Overall, for Equation 4.9, it was stated that "*the predicted transport loads are about a factor of 5–10 larger than the observed values*"; however, this overestimation depended on the uncertainty of the aforementioned hydraulic parameters C and d/D_m.

To confront this problem, an alternative proposed here consists of combining the asymptotic limb of Eq. 4.4: $\Phi = 14\tau^{*2.5}$ with the friction law proposed in Equation 4.6, considering the dimensionless discharge $q^* = q/\sqrt{gSD^3_{84,BS}}$, which, taking into account a *30%* void in the deposit, a sediment density of 2.65 and a rectangular channel hypothesis, leads to:

$$Q_{sv} = \frac{5.8 \times 10^{-4}}{p^{6.25} g^{2.5p}} W D_{84,BS}^{1.5-7.5p} q^{5p} S^{2.5(1-p)} \tag{4.10}$$

where $p = 0.24$ if $q^* < 100$, and $p = 0.31$ if $q^* > 100$.

This equation has been tested on the Roize for event related transport (Lamand et al., 2015). As detailed previously, the Roize is known to occasionally experience bedload transport of dozens of thousands of cubic meters, as was the case in 1971. As a rough case study, the 100-yr return period peak discharge was determined using classical hydrology methods (CFGB, 1994; Mathys et al., 2013). Its value remains uncertain due to the necessary regionalization (no data on the Roize), combined with extrapolation towards high magnitude events; however, the target accuracy was only concerned with orders of magnitude. Hy-

Table 4.2 – Comparison of event-related sediment transport at the Roize apex

Transport equation	$Mean \pm \sigma$
Units	[m^3]
Eq. (4.4)	$2,000 \pm 1,500$
Eq. (4.10)	$23,000 \pm 15,000$

drographs were created with varying durations: three values enveloping the variability range were considered (floods lasting 4 hr, 8 hr and 16 hr). The classical Equation 4.4 and the new Equation 4.10 were both applied to the reach located directly upstream of the fan apex (Table 2). The quite strong variability in the computation results is related to the varied duration of floods.

The normal transport equation (Eq. 4.4) is used with $D_{84,BS}$, as the paved bed surface is assumed to be transported for such rare events. This results in dramatic underestimation of the transport volume, on the order of a few thousand cubic meters of transport; events that regarding the sediment trap dredging data are certainly more common than a 100-yr return period (Fig. 4.4). Conversely, the asymptotic approach of Eq. 4.10 provided reasonably consistent estimations, within a few dozens of thousands of cubic meters.

The asymptotic approach proposed for high magnitude events in Equation 4.10 seems consistent with the basic and uncertain data available for the Roize. It deserves to be tested on other strong sediment transport events, with sufficient data available. This would allow testing whether it could make reliable predictions within the correct order of magnitude, in high magnitude sediment transport computation.

4.5. Conclusion

Bedload transport computation in mountain streams is still a challenging issue. In addition to the natural complexity of the process itself, some streams experience strong influences from their environments. One possible consequence of the coupling between streams, their underlying bedrock, and surrounding hillslopes, is a general trend to be armored, sometimes by boulders that are seldom moved by the flow. Transported material may consequently be very different from armor material. Depending on the sediment source and hillslope activity, a calm brooklet may sometimes became a rushing torrent prone to debris flows (Chen et al., 2015). In essence, sediment transport in mountain streams is necessarily a multidisciplinary topic combining (Church and Ferguson, 2015):

- Geomorphology through the distinction of process types and the relative activity of catchment sources, with
- Physics through the varied sediment transport formulae and their physical meaning.

This makes the subject both complicated, because of difficulties in attaining measurements, and complex because of feedback loops and couplings between processes, which may generate unexpected outcomes (Keiler, 2011).

This work continues from that of Recking et al. (2016), who demonstrated the importance of accounting for morphology in the bedload computation strategy. Within the present work, we additionally demonstrate the importance of paying attention to the material that structures the morphology of mountain streams; material that may be different from that transported. Three geomorphological situations that necessitate distinct computational strategies have been presented within this paper:

- Streams fitting more classical descriptions usually only transport the material present at their bed surface. In their headwaters, there are no significant sediment sources that would supply relatively fine sediment. Such streams usually experience relatively low sediment transport considering their

gradient, and are variably paved. Application of the classical bedload computation approaches, *e.g.*, Recking (2013b) and Recking et al. (2016), seems reasonable in these cases.

- Some mountain streams have inherited mostly paved beds from their geomorphic construction, but are currently supplied by sediment sources providing finer material. This material is eventually massively transported downstream, with marginal interaction with the bed structural morphology. Such travelling bedload necessitates a specific computation approach, as presented in this work.

- Bed armor breakings sometimes occur. The release of the fine subsurface and some self-reinforcing feedbacks then enhance the sediment transport efficiency. Alternative equations, based on knowledge of the high intensity sediment transport asymptotic behavior, must be used in these situations. A simplified equation has been proposed for such cases.

Mountain streams are high energy systems because of their gradients. Self-stabilizing processes, such as heavy armoring, limit the erosion rate and the transport of material in the downstream fluvial system. Many streams are thus mostly dormant, despite their steep slopes. However, sediment sources erratically provide massive sediment amounts to mountain streams, which may possibly change their activity. Extreme hydrological events may also trigger general armor breaking. This work aimed to clarify how such geomorphic processes affecting stream sediment supply and bed stability may fundamentally influence sediment transport, and how this perspective should influence the computation strategy used in prediction.

More generally, performing such computations for mountain streams with only poor knowledge of the geomorphic processes affecting sediment supply, would be unreasonable, if not irresponsible, when focusing on hazard assessment.

Acknowledgments

This study was funded by Irstea and the federative research structure VOR (Vulnératiblité des Ouvrages aux Risques) through the project " Le transit de la charge de fond dans les ouvrages torrentiels : quelles interactions entre barrages et flux sédimentaires?"' granted to EDYTEM (UMR 5204 CNRS) & IRSTEA. The authors would like to thank Elie Lamand and Segolène Mejean who performed the field work and preliminary analysis, as well as the Isère ONF-RTM service for providing archive data.

Notation

The following symbols are used in this paper:

= **Parameters:**

C = Chézy coefficient (-);

$D_{bedload}$ = sediment diameter to use in sediment transport formula (m);

$D_{friction}$ = sediment diameter to use in friction law (m);

D_m = mean sediment diameter (m);

D_X = sediment diameter such that $X\%$ of the mixture is finer (m);

$D_{84,BS}$ = bed surface D_{84} (m);

$D_{84,TraBL}$ = Travelling bedload D_{84} (m);

d = water depth (m);

g = gravitational acceleration (m/s^2);

Q = water discharge (m^3/s);

Q^* = pseudo-specific water discharge = $Q/S_{BV}^{0.75}$ (m^3/s.km$^{1.5}$);

Q_{sv} = volumetric sediment discharge (m^3/s);

q = water unit discharge = Q/W (m^3/s.m);

q_{sv} = volumetric sediment unit discharge = Q_{sv}/W (m^3/s.m);

q_s = sediment unit discharge (g/s.m);

q^* = dimensionless water unit discharge = $q/\sqrt{gSD_{84,BS}^3}$ (-);

p = dimensionless transition parameter between intermediate and high submersion (Eq. 4.6) (-);

R = hydraulic radius (m);

S = slope (m);

S_{BV} = catchment surface area (km^2);

U = water mean section velocity (m/s);

u^* = shear velocity = $\sqrt{gRS}$ (m/s);

W = channel - bed width (m);

V_{an} = mean annual sediment production (m^3/yr);

Z_{Bed} = channel bed elevation at the catchment outlet (m.osl);

Z_{MAX} = maximum catchment elevation (m.osl);

β = dimensionless coefficient of Eq. 4.8, =6.3 on average (m);

$\Delta Z = Z_{MAX} - Z_{Bed}$(m);

Φ = Einstein parameter: dimensionless solid discharge (Eq. 4.3) (-);

σ = standard deviation of the transported volume (m^3);

ρ_s = sediment density (kg/m^3);

ρ = water density (kg/m33);

τ^* = Shield parameter: dimensionless shear stress (Eq. 4.2) (-);

τ_m^* = dimensionless transition parameter between partial and full mobility (Eq. 4.5) (-);

= **subscripts:**

$\ldots_{X\%}$ = quantile of ... with probability X;

"la correction d'un torrent se borne le plus souvent à le contraindre à délivrer "au détail" ce qu'il livrait trop brutalement "en gros"."

Marcel Widmann in Poncet (1995, p. 713)

CHAPTER 5

Effects of check dams on bed-load transport and steep-slope stream morphodynamics

Guillaume PITON[a] and Alain RECKING[a]

[a] Université Grenoble Alpes, Irstea, UR ETGR, St-Martin-d'Hères, France.

Since the physics of sediment transport in steep slope streams is still an unresolved issue (Chap. 4), one can imagine that the question of the possible emergence of retroactive loops between bed-load transport and artificial structures are even more fuzzy.

The simple experiments reported in this recently published[1] chapter, were undertaken in a "*reduced complexity approach*" (Paola and Leeder, 2011). They aimed at exploring the possible effects of check dams on sediment transport within classical flume experiments. Trying to observed the possible sediment transport regulation pointed in Chapter 1 was the leading idea.

NOTA: The modifications brought to this chapter since its journal publication are highlighted in grey.

[1] Piton, G. Recking, A. "Effects of check dams on bed-load transport and steep slope stream morphodynamics", in *Geomorphology*, 2016, (in press.) DOI:10.1016/j.geomorph.2016.03.001

Abstract

Check dams are transversal structures built across morphologically-active streams in mountainous regions. These structures have been used widely in torrent-hazard mitigation for over 150 years. Thousands of them are regularly maintained by stream managers and torrent-control services. The stabilization role of these structures is well known, *i.e.*, they durably constrain the stream-bed through the creation of vertical and planar fixed points. What is not yet clear is to what extent check dams influence bed-load transport: How do peak solid discharge or flood-transported volume change when check dams are added to a reach? To address these questions, long-lasting small-scale experiments were conducted in a 4.8-m-long flume with either one, three or no structures. The results show that the addition of structures creates independent compartments in the bed level, which have a strong influence on bed surface armouring and stream morphodynamics: the consequence is that instantaneous transport intensities are unchanged, but peak solid discharge occur more often and for shorter duration. This results in the same total transported volume over the long term, but reduced volume for a single transport event. It reaffirms the observation of pioneering authors of the mid-19^{th} and early 20^{th} century who conceptualized the possible sediment transport regulation function of check dams: in addition to stabilizing the stream-bed, check dams influence bed-load transport through a buffering effect, releasing frequently and in small doses what, in their absence, would be transported abruptly en masse during rare extreme events.

Author key words: *torrent control works; bed-load transport; mountain streams; small scale models*

5.1. Introduction

Some steep slope streams (*i.e.*, with slope $S >$ 2% approximately) are characterized by flash floods with intense solid transport (Fabre, 1797). In such streams, the transport of substantial amounts of sediment increases flood hazards and related costs to society (Badoux et al., 2014). Since the mid-19^{th} century, special attention has been paid to curtailing part of the sediment transport by the use of soil conservation and stream bed stabilization measures, especially check dams (Surell, 1841; Gras, 1857; Demontzey, 1882).

The origins of the first grade control structures are unknown, however, they are probably very old (Jaeggi and Pellandini, 1997; Doolittle, 2013). To our knowledge, only occasional and very few high check dams were built before the 19^{th} century (see Armanini et al., 1991; Okamoto, 2007, for examples of early descriptions). Watershed-scale erosion-control plans emerged in European mountains in the mid-19^{th} century, in order to protect strategic network facilities such as roads, railways and fluvial embankment systems (Liebault and Taillefumier 2000, Vischer 2003, Hugerot 2015, Piton et al., *sub.*). The specific-features of torrents and the geomorphic processes leading to torrential hazard were theorized and highlighted during this period (Surell, 1841; Gras, 1857). In addition to soil conservation measures, drainage networks and reforestation, streams and gullies have been stabilized using longitudinal structures as groynes, dykes, bank protection and transversal structures (Fig. 5.1) such as check dams (Van Effenterre, 1982; Chatwin et al., 1994; VanDine, 1996).

Guidelines from the 19^{th} century list the varied purposes of check dams (Piton et al., *sub.*):

Figure 5.1 – Check dam series in the Saint Julien Torrent (73) Fr – 2015, grade control structure built above the bed level (photo courtesy of S. MEJEAN)

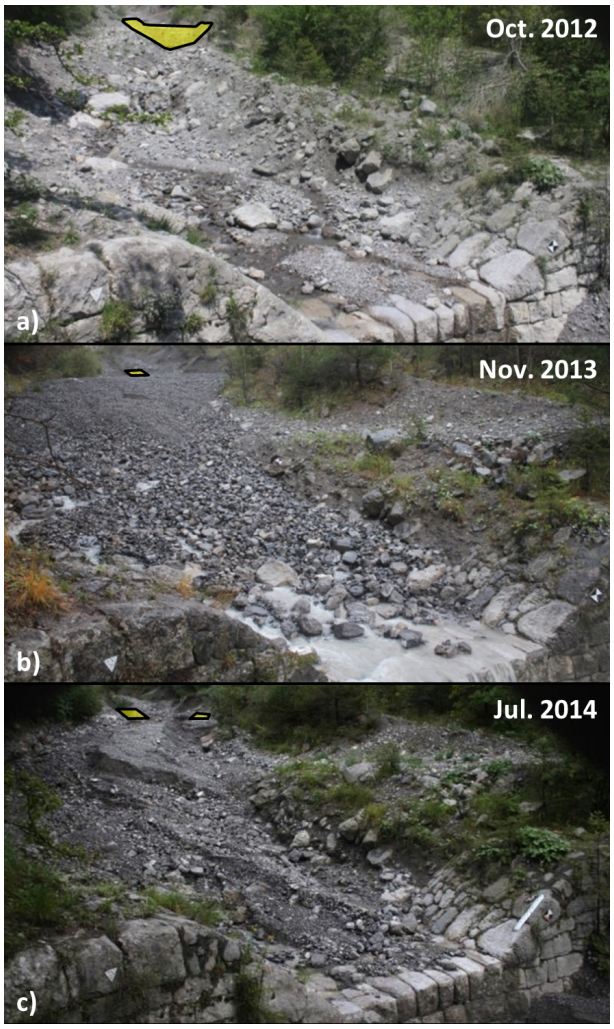

Figure 5.2 – Illustration of slope fluctuations in the vicinity of old check dams in the Manival torrent -Fr. (visible part of the upstream check dam colored in yellow): a) eroded reach with a mild slope in Oct. 2012, b) filled reach with a steeper slope, deposit burying the upstream structure in Nov. 2013 and c) partially eroded deposits in Jul. 2014 (Photos courtesy of C. BEL)

(i) bed stabilization: fixation of the stream longitudinal profile to prevent long term incision and lateral shifting, (ii) hillslope consolidation: elevation of the stream bed specifically to slow down unstable hillslope activity and the related sediment supply, (iii) decrease in slope: settling of an alluvial backfilled reach with a gentler slope compared to the initial torrent slope in order to limit flow energy and capacity to transport large boulders; (iv) retention: long-term trapping of a maximum volume of sediment in an area where a strong aggradation is acceptable (this effect stops once the structure is filled) and (v) solid transport regulation by temporary deposition of sediment. This later effect results from the natural bed-level fluctuation that commonly occurs in these streams (Fig. 5.2).

Functions (ii–v) are all consequences of the fact that check dams are usually built above the initial stream bed longitudinal profile (Fig. 5.1) (Thiéry, 1891; Bernard, 1927; Deymier et al., 1995). After a given time and sufficient sediment supplies, structures are filled and alluvial reaches are created upstream of structures. An alluvial dynamic then takes place on the reaches (function (iii)) with regularly reported deposition and re-erosion processes (function (v), Fig. 5.2). The initial check dam filling that usually results in nearly total bed-load trapping (function (iv)) may take some times, possibly dozens of years (e,g., Rickenmann and Zimmermann, 1993). However, hazard mitigation structures are built for much longer life duration. To better highlight the effect of the numerous check dams built for decades, this paper study the long term dynamic equilibrium (see López et al., 2010a; 2010b; 2010c; Zou et al., 2014 for studies addressing the transient initial filling period).

Nowadays river managers are maintaining thousands of check dams in mountainous catchments

(Carladous et al., 2016a) which is a complex and endless task (Van Effenterre, 1982). A better understanding of the influence of check dams on solid transport dynamics in streams is needed, in order to determine how to take them into account in downstream mitigation measures such as hazard mapping, land use plans, design of sediment traps and channel management on fans. More fundamentally, an improved understanding is also required in order to better adapt maintenance plans. In terms of risk mitigation, it will help to judge the relevance of continued maintenance of structures in hard to access headwaters and allow comparison with alternative structures, such as open check dams, which have emerged since the advent of mobile earth-moving machinery (Piton and Recking, 2016a; 2016b).

To what extent sediment transport dynamics are influenced by check dams is still poorly understood. The effect of check dams on sediment transport rate, on mean and peak values or on transient bed storage dynamics is not yet clear. Also to be discerned is the influence of structures on the temporal fluctuations of solid transport and bed level and their characteristic frequencies.

In this paper we describe new flume experiments to investigate the effects of check dams on bedload transport. We focus particularly on how check dams interfere with the highly fluctuating nature of bed-load transport on steep slope streams. After a presentation of the experimental conditions, the key results highlighted by our experiments are presented, discussed and compared with field examples.

5.2. Material and methods

5.2.1. Flow specificities

Flows in a reach downstream of a check dam typically take three specific forms (Figure 3 and Whittaker 1987): (i) a jet flow, plunging as a chute from the check dam crest, (ii) a tumbling flow, highly turbulent, dissipating the energy of the jet in rollers and digging a scour-hole; and (iii) a more uniform flow on the downstream alluvial section with established sediment transport. Each form can be more or less developed depending on the distance L from the next structure (Lenzi et al., 2003b; Marion et al., 2004; Comiti et al., 2013).

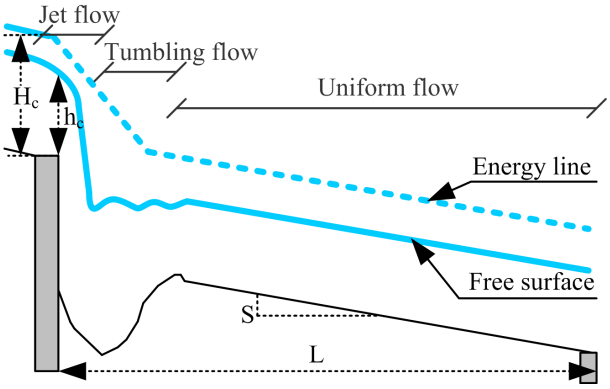

Figure 5.3 – Flow configuration in a reach between two check dams: the uniform flow length mainly depends on L the distance between structures.

The plunging flow development is related to the check dam height over the downstream stream bed and also to the initial velocity, which will control the parabolic trajectory of the jet. The scour-hole depth results from the erosion power of the turbulent flow dissipating the energy in the tumbling-flow. Scour-hole development has been widely studied (Veronese, 1937; Couvert et al., 1991; D'Agostino, 1994; Gaudio et al., 2000; Lenzi et al., 2002; Lenzi et al., 2003b; Lenzi et al., 2003a; Marion et al., 2004; Marion et al., 2006; D'Agostino and Ferro, 2004; Comiti et al., 2005; Comiti et al., 2006; Lin et al., 2008; Comiti et al., 2013) .

Lenzi et al. (2003b) demonstrated that when check dams are close enough to each other, scour-hole dimensions tended to decrease for equivalent discharge and check dam height, thus limiting the scouring threat to structures. They called *"geometrical interference"* this influence of the downstream structure on the upstream scour-hole. In streams with very steep slopes the distance between structures can be comparable to the stream

width. In this case, the alluvial part of the reach almost disappears, check dam series resemble step pool rivers (Whittaker, 1987; Jaeggi, 1992; Lenzi, 2002) and the energy dissipation by tumbling flows are maximized (Canovaro and Solari, 2007).

For structures spaced more than 15 to 20 H_c (with H_c the critical flow energy $\approx 1.5h_c$ and h_c the critical flow depth), the geometrical interference is considered to be negligible (Lenzi et al., 2003b; Comiti et al., 2013). In such conditions it can be assumed that the bed development is not influenced by by the upstream scour-hole flow. The slope of this reach can thus be considered as an "alluvial slope" with slope S dependent on hydrological and solid transport features (Fig. 5.3). This analysis focuses on such widely spaced structures, *i.e.*, with $L >> H_c$.

5.2.2. Experimental set-up

New experiments[1] were performed in the manner described in a previous analysis of the bedload transport dynamics in a steep slope flume (Bacchi et al., 2014). A titling flume 4.8 m long, 0.107 m wide, and 0.4 m deep was set to a slope of 12% (Fig. 5.4).

Three configurations were tested (Fig. 5.4): (i) noCD: a reference test without a structure in the flume, (ii) 1CD: one check dam in the middle of the flume, and (iii) 3CD: flume with three equally spaced check dams. In the case of the noCD test, the experiment was allowed to run for 20 h in order to be sure to to reach a dynamic equilibrium, following which 30 h of measurements were undertaken (actually a shorter period than 20-h would have been sufficient, as to our experience, two cycles of complete aggradation and degradation lasting 8-10 h were expected. In the case of the present study, the 30-h of experiments were sufficient to highlight the changes in the 1CD and 3CD tests, the statistical analysis has thus been performed with the end of the 50-h time series of the noCD test). Shorter periods of stabilization were required for 1CD and 3CD tests due to the shorter distances concerned. Check dams were modelled by horizontal plastic plates fixed across the entire flume width. The possible effects of the spillway design or of permeable body, *e.g.*, for structures made of gabions, are thus neglected in this study. Small counter check dams were added to each check dam toe in order to limit scour depth, as is usually done in the field (Demontzey, 1882). Grains with diameter between D_{16} and D_{84}, with D_x the sediment mixture diameter such that $x\%$ are finer, were glued onto the side-walls to reproduce the natural roughness of steep slope stream banks (Fig. 5.5).

[1] See details in measurement and setup definition in §5.7, p. 121.

Table 5.1 – Grain size distribution features

D_{min} [mm]	D_{50} [mm]	D_{84} [mm]	D_{max} [mm]	D_{mean} [mm]
0.8	3.0	8.2	20	5.6

Note: D_{min} and D_{max}, minimum and maximum sediment diameter respectively and D_{mean}, mean arithmetic sediment diameter.

5.2.3. Sediment mixture

A poorly sorted natural sediment mixture was constructed with respect to grain size distribution ratios observed by Recking (2013a) in a large gravel bed river dataset. The grain size distribution features of this mixture are summarized in Table 5.1. To highlight grain size sorting, coarse grains were painted in red and green, the coarsest fraction was painted in blue. The medium sizes were naturally brown and grey while the fine fraction was naturally white.

5.2.4. Supply conditions

In order to identify the intrinsic average response of a check dam to a long hydrological period, the water and solid discharges were set at a constant rate during all runs. The water discharge was recirculated and fixed to $0.55l/s$ ($\pm 0.03l/s$) with a constant-head reservoir. It was controlled

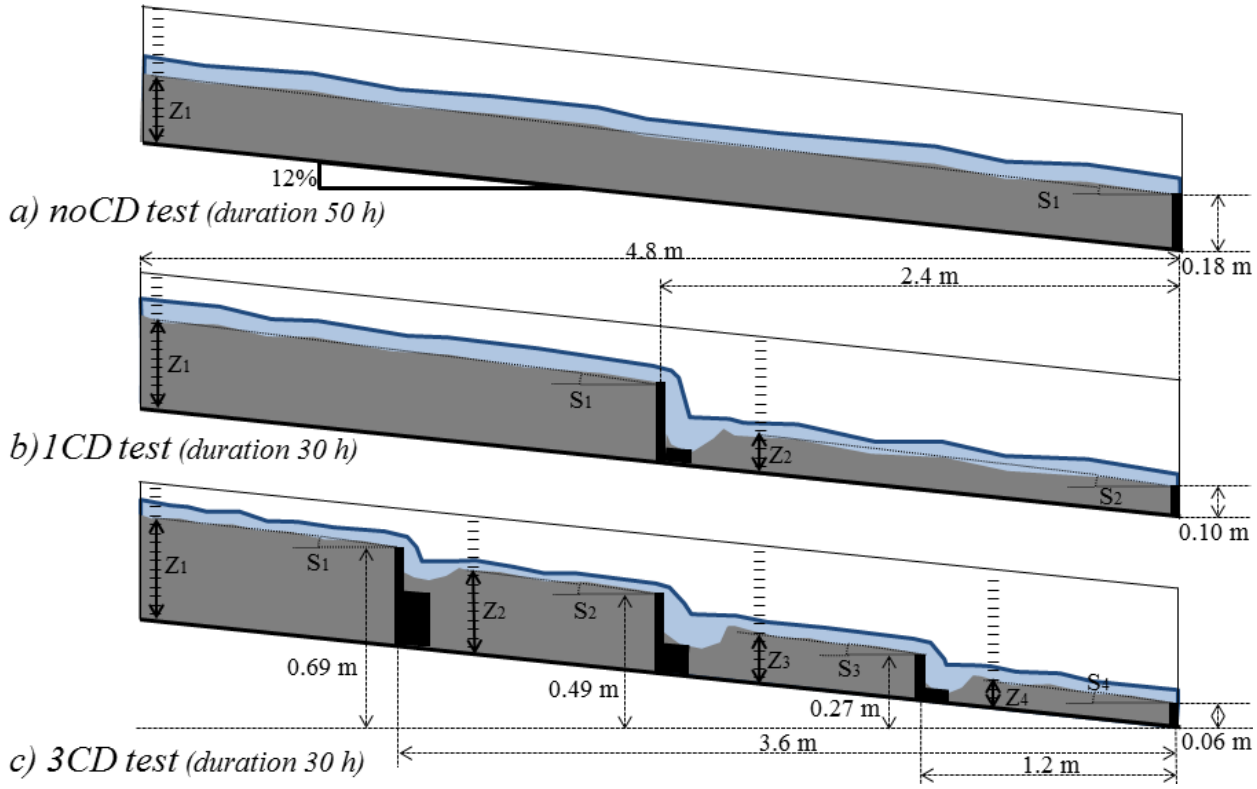

Figure 5.4 – Flume configuration: a) noCD test: reference test without structure in the flume, b) 1CD test: one check dam test with one structure in the middle of the flume and c) 3CD test: three check dam test with three structures regularly installed along the flume. Reaches between structures are numbered from upstream to downstream.

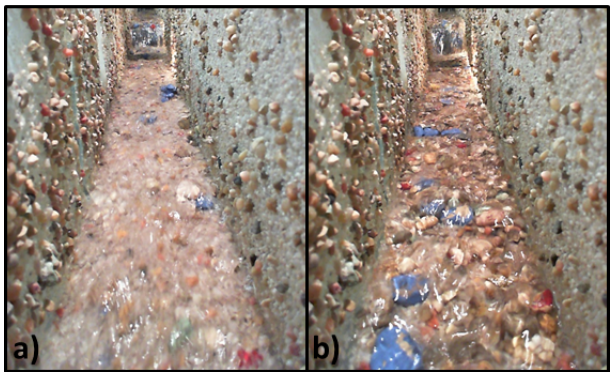

Figure 5.5 – Rough flume side walls and bed states at the same position at different time: a) fine bed during a bed-load sheet event, b) paved bed with high grain protrusion, 3'30" later

and recorded by an electromagnetic flowmeter at a 10-Hz frequency. The solid discharge of $44g/s$ ($\pm 2g/s$) was fed by a hoper delivering sediments to a velocity-controlled conveyor belt which was also measured at a 10 Hz frequency. The system was a sediment fed configuration according to the definition of Parker and Wilcock (1993). Sediments were carefully mixed before introduction to the hoper in order to ensure a constant grain size distribution at the inlet. The experimental conditions were chosen very similar to those used in Bacchi et al. (2014) to make possible some comparison.

5.2.5. Measurements

The outlet solid discharge (Qs) was measured by weighing the cumulative solid discharge every 3 to 4 minutes ($\pm 1g/s$). A correction factor for the water content of the measured solid discharge was derived by drying 32 randomly selected samples. The bed levels (z_i) of the reach

(i), numbered from upstream to downstream, were measured in the upstream part of each reach (Fig. 5.4), downstream of the scour-hole extension and with a precision of $\pm 2mm$. The measurements were performed visually using staff gauges on the side walls viewed through windows pierced in the glued grains. Complementary measurements were done using ultrasonic sensors at the staff gauge abscissa. The bed-level under the ultrasonic sensor was computed assuming a constant water depth: the bed level is considered to be the free surface level (measured by ultrasonic sensors) minus the water depth. The latter is considered constant and equal to the mean computed value of Table 5.2. The precision of the measurement using this assumption is degraded compare to direct visual measurement and was considered to be of $\pm 5mm$ mainly due to the varying water depth which was dependent on bed state and roughness (see *e.g.*, Fig. 5.5 or Ghilardi et al., 2014b). Such variations of the water depths ($\pm 5mm$) are equivalent to variations in the $Froude$ number between 0.7 and 2.4: a pretty large range, for instance compared to Froude number variations observed in constant feeding long lasting experiments by Ghilardi et al. (2014b) (Slope: 0.067, $Fr = [0.6;1.14]$, presence of immobile boulders in the flume) or regarding the variations of measured velocity and water depth (Table 2); the $\pm 5mm$-uncertainty range is thus considered conservative.

At the reach scale, *i.e.*, between two dams, the reach mean slope can be deduced from the bed level and assuming a constant level of the bed fixed by the check dam crest level (Fig. 5.4):

$$S_i = \frac{z_i - z_{dam,i}}{L_i} \tag{5.1}$$

with S_i, the slope of the i^{th} reach, z_i and $z_{dam,i}$ the bed level of the upstream part and the dam level downstream of the i^{th} reach, and L_i the length of the i^{th} reach. Complementary intra-reach ultrasonic measurements taken just upstream of the check dam suggested that the hypothesis of a constant bed level at the check dam abscissa was reasonable. An error analysis concluded on a slope precision of ± 0.005 (c.f. § 5.7).

5.2.6. Main flow conditions

The main characteristics of the flow conditions are reported in Table 5.2, they were estimated through 3 independent approaches that gave very consistent results.

1. The mean water velocity U was measured by manually tracking the trajectories of 92 polystyrene beads individually released in the 1CD test ($> 4,400$ instantaneous bead velocity measurement, *i.e.*, couple of frames). The video (30 frame/s) was filmed from the ceiling (see timelapse video in supplementary material). This surface velocity estimation was corrected by a factor of 0.85 to compute the mean velocity, following the recommendation of Muste et al. (2010).

2. The water depth was independently measured during the noCD test on a series of 68 side pictures of staff gauges.

3. The velocity was also computed using the Rickenmann and Recking (2011) equation and results are consistent with the measurements (Table 2):

$$\frac{U_{calc}}{\sqrt{gSD_{84}}} = 1.443 q^{*0.6} [1.+(\frac{q^*}{43.78})^{0.8214}]^{-0.2435} \tag{5.2}$$

with $q* = Q/W\sqrt{gSD_{84}^3}$.

From either water depth or velocity measurements, it is possible to computed the other parameter from the mass conservation equation $Q = WdU$ (where W was the flume width). We computed the Shields stress $= Sd/\Delta D_{84}$, the Froude number $Fr = U/\sqrt{gd}$, the flow and grain Reynolds numbers $Re = Ud/\nu$, and $Re* = D_{50}\sqrt{gdS}/\nu$ (where ν is the kinematic viscosity) for measured and computed estimations of the flow parameters. The critical shear stress, $\tau*_{cr} = 0.15S^{0.275}$, was

considered slope dependent according to Recking et al. (2008b). As sediment and water discharges were kept constant using the same grain size distribution, providing that the mean slope weakly varied (see later), the main flow features summarized in Table 5.2 are assumed not to change between the 3 tested configurations.

5.3. Results

5.3.1. General observations

All runs (noCD, 1CD and 3CD) showed dramatic changes in bed state (see videos in supplementary materials), ranging from highly mobile bed-load sheets during bed erosion events (Fig. 5.5a) to nearly fixed paved beds (Fig. 5.5b). These effects were consistent with previous observations (*e.g.*, Kuhnle and Southard, 1988; Ghilardi et al., 2014b; Bacchi et al., 2014) and could be attributed to kinetic sorting (Frey and Church, 2009; 2011). A complete description of this natural and autogenic (internally generated) process of fluctuations in constantly fed flume can be found in Kuhnle and Southard (1988); Recking et al. (2008b); Recking et al. (2009); Ghilardi et al. (2014b); and Recking (2014). It may be summarized as follows Recking et al., 2009; Bacchi et al., 2014: during armouring, coarse grains are trapped by the protrusion of other coarse grains at rest and create a rough and paved bed surface. At the same time, fine grains are efficiently trapped in the armour porosity by kinetic sieving, creating a layer of fines below the armour. The combination of a stable rough surface layer, with a fragile subsurface layer of fines leads to unstable slopes. The rough bed aggrades until the armour is destabilized due to steepness or by a stochastic destabilization of key grains in the armour force chains. Once the armour starts breaking, the fine sub-surface released in the transport layer smoothes the bed and leads to high transport efficiency of the coarse fraction and strong bed erosion. This sediment flushing develops until a new milder equilibrium slope is reached on which sediment transport is no longer possible. A new cycle of aggradation then begins. As a consequence the bed slope and solid discharge fluctuate with time, and sediment is transported through some kind of sediment wave, as observed in previous similar experiments, *e.g.*, Kuhnle and Southard (1988) and Whittaker (1987).

Evolution over time of the downstream reach mean slope and solid discharge at the flume outlet are shown in Figure 5.6 for the three runs. The initial evidence is that for identical flow and sediment conditions (identical flume slope, grain size, and feeding), the presence of check dams strongly affects the fluctuation process observed both in the flume and at the outlet, through an increase in the frequency of fluctuation. The changes in the outlet solid discharge signal of Fig. 5.6c are not as obvious as the changes in the slope signal: due to technical limitation it was not possible to perform a high frequency measurement of the outlet solid discharge (limited to once every 3 to 4 minutes). On the contrary, the use of ultrasonic sensors made it possible to measure bed fluctuations at a frequency of 10 Hz during the 3CD test. Comparison with the ultrasonic measurements on the 1CD test demonstrated that visual measurements every 3-4 minutes were sufficient to catch the fluctuation cycles without subsampling (c.f. § 5.7).

5.3.2. Instantaneous solid discharge variations

Due to successive phases of bed armouring and erosion, the outlet solid discharge varied substantially between 1% and 300% of the feeding rate (Fig. 5.6). The strong grain size sorting observed on the bed state was confirmed in the transported material which, during aggradation events, consisted mainly of medium diameters *i.e.*, transient reversed mobility events were observed (*sensu.* Solari and Parker, 2000), as fine and coarse grains were preferentially trapped by the above men-

Table 5.2 – Main flow features

Parameter	U	d	Fr	τ^*_{84}	$\tau^*_{84,cr}$	$\tau^*_{84}/\tau^*_{84,cr}$	Re	$Re*$
Units	$[m/s]$	$[mm]$	$[-]$	$[-]$	$[-]$	$[-]$	$[-]$	$[-]$
$U_{measured}$	0.46 ± 0.10	$11^\dagger$	$1.4^\dagger$	$0.099^\dagger$	0.083	$1.3^\dagger$	$5,150^\dagger$	$344^\dagger$
$d_{measured}$	$0.37^\dagger$	13 ± 3	$1.1^\dagger$	0.115	-	1.5	-	371
$Computed$	0.42	$12^\dagger$	$1.2^\dagger$	$0.109^\dagger$	-	$1.4^\dagger$	-	$360^\dagger$

†: Deduced from the mass conservation, *i.e.*, through $Q = WdU$.

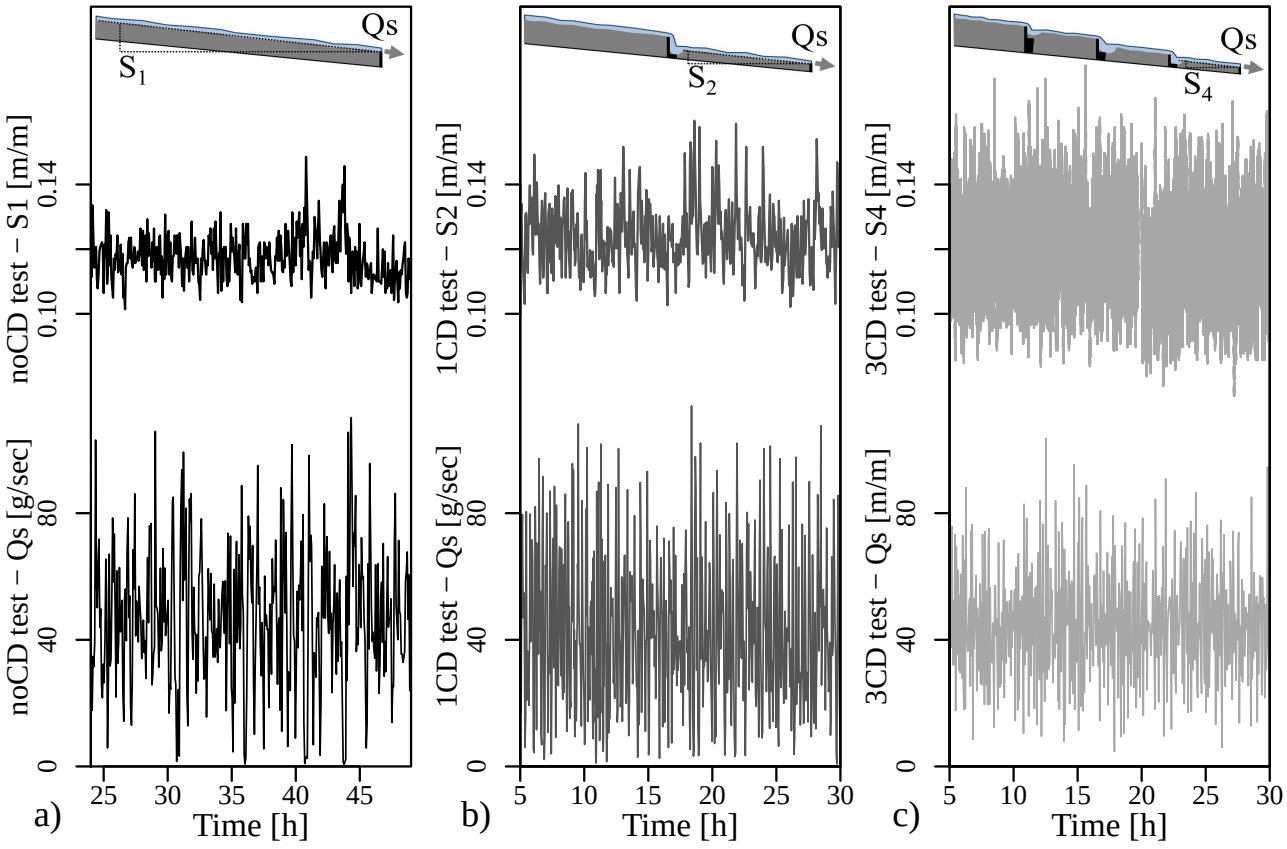

Figure 5.6 – 25-h time evolutions of solid transport Qs and downstream reach slope Si for the 3 configurations tested: a) noCD test without structure, b) 1CD test with one check dam and c) 3CD test with three structures; illustration of the increase in fluctuation frequency with segmentation of the flume by structures

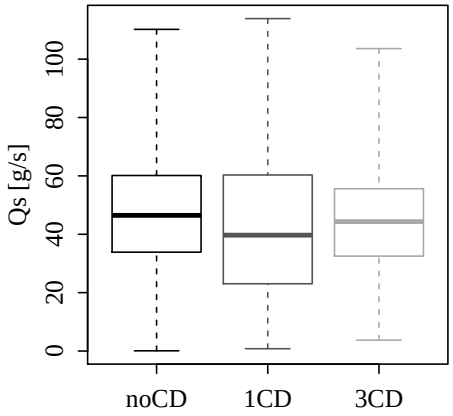

Figure 5.7 – Statistics of the outlet bed-load discharge Qs: no consistent trend to smaller or higher variation of the instantaneous solid discharge with and without structure

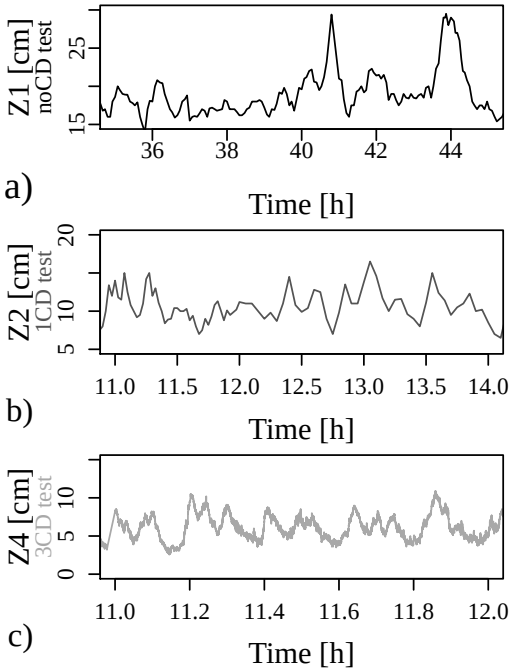

Figure 5.8 – Bed level z_i fluctuations measured in each downstream reach for different time duration: a) 10 h of noCD test without structure, b) 3 h of 1CD test with one check dam and c) 1 h of 3CD test with three structures. Illustration of the acceleration of the fluctuation periods

tionned grain size sorting process. During erosion events the transport rate increased and fines and coarse sediments were released from the bed and transported as bed-load sheets with clearly higher transport efficiency consistently with Kuhnle and Southard (1988).

Despite these high temporal fluctuations, the solid discharge values at the outlet were nearly statistically identical in the three configurations (Fig. 5.7), demonstrating that the instantaneous intensity of the transport rate seems to be poorly influenced by check dams. Conversely, changes in fluctuation frequencies and durations play a key role that is discussed later.

5.3.3. Bed level and slope fluctuations

A time-fluctuating outlet sediment transport, observed in constant solid feeding conditions, necessarily imposes, by mass conservation, a fluctuating storage in the flume bed. Indeed, bed level variations were observed during all experiments with amplitude of several times the coarse grains' diameter. However, the frequencies of these fluctuations tend to collapse when check dams segment the flume (Fig. 5.8). Bed fluctuations can be observed as reach mean slope fluctuations (see Eq. 5.1 & Fig. 5.6).

One important result we would like to highlight here is that contrary to what is often reported (Iroume and Gayoso, 1991; Kostadinov, 1993; Porto and Gessler, 1999; Porto and Gessler, 1999; Ferro and Porto, 2011; Kostadinov and Dragović, 2013), the addition of check dams does not necessarily lead to a decrease in slope[1] (Fig. 5.9). This result is important in terms of structure de-

[1] During the PhD defence, Dieter Rickenmann pointed that the total slope increased with the addition of check dams.
When asserting that "the addition of check dams does not necessarily lead to a decrease in slope", we mean that the slope of sediment deposition - more precisely its mean temporal value, when compared to a similar alluvial reach with unchanging supply conditions - does not change (see later). However, since the total profile elevation is the cumulation of each check dam heights, plus the reaches' own slope elevation, we introduced an increase in the average river slope with our check dams addition. The check dams have been built above the initial bed level, as done in the field. In our case high enough never to be buried despite bed level fluctuations. The check dams progressively elevate the bed level. They are consequently representative of a consolidation check dam series (*sensu* Chap. 1). It does not change the important result that the deposition slope is not strongly related to the presence of structure in our quite-spaced structures' configuration.

sign as it contradicts the classical design criteria $S \approx 2/3 S_{init}$, with S_{init} the initial slope of the stream before check dam construction (Fig. 5.9), a criteria which is regularly reported in the literature (Sabo Department., 2000; Böll et al., 2008; Osanai et al., 2010; Kostadinov and Dragović, 2013). These different conclusions are not inconsistent, and can be explained when the alluvial nature of the initial bed and the supply condition of the system is considered (see discussion section). Another point worthy of discussion is that the range of fluctuation in slope tends to increase from upstream to downstream in a given configuration, *i.e.*, with an increasing number of reaches between the constant supply point and the analysed reach.

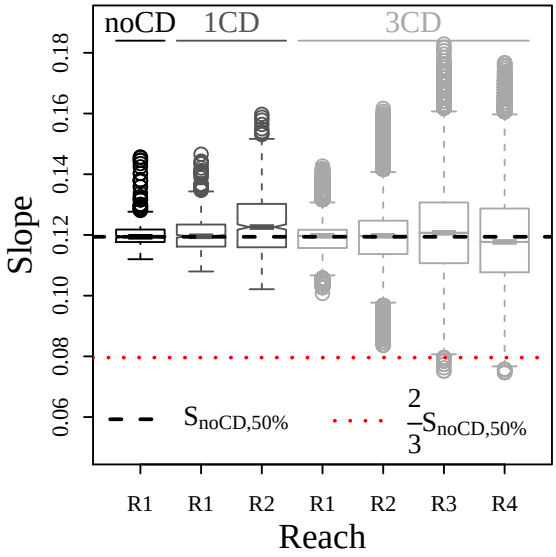

Figure 5.9 – Mean slope Si statistics of reaches on 25-h experiments compared to the median slope value of the noCD test, $S_{noCD,50\%}$. Median values are fairly stable while extreme values evolve from upstream to downstream direction in each configuration.

5.4. Analysis of Results

5.4.1. Fluctuation period

A Fast Fourier Transform (FFT) of the slope signals presented in Fig. 5.6 demonstrates that the signal-power shifts from low frequencies to high frequencies with the flume segmentation (Fig. 5.10): in the noCD test the highest power frequency were made at 7 and 10 h cycles. These decreased to 1 and 2 h in the 1CD test and finally collapsed to 9 and 7 min in the 3 CD test.

It is likely to be the result of equivalent sediment discharge (Fig. 5.7) feeding smaller volumes, thus filling them more rapidly. The active volume of a reach i, $V_{act,i}$, *i.e.*, the maximum volume filled and eroded in the reach, can be expressed by:

$$V_{act,i} = W.L_i^2(S_{i,max} - S_{i,min}) \qquad (5.3)$$

where W is the flume width, L_i its length, $S_{i,max}$ and $S_{i,min}$ the maximum and minimum slope values. For slopes with the same order of magnitude (Fig. 5.9), the volume of sediment that can potentially be stored and released by a reach is thus mainly controlled by the square of its length (Eq. 5.3).

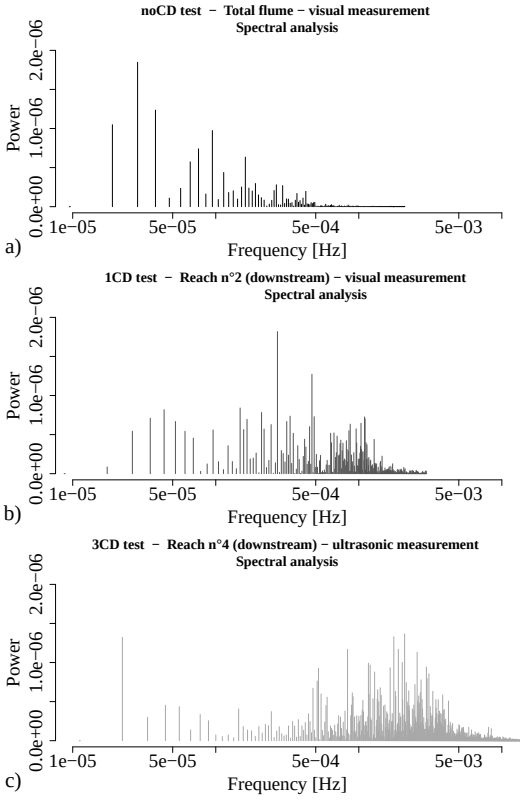

Figure 5.10 – FFT of slope signals Si shown in Fig. 6, demonstrating higher frequency fluctuations with increase in number of check dams: a) noCD test, b) 1CD test c) 3CD test

The whole flume active-volume decreases when structures are added (Eq. 5.3. & Fig. 5.4). Smaller reaches located behind each check dam have shorter time responses to boundary solicitations (Jerolmack and Paola, 2010). As a consequence, for a given feeding rate, the bed active volumes are filled and emptied more rapidly, and bed level fluctuations (*e.g.*, Fig. 5.2) are more frequent in check dam equipped streams than in streams without structure, where bed recharge takes much longer.

5.4.2. Solid transport autocorrelation

Signal-autocorrelation in time-series eventually results in what is sometimes called the "Hurst phenomenon", also known as long memory or multiscale fluctuations (Koutsoyiannis, 2002; Koutsoyiannis and Montanari, 2007). In the case of sediment transport, it would essentially be the tendency of high or low solid discharge values to form temporal clusters, rather than being randomly distributed (Ghilardi et al., 2014b). In other words, studying autocorrelation highlights and quantifies a kind of system memory (Koutsoyiannis and Montanari, 2007). A memoryless system, for instance a random signal, would not be autocorrelated. On the contrary, a long-memory system could show tendencies for multiscale fluctuations, with increases in activity during some periods while other periods would experience weak activity. The autocorrelation on a given time window of duration l can be analysed by computing the autocorrelation factor γ_l defined by Eq. 5.4 in the case of solid transport time series.

$$\gamma_l = \frac{\sum_{i=l+1}^{N}(Qs_i - \langle Qs\rangle)(Qs_{i-l} - \langle Qs\rangle)}{\sum_{i=1}^{N}(Qs_i - \langle Qs\rangle)^2} \quad (5.4)$$

with Qs_i, the outlet discharge at time i, $\langle Qs\rangle$, the mean value of the Qs time series and N the number of measurements in the Qs time series.

The autocorrelation factor γ_l varies in the range $[-1;1]$. A "*white noise*" (*i.e.*, random) signal would not show any autocorrelation, and would have a theoretical $\gamma_l = 0$ (though it can be slightly positive or negative due to sampling effect; see later). A positive autocorrelation, *i.e.*, $\gamma_l > 0$, means that $Qs(t)$ and $Qs(t+l)$ are correlated, having similar differences with the mean value of the time series $\langle Qs\rangle$. A negative autocorrelation, *i.e.*, $\gamma_l < 0$, means that $Qs(t)$ and $Qs(t+l)$ are distributed around $\langle Qs\rangle$, with sort of out-of-phase signals around the mean.

The autocorrelation factor γ_l had been calculated for the Qs time series of the three configurations for values of l varying between 1 minute and 6 hours (Fig. 5.11). Random "*white noise*" signals were also created in order to highlight the statistical significance of the experimental γ_l values: one thousand 30-h time series were randomly generated based on a normal distribution with the same mean and standard deviation as Qs_{noCD}. For each l value, 1000 γ_l values were computed (one per random time-series) from which the γ_l quantiles with probability 0.005 and 0.995 were extracted. The range between these two quantiles is drawn in red on Fig. 5.11 to represent the extent of γ_l variation of a signal with no autocorrelation. In other words, only γ_l values outside of the red range have autocorrelation higher than a random signal at a statistical significance level of p = 0.01.

On one hand, Fig. 5.11 indicates that for long time periods ($l >$ 60–90 min), γ_l fall within the red range, *i.e.*, the Qs time-series show little or no correlation over such long periods. On the other hand, γ_l values may be high for short time periods (10 min for Qs_{noCD} to 1 min for Qs_{3CD}), illustrating that high or weak sediment transport events tend to last longer than 1 min, even regularly attaining around 10 min in Qs_{noCD}. Conversely, after such strong positive autocorrelation occurs, all signals then show inverse correlation, *i.e.*, γ_l <0, which means that after a given period of strong or weak sediment transport, the trend

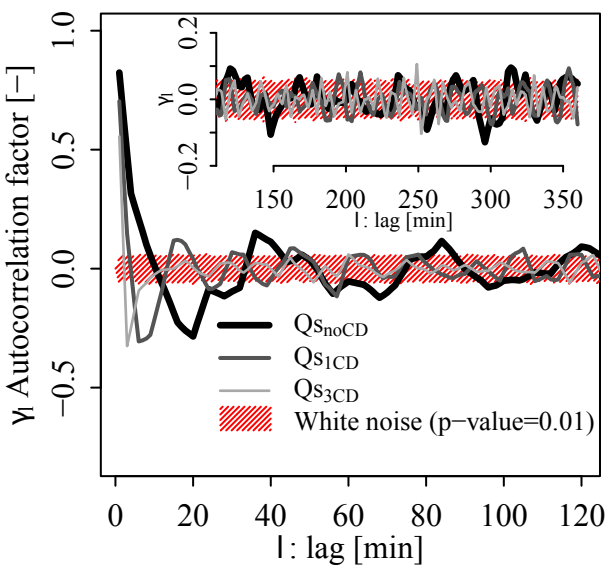

Figure 5.11 – Autocorrelation coefficients vs lag duration for solid transport Qs time-series of noCD, 1CD and 3CD experiments; White noise p-value extracted from 1000 random signals with similar mean and standard deviation than Qs_{noCD}. Positive autocorrelation can be seen for a short time, rapidly followed by negative autocorrelation. These autocorrelated periods shorten when structures are added to the flume.

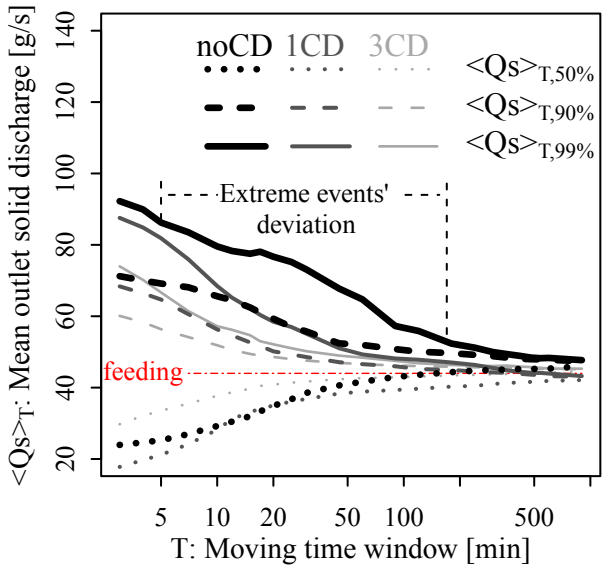

Figure 5.12 – Outlet solid discharge quantiles of $\langle Qs \rangle_T$ the mean solid discharge on variable averaging time windows of duration T. Evidence of long-lasting and intense solid transport events (deviation on the noCD data), which tend to disappear with the flume segmentation

tends to inverse. As our feeding conditions were constant in time, all erosion events were followed relatively rapidly by aggradation events and vice versa. Finally and more interestingly, the duration of periods with strongly autocorrelated values tends to collapse dramatically with flume segmentation, *i.e.*, long-lasting erosion or aggradation events disappear and fast cycles of storage and release emerge when check dams are added to the system. In other words, the 'memory' that allows multiscale fluctuations to occur in a natural bed tends to disappear when check dams are added.

5.4.3. Extinction of extreme solid transport events

To confirm the disappearance of extreme erosion events, the outlet solid discharge was averaged over a moving time window (T) with duration varied from 1 min to 10 h. The medians $\langle Qs \rangle_{T,50\%}$ and quantiles $\langle Qs \rangle_{T,90\%}$ and $\langle Qs \rangle_{T,99\%}$ (*i.e.*, with probability of 0.9 and 0.99, respectively) for all T-values and each run are presented in Fig. 5.12.

The first conclusion from Fig. 5.12 is that with increasing window T, all series converge toward the value of the feeding rate (≈44 g/s). This illustrates that on average the flux is balanced: *i.e.*, when T is longer than several cycles, the mean outlet flux is equal to the mean inlet flux.

For time windows shorter than 120 min, different trends appear: first, the medians, $\langle Qs \rangle_{T,50\%}$ are inferior to the feeding rate, which means that the flux is unbalanced toward storage in the flume (the bed was aggrading more than 50% of the time with a low intensity, on the contrary erosion are shorter and more intense). Secondly, the rare and strong events, represented by $\langle Qs \rangle_{T,90\%}$ and $\langle Qs \rangle_{T,99\%}$, decrease with time window duration, illustrating that bed-erosion events and sediment recruitment from the bed are finite in volume and cannot last infinitely. Finally $\langle Qs \rangle_{T,90\%}$ and $\langle Qs \rangle_{T,99\%}$ decrease more rapidly when the

flume is segmented by check dams, whereas a sudden deviation exists in the noCD experiment data: This is the signature of rare but long-lasting and intense sediment-release events (global bed erosion) which no longer exist when the flume is segmented.

An analysis of bed volume fluctuations has been undertaken to confirm the signature of erosion events in the outlet solid discharge. The erosion event volumes V (continuous negative evolution of volume stored in the bed, integrated over the duration of each event) have been computed based on the z_i time-series. These volumes have been made dimensionless by dividing them by the active volume of the noCD test (computed with Eq. 5.3). They are hereafter called V^* and are analysed in Fig. 5.13.

Two erosion events with $V^* > 0.5$ occurred in the noCD test (Fig. 5.13a). They corresponded to global armour breakages concerning the whole flume length generating big sediment pulses at the outlet. When check dams were added to the flume, the erosion-event volumes decreased and extreme armour-breaking events disappeared. One must note that the 3CD test volumes are overestimated: they had been computed based on one bed level visual measurement per 3 min period and thus comprised multiple smaller events in each represented event (ultrasonic measurements were not taken in all reaches, making a 10-Hz total flume volume estimation impossible). Despite this overestimation, the trend towards decreasing event volumes remains visible. The reduction should actually be stronger in Figure 5.13c.

Event durations were also extracted from the times series. Event volumes and durations are plotted in Fig. 5.14 to take into account not only the magnitude of events, but also their intensities. Two lines, one representing the dimensionless supply sediment discharge $\langle Qs \rangle^*$ and the other 50% of $\langle Qs \rangle^*$ (rendered dimensionless with the same method as $V*$) are plotted to act as comparison elements. As an interpretive example, an erosion point located on the $0.5\langle Qs \rangle^*$ line would correspond to a continuous recruitment of a volume V^* during a given duration which would be equivalent to an average rate of $0.5\langle Qs \rangle$. Consequently, the outlet flux would on average be $1.5\langle Qs \rangle$ during this erosion event.

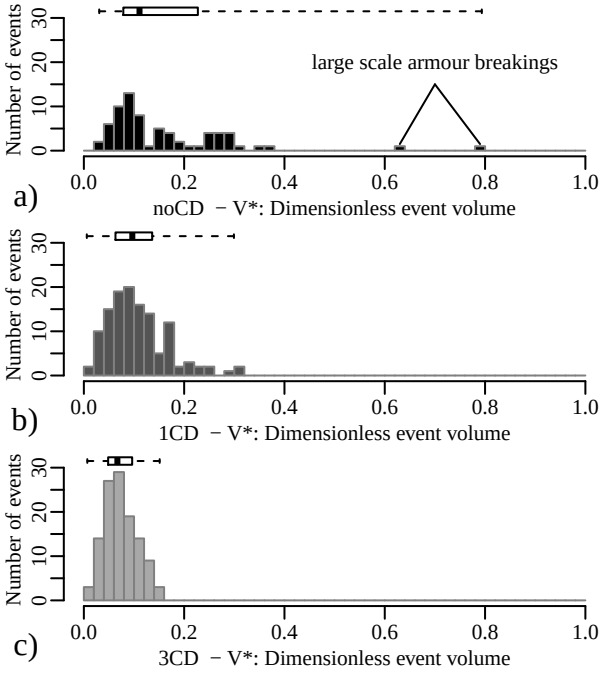

Figure 5.13 – Number of events depending on their dimensionless erosion volume (V^*=Erosion event volume divided by the active volume of noCD test) for a) the noCD test; b) the 1CD test and c) the 3CD test. There is a a general trend to a decrease in erosion volume with flume segmentation and disappearance of extreme events recruiting more than half of the active volume ($V^* > 0.5$)

Multiple points appear between the two lines, including most of the strong magnitude intense events (*e.g.*, V^*>0.3) with recruitment from the bed constituting 1/3 to 1/2 of the outlet flux. Sediment coming from the bed would thus often constitute a significant part of the outlet flux.

As mentioned previously, the number of events increases with the presence of check dams, however, the cumulative effects of multiple small erosion events (Fig. 5.14c) do not exceed rare but intense global armour breaking occurring during the noCD test (Fig. 5.14a). As a consequence, check dams generate a decrease in outlet sediment

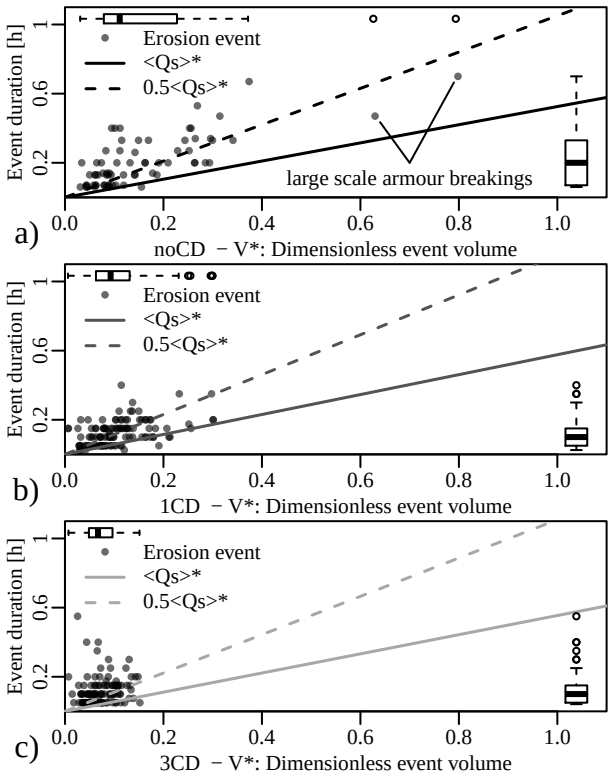

Figure 5.14 – Erosion event duration vs Erosion event dimensionless volume (V^*) and comparison with the dimensionless feeding rate $\langle Qs \rangle^*$ for a) the noCD test; b) the 1CD test and c) the 3CD test. Extreme events recruiting more than half of the active volume (V^*>0.5) disappear when check dams are added. In addition the event volumes and durations tend to decrease with segmentation of the flume (side boxplots).

discharge over periods longer than a few minutes (Fig. 5.12); *i.e.*, they regulate sediment transport.

5.5. Discussion

5.5.1. Comparision with sand bed experiments

The results presented in this paper somewhat depend on the grain size distribution shape (poorly sorted) and on the transport stage ($\tau^*/\tau^*_{cr} \approx 1.2 - 1.4$, *i.e.*, low). For instance, quite similar experiments have ever been performed by Martìn-Vide and Andreatta (2006; 2009), but addressing gentler slopes (0.01-0.04) and, most importantly, using a nearly uniform sand ($D_{84}/D_{50} \approx 1.2$) in very high transport stage ($\tau^*/\tau^*_{cr} \approx 12$). Different results were observed, which can be explained by two reasons investigated in Recking et al. (2009): i) bedload transport fluctuations tend to disappear when transport stage increases and, ii) the fluctuations are, at least partially, a consequence of a very intense grain size sorting which weakly develop on uniform grain size mixtures. Steep Alpine streams where check dams are regularly built have generally very poorly sorted cobble and gravel beds. In addition, transport stages in such streams are seldom very high (Parker et al., 2007; Recking et al., 2012a). This context justified the studied experimental conditions that are fundamentally different from the milder rivers with stronger discharges modelled by Martìn-Vide and Andreatta (2006; 2009).

5.5.2. Influence of structures on slopes

A. A cascading process

Check dams partially segment the flume creating sediment barriers following the Fryirs (2013) definition, *i.e.*, structures that *"disrupt longitudinal linkages in the sediment connectivity through their effect on the base level or bed profile of a channel"*. In the reaches downstream of a check

dam sediment supply directly depends on the upstream reach dynamics. For example, during an aggradation of reach n, reach $n+1$ is partially sediment starved and often tends to incise. In an alluvial reach without structures, a downstream incision would destabilize the upstream bed by backward erosion propagation. Once check dams have been built, this propagation is no longer possible. A nearly total trapping in reach n, starves reach $n+1$ inducing its incision, but this downstream lowering of the bed level no longer destabilizes the upstream reach bed n. Partially independent compartments (*i.e.*, independent in term of bed level but dependent considering the sediment cascade process) have been created by adding check dams.

As distance from inlet increases, the more the sediment supply depends on varied upstream reachs' dynamics, and the longer the starving period can last. Consequently, a deeper incision can develop as suggested by the decreasing minimum slope in the downstream direction (Fig. 5.9). Symmetrically, the shorter the reaches, the smaller are the volumes to fill and the closer are downstream stable check dam crests. These changes, when compared to an alluvial structureless reach, promote higher maximum slope values in the downstream direction.

B. Project slope

The great majority of studies examining a new equilibrium after torrent control works report milder slope between structures than existed before construction (Ratomski, 1988; Iroume and Gayoso, 1991; Kostadinov, 1993; Porto and Gessler, 1999; Porto and Gessler, 1999; Conesa-Garcia et al., 2007; Böll et al., 2008; Ferro and Porto, 2011; Kostadinov and Dragović, 2013). Following the results presented above, the authors hypothesize that "the effect of check dams on the mean-slope of an alluvial reach is nearly null, under similar supply conditions". Reaches with colluvial or bedrock influences, *i.e.*, non-alluvial reaches, and reaches with changing feeding conditions present two situations where structures are often encountered in the field and that do not fulfil the conditions of the hypothesis. These may go some way in explaining the widely observed decreases in slope after check dam construction.

Non alluvial channel

On mountains and hills, a large number of streams flow on beds with material supplied by alluvial and more importantly in this analysis, colluvial processes, *i.e.*, debris flows, avalanches, rock falls, landslides and bedrock outcrops. Thus, the initial reach can either be bedrock or large boulder covers, with steep slopes generally poorly representative of the upstream water and sediment supplies, *i.e.*, steep slope streams are often sediment supply limited (Montgomery and Buffington, 1997).

Check dams are usually built above the initial bed level (Piton et al., *sub.*). When building a structure above a steep boulder paved bed, a purely alluvial reach can develop. It settles with a slope representative of the real solid transport occurring in the stream, in terms of rate and grain size. This slope is generally milder than the initial colluvial or bedrock slope. Conversely, bed-sills in lowland alluvial rivers generally generate a step in the river longitudinal profile but no decrease in slope, because of this lack of colluvial influence (Malavoi et al., 2011).

For this reason old torrent control guidelines recommended building check dams at the initial bed level in alluvial fans, like ground sills, and not to build check dams above the bed level (Breton, 1867; Piton et al., *sub.*). This would help to avoid a fast aggradation upstream on a thickness equivalent to the check dam height (which is generally not desirable to limit flood hazard).

Varying supply conditions

With or without colluvial influence, changes in water and/or sediment supply often generate bed-slope adjustments. It can be due to increase in

water supply following land use changes (Martìn-Vide and Andreatta 2006; 2009; Wohl, 2006), or to sediment supply decrease due to gravel mining (Liébault and Piégay, 2002; Martson et al., 2003), dam constructions (Brandt, 2000) or medium term climatic evolutions and related vegetation adaptation (Liébault and Piégay, 2002; Liébault et al., 2008). Finally, torrent control works were undertaken with the objective to curtail sediment supply from soil and streambed erosion (Demontzey, 1882; Thiéry, 1891; Liébault and Zahnd, 2001; Evette et al., 2009). In all these watersheds, the alluvial-equilibrium slope diminishes when the sediment supply decreases or the water discharge increases. Both these effects can thus result in river bed incision.

As a counterexample, in streams with an increase in sediment supply, for instance resulting from landslide reactivations, check dams series are generally partially or totally buried while the equilibrium slope increases (Logar et al., 2005; Koulinski, 2010). Examples of check dam series built in aggrading streams are scarce, but clearly demonstrate that check dams do not intrinsically generate decreases in slope.

5.5.3. Consequences for risk mitigation

A. Influence of structures on bed-load transport dynamics

The high instantaneous variability of the bed-load transport rate for equivalent flow conditions no longer needs to be demonstrated (Whittaker, 1987; Kuhnle and Southard, 1988; Warburton, 1992; Whitaker and Potts, 2007; Jerolmack and Paola, 2010; Van De Wiel and Coulthard, 2010; Ghilardi et al., 2014b). The stochastic nature of supply conditions in mountain catchments is a first cause of fluctuations (Recking, 2014). However, Jerolmack and Paola (2010) considered that systems driven by nonlinear threshold processes, such as bed-load transport, can completely obliterate sediment supply signals depending on the timescale of their fluctuations, *i.e.*, the downstream sediment flux signal can be significantly different from the upstream signal due to a sort of transport-system filtering. Recent works have demonstrated a grain size sorting influence on the autogenic fluctuating trends of sediment transport in gravel bed rivers (Recking, 2006; Recking et al., 2008b; 2009; Bacchi et al., 2014).

In our experiments, as the local alluvial behaviour is little changed when check dams are added, no clear influence on the instantaneous bed-load transport intensity was detected. However, the main influence of check dams was observed when transported volumes were considered through varied time windows.

B. Influence of structures on erosion volumes

The problem brought by torrential floods is more related to the volume of sediments transported and deposited during short and intense events than to the instantaneous transport intensity (Costa de Bastelica, 1874; Armanini et al., 1991). It is thus highly related to sediment supply and availability. In addition to colluvial processes, armour-breaking will allow erosion in the stream-bed which may supplies a substantial part of the transported volume during catastrophic events (Lenzi, 2001; 2002; Vericat et al., 2006; Theule et al., 2012; 2015; Recking, 2014).

Our results demonstrate that check dams can considerably reduce the sediment transported volume recruited in the bed. Consistent with this, Jaeggi and Pellandini (1997) pointed out that the role of check dams is partially to prevent stream bed material recruitment. The creation of partially independent compartments and the related decrease in active volumes prevents large-scale armour breaking from inducing massive stream bed sediment recruitments. The system is even able to regulate upstream supply by temporarily storing sediment.

This effect of sediment transport regulation by check dams was theorized by Gras (1857). Nearly 150 years later, after decades of field observations, Poncet (1995) stated that "Check dams are built to deliver in small amounts, what the torrent would have release abruptly en masse". Downstream of a series of check dams with alluvial reaches long enough to allow significant transient storages, *i.e.*, buffer effects (Jaeggi, 1992), sediment releases are probably more frequent but each volume is smaller on average, thus easier to manage regarding hazard mitigation.

5.5.4. Flume limitation

A. Lateral confinement

Our model forbade lateral erosion and flow spreading. The authors assume that it could be compared to check dams built in the gorge part of a catchment; area prone to high bed fluctuations. In the more classical case of a wider valley, high aggradation would result in flow spreading and lateral sediment deposit in the flood plain. Conversely, high incisions would result in bank and hill-slope destabilizations and lateral sediment supply. Both effects may diminish the vertical development of bed fluctuations. As a consequence, the fluctuation trends in our model may be exacerbated.

However, feedback from French and Italian practitioners confirms the existence of fluctuations in most studied torrential stream beds, sometimes measuring several meters in height, such as the example presented in Fig. 5.2 (see also Fabre, 1797; Glassey, 2010; Astrade et al., 2011; Theule et al., 2012; Theule et al., 2015). These observations let us think that the observed fluctuations in the flume are not model effects.

B. Steady supply

In the field, water and sediment supply are highly transient, *i.e.*, often occurring during flash floods, one of the most characteristic features of torrential streams (Fabre, 1797). In these experiments undertaken in a reduced complexity approach (Paola and Leeder, 2011), the water and sediment supplies were constant. Indeed, it is interesting to denote that even in completely constant feeding conditions, sediment transport and storage demonstrated autogenic fluctuating dynamics.

Transient hydrology and sediment supply would make it more complex and probably create a superimposition of autogenic fluctuations on supply forcing fluctuations (Van De Wiel and Coulthard, 2010). In the case of extreme floods, the significance of check dam influence on sediment transport depends on the volume brought by the external supply source (*e.g.*, landslides) when compared to the system volume. Jerolmack and Paola (2010) demonstrated that above a given sediment input amplitude the filtering effect of a sediment transport system has little effect on the input signal: "*a sufficiently large-amplitude input signal must be able to overwhelm the autogenic dynamics and pass through the transport system regardless of its time scale*". Complementary experiments addressing varying magnitude transient supply conditions should be performed to confirm the results of this preliminary work.

To finish, our study concerned streams with noticeable sediment supply, which are those usually equipped with check dams. Many mountain streams are supply limited and develop stable step-pool morphologies; they were not considered here.

5.6. Conclusions

Check dams are grade control structures that are often presented as simply stabilizing stream beds with the purpose of preventing long term incision and lateral bed shifting. They have been built for over 150 years, mainly in streams showing high transport rates and long term incision trends. These trends can be due to changes in feeding condition or to long term disequilibrium in streams initially influenced by colluvial processes, *i.e.*, in supply-limited streams.

Building check dams affects the sediment cascade by fixing, and more generally elevating, the stream base level, thus creating bed-level independent compartments. Slopes representative of an alluvial (dynamic) equilibrium can settle in these compartments. In many streams (not initially at equilibrium) they result in milder slopes as the initial slopes were not yet representative of a purely alluvial equilibrium.

The experiments presented in this paper demonstrate that check dams do not intrinsically induce lower slopes or changes in instantaneous solid discharge when compared to structure-less alluvial streams. However, they change the dynamics of the natural erosion and deposition propagation in the streams. In the long term, once filled, they do not change the total sediment yield (fluxes are balanced). However, at the flood scale or at a bedload pulse scale, they are able to temporarily store and then later release sediment. By creating independent compartments the effect of the stream on the sediment discharge signal changes depending on the distance between dams, consistent with the theory of Jerolmack and Paola (2010). Interestingly, strong sediment release events tend to disappear and a more regulated sediment transport emerges.

This effect must be confirmed for extreme events and is important in torrent hazard mitigation; deeper attention should be paid to it in the future. Further field and laboratory experiments could identify in which configurations, sites and contexts, this effect is the most pronounced. This would allow practitioners and researchers to take the effect into account when estimating torrential hazard and sediment transport downstream of check dam-equipped streams.

Acknowledgments

This study was funded by Irstea, the INTEREG ALCOTRA European RISBA project and the ALPINE SPACE European SEDALP project. The authors would like to thank Francesco COMITI, Frederic LIEBAULT and Joshua ROERING for key discussions on the results of this paper, Guilhem HOYAUX for the PTV tracking, Gabin PITON and Matteo SALETTI for advices in the statistical analysis and Coraline BEL and Ségolène MEJEAN for kindly providing the field images that illustrate the paper. In addition, two anonymous referees helped us to improve the paper by their comments.

Notation

The following symbols are used in this paper:

= **Parameters**:

D_x = Diameter such that x% of the mixture is finer (m);

d = water depth (m);

Fr = Froude number $\approx \frac{U}{\sqrt{gd}}$ (-);

h_c = critical water depth (m);

H_c = critical energy (m);

g = gravitational acceleration = 9.81 (m/s^2);

L = distance between check dams (m);

l = lag time (s);

Q = water discharge (m^3 /s);

Q_S = sediment discharge (g/s);

$\langle Q_S \rangle *$ = Dimensionless feeding rate, see text. (-) ;

q^* = dimensionless water discharge $= Q/W\sqrt{gSD_{84}^3}$(-);

Re = Flow Reynolds number Ud/ν (-);

$Re*$ = Grain Reynolds number $D_{50}\sqrt{gdS}/\nu$ (-);

S = Slope (m/m);

T = Time window (s);

U = water mean section velocity (m/s);

V = Volume of sediment (m^3);

V_{act} = Active volume of sediment (Eq. 5.3) (m);

$V*$ = Dimensionless volume of sediment $= V/V_{act}$ (m);

W = Flow width (m);

z = bed level elevation (m);

z_{dam} = dam crest elevation (m);

Δ = sediment submerge density (-);

γ_l = Autocorrelation factor for lag time l (Eq. 5.4)(-);

ν = water kinetic viscosity (-);

$\tau*$ = Shields number $Sd/\Delta D_{84}$ (-);

$\tau*_{cr}$ = Critical Shields number (-);

= **Subscript**:

$\ldots_{noCD}$ = Value of the $noCD$ run ;

$\ldots_{1CD}$ = Value of the $1CD$ run ;

$\ldots_{3CD}$ = Value of the $3CD$ run ;

$\langle \ldots \rangle$ = Mean value of ... ;

$\langle \ldots \rangle_T$ = Mean value of ... on a time window of T duration ;

$\ldots_{max}$ = Maximum value of ... ;

$\ldots_{min}$ = Minimum value of ... ;

$\ldots_{X\%}$ = Quantile of ... with probability X%;

$\ldots_i$ = ... of reach i;

$\ldots_{Calc}$ = Computed value of ...;

$\ldots_{Meas}$ = Measured value of ...

5.7. Narrow flume experimental details

This sub-chapter provides additional information on the experimental setup used for the Chap. 5's experiments.

Preliminary remark: some details on error propagations methods are provided in Appendix A.

5.7.1. General approach

A few words about error assessment and propagation.

A. Measurements' uncertainties

For each primary measurement X_i, we made a first assessment of the uncertainty $u(X_i)$. When it was possible (technically and in a reasonable time), several measurements were done to use standard error approaches and thus reduce the uncertainty (see Appendix A). The variance and standard error were then deduced. However, in some cases where an alternative independent measurement, or multiple measurement of the same phenomena, were too complicated to perform, the uncertainty on the measurement was based on expert assessments which are detailed within the text.

B. Uncertainty / Error propagation

In further steps, for each secondary variable Y_i, *i.e.*, compound variable estimated through formula involving primary and/or other secondary variables $Y = f(x_1, \cdots, x_j, y_{j+1}, \cdots, y_n)$, the classical error propagation formula[1] was used. It combines the basic uncertainties estimated at the previous step for each direct measurement and compound uncertainty defined through error propagation (later we will not differentiate primary or secondary variable, all being called x_i). All the details of the derivative equations are not detailed in the text, we simply recall the basic function $Y = f(x_1, \cdots, x_n)$, the values of the basics uncertainties $u(x_i)$, $\forall i$ and the resulting uncertainties on Y, $u(Y)$. $u(Y)$ designate the standard uncertainty, the uncertainty range $U(X)$ is not recalled but may be deduce by multiplying $u(Y)$ with a simple factor depending on the confidence interval, *e.g.*, 1.96 for a confidence interval $\pm 95\%$ (see details in Appendix A). A constant physical scale Y is thus expressed as $Y = \langle Y \rangle \pm u(Y)$.

[1] (Eq. (A.3) of Appendix A)

5.7.2. Narrow flume experimental setup

All the laboratory experiments presented in this thesis had been undertaken in the IRSTEA laboratory of Grenoble. This work had the opportunity to re-use the Grenoble Multi-Use Flume, after three previous PhD works: Recking (2006); Bacchi (2011); Leduc (2013). Alain Recking, in particular, spent a lot of time to develop the sediment feeding system, its stability is thoroughly analysed and described in his PhD thesis (Recking, 2006). Ten years after his defence, the setup is still very adapted to our experiments.

Two sets of experiments had been done within this PhD work. The first one deals with the effect of check dams on bed-load transport and is described in the present chapter. Its experimental setup was basically the same than Bacchi (2011). Following this first set of experiment, adaptations of the feeding conditions and of their remote control had been done. They are detailed in chapters 6 and 7.

A. The flume

The experimental area of investigation is built on a 6-m long, 1.25-m wide, 0.40 m deep titling flume. Its slope varies from 0 to 12% (0-6.8°). In the first set of experiments, only 4.8 m of the flume were used because the constant head reservoir occupied the elevating table and the sediment feeding system occupied the 1.2 m of the upper flume part (see later). The glass side walls can be moved to decrease the flow width. It has been fixed to 0.115 m, taking into account the wall artificial roughness.

Despite the great interest of keeping transparent side walls to be able to observed flow and solid transport processes, we decided to use relatively rough side surfaces (Fig. 5.5): If most of low lands natural rivers have generally quite high *width / depth* ratios (Yalin, 1992, p.1), mountain rivers often flow in impressively rough beds with quite low *width / depth* or *width / boulder diameter* ratios. Channel armouring was expected to be an important process in our observations of steep slope stream morphodynamics. The armouring development was expected to be partially related to chain force formation from stable points of the bed (*e.g.,* boulders, bedrock outcrops, check dams - Church and Zimmermann, 2007). To ensure that no unreasonable armour instability emerge from a model effect (*i.e.*, unreasonably smooth walls preventing side force chains' creations), poorly sorted sediment with diameter between the D_{16} and D_{84} of the sediment mixture, randomly distributed, were glued on the walls. For very stable system as step-pool streams, even greater side roughness may be used (*e.g.,* Zimmermann, 2009).

In addition to the creation of probably stronger armours, an obvious consequence of this adaptation is an increase in the energy dissipation by friction on the side walls. These combined effect of stronger armour and increased flow friction results in (fortunately but unexpected) very similar average equilibrium slope in both Bacchi et al. (2014) and our experiments, though his solid discharge was 60 g/s while our is only of 44 g/s. This observation is not investigated further, but it demonstrates that the choice of rough against smooth side walls in a flume is possibly equivalent to an increase of $\approx$ 40% of the solid discharge. This effect likely depends on the flow aspect ratio ($W/d \approx 10$ in our case).

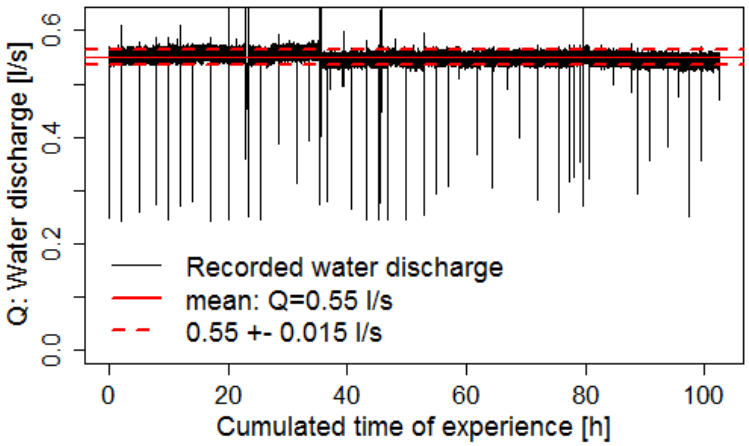

Figure 5.15 – Water discharge during the 110 h of experiments in the narrow flume. Some noise can be seen on the signal, a low amplitude ($\approx \pm 0.015 l/s$) and few peaks of high amplitude that we relate to experiment stop and to problem in the record. A 'step' can be seen at about 40 h, we do not know what is it source; taking it into account, $Q = 0.55 \pm 0.03 l/s$

B. Water feeding

The water discharge was recirculated with a pump from a 1,500-l reservoir at the flume outlet to a 1,000-l reservoir upstream of the flume, put on an elevating table. The upstream reservoir had a nearly constant head level thank to an overflowing orifice. From the constant head reservoir, water passed by a flowmeter (electromagnetic Khrone Model), a spherical valve adjusted to fix the discharge thanks to its head-loss and finally flowed at the flume inlet. The valve as been adjusted at the beginning of the NoCD run and never touched before the end of the 3CD run.

The stability of the system is considered as satisfying (Fig. 5.15) with instantaneous measured fluctuations of less than 2% of the water discharge, fluctuation that probably have a partial electronic source. One can see the range $\pm 0.015 l/s$ envelop most of the measurements, thus we empirically conservatively defined $u(Q) = 0.03\ l/s$, *i.e.*, $Q = 0.55 \pm 0.03\ l/s$.

C. Sediment feeding

The solid discharge was fed using the device developed by Recking (2006). It consists in a nearly 200-l transparent hooper that delivers sediment on a conveyor belt. The sediment discharge is not fixed by the hooper orifice (that is oversized), but by the belt velocity (controled by a brushless-motor). An additional special tachometer device (an adapted potentiometer) was fixed on one of the conveyor belt axis and measured its velocity. This experimental setup allows to use wet sediment which is an important point to facilitate experimental procedures; however, it makes necessary to supply a thin water layer on the belt to make sure that surface tension do not glue the finest grains to the belt (see for details Bacchi, 2011; Leduc, 2013).

The experimental setup was used in a 'sediment fed' configuration (definition of Parker and Wilcock, 1993). Relatively long lasting experiments were planned with steady supply conditions. Bed-load transport autogenic fluctuations were expected. If the feeding system itself amplified any fluctuations, it would had been impossible to judge whether the fluctuations: i) were generated by the sediment transport process or; ii) they were simple 'noise' multiply amplified by the feeding system, which would had been possible in a 'sediment recirculation' configuration (Parker and Wilcock, 1993).

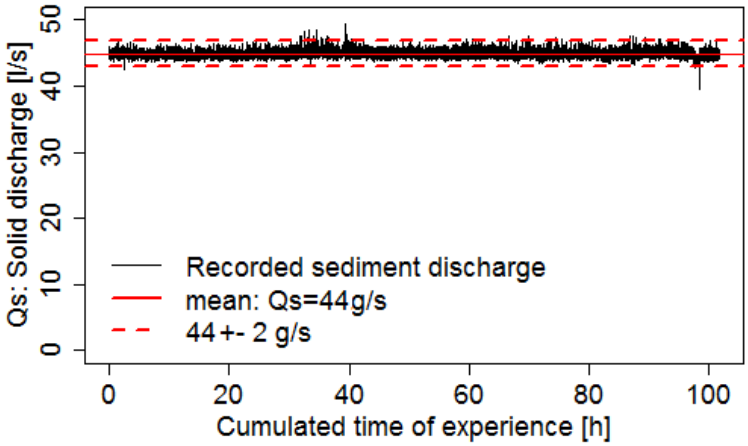

Figure 5.16 – Sediment discharge deduced from the belt velocity during the 110 h of experiments in the narrow flume. A low amplitude noise ($\approx \pm 1\ g/s$) can be observed, it is related to the tachometer sensor that was not perfectly aligned on the conveyor belt axis; a small axis oscillation resulted in the oscillating measurement. Considering how complicated it can be to obtain a stable sediment feeding device, this signal is considered as fully satisfying.

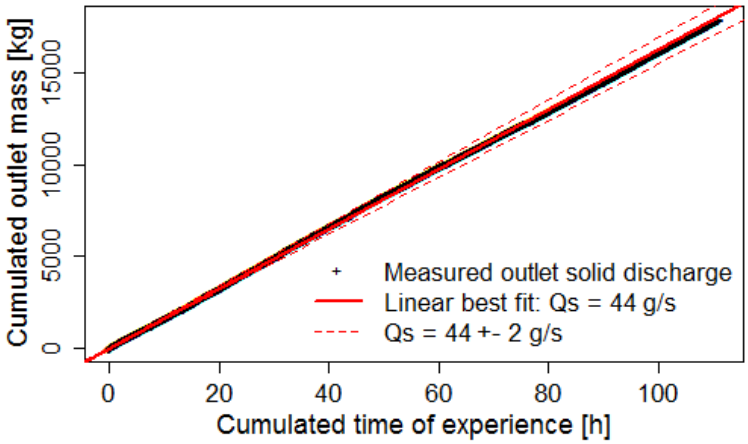

Figure 5.17 – Cumulated solid discharge at the outlet of the flume. Linear best fit give an average solid discharge of $44g/s$, the range $\pm 2\ g/s$ give a satisfying envelop of the inlet discharge considering that storage and release occur in the flume.

Fig. 5.16 shows the sediment discharge deduced from the belt velocity measurement. It was stable in time and considered to be of $44g/s \pm 2g/s$ on average (Fig. 5.17).

D. Sediment mixture

D.a. Grain size distribution choice

The sediment mixture has been reconstructed to be compared to the mixture used in the experiments of Bacchi (2011). About 500 kg of poorly sorted sediments, with diameter ranging from 0.8 to 30 mm, were separated using sieves of 2, 5, 8, 9, 10, 14, 15, 18, 20 and 40 mm. Only gravels coarser than 5 mm were re-used. For the portion finer than 5 mm, the coarse white sand of Leduc (2013) has been used. We were then able to reconstruct a grain size distribution with a greater detail than the data available to describe the Bacchi (2011) material. The model for grain size distribution reconstruction proposed by Recking (2013a) has been used to determine the detailed shape of a 'natural'

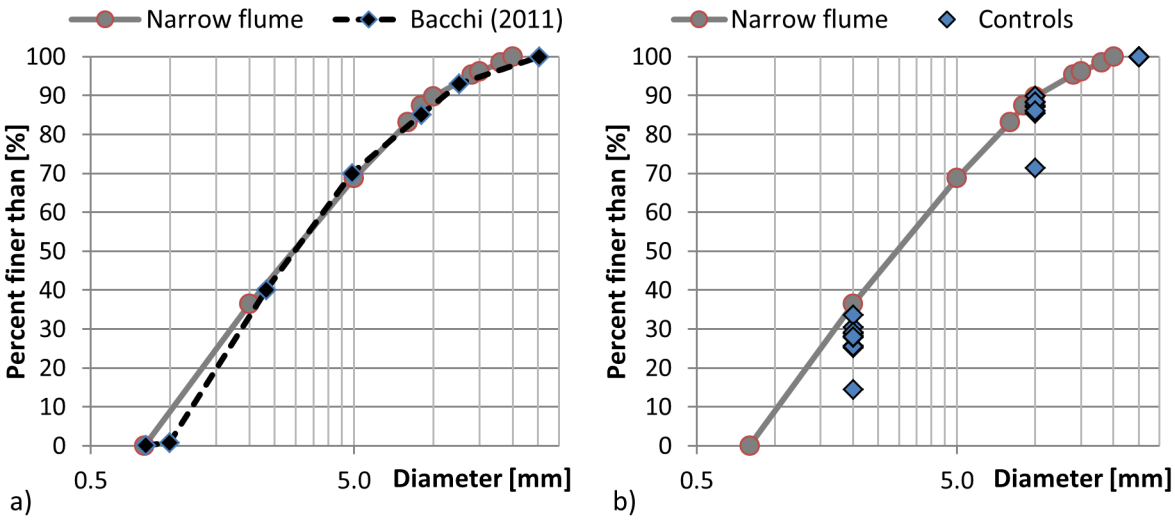

Figure 5.18 – Grain size distributions: a) comparison of Bacchi (2011) and Chap. 5 sediment mixture and b) result of control of the grain size distribution randomly sampled in the hooper during the experiments: reasonably stable, though a bit coarser than expected.

Figure 5.19 – Sieved sediment after a hooper mixture control: coarse white sand finer than 2 mm, brown and grey gravel [2;10mm] and partially painted gravel coarser than 10 mm.

grain size distribution that fit the Bacchi (2011) main features. Fig. 5.18a illustrates the Bacchi (2011) and our grain size distributions, they can be considered as fairly similar.

D.b. Grain size distribution stability

The sediment mixture transported in the flume was subject to a very intense sorting process. To ensure the stability of the grain size distribution at the inlet, the mixture was carefully manually mixed before to be reintroduced in the hopper. The homogeneity of the mixture and the absence of sorting was verified visually during all runs. In addition, 11 samples were randomly taken from the hooper, dried and sieved with sieves of 0.8, 2, 10 and 25 mm (Fig. 5.19), to verify the overall stability of the mixture. Fig. 5.18b shows the results of these controls. Two remarks: i) the grain size distribution was reasonably stable on time, one sample showed a globally finer distribution but, on average, the grain size distribution is very stable taking into account the huge variability of the outlet sediment mixture, but ii) the finest part was finally a bit coarser than expected (the introduction of the fine white sand has been based on the Leduc (2013, p.53) sieving data).

D.c. Painting gravel: the 'Canadian trick'

Painting gravels without making them sticking to each other is not straightforward. We used a cunning and helpful 'trick' reported by Jeremy G. Venditti from UBC that was used for the experiments reported in Sklar et al. (2009); Venditti et al. (2010): put gravels in a concrete mixer, add paint (not too much, it would make the mixture too viscous and make the concrete mixer forcing to mix it) and make the concrete mixer turning several hours until the paint is closed to be dried or even completely dry (but you then obtain a nice coloured concrete mixer). We use paint with strong resistance to abrasion that is normally dedicated to road marking (heavy traffic type). The pebbles kept their color about $400 - 500$ h of experiment.

E. Measurments

As presented before, the water discharge and the inlet sediment discharge (trough the belt velocity) were measured and recorded on a computer at a 10-Hz frequency. Their respective uncertainties were $u(Q) = 0.03$ l/s, determined from constructor informations and $u(Qs) = 2$g/s, determined from the calibration data.

E.a. Outlet solid discharge

The cumulated outlet solid discharge was weighted each 3 to 4 minutes after being drained. Sediments were still wet during the measurement. We weighted, dried and re-weighted 31 samples of 3-6 kg of randomly selected samples from the outlet measurements. Water contents ($W\% = \frac{Mass_{wet} - Mass_{dry}}{Mass_{dry}}$) varied between 0.03 and 0.068 ($\langle W\% \rangle = 0.044$, $u(W\%) = 0.002$ by Eq. A.1). All the solid discharge measured at the outlet of the flume were thus corrected by a factor $\frac{1}{1+\langle W\% \rangle} = \frac{1}{1+0.044}$.

The outlet solid discharge is finally estimated by:

$$Qs = \frac{1}{1 + \langle W\% \rangle} . \frac{Mass_{sediment+bucket} - Mass_{bucket}}{\Delta t} \tag{5.5}$$

with the time duration from the last sampling Δt ($\langle \Delta t \rangle = 240s$, $u(\Delta t) = 5s$ based on our experience), the weight of the bucket filled by wetted sediment and the bucket weight: $Mass_{sediment+bucket}$ and $Mass_{bucket}$, respectively ($\langle Mass_{sediment+bucket} \rangle = 12.22kg$, $\langle Mass_{bucket} \rangle = 0.66kg$ & $u(Mass_i) = 0.01kg$ from the weighting scale constructor information) and $u(W\%) = 0.002$ as mentioned previously.

The uncertainty on the outlet solid discharge is estimated as $u_c(Qs) = 1g/s$ by using Eq. (A.3), mainly due to the uncertainties on the water content of the wet sediments.

E.b. Bed level measurements

Visual measurements

Windows pierced in the wall roughness and equipped with transparent staff gauge were used to perform bed level measurements (Fig. 5.20). Staff gauges were *mm*-accurate, however the measurement is less precise mainly because of the bed coarse, granular constitution makes its representative level leaving room for interpretation. We considered the bed level to be the *average level of unmoving bed materials* (on the width of the window *i.e.*, 2-4 cm). This wider window than the unique staff gauge abscissa allowed to take into account, for instance, the presence of one coarse

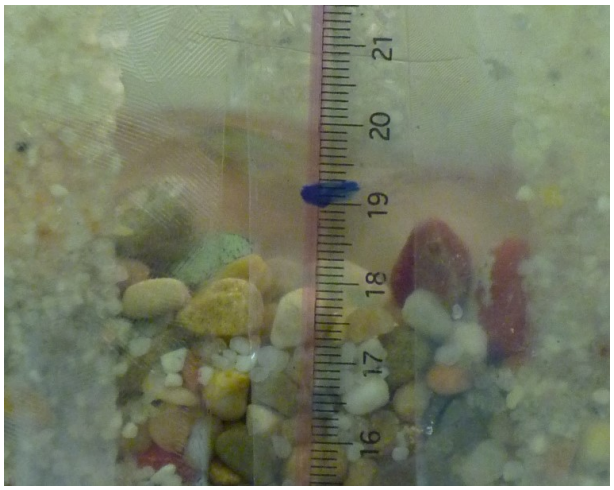

Figure 5.20 – Picture of a bed level measurement window with the transparent staff gauge. The coarse material of the bed was the biggest source of uncertainties. Here, for instance, the bed level would have been estimated as $18.1 \pm 2\ mm$

grain protruding over a lower bed and to consider the average bed level. Mobile grains passing the window during the measurement were considered to belong to the flow and not to the bed. The uncertainty on this measurement is assumed to be $u(z_i) = 2\ mm$, which is close from the $D/4$ criteria adopted by Recking (2006), with D the sediment diameter.

Ultrasonic measurements

Ultrasonic sensor were installed and moved at different points of the flume during the 1CD run and durably installed at the upper part of reaches 2, 3 and 4 during the 3CD run. They were installed 20-cm downstream of the PVC plates figuring check dams (Fig. 5.21 (a)). These sensors measure, on a range of 5-25 cm, the distance between the water surface and the sensor head. We installed them on PVC plates, whose altitude were tuned to ensure that the bed level and the water surface fluctuated in the measurement range.

While the visual measurement is a direct measurement of the bed level, the ultra sonic sensor measured the water surface level. An additional assumption on the water layer thickness had to be done. The water depth had been considered equal to 12 mm. This average water depth was consistent with both theoretical formula and few rough Particle Tracking Velocimetry measurements (Table. 5.2). This assumption is obviously questionable. Depending on the bed state, the bed roughness evolved and consequently, the Froude number and flow thickness (discharge was fortunately constant). The measurement uncertainties of the bed level has been considered to be $\pm 5\ mm$ when using ultrasonic sensor. Assuming that this uncertainty mainly come from the varying water depth, a 5 mm variation in the water depth (compare to the mean) would be equivalent to a variation of the Froude number between 0.7 and 2.4, compare to the mean value of 1.2. Such variations of the Froude number seems relatively high but reasonable, which lead us in adopting $u(z_{i,ultrasonic}) = 5\ mm$.

The visual and ultrasonic measurements of the bed level at a given position during the 1CD run are compared on Fig. 5.21 (b). It demonstrates that the relatively low frequency of the visual measurement (one every three minutes) was sufficient to catch the high amplitude cycles of the bed level.

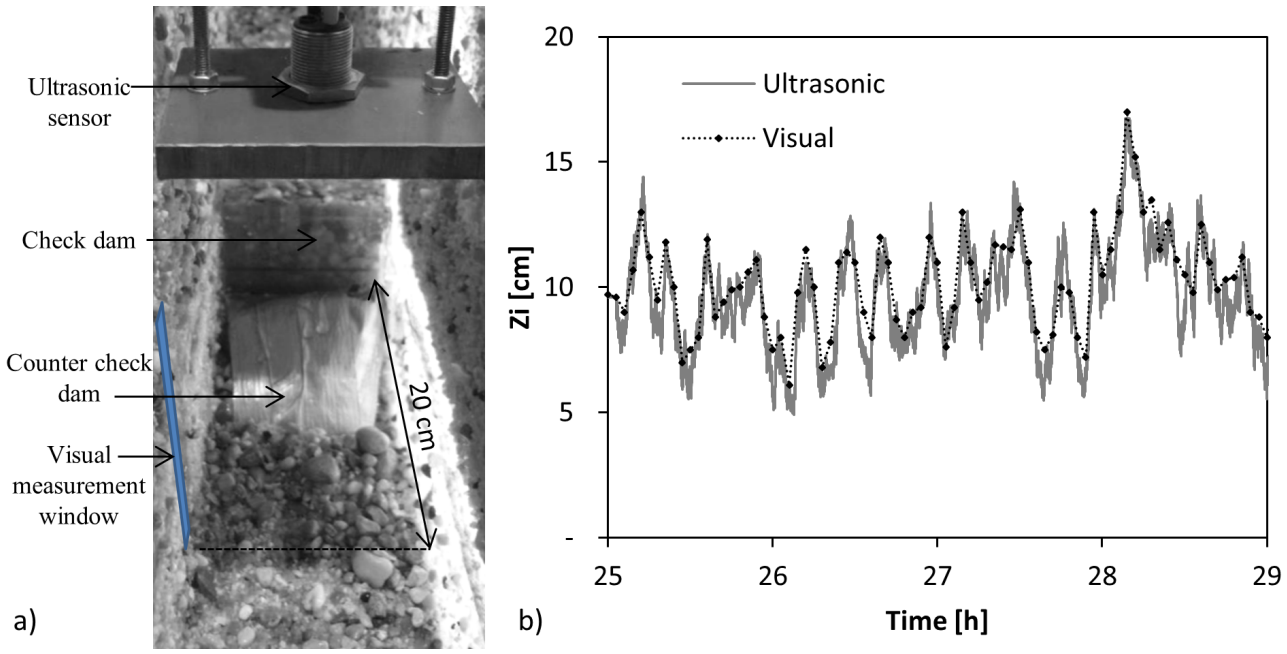

Figure 5.21 – a) Illustration of the configuration of a check dam, its counter dam, the window and ultrasonic sensor; and b) Comparision between ultrasonic and visual measurement of the bed level: fluctuation amplitude are correctly cough, though a weak under-sampling may appear on the fastest fluctuations.

High frequency - low amplitude fluctuations can be observed on the ultrasonic measurements. They are likely the mixed consequences of (i) water depth variation and waves, classical features of supercritical flows, (ii) coarse sediment protruding over the free surface; and (iii) fast moving congested grains that create a moving obstacle to the flow, increasing transiently the free surface level. We do not seek to analyse them, only bed variation of several times the coarse grain diameter are considered as meaningful.

An equivalent comparison had been performed on the result of the 3CD test showing clear subsampling. The high magnitude cycles of the bed fluctuations of the 3CD had thus been correctly grasped only using ultra-sonic sensor. We maintained the visual measurements to get additional data to validate the magnitude of the cycles, conversely their frequency were not correctly grasped too (Shannon law violation).

Reach' geometrical mean slope

The mean geometrical slope of each reaches had been deduced from the bed level z_i using Eq. 5.1 that we remind here:

$$S_i = \frac{z_i - z_{dam,i}}{L_i} \tag{5.6}$$

with the slope of the i^{th} reach S_i, the check dam elevation downstream of the i^{th} reach $z_{dam,i}$, and the distance between the staff gauge and the check dam downstream of the i^{th} reach L_i . L_i varied between runs: from 4.2 m during the NoCD run to 1.0 m during the 3CD run. The L_i accuracy depends on where exactly was taken the bed level within the staff gauge window (Fig. 5.20), we assume that $u(L_i) = 1\ cm$.

For the sake of simplicity, the worst case is taken into account for uncertainty assessment, *i.e.*, $L_i = 1.0m$ (3CD run) and $u(z_i) = 5\ mm$ (for ultrasonic measurements, see above). The PVC plates figuring the dams were carefully made and fixed with a millimetric precision, the uncertainty on their final level is considered to be $u(z_{dam,i}) = 2\ mm$. $\langle z_i - z_{dam,i} \rangle \approx 0.12\ m$ in the 3CD run. The standard uncertainty on the reach' geometrical mean slope is finally estimated as $u_(S_i) = 0.0055$ by using Eq. (A.3).

"There is a clear need for further research directed toward identifying effective topographic indices of resistance, and for detailed flow and turbulence measurements in streams or self-formed laboratory channels to help elucidate the physics of shallow flows over irregular beds."

Rob Ferguson (2007), *Water Resour. Res.* **43** p. 12

CHAPTER 6

Combining LS-PIV and photogrammetry to capture complex flows with low submergence and highly mobile boundaries

Guillaume PITON[a], Alain RECKING[a], Jérôme LE COZ[b], Hervé BELLOT[a], Alexandre HAUET[c], Magali JODEAU[d]

[a] Université Grenoble Alpes, Irstea, UR ETGR, St-Martin-d'Hères, France.

[b] Irstea, UR HHLY, Hydrology-Hydraulics, Villeurbanne, France.

[c] Electricité de France, DTG, Grenoble, France.

[d] Electricité de France, LNHE, Chatou, France.

This chapter describes a measurement procedure that has been developed to get insights from flows over massive bedload depositions. Namely, laterally constrained flows in steep slope channels yet show complex behaviours with sorting and armor breaking issues (Chap. 4) and exchanges between bed and flows, resulting in changes in sediment transport signals (Chap. 5). When entering a wide sediment trap basin, sediment-laden flows spread, depositing their load and building new bed topographies. This out-of-equilibrium process was poorly known, though its comprehension is required to secure and improve structure design (Chap. 2). It was thus worthy of investigation. This chapter presents the measurement procedure, while Chapter 7 reports a preliminary analysis of the measurement results.

Abstract

Steep slope streams with massive sediment supply are among the most complex systems to study, even in the laboratory. Their shallow sediment-laden flows create self-adjusting bed geometries that rapidly evolve. Consequently morphological changes and flow processes cannot be dissociated. Because these very shallow and unstable flows cannot be equipped with measurement sensors, image analysis techniques, such as photogrammetry and Large Scale – Particle Image Velocimetry (LS-PIV) are interesting alternatives to capture descriptions of these systems. The present work describes a complete procedure using both techniques to measure bed geometries (deposit pattern, channel slope, local roughness) and flow spatial distributions (surface velocity). The velocity data are used to assess the local flow directions and to extract the flow slope and roughness from the photogrammetry digital elevation models. In a second step we used the collected data with the Ferguson's friction law (previously validated by comparison with a few local flow depth measurements) for reconstructing a complete mapping of the hydraulics. The assumptions, details and limits of the procedure and possible sources of errors are discussed in the paper, as well as improvement possibilities. Overall, this affordable and simple-to-implement procedure can provide large amount of data for complex hydraulic systems.

Author key words: *Small Scale Model, Large Scale Particle Image Velocimetry, Photogrammetry, Friction Laws, Hydraulic Inverse Problem*

6.1. Introduction

Measuring appropriate hydraulics parameters (water depth, velocity) is the keystone and challenge of most hydraulics studies; especially in small scale models, which are commonly used for cases with sediment transport and geomorphic changes (Oda et al., 2002; Paola et al., 2009). Small scale models are particularly useful in steep slope streams studies (*i.e.*, with slope > 0.02) because, i) on the one hand, the physics of sediment transport and steep slope hydraulics is not sufficiently understood which limits the capacity of numerical models (Ferguson, 2007); and ii) on the other hand, the rough beds of mountain streams minimize unwanted scale effects related to Grain Reynolds similitude relaxation (Peakall et al., 1996; Kleinhans et al., 2014). The theoretical suitability of steep slope flows to be studied in small scale models is however strongly jeopardized by the difficulty of measuring such shallow and morphologically active systems (Fig. 6.1). Water depth measurement may be done at specific locations using a point gauge (Fig. 6.1a). However, few millimeters to centimeters-deep, steep, shallow flows on rough beds tend to have a fluctuating free surface (traveling and standing waves, hydraulic jumps, boulder wake), making its elevation measurement using a point gauge quite inaccurate. It is even worse for the bed elevation measurement, which is possibly moving by bedload transport. Modern techniques like ultrasonic sensors and laser distance-meter are possibly more accurate, but still only give a local measurement. In brief, even in small scale models, flow depth measurements in steep sediment-laden flows are complicated and necessarily affected by large errors.

More generally all direct measurements with intrusive velocity sensors (*e.g.*, ACVP, flow-meters) are impossible or dangerous because: (i) the sensor size can be larger than the flow depth, (ii) sediments can potentially damage sensors (for in-

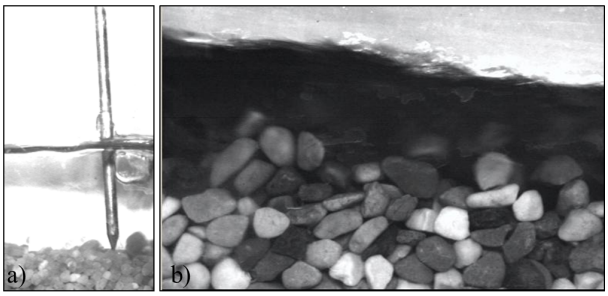

Figure 6.1 – View through a flume glass side of steep flows over a mobile bed made of nearly uniform grains: a) illustration of the use of a point gauge: intrinsic uncertainty related to the variable bed level and free surface, b) side view showing mobile grain clusters and perturbed free surface highlighting how uncertain/variable is the water depth

stance the flow meter propeller), and (iii) the sediment transport intensity make flow paths unstable, shifting and wandering in the flume. In addition to the planimetric instability, the vertical bed adjustment may be of several times the water depth, so that the sensors are intermittently buried in sediment or perched over an eroding channel. Overall, it is quite complicated to equip channels with intrusive sensors in steep, freely adjusting bed geometry, with high solid transport, and thus, bed mobility.

To face the above limitations, steep slope flow velocities have traditionally been measured by injection of tracers. For instance the salt tracing technique uses the electrical response of two pairs of electrodes to a saline marker injected into the flow (Smart and Jaeggi, 1983; Cao, 1985; Rickenmann, 1990). Such technique has two limitations, especially in shallow flows with sediment transport: firstly it is intrusive (electrodes); secondly the shape of the electrical response may be very deformed by interactions with the sediments, making the reading of the output signal very difficult and uncertain (Cao, 1985). To face the intrusive problem, the measurement of salt with electrodes was replaced by the dye measurement by image capture (Recking et al., 2008a; Ghilardi et al., 2014a). However specific problems persist in very shallow flows because partial infiltration of the injected tracer in the alluvial material and later restitution to the main flow bias measurements toward underestimation (Recking, 2006, p. 25). In addition, such methods present some problem in multichannel flows, *e.g.*, braided patterns, in which the response signal is strongly deformed by diffusion in the multichannel flow system (Leduc, 2013). Finally these techniques measure a value of flow velocities integrated over space, velocity that may be of secondary interest in some varied environments as braided patterns.

Considering all the difficulties to measure the depth average velocity, an alternative consists in measuring the surface flow velocity by image tracking of floating particles. In the field, the LS-PIV (Large Scale Particle Image Velocimetry) technique (Fujita et al., 1998) enables measurements in difficult flow conditions (Jodeau et al., 2008; Dramais et al., 2011; Le Boursicaud et al., 2016). It has also been used in the laboratory to measure flow velocities in small scale models (Weitbrecht et al., 2002; Admiraal et al., 2004; Kantoush et al., 2008; Le Coz et al., 2010; Kantoush et al., 2011; Legout et al., 2012; El Kadi Abderrezzak et al., 2014), though, to our knowledge, never on rapidly evolving geomorphic systems. The simplest practice consists in measuring the velocity of floating tracers, *e.g.*, polystyrene balls, small wood marbles, confettis. However, in low submergence flows, such large particles can strongly interact with the emerging roughness or the banks, leading to severe underestimation of the surface flow velocities (Bacchi, 2011; Leduc, 2013). Such measurement needs the user to carefully select the few particles which are maintained in the center of the flow, which makes its automatization difficult. An alternative consists in using very small particles easily transported by the main flow; however it requires accurate surface images, complicated to acquire on wandering channels.

The present work takes advantage of the development of a user-friendly LS-PIV, free software (Fudaa LS-PIV – Jodeau et al., 2013; Le Coz et

al., 2014) combined with detailed photogrammetry measurements, two affordable image-analysis measurement techniques, to reconstruct detailed flow fields of steep, low submergence and freely adjusting systems as well as their geomorphic adjustments. Because the objective was to develop a methodology for measuring complex hydraulics, we chose to reproduce in the flume the fan-like deposition process occurring in sediment traps located in mountain streams, a topic which is still poorly known (Piton and Recking, 2016a). It is possibly one of the most restrictive situations, with sometimes very low relative depths, over very coarse sediments in highly mobile, out of equilibrium and rapidly evolving beds.

This paper proposes a complete methodology comprising (i) the LSPIV measurement of surface velocity, (ii) the photogrammetry measurement of the bed topography and bed roughness measurement deduced from the bed topography, and (iii) a friction law inversion procedure for determination of the 2D flow depth from the measured slope, roughness and flow velocity. Some possible improvements of the technique are finally discussed.

6.2. Materiel and Methods

Bedload laden flows in laterally unconfined beds have freely adjusting morphology. Water flowing on coarse and steep beds tends to have quite low submergences (Fig. 6.1), to be highly mobile and overall to be really poorly known (Ferguson, 2007). In such complex environment, topographical adjustments by sediment transport are fast and fundamentally driven by hydraulics; while the flow features (friction losses and energy balance) are themselves back-influenced by the sediment transport (Recking et al., 2008b; Recking, 2009; Revil-Baudard et al., 2015). Detailed hydraulics features have ever been studied in 1D flumes (Recking et al., 2008b; Ghilardi et al., 2014b) but, to date, the relaxation of the lateral constraint has been poorly addressed. Nevertheless, a better understanding of the coupled hydraulics - morphodynamics is increasingly possible using recent techniques. A first step will be to make possible flow spatial distribution measurement, with a better accuracy than local point gauge measurements and averaged injection velocity measurements.

6.2.1. Experimental set up

The flume of IRSTEA Grenoble, ever presented in Bacchi et al. (2014) and in Piton and Recking (2016c) has been used to perform the experiments.

A. Flume features

The flume was 6-m-long, 1.25-m-wide and 0.4-m-deep (Fig. 6.2). Its varying slope (0-12%) has been fixed at 10% (5.7°) for all experiments. A 2.5-m long basin, the investigation area, was constructed in the flume (Fig. 6.3). Sediments were glued on the side walls to make them rough, similarly to rip-rap or sediment covered dikes.

Three configurations were tested (Fig. 6.3 & Table 6.1): the first with a slit dam at the outlet (details on the flume shape are given in Carbonari, 2015); the second and the third with a simple ground sill at the outlet across the entire basin width (details in Mejean, 2015). The basin maximum width was 1.25 m in the two first set of experiments and 0.62 m in the third one. The flume was manually dredged at the beginning of each experiment, leaving behind a transversally flat bed with a sediment thickness of 5 cm. This preparation, without pre-existing channels, is purely artificial and figured the mechanical excavation that is normally done in sediment trap basins after each sediment supply.

In the first configuration, the slit was wide enough (60-mm, *i.e.*, $\approx 3D_{MAX}$) to prevent any coarse grain jamming (Piton and Recking, 2016a). The structure thus generates a mere "hydraulic control" of the deposit, *i.e.*, sediment formed a

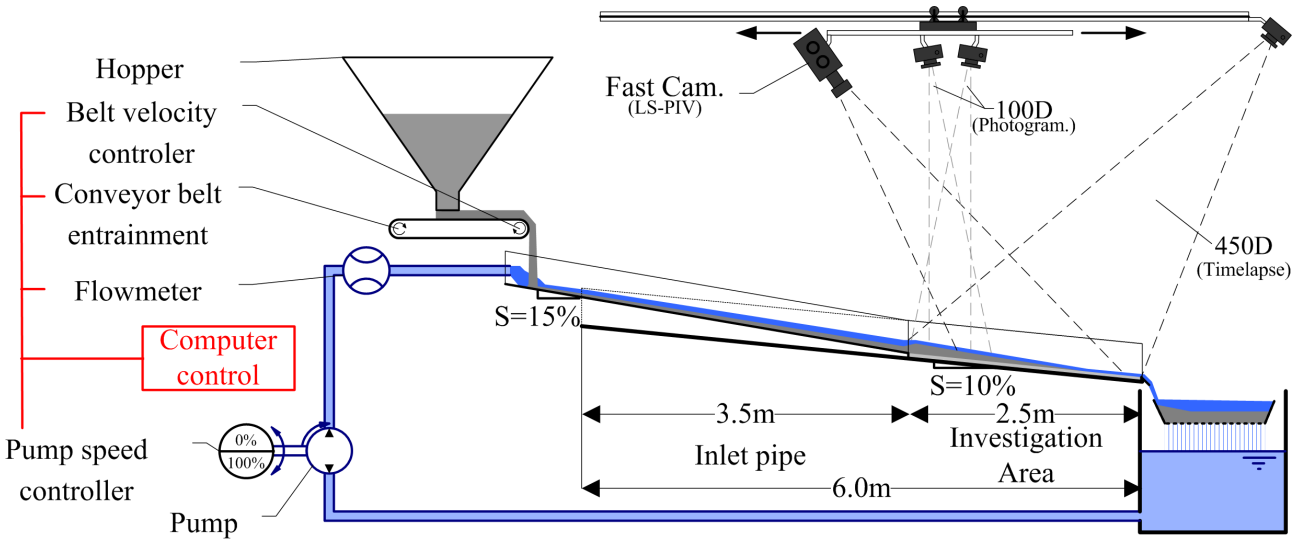

Figure 6.2 – Experiment set up : sediment fed configuration and recirculation of water Investigation area

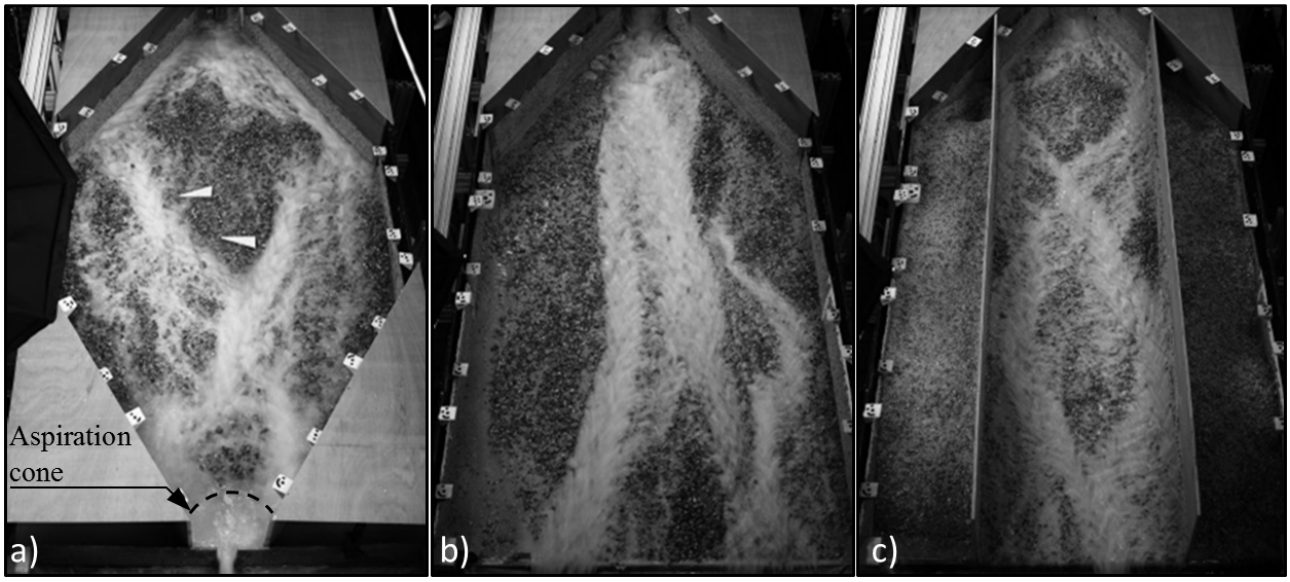

Figure 6.3 – Basin shape configurations: a) slit dam and simple bed sill at the outlet with b) basin width=1.25 m; and c) basin width=0.62m

delta in the high water depth area located directly upstream of the dam. This backwater area is a simple consequence of the head loss related to the slit contraction. The delta prograded toward the slit, down to fill the backwater area and only leave an 'aspiration cone' (Fig. 6.3a) in the direct vicinity of the slit, where velocities remain high enough to entrain all grains (Zollinger, 1983). In the second and third configurations, channels could freely flow at any point of the outlet bed sill (Fig. 6.3b & c).

A.a. Water and sediment supply/feeding

The water was recirculated directly from the pump, without constant head reservoir (Fig. 6.2). The water discharge Q was remotely controlled by a computer through the pump speed controller. Unsteady hydrographs were used with a maximum discharge of 2.75 l/s (Fig. 6.4): The computer interpolated a given time series of water discharge at a 10-Hz frequency and consequently varied the pump speed according to a preliminary calibrated pump speed – discharge equation. The water discharge was measured with a flowmeter at a 10-Hz frequency (accuracy $\pm 0.03 l/s$) and recorded on a computer.

The sediment feeder was composed of a hopper associated with a conveyor belt, with a maximum solid discharge capacity of 292 g/s and 214 g/s with two distinct grain size distributions (GSD), respectively (see later). The system works in a sediment-fed configuration (*sensu.* Parker and Wilcock, 1993). The conveyor belt delivered sediment in a 3.5-m-long, 15%-steep pipe, where water and sediment mixed. The pipe figured the stream bed upstream of the basin. It had coarse grains (15-20 mm in diameter) glued on the bottom and sides to prevent excessive Froude numbers at the inlet flow. No depositions were observed in the pipe (except due to backfilling from the basin), so the instantaneous sediment and water discharges Qs and Q at the basin inlet are assumed to be equal to the belt and pump-delivered discharges.

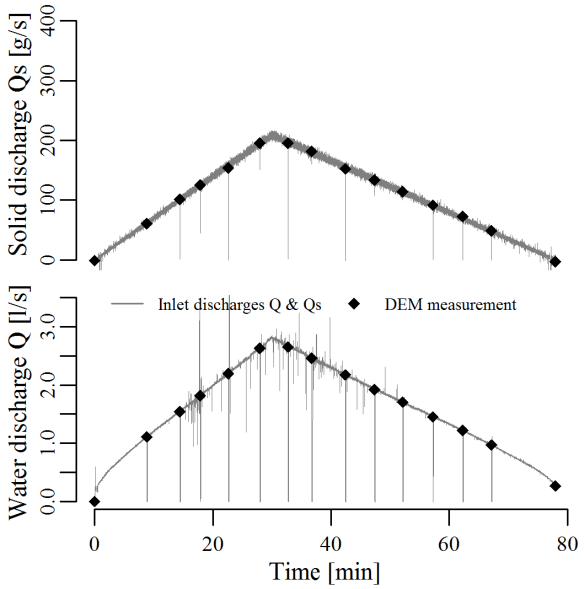

Figure 6.4 – Typical boundary conditions: solid and water discharges at the inlet and times of DEM measurements.

A.b. Boundary conditions

This work did not aim at studying a specific stream, but rather to be a "*generic*" study of flows in steep and wide streams (Peakall et al., 1996) addressing the influence of i) transient flows, ii) unsteady sediment load, iii) varying sediment mixtures, iv) varying lateral confinement and v) low submergence. Floods and sediment supply in mountain streams being a complex problem (Van De Wiel and Coulthard, 2010), several simplification assumptions must be taken, accepting that the study is done in a "*reduce complexity approach*" (Paola and Leeder, 2011).

Simple triangular hydrographs were used with a recession duration 1.7-time longer than the rising limb (Fig. 6.4, same shape as in Armanini and Larcher, 2001): slightly longer recession limbs are generally observed in torrent floods (*e.g.*, D'Agostino and Lenzi, 1999; Rickenmann et al., 1998; Lenzi, 2001; Turowski et al., 2009).

A correction regarding the infiltration must be considered: the water discharge necessary to saturate the initial sediment layer (0.23 l/s) has been added to all hydrographs. It is assumed to infiltrate and not to participate to surface run-

Table 6.1 – Experimental plan

Code	Slit	GSD	Basin width	Q	Qs	Tpeak	C=Qs/Q	N_{DEM}	N_{PIV}	$N_{water\ depth}$
Units	dam	code	[m]	[l/s]	[g/s]	[min]	[%]			
DaG1/C0. 1	Yes	1	1.25	2.75	73	90	1	6	3*	8*
DaG1/C0.2	-	-	-	-	146	45	2	8	6*	12*
DaG1/C0.3	-	-	-	-	219	30	3	4	2*	4*
DaG1/C0.4	-	-	-	-	292	22.5	4	5	3*	6*
nDG1/C0.1	No	-	-	-	73	90	1	7	5	10
nDG1/C0.2	-	-	-	-	146	45	2	6	4	8
nDG1/C0.3	-	-	-	-	219	30	3	4	2	4
nDG1/C0.4	-	-	-	-	292	22.5	4	5	3	6
nDG2/C0.2	-	2	-	-	146	45	2	6	2	4
nDG2/D0.2	-	-	-	-	-	-	-	6	5	10
nDG2/C0.3	-	-	-	2.69	214	30	3	4	2	4
nDG2/D0.3	-	-	-	-	-	-	-	16	14	19
nDG2/C0.4	-	-	-	2.02	-	-	4	4	2	4
nDG2/D0.4	-	-	-	-	-	-	-	9	7	11
nDG2/C0.5	-	-	-	1.62	-	-	5	4	1	2
nDG2/W2.3	-	-	0.62	2.69	-	-	3	10	7	7
nDG2/W2.4	-	-	-	2.02	-	-	4	9	7	7

Note: Q: peak water discharge; Qs: peak solid discharge, Tpeak: duration before hydrograph peak, C: sediment concentration (assuming a sediment density of 2.65), N_{DEM}: number of DEM acquisition; N_{PIV}: number of LS-PIV acquisition; and $N_{waterdepth}$: number of reference points , *i.e.*, water depth measurement using the point gauge.

*The first LS-PIV measurements were done without crushed charcoal seeding; the velocity fields are thus questionable and were excluded from the dataset.

Table 6.2 – Grain size distribution features

GSD	D_{16}	D_{50}	D_{84}	D_m
Units	[mm]	[mm]	[mm]	[mm]
GSD1	1.7	3.8	8.1	6.4
GSD2	1.2	2.4	6.2	4.9

D_X diameter such that $X\%$ of the mixture is finer, D_m mean arithmetic diameter

off; consequently this infiltrated discharge is not drawn in the graphs nor taken into account in the computations presented later on.

The sediment discharge was arbitrarily set proportional to the water discharge. Various sediment concentration $C = Qs/Q \in [0.01; 0.05]$ were used in order to observe varying deposition intensity: from near equilibrium up to nearly total deposition. Conversely, to compare the various experiments the total volume injected was kept constant between runs ($\approx 500kg$). Maintaining a total sediment supply while varying the instantaneous concentration imposed either: (i) to modify water discharge, or (ii) to keep the water discharge magnitude constant while changing the flood duration. The second option was chosen to keep a maximum instantaneous water discharge, whenever it was possible. As a consequence, the experiment durations were inversely proportional to the concentration and the water discharges were maintained as high as possible. Table 1 summarizes the experiment plan.

A.c. Sediment mixtures

Two sediment mixtures were used, hereafter referred to as GSD1 and GSD2, consisting in natural poorly sorted sediment with diameter from 0.2 to 20 mm (Fig. 6.5 & Table 6.2).

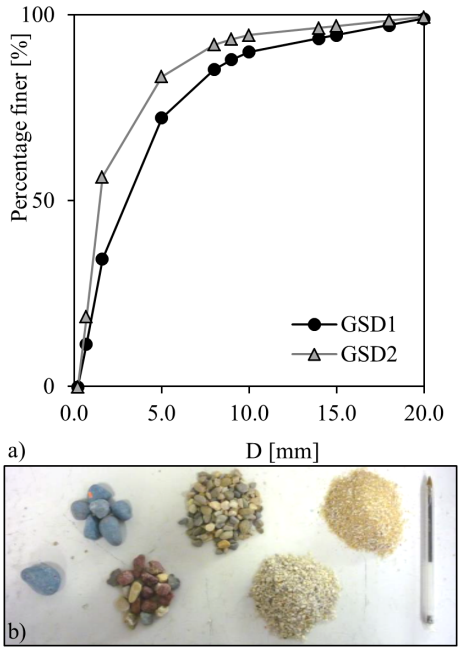

Figure 6.5 – Grain size mixtures: a) grain size distribution of the two mixtures GSD1 and GSD2; and b) picture of the colouration of the different grain sizes: blue for the coarsest fraction, red, brown and grey for the intermediate, white and beige for the finest.

B. Image analysis techniques

A 6-m-long rail was fixed to the ceiling of the laboratory, about 2 m above the flume axis (Fig. 6.2). A trolley circulated on the rail, carrying a high speed camera Phototron FASTCAM (equipped with a polarizing filter minimizing light reflections on the free surface, focal length: 35 mm, 10 Mpix/frame) and two CANON 100D cameras (focal length: 28 mm, 18 Mpix/frame). In addition, a CANON 450D camera (focal length: 32 mm, 12 Mpix/frame) was fixed at the downstream end of the rail, taking pictures (cf. Fig. 6.3) every 5 seconds to later construct a time-lapse video of each experiment. All the cameras were remotely controlled from a computer. A special attention has been paid to ensure a homogeneous distribution of the light intensity, a key point in LSPIV (Muste et al., 2004; Kantoush et al., 2011): 4 lights were installed at the edges of the flume (2×250 W+2×500 W - continuous current necessary if videos are acquired at frequency $>$ 50-60 Hz).

B.a. Photogrammetry

The pump was switched off immediately after the fast camera acquisitions, stopping the flow nearly instantaneously and draining the deposit with marginal relief changes: the photogramme-

try measurements were then undertaken. High quality pictures of the flume ($\approx$ 30 images) were taken with the trolley cameras to be used in a photogrammetry software (Agisfost Photoscan). The overlapping was quite high, since most points of the flume were covered by at least 10 images taken from different positions (6 images minimum for any point). Twenty-four ground control points were used to scale the images (white targets in Fig. 6.3). Their X, Y, Z positions were measured with a total station (accuracy ± 1 mm in all directions). The classical photogrammetry procedure has then been applied (Agisoft LLC, 2014): i) positioning of the ground control points in each image (semi-automatic in Agisoft Photoscan), ii) back calculation of camera alignments, iii) construction of a dense point cloud by cross-correlation between images, iv) construction of a 3D polygonal mesh based on the dense point cloud. In addition, v) orthorectified HD images of the complete flume were reconstructed (25 pix/mm^2) and vi) high density Digital Elevation Models (DEM) were extracted from the mesh as bed elevation matrices $Z_{X,Y}$ ($\Delta X = \Delta Y = 1mm$, *i.e.*, 3,125,000 elevation points per acquisition). Considering the image resolution and coverage, it would have been possible to increase the DEM density by one order of magnitude. However, the data density of these DEMs was yet greatly sufficient to describe the relief and armoring of the deposits, while being reasonably heavy to handle. The vertical accuracy of the measurement is considered to be $\pm 1mm$ (Le Guern, 2014).

B.b. LS-PIV

Large Scale – Particle Image Velocimetry (LS-PIV, Fujita et al., 1998) has been used to measure surface velocity fields. The technique proved to be robust in highly varied contexts (Muste et al., 2010). The Fudaa LS-PIV software has been used (Jodeau et al., 2013; Le Coz et al., 2014; Hauet et al., 2014). This technique showed satisfying performances in small scale models measurements with low submersion and relatively steep slopes (Nord et al., 2009; Legout et al., 2012) as well as for fast torrential flows in the field (Le Coz et al., 2014; Le Boursicaud et al., 2016).

The same ground control points as for the photogrammetry were used to scale the images and orthorectify them. Fifteen to twenty points were manually identified in each picture series. The minimum of 10 ground control points per image to fully constrain the orthorectification equations involved in the procedure, and to allow a verification of the points coordinates, has thus systematically been respected (Jodeau et al., 2013). The errors of the ground control point planar coordinates, after orthorectification, were generally of $2 \pm 1mm$; a satisfying result equal to the fast camera pixel size.

Several times in each run, the fast camera took videos of the flow at 125 $frames/s$ during 10 seconds. A series of N=50 images lasting for 0.4 s was selected to be subsequently analyzed. It is assumed that the flow velocity did not significantly vary during the 0.4 s of measurement. In their parametric study, Legout et al. (2012) demonstrated that 50 images were sufficient to grasp a correct value of the velocity and that more images did not improve the results. Based on these N images, correlation analysis built N-1 velocity spatial distributions by tracking the displacements of patterns in the orthorectified-image pairs (Jodeau et al., 2013). At each calculation point, the correlation is computed on interrogation areas which are 20-pixels side squares, size large enough to comprise the typical greyscale pattern sizes, while smaller than braided channel width. The searching area, in which the patterns are tracked, has been defined to be able to handle velocities up to $2m/s$, a value that has never been reached in the measurement.

Some classical experimental adjustments have been necessary to adapt the measurement to our complex hydraulics (see Muste et al., 2004; Kantoush et al., 2011 for recommendations). First,

manual particle tracking (PTV) measurements of confetti seeded in the flow were used for comparison (Carbonari, 2015). A few red confettis were manually seeded in the inlet pipe during fast camera acquisitions. Manual tracking of these floating materials was then performed on orthorectified pictures to measure the local velocities along their trajectories. The LSPIV velocity was interpolated precisely at each confetti PTV measurement. Both velocity estimations are compared in Figure 6.6. PTV is a reliable estimate of the surface flow velocity and can be used as reference measurement, but is fastidious because, in our experimental conditions, the particles must be tracked individually, excluding all particles interacting with the channel banks.

The LS-PIV technique is basically able to inform us on the velocity of what is being seen as moving on the videos. The problem is that in clear water flows, one can see not only surface water movements (travelling perturbations, standing waves, tracers) but also sediment movements beneath the water surface and sometimes tracer shadows on the bed. These two different movements resulted in highly variable velocity fields, which in our case globally underestimated the actual flow velocity by a factor of 3.3 ± 2.2 (mean $\pm$ standard deviation - Fig. 6.6), when LSPIV measurements are compared to PTV assessment. TiO_2 powder has been used to dye the water, thus removing the bed grain movements from the pictures, and resulting in a lower underestimation of the LS-PIV measurements ($V_{PTV}/V_{LSPIV} = 1.8 \pm 0.8$). Finally, correct, though not perfect, estimations of the velocities were obtained using TiO_2-dyed water and seeding the flow with crushed charcoal powder directly injected to the flow just before triggering the fast camera acquisition. Charcoal powder created black patterns advected by the flows which improved significantly the measurement performance: $V_{PTV}/V_{LSPIV} = 1.2 \pm 0.4$. Despite its uncertainty, this result is considered satisfying in the context of such rapidly mobile, low submersion and perturbed flows.

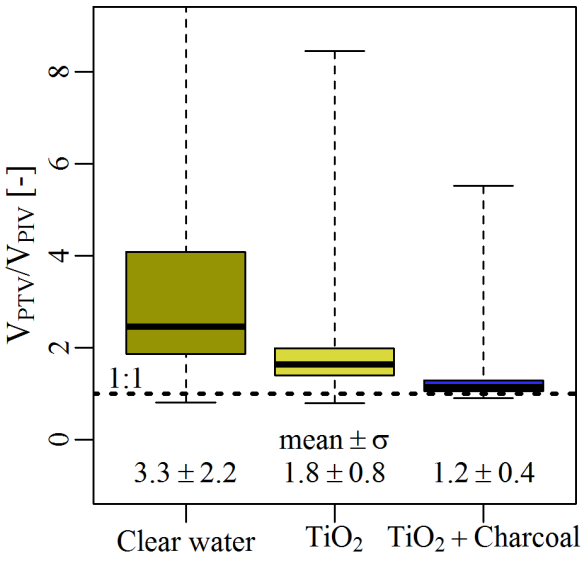

Figure 6.6 – Influence of the dying and seeding of flows analyzed through the ratio between manual particle tracking velocities, V_{PTV}, considered as references and the LS-PIV velocities, V_{LSPIV} : only combined TiO_2 and Charcoal seeding gave satisfying approximation of the surface flow velocities

Surface velocity fields V_{LSPIV} that contained $\approx 20,000$ calculation points (on an irregular centimetric grid with a total area $\approx 1\ m \times 2\ m$, Fig. 6.7a) have been transformed into mean velocity fields on the entire water depth $V_{X,Y}$ by multiplying V_{LSPIV} with the velocity index α = mean water depth velocity/surface velocity. Muste et al. (2010) report that α weakly varies, even in relatively low submergence (Polatel, 2006; Le Coz et al., 2010; Welber et al., 2016). It has thus been assumed that $\alpha = 0.85 \pm 0.04$ based on Muste et al. (2010) recommendations and Polatel (2006, p. 39) variability data. Finally, velocities were interpolated on a regular grid using a homemade code (R software). This grid, that supported the resulting flow field (Fig. 6.7b), is coarser than the elevation grid ($\Delta X = \Delta Y = 5mm$, *i.e.*, $\approx 75,000 V_{X,Y}$ points per acquisition; more detailed grids can be built, it requires more computational time and was not necessary in this study).

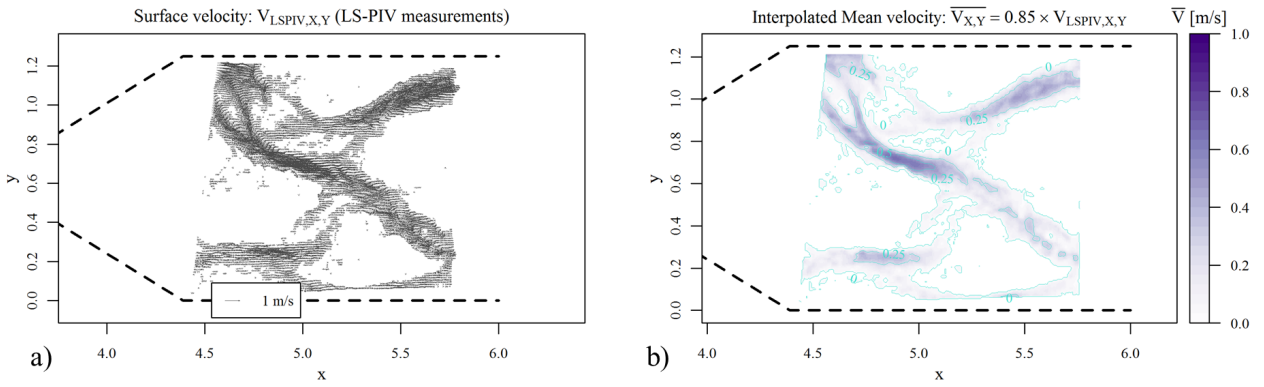

Figure 6.7 – Velocity surface distributions: a) LS-PIV velocity vectors $V_{LSPIV,X,Y}$ on an irregular grid; b) Interpolated mean velocity $V_{X,Y}$ on a regular grid ($\Delta X = \Delta Y = 5mm$)

C. Water depth

A movable point gauge (Fig. 6.1a) was used for flow surface and bed level measurements. The accuracy of the sensor itself is as low as 0.01 mm. However, the highly perturbed free surface typical of steep flows on rough beds (*e.g.*, Fig. 6.1b); and the dyed opaque flows with moving sediment transported on the bed (*e.g.*, Fig. 6.3), made the measurements very inaccurate. The uncertainties are assumed to be of the order of a grain diameter, $\pm 2mm$ for the free surface level Z_{FS} and $\pm\ 5mm$ for the bed level Z_B. As a consequence, the accuracy of the water depth ($d = Z_{FS} - Z_B$) is $\pm 6mm$ (quadratic sum used in error propagation, JCGM, 2008). One or two point gauge water depth measurements were done before each LS-PIV measurement (Table 6.1). They are hereafter referred to as "reference points".

6.2.2. Photogrammetry analysis

Several proxies of both the deposit thickness and the surface roughness were extracted from the DEMs and the HD orthorectified images (Fig. 6.8).

A. Relief data

The elevation field $Z_{X,Y}$ could be used to observe the bulk deposit relief (Fig. 6.8a). By subtraction of the flume bottom slope, the deposit thickness $T_{X,Y}$ is deduced (Fig. 6.8b). This flume-slope de-trended elevation yields a clearer view of the deposit morphology.

A local roughness indicator $Ks_{X,Y}$ has been computed by subtracting the mean local bed elevation to the point bed elevation $Z_{X,Y}$. The mean local bed elevation is averaged over a D_{MAX}-side square, centered on the point (one value per mm^2-pixel), with D_{MAX} the coarsest grain diameter (20 mm). $Ks_{X,Y}$ is an indicator of the pixel elevation compared to the local mean elevation. It tends to 0 in smooth areas (Fig. 6.8c), while it is positive or negative where grains protrude from the bed level. Smooth and rough areas, *i.e.*, covered with fine sands or paved by coarse gravels can easily be distinguished on the Ks maps.

B. Flow slope

A key parameter for hydraulics and sediment transport is the energy slope S, hereafter considered to be equal to the bed slope following the flow paths $S_{X,Y}$. The flow being generally close to the critical regime in rough and steep streams (Grant, 1997; Ghilardi et al., 2014b; Schneider et al., 2015; Ran et al., 2016), it is assumed that the free surface is locally adjusted to the slope and roughness. Free surface is thus assumed to be globally parallel to the bed slope, *i.e.*, that no extensive backwater effects occurred, a result observed in steep slopes by Ran et al. (2016) (a possibly excessive assumption in other configurations with gentler slopes). Namely, as water flowed in

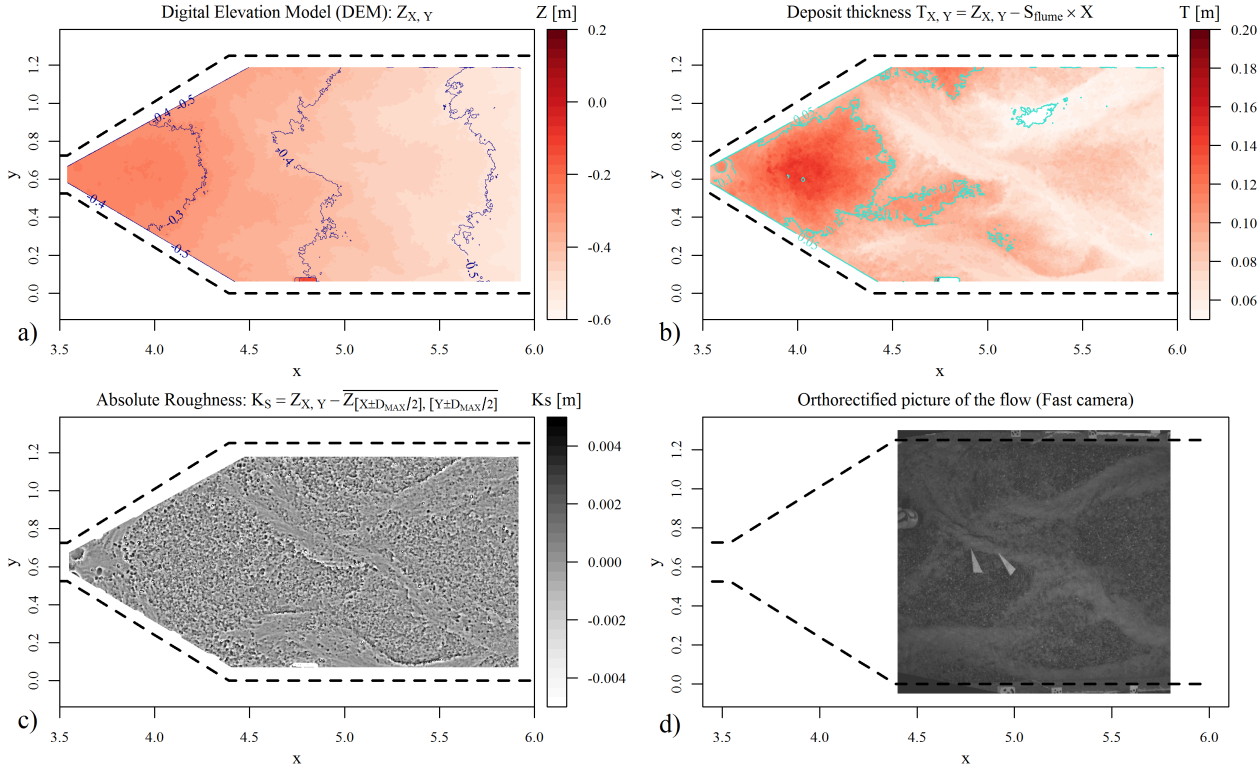

Figure 6.8 – Relief proxies and image of the flow field: a) Bed elevation $Z_{X,Y}$; b) Deposit thickness $T_{X,Y}$; c) Surface roughness $Ks_{X,Y}$; and d) orthorectified grey-levels image taken from LSPIV results.

sometimes poorly-defined channels shifting and wandering on the deposit (*e.g.*, Fig. 6.8d), the flow slope $S_{X,Y}$ is sometimes lower than the deposit slope $_{Sdep}$ along the X axis. In other words the curvilinear flow direction is often longer than the deposit main axis. $S_{X,Y}$ was measured at a given position X,Y following several steps summarized in Figure 6.9:

1. $V_{X,Y}$ is interpolated based on the LS-PIV velocity vector field (Fig. 6.7a & b);
2. A transversal profile, perpendicular to the flow direction is defined;
3. The flow width is defined as the transversal profile length such that $V > V_0 = 0.02m/s$: with V_0 lower limit velocity; defined such that the water depth is negligible and no geomorphic activity occurs;
4. A local main longitudinal profile axis, was considered over a distance equal to 3 times $W_{X,Y}$, defined parallel to the flow direction, *i.e.*, along the surface streamline passing by the point (X, Y).
5. A linear fit of the bed elevation along the curvilinear abscissa of the longitudinal profile defines the local flow slope $S_{X,Y}$.

Specifically at the reference point locations additional extractions were performed to quantify the uncertainties (Fig. 6.9). Four additional profiles were defined whose slope was also extracted. The Slope uncertainty $u(S)$ at the reference points was considered to be the standard deviation of the five profiles slopes values: $u(S_{X,Y}) = \sigma_{S_{X,Y}}, \forall$ 5 profiles$_{X,Y}$.

The procedure has been applied in all flowing areas of the flume (Fig. 6.10a), determining the field of flow Slope $S_{X,Y}$.

C. Flow roughness proxies

In addition to slope, flow features are fundamentally correlated to the bed roughness. The roughness of gravel bed rivers is classically de-

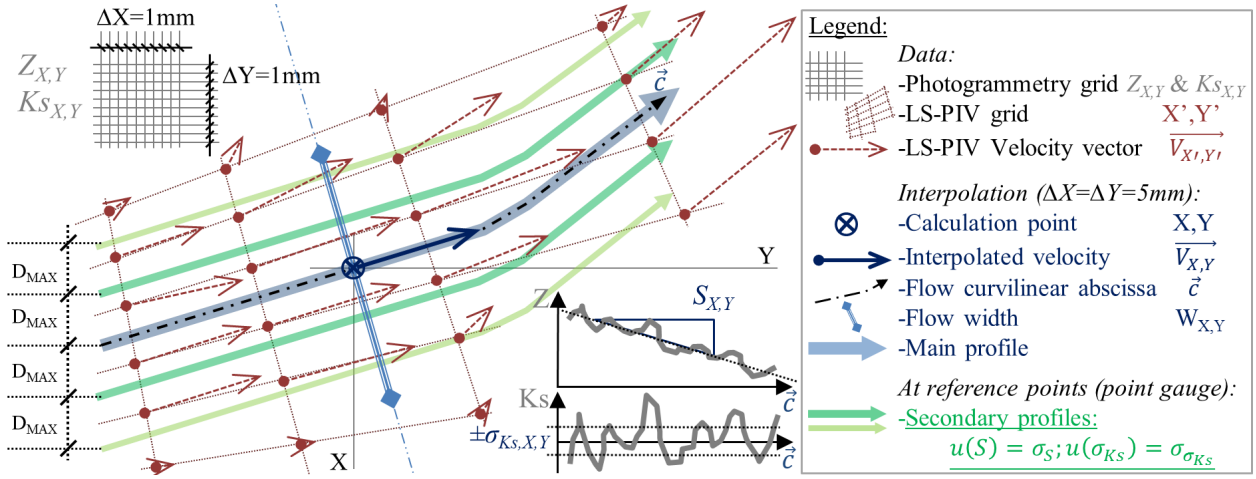

Figure 6.9 – Sketch of the friction law parameters extraction algorithm: extraction of the flow slope $S_{X,Y}$ and roughness standard deviation $\sigma_{K_{X,Y}}$ along curvilinear profiles following the flow direction defined by LS-PIV velocity data. Main profile defined parallel to the main stream line passing by X,Y and additional uncertainty measurements at reference points (underlined steps).

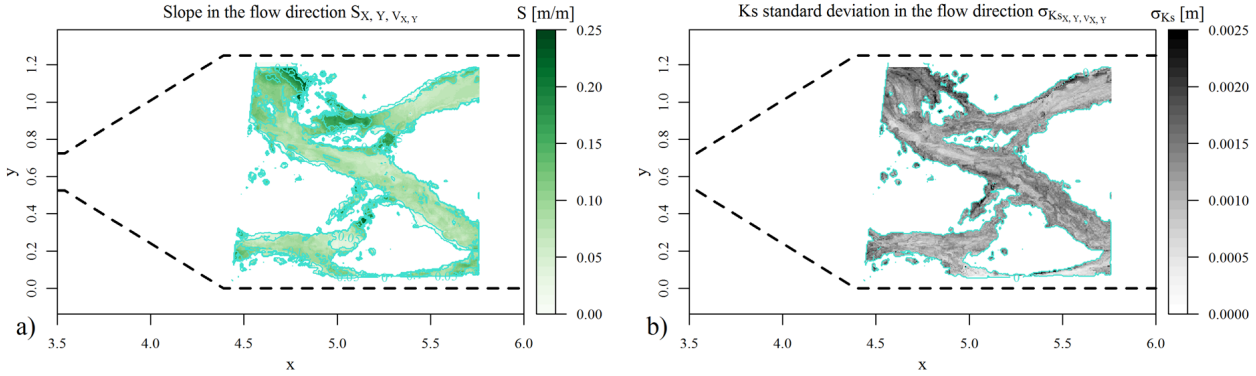

Figure 6.10 – Friction law parameters: a) Slope in the flow direction $S_{X,Y}$; and b) Roughness standard deviation in the flow direction $\sigma_{Ks_{X,Y}}$

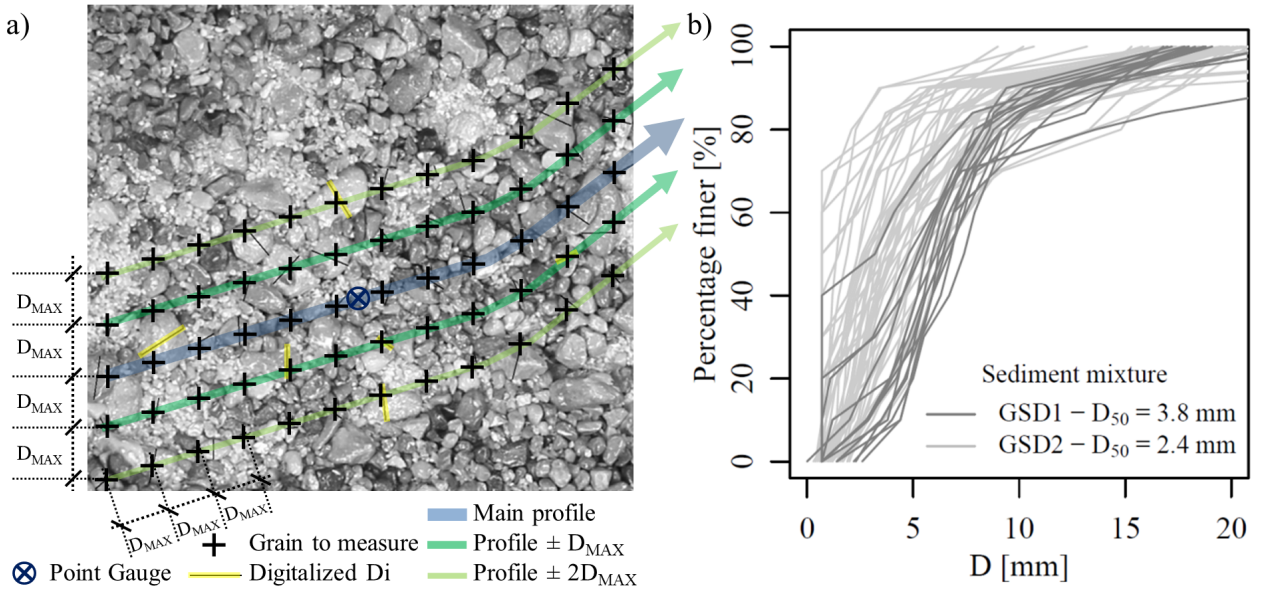

Figure 6.11 – a) Detailed implantation of the 5 longitudinal profiles defined at each reference points supporting both the Wolman count marks and the $u(S_{X,Y})$ and $u(\sigma_{Ks_{X,Y}})$ computations; and b) Grain Size Distributions defined by Wolman counts: illustration of the great variability of the bed texture due to intense grain size sorting

scribed using a proxy D_i often derived from the grain size distribution of the surface material, usually D_{50} or D_{84} (Ferguson, 2007). However, the advent of accurate topographical measurement devices increasingly results in the use of alternative roughness indicators such as the standard deviation of the bed elevation (Aberle and Smart, 2003; Nitsche et al., 2012; Schneider et al., 2015). Both approaches were considered here.

C.a. Wolman count

Classical GSD measurements were done with the Wolman surface counting method (Wolman, 1954). To later look at representativeness and correlation of the various proxies, the counting was also performed precisely along the aforementioned profiles characterizing the reference points' vicinity (Fig. 6.11a): The HD-orthorectified images of the bed surface coming from the photogrammetry analysis were displayed, with marks spaced of $D_{MAX} - mm$, along the 5 longitudinal profiles. The diameter of the grain located under each mark was measured manually.

An average number of 112 ± 45 pebble diameters were measured at reference points (55 to 260 pebbles, depending on the profile length $= 3W_{X,Y}$). The distributions (Fig. 6.11b) and their quantiles D_{50} and D_{84} are proxies of the local bed roughness. Through error propagation, the accuracy of the grain size measurement is estimated to be $\pm 0.6mm$ as digitized points have an accuracy of ± 1 pixel and that the pixel size is $0.2mm$.

C.b. Roughness along streamlines

The standard deviation of Ks was computed along the flow longitudinal profile (Fig. 6.9) at each pixel of the rough grid (Fig. 6.10b). Like $S_{X,Y}$, this parameter depends on the flow direction and is not computed out of flooded areas, contrary to $Ks_{X,Y}$.

In order to quantify the uncertainty of this parameter at reference points, the roughness standard deviations $\sigma_{K_{X,Y}}$ along the secondary longitudinal profiles have also been computed at these specific locations. The uncertainty of $\sigma_{K_{X,Y}}$ is considered to be standard deviation of the five profiles $\sigma_{Ks_{X,Y}}$: $u(\sigma_{K_{X,Y}}) = \sigma_{\sigma_{K_{X,Y}}}$, $\forall$ 5 profiles$_{X,Y}$.

6.2.3. Hydraulics reconstruction by Friction law inversion

Some authors used spatial distribution of flow features (*e.g.*, free surface width, free surface elevation) and a suitable friction law to reconstruct unmeasured data by inversion problem. Roux and Dartus (2008) implemented an optimization approach to reconstruct bed topography only based on flooded area limits and discharge. Bed elevation were also reconstructed using discharge data and free surface elevation from LIDAR (Smart et al., 2009), or free surface computation and laboratory measurements (Gessese et al., 2011; 2013). Their approaches are usually iterative or based on data assimilation due to lack of data concerning the flow features.

Friction laws are equations that relate flow velocity to flow depth (or alternatively hydraulic radius or specific discharge, Rickenmann and Recking, 2011). Their simplest forms relate the velocity V to the water depth d, flow slope S and a roughness parameter K through an equation generally given in the dimensionless form:

$$\frac{V}{u^*} = f(S, d, K) \tag{6.1}$$

where $u^* = \sqrt{gdS}$ is the shear velocity. Several friction laws were proposed in the literature. The Manning-Strickler formula is likely the friction law most commonly used in gravel-bed rivers. The version of the Manning Strickler formula retained here is (Rickenmann and Recking, 2011):

$$\frac{V}{u^*} = 6.5 \left(\frac{d}{D_{84}}\right)^{1/6} \tag{6.2}$$

D_{84} is considered as the best suited roughness parameter rather than D_{50} because the coarsest

grains are often the main source of friction loss in gravel bed rivers (Ferguson, 2007; Nitsche et al., 2012). The Manning-Strickler formula is particularly suited for high submersion flows, *i.e.*, for d/D_{84}>7-10 (Ferguson, 2007; Rickenmann and Recking, 2011).

Aberle and Smart (2003) proposed a friction law specifically adapted to low submergence depths of steep, boulder-paved mountain streams. Pointing out that D_X-based indicator do not consider the possible bed structuration, *e.g.*, step-pools, Aberle and Smart (2003) retained the standard deviation of the bed surface elevation as the most relevant roughness parameter:

$$\frac{V}{u^*} = 0.91\frac{d}{\sigma_{Ks}} \tag{6.3}$$

The resulting friction law has a different power coefficient than the Manning Strickler equation, which illustrates the changes in the flow profile related to the lower submersion. Gathering these two asymptotical forms (or similar equations from other works), Ferguson (2007) built a so-called variable power equation:

$$\frac{V}{u^*} = \frac{2.5(d/D_{84})}{\sqrt{1+0.15(d/D_{84})^{5/3}}} \tag{6.4}$$

Rickenmann and Recking (2011) tested several friction laws on a large gravel bed rivers data set. They observed that Equation 6.4 had the best performances, this from low to high submergence.

Determining d from the measured V, S and D_{84} or σ_{Ks} is an inverse problem (see Gessese et al., 2013 for a complete presentation of the problem). It is straightforward for Equations 6.2 and 6.3, *i.e.*, the function $d = f^{-1}(V, S, K)$ has an obvious explicit form. Conversely, the water depth d computed using Equation 6.4 is the numerically solved solution on d of equation:

$$V_{X,Y} - \sqrt{gdS_{X,Y}}\frac{2.5(d/D_{84})}{\sqrt{1+0.15(d/D_{84})^{5/3}}} = 0 \tag{6.5}$$

Equation 6.5, or an equivalent with another friction law, may be applied to the entire flooded area, providing that: (i) it has been determined which friction law is best suited to describe the measured flows, and a surface distribution of D_{84} is available. With such a method, it is possible to reconstruct 2D flow fields of water depths d based on 2D spatial distribution of mean depth velocities V, flow slope S and roughness parameter D_{84} (by large scale image analysis, *e.g.*, Leduc et al. 2015) or its proxy (using a direct roughness measurement as σ_{Ks}).

6.3. Results

6.3.1. Comparison of roughness proxies

Both the grain size distribution and the roughness standard deviation were measured along the longitudinal profiles defined at the 96 reference points (point gauge depth measurements). The correlations between these roughness proxies are analyzed in Figure 6.12.

A natural and obvious correlation exists between D_{84} and D_{50} ($D_{84} \approx 2D_{50}$ - Fig. 6.12a). Small scatter remains related to the various shapes of GSDs (Fig. 6.11b). Similarly, coarser profiles are also rougher since $D_{84} \approx 7\sigma_{Ks}$ (Fig. 6.12b) and $D_{50} \approx 3\sigma_{Ks}$ (Fig. 6.12c).

The correlations relations were chosen proportional ($D_X = A\sigma_{Ks}$) rather than linear ($D_X = A\sigma_{Ks} + \sigma_0$) to simplify the approach, thus creating a simple dimensionless ratio between D_X and σ_{Ks}. Consequently these linear models do not contain a dimensional term origin.

The scatter remains quite high, which demonstrates that similar gravel mixtures (same D_X) may have variable granular arrangements and interlocking, leading to variable surface roughness (Smart et al., 2002). In other words, similar mixtures with very different imbrication will present different vertical roughness, *i.e.*, roughness to the

flow. This drawback of the Wolman count has ever been pointed by several authors (Aberle and Smart, 2003; Ferguson, 2007). However, increasing roughnesses are definitively related to increasing sizes of sediments and equations using D_{84} may be tested with an estimation of D_{84} based on another roughness proxy and its linear regression (see later).

6.3.2. Friction law validation

At the 96 reference points, 7 outliers were removed because of the large uncertainties of their roughness due to their uncertain X, Y locations and proximity to intensively sorted areas. The $S_{X,Y}$ and σ_{Ks} extraction procedure and the three aforementioned friction laws were applied at all reference points. The reference points' water depths and the computed water depths can be compared to test the relevance of each friction law in describing the measured flows (Fig. 6.13).

The Manning-Strickler formulation shows a general trend to underestimation of the measured depth (Fig. 6.13a), as do the Aberle and Smart (2003) formulation (Fig. 6.13b). On the contrary, despite being inevitably scattered considering the depth measurement uncertainties, the data are centered on the equality line using the Ferguson (2007) formulation (Fig. 6.13c). The scatter remains very high and is related, on one hand, to the natural variability of sediment-laden flows on such steep and rough beds and, on the other hand, to quite high measurement uncertainties (see below). Actually, measuring any of the 4 studied parameters (*d, V, S* and σ_{Ks} or D_{84} - all being necessary for closing and validating the equation), is a simple experimental nightmare in such rapidly shifting, heavily active and intrinsically complex flows.

Fig. 6.14 show that, using the Fergusson law, the ratio computed / measured velocity has a statistical distribution with mean and median values centred on one, *i.e.*, underestimations balance overestimations. These deviations are likely due, at least partially, to the quite high uncertainties on the measured values; in addition to the intrinsic imperfection of an equation as simple as Eq. 6.4: its author for instance wrote "*it is unlikely that any single relation does exist between d and V if there is a combination of skin and drag resistance*" (Ferguson, 2007). Overall, we considered that the results are quite satisfying considering the complexity of the problem and that the best suited friction law to describe the measured flow is the Ferguson (2007) formulation. This is consistent with the results obtained by Rickenmann and Recking (2011) on a large data set comprising well controlled flow conditions or (Schneider et al., 2015) in a steep heavily paved stream.

A specific attention has been paid to uncertainty quantifications. The error propagation has been done through classical analytical uncertainties combinations, whenever a model related an estimation y to its estimator x_i, *i.e.*, if the relationship $y = f(x_1, x_2, \dots x_n)$ is known (JCGM, 2008). Eq. 6.4 has a formulation depending on both d and $d^{5/6}$, which make it unsuitable to direct analytical error propagation. A numerical approach has thus been implemented: the uncertainties *u(V)*, *u(S)* and $u(\sigma_{Ks})$ have been inserted in Equation 6.5 to compute the resulting water depth uncertainty *u(d)*. A Monte Carlo simulation generated 10,000 values of (small) parameter variations ∂V, ∂S and $\partial\sigma_{Ks}$ from normal distributions ($\bar{x_i} = 0$ and $\sigma_{x_i} = u(x_i)$). These variations were introduced in Equation 6.5 and the corresponding water depth $d' = d + \partial d$ was computed. The water depth uncertainty *u(d)* is considered to be the standard deviation of the $10.000d + \partial d$ sample.

The method proved to give similar results as analytical methods, when applicable. Error bars plotted in Figure 6.13 correspond to $u(d_{X,Y})$ at each data point determined through error propagation, thus depending on the local value of the parameters $x_i = (V_{X,Y}, S_{X,Y}, D_{84,X,Y}, \sigma_{Ks,X,Y})$ and on their related uncertainties $u(x_i)$, either determined analytically, whenever possible (mea-

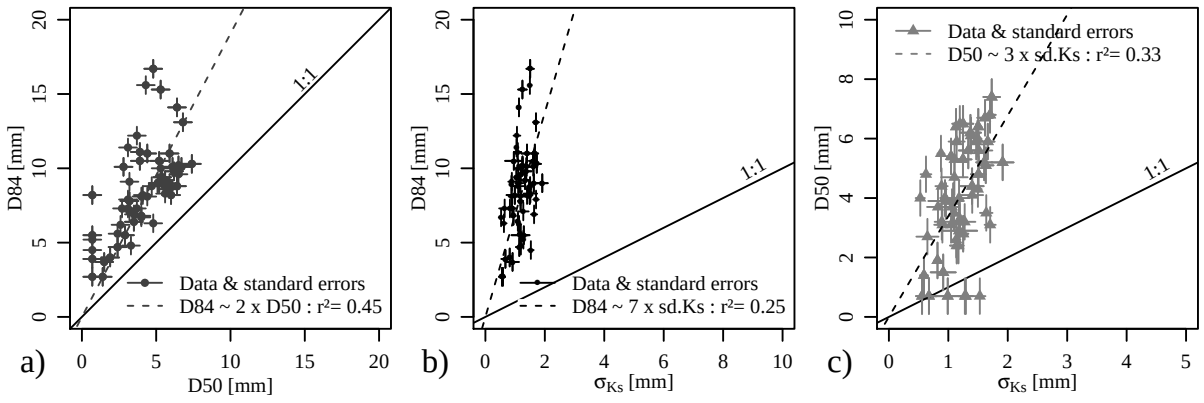

Figure 6.12 – Statistical correlation between roughness proxies: a) $D_{84} \approx 2D_{50}$; b) $D_{84} \approx 7\sigma_{Ks}$ and c) $D_{50} \approx 3\sigma_{Ks}$

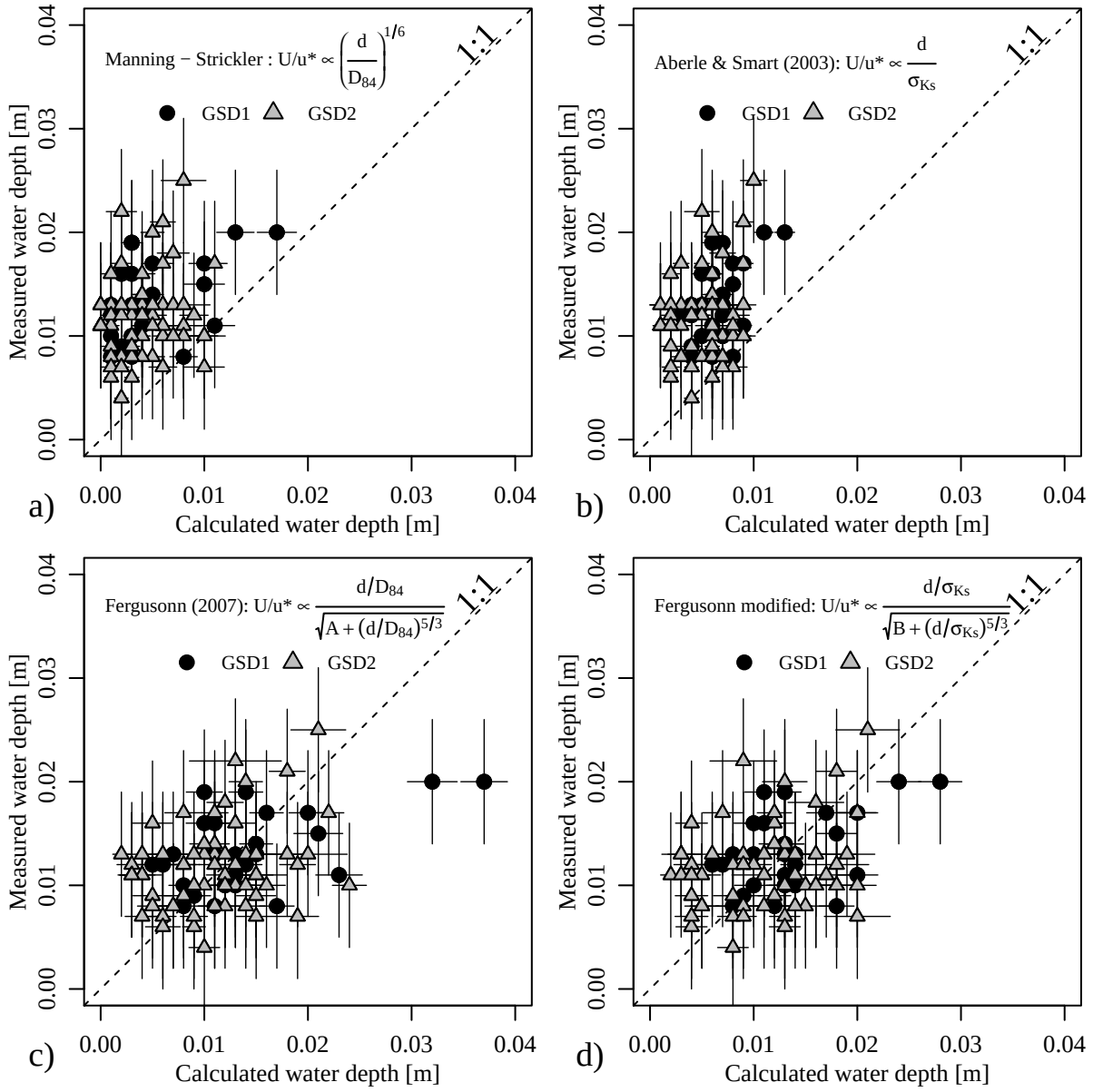

Figure 6.13 – Comparison between measured and computed water depths at reference points with: a) Eq. 6.2; b) Eq. 6.3; c) Eq. 6.4 and d) Eq. 6.6. The underestimation observed in the two first Eqs. is not present using the Ferguson (2007) equation which take into account the changing flow hydraulics related to varied submersions

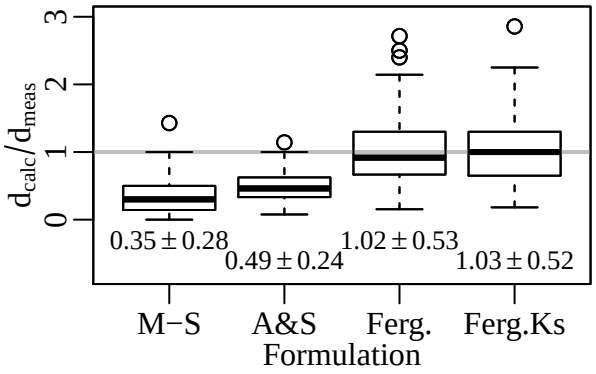

Figure 6.14 – Statistical distribution of the ratio computed water depth / measured water depth, water depth computed using the Manning-Strickler form (M-S); the Aberle and Smart (2003) form (A&S); the Ferguson (2007) form (Ferg.) and the modified Fergusson form using σ_{Ks} as roughness parameter (Ferg.Ks) (Numbers under boxes are mean values ± standard deviation).

surement, Eqs. 6.2 & 6.3), or numerically (Eqs. 6.5 and 6.6).

6.3.3. Reconstitution of 2D flow fields

Considering that the Fergusson formulation is suitable to describe our small scale model flows, it may be used for an inverse computation of the water depths. It is possible to rebuilt 2D water depth spatial distribution if spatial distributions of velocities, slopes and roughness (D_{84} in Eq. 6.4) are known. The roughness standard deviation was used by injecting the linear relation between D_{84} and σ_{Ks} (Fig. 6.12b) in the inversed friction law (Eq. 6.5):

$$V_{X,Y} - \sqrt{gdS_{X,Y}} \frac{2.5(d/7\sigma_{Ks,X,Y})}{\sqrt{1+0.15(d/7\sigma_{Ks,X,Y})^{5/3}}} = 0 \quad (6.6)$$

The performances of this modified Fergusson equation in estimating the water depths are equivalent to the initial formulation using D_{84} (centered median and mean, fewer outliers - Fig. 6.13d & Fig. 6.14). This result was actually expected considering that D_{84} is used as an indirect roughness proxy, while σ_{Ks} is a direct roughness measurement, thus more robust and increasingly used in the field (Nitsche et al., 2012; Schneider et al., 2015).

From the measured flow velocity it is possible to map all hydraulics parameters, as illustrated in Figure 6.15 for Run nDG1/C0.3 (Table 6.1). Water depth 2D fields can be rebuilt by applying the complete procedure of velocity measurement, $S_{X,Y}$ and σ_{Ks} extraction and application of Equation 6.6 to the entire LS-PIV measurement area (Fig. 6.15a). Other meaningful flow dimensionless parameters based on the computed data, such as the relative submergence (here defined as $d/7\sigma_{Ks} \approx d/D_{84}$), the Froude number (here defined as $V/\sqrt{gd}$) or the Shields number (here defined as $= Sd/(s-1)7\sigma_{Ks} \approx Sd/(s-1)D_{84}$ with the sediment density s, can also be mapped allowing detailed analysis of flow features (Fig. 6.15b, c & d).

6.4. Discussion

6.4.1. A simple and affordable technique

This procedure could be extended to other experimental conditions, including field studies, and seems promising considering that: (i) it is relatively simple to implement (the authors are happy to share the code with anybody interested), and (ii) the necessary equipment such as cameras and a photogrammetry software is quite affordable.

Videos filmed at 60 frames/s – classical on modern HD-cameras – are sufficient in most cases (see review of Kantoush et al., 2011). The fast camera was needed in our case only because of the particularly high velocity of the chosen experimental conditions (V up to $1m/s$).

The application of the technique is however limited to flow conditions with reasonably limited 3D-flow patterns since it only takes the surface velocity as a proxy of the flow field. Secondary cur-

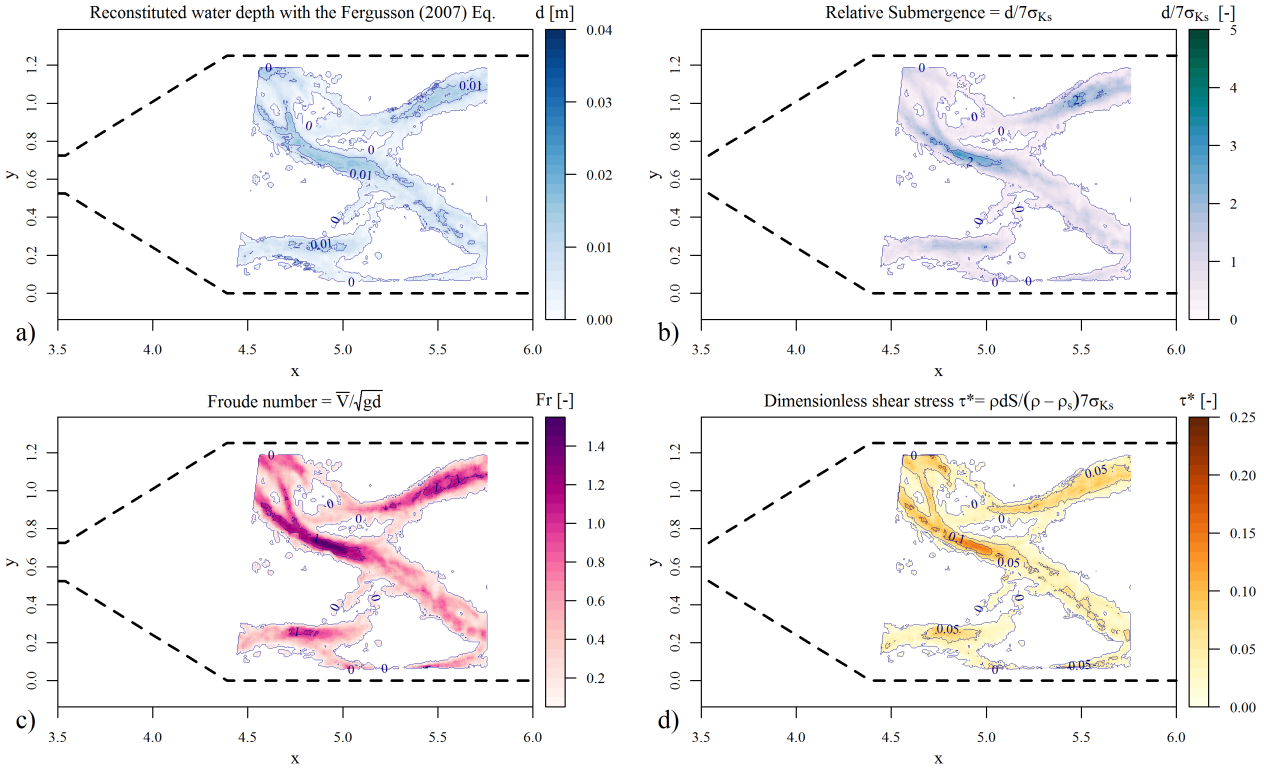

Figure 6.15 – Inversely computed flow fields: a) water depth d, b) relative submergence $d/7\sigma_{Ks}$, c) Froude number $V/\sqrt{gd}$ and, d) Shield parameter $Sd/(s-1)7\sigma_{Ks}$

rents cannot be directly measured or indirectly as deviations from the nearly uniform reconstructed flows. Configuration with marked backwater effects, where energy slopes are not equal to bed slopes, are not favorable as well, in the present version of the procedure, though simple improvements would make such configurations measurable.

6.4.2. Improving the technique

A. Horizontal flow surface assumption

The horizontality of the free surface is implicitly assumed in LSPIV which seems reasonable in most laboratory application (*e.g.*, Fujita et al., 1998; Kantoush et al., 2011). Recent applications in steep slope contexts addressed the possible bias resulting from an excessively steep free surface (Le Boursicaud et al., 2016; Ran et al., 2016) or from 3D flow patterns related to obstacles (bridge piers, protruding boulders – Dramais et al., 2011). To resolve this problem, Ran et al. (2016) performed stereo-picture acquisitions and compute the free surface as a bi-dimensional plane with a variable slope. In the same idea, for more controlled laboratory applications, an alternative could be to orthorectify the fast camera pictures in the flume-plan rather than horizontally. It would then be possible to perform the velocity computation in this local referential system, and to later bring back these results in the laboratory referential system. More complicated and rigorous 3D flow analysis could be performed by projecting the flow pictures on the DEM and tracking pattern correlation on this 3D shapes.

B. Improving flow depth measurements

The determination of the suitable friction law to use in the inversion procedure is a key step. The reference depth measurements that have been used in this work have strong uncertainties that encourage us to prudent conclusions concerning the reconstructed flow fields. In future similar flow depth reconstruction, the use of more precise reference depth measurement techniques, for the

friction law validation step, is recommended. Providing that the water surface must be dyed and seeded with black patterns, its elevation measurement seems possible using photogrammetry, just as the bed surface.

The technical challenge here is to take enough pictures of the flume at exactly the same time in order to capture an instantaneous image of the flow surface with its patterns. It would need several cameras and, according to dynamic photogrammetry monitoring of avalanches (Pulfer et al., 2013) and torrential flows (Ran et al., 2016), the use of accurate remotely control camera triggering.

This image acquisition would optimally be simultaneous with the LS-PIV measurement. The flow must subsequently be stopped, as fast as possible, to prevent bed geometry and roughness adjustments between the flow measurement and its representative bed measurement. Using such a technique would theoretically allow surface-flow DEM computation, which by difference with the bed level DEM (and providing that bed changes between both measurements are reasonably small), would give us the spatial distribution of water depths.

A specific attention must be paid to error propagation when manipulating such great amount of partially automatically computed data. Comparison between reconstructed and measured flow depth fields should come with 2D spatial distribution of measurement uncertainties, after combination and propagation of the spatially distributed input parameter uncertainties. This would extend the validation dataset of the friction law selection and give additional information on its accuracy and bias. It would eventually allow the development of new and more accurate friction laws based on new flow, relief and roughness proxies.

C. Stream line tracking

Friction laws are basically closure equations of the Bernoulli equation which express the evolution of the flow energy along stream lines, *i.e.*, along lines tangent to the velocity vectors (Lencastre, 1983). The slope and roughness parameters should thus been computed along the streamlines. Surface streamlines can be computed from surface velocity measurements (*e.g.*, Weitbrecht et al., 2002; Muste et al., 2004). Assuming that secondary currents are negligible compared to horizontal flow patterns (a reasonable assumption in context of application of the shallow water equation - Muste et al., 2004), surface streamlines are an interesting proxy of the mean flow local directions.

In a narrow flume or along a given river reach, the streamlines are assumed to follow the flume or river main direction. Conversely, in 2D flow computations or reconstructions, flow directions are not systematically parallel to the average flume/river direction. In our case, they are rather locally diverging, converging and wandering over the deposit. As discussed previously, the slope and roughness estimations have thus not been computed along the flume direction (X-direction in our case) but on local, 3W-long longitudinal profiles, defined parallel to the flow direction (an initial step toward a streamline computation). The procedure is assumed to be reasonably correct as long as the flow curvature radius is small compared to the flow width. For highly meandering flows with curvature radius of the order of magnitude of the flow width, the procedure may fail and the σ_{Ks} and S extractions should be done along the curved streamlines rather than along profiles locally parallel to the stream line.

D. Surface velocity correction

A strong hypothesis of this work is the use of a constant velocity index α=0.85 between the surface velocity and the mean depth velocity. The α parameter fundamentally depends on the vertical velocity profile (Le Coz et al., 2010), which itself varies depending on the flow aspect ratio, micro and macro-roughness, Froude and Reynolds numbers and macro-roughness relative submergence

(Muste et al., 2010). Polatel (2006, p. 39) undertook a comprehensive study of the α variation depending on flow velocity and macro-roughness sizes in a 1D flume, tested with smooth bed and with bed cover of dunes and ribs. Her experimental conditions covered a range of relatively low submergence (d/macro-roughness vertical size = 3-10) with subcritical flows ($Froude = 0.39 - 0.51$) and resulted in a α-range of variation fairly small: 0.88±0.04 (mean $\pm\, \sigma$; envelop: *0.80-0.94*). Such values are typical of uniform flows (Costa et al., 2006; Le Coz et al., 2010), even for higher submergence, though it is generally slightly lower (AFNOR, 2009; Dramais et al., 2011). The extensive analysis of Welber et al. (2016) highlights the major influence of the roughness submergence on α.

Similar works addressing nearly critical and super-critical flows, as well as, even lower submergence down to $d/Ks \approx 1$, eventually with sediment transport, are however still lacking, an issue regularly pointed in the literature (Le Coz et al., 2010; Dramais et al., 2011; Ran et al., 2016; Welber et al., 2016). It would possibly lead to different results than Polatel (2005) since two layers flows (a slow sub-layer under macro roughness height, below a faster layer overflowing the macro-roughness, Aguirre-Pe and Fuentes, 1990) are expected in steep rough channels. This change in the flow profile and the influence of the submergence is fundamentally the reason of the difference between the Manning Strickler (Eq. 6.2) and the Aberle& Smart (Eq. 6.3) formulations that drove Ferguson (2007) in proposing his Variable Power Equation (Eq. 6.4). Additional modification of the flow profile may emerge from feedback related to sediment transport (Recking et al., 2008b; Revil-Baudard et al., 2015). In the current state of knowledge, the authors must assume the recommended *0.85* value of α (Muste et al., 2010).

6.5. Conclusions

The present work describes a measurement procedure that takes advantage of the recent development of affordable HD-cameras and of user-friendly image-analysis software. Using HD-pictures of the flows and the beds, it is now easily possible to reconstruct *mm*-accurate elevation models and detailed velocities spatial distribution. Combining the resulting data make it possible to describe the spatial distribution of deposit thickness, slope S, roughness σ_{Ks} and velocity V at unprecedented spatio-temporal resolution. Care has been paid to measuring slope and roughness along the flow directions which, in freely adjusting beds, are often not the main flume direction. A set of manual water depth measurements were used to test several friction laws in their ability to describe the measured velocity and depth under their slope and roughness conditions. The Ferguson (2007) Variable Power Equation (Eq. 6.4) has, once again, proved to be the best suited to our steep variably-deep flows. Using the local standard deviation of the bed roughness σ_{Ks} as a proxy of the D_{84} parameter in the Ferguson (2007) friction law, it proved to be possible to extend the water depth computation by inverting the friction law ($d = f^{-1}(V, S, \sigma_{Ks})$) throughout the entire flooded area. Complete spatial distribution of the flow features (flow slope, roughness, mean depth velocity and depth) can be reconstructed thus providing numerous data on these freely adjusting systems, currently still poorly known. The method is simple in essence and relatively affordable regarding the amount of data it can produce. The authors hope that it will be tested and improved in other experimental situations, including field observations, and help understand the dynamics of freely adjusting geophysical flows.

Acknowledgments

This study was funded by Irstea, the INTEREG-ALCOTRA European RISBA project, and the ALPINE SPACE European SEDALP project. The authors would like to thank Benoit CAMENEN for the idea of using Fudaa-LSPIV, Guillaume NORD and Cédric LEGOUT for the TiO_2 trick, Jules LE GUERN, Costanza CARBONARI, Ségolène MEJEAN, Firmin FONTAINE and Coraline BEL for their help in the experimental setup development and experience performance.

Notation

The following symbols are used in this paper:

C = sediment concentration = Q_S/Q (-);

D = sediment diameter (m);

d = water depth (m);

$\partial \ldots)$ = small variation of ... used in error propagation ;

g = gravitational acceleration = 9.81 (m/s^2);

K_S = local bed roughness = $Z_{X,Y} - \bar{Z}_{X\pm D_{MAX}/2,Y\pm D_{MAX}/2}$ (m);

Q = water discharge (m^3/s);

Q_S = sediment discharge (g/s);

S = slope (m/m);

s = sediment density = 2.65 (-);

T = deposit thickness, de-trended bed elevation, *i.e.*, = $Z_{X,Y} - S_{flume} \times X$ (m);

T_{peak} = hydrograph rising limb duration (min);

$u(\ldots)$ = uncertainty on ... used in error propagation ;

u^* = shear velocity = $\sqrt{gdS}$ (m/s);

V *or* $\bar{V}$ = mean velocity integrated over the flow depth(m/s);

V_0 = threshold velocity below which no d inversion is done (m/s);

V_{LSPIV} = surface velocity measured by LSPIV (m/s);

V_{PTV} = surface velocity measured by PTV (m/s);

W = flow width (m);

X, Y = point spatial coordinate (m);

Z = bed elevation (m);

Z_B = bed elevation, measured with the point gauge (m);

Z_{FS} = free surface elevation, measured with the point gauge (m);

$\sigma_{\ldots}$ = standard deviation of ...;

α = velocity index = $\bar{V}/V_{surface}$ (-);

$\Delta X, \Delta Y$ = grid size in the X and Y direction, respectively (m);

$\bar{\ldots}$ = mean value of ... ;

$\ldots_{MAX}$ = maximum value ... ;

$\ldots_m$ = mean arithmetic value ... ;

$\ldots_{X,Y}$ = value of ... at the coordinate X, Y;

$\ldots_{X\%}$ = Quantile of ... with probability $X\%$;

$\ldots_i$ = i^{th} element of ...;

"Simple interactions at small scales can produce complex behaviours at larger scales; and complicated small-scale processes can add up to relatively simple large-scale dynamics."

Chris Paola (2011), *Nature* **469** p.38.

CHAPTER 7

Hydraulics and geomorphic dynamics in bedload deposition basins: A generic Froude scale model study

Guillaume PITON[a], Alain RECKING[a], Ségolène MEJEAN[a], Costanza CARBONARI[a,b] , Jules LE GUERN[a]

[a] Université Grenoble Alpes, Irstea, UR ETGR, St-Martin-d'Hères, France.

[b] University of Florence, Dipartimento di Ingegneria Civile e Ambientale, Firenze, Italy.

Our study of the general process of bedload deposition in wide basins required several experimental choices that are presented in the first part of this chapter. The second part is a preliminary analysis of our results. I must confess that we were surprised by the complexity and the changing aspect of the depositions observed in the model. I am now convinced that they are not mere model effects. Since they may be observed in the field, we spend time to describe them and explain their origins. In a second step, we performed simple analysis of the deposition slopes and Froude numbers, with quite consistent results. It is somewhat reassuring that, as regularly stressed by Chris PAOLA (Paola et al., 2009; Paola and Leeder, 2011), *complexity is a matter of scale*, and that engineers will obviously not have to wait for a complete deterministic description of bedload / water mixtures to obtain simple criteria for structure design, although we must accept that our criteria are necessarily partially wrong and unable to grasp the complete complexity of Nature.

Abstract

Sediment trapping structures, such as gravel deposition basins, are regularly implemented in mountainous context for flood hazard mitigation. These structures should ultimately trap gravels when their excess may aggravate the downstream flood hazard, while, the remaining time, allowing a suitable background sediment continuity. Such optimized designs require a sufficient knowledge of the flow features and geomorphic processes implied in gravel trapping. A generic Froude scale model of a 10%-steep, bedload deposition basin, with a slit dam and without outlet structure, is presented in this paper. Accurate photogrammetry and large scale particle image velocimetry (LS-PIV) were combined to study the geomorphic patterns and to reconstruct the flows. The emergence of self induced cycles of braided and channelized flows, with intense grain size sorting, is described. It sheds light on the similarity of bedload trapping with alluvial fan formation or fluvial delta development. The deposition slope, a key parameter in the structure design, is more precisely studied. The measurements are correctly estimated by a new simple equation, which is developed from prior works dedicated to steep slope stream hydraulics and bedload transport. The analysis demonstrates additionally that, despite the steepness of the studied conditions, most flows are subcritical due to roughness adjustment. We finally highlight that morphologically-active flows, *i.e.*, with dimensionless shear stress higher than the threshold for motion, have Froude number ≈ 1; *i.e.*, that a critical flow hypothesis seems reasonable, as a first approximation, to describe flows over massive bedload depositions. This new dataset, with complete geomorphic and flow measurements, in diverse conditions, may be used as reference to try and test numerical approaches of the phenomena.

Author key words: *Generic Froude Scale Model, Large Scale Particle Image Velocimetry, Autogenic Cycles, Deposition Slope Estimation, Critical Flow Hypothesis.*

7.1. Introduction

Damages induced by floods in mountains streams are significantly related to excess in sediment supply (Badoux et al., 2014; Rickenmann et al., 2015). Sediment trapping structures are consequently regularly implemented to protect urbanized areas or strategic transportation networks (Van Effenterre, 1982; Zollinger, 1984b; Ikeya, 1989; VanDine, 1996). Gravel deposition basins were for instance built as soon as 1843 in Switzerland (Vischer, 2003). They considerably increased in number since the advent of mobile earth-moving machinery allowing affordable basin dredging (Van Effenterre, 1982).

Sediment trapping structures are basically composed of an artificially widened river reach, constituting their basin. Their outlet section is usually equipped with a ground sill. Some outlet sills have an open check dam built atop, with a specific shape depending on the expected structure function, *e.g.*, total retention, woody debris and boulder filtering, solid discharge dosing (Zollinger, 1984b; Ikeya, 1989; Piton and Recking, 2016a; 2016b). These functional check dams, with an optimized design adapted to the site-specific hazards (Armanini et al., 1991), are expected to progressively replace some older structures whose effect was usually to excessively trap the sediment load (Mizuyama, 2008; Papež et al., 2015), this even during mere high flows that do not threaten elements at risk.

Using functional check dams, in addition to classical check dams, is desirable for two main

reasons: (i) it is necessary to mechanically excavate and evacuate sediment supplied by extreme floods - fundamental function of the structure - but also the background sediment supplied by small floods, the latter sometimes deeply impacting the structure maintenance costs (Dodge, 1948; Mazzorana et al., 2015). In addition, (ii) excessive sediment trapping induce sediment starvation downstream of dams, leading to incision and downstream structures destabilization (Brandt, 2000). At a broader scale, sediment disconnectivity impairs ecological status of fluvial systems (EU, 2000, p. 40). In some catchments (with sufficient downstream sediment transport capacity), a better sediment continuity of open check dams seems desirable. Adaptations and optimizations of existing and new structures are necessary, which requires a sufficient comprehension of the hydraulics and sediment processes occurring inside the deposition basins, not to impair their hazard mitigation effects.

Defining guidelines for such adaptations is challenging because: i) the diversity of catchments make the flood processes even more diverse (from clear water transporting woody debris to large scale debris flows related to natural dam outbursts, Schuster, 2000; D'Agostino, 2013a; Hungr et al., 2014); and consequently, ii) the seldom directly-observed, violent and fast trap filling processes, which are likely as diverse as the flood types, are poorly known. Piton and Recking (2016a) reviewed the existing design criteria and highlighted that some simple questions necessary for sediment trap design or optimization are far from having clear answers, *e.g.*, i) how to compute the deposition slope in the basin?; or ii) what are the typical flow conditions during massive bedload deposition?

Design and optimization of deposition basins are consequently a regular subject of investigation, particularly using small scale models, often for specific case-studies (Zollinger, 1983; Ishikawa and Mizuyama, 1988; Armanini and Larcher, 2001; Lefebvre and Demmerle, 2004; Itoh et al., 2011; Kaitna et al., 2011; Shrestha et al., 2012; Ghilardi et al., 2012; Itoh et al., 2013; SedAlp, 2015b). The understanding of the morphodynamics is increasingly enhanced by additional and always more accurate topography measurements technique (laser-scan or photogrammetry), down to grain size sorting assessment (Leduc et al., 2015). Cross-comparison with numerical models complete laboratory experiments with a twofold general objective: developing operational design tools and improving the comprehension of the processes from a scientific perspective (Kaitna et al., 2011; Shrestha et al., 2012; Itoh et al., 2013; Gems et al., 2014; Canelas et al., 2015).

However, dynamics acquisitions of the flows features are lacking most of the time. Consequently, the numerical models are indirectly validated by comparing the resulting computed and measured deposit patterns, without validation of the flow conditions. This global lack of knowledge concerning the flow features impairs design optimizations because: (i) the use of numerous design criteria necessitate to know some flow and geomorphic parameters, usually unobtainable out of laboratory experiments, *e.g.*, velocity, depth, Froude number, Shields number, depostion slope (*e.g.*, Armanini and Larcher, 2001; Schmocker and Hager, 2013; Di Stefano and Ferro, 2014); (ii) considering that we do not really know in which extend the numerical models can be trusted in extreme flow conditions, their use must be profoundly cautious in the design of key hazard mitigation structures in the highly varied situations encountered in the fields.

Investigation of both the morphodynamics and the flows are necessary to improve our comprehension of their coupling and to constitute complete data set for eventual complementary validations of numerical approaches.

Here we used the flow reconstruction procedure by inverse approach presented in Chapter 6, to investigate a generic Froude scale model of bedload deposition basin (*i.e.*, a model that is

not site or scale-specific but rather seek to figure a typical deposition basin). This chapter details how has been defined the experimental conditions, based on literature dataset whenever existing, and on field surveys when the typical prototype features were not known. It secondly describes the morphodynamics and flow features that were observed under massive bedload supply, in basins equipped with a slit dam or without open check dam. These results are finally discussed and synthesized.

7.2. Materiel and Methods

The technical details concerning the experimental set up used for this chapter has been thoroughly presented in Chap. 6. Some details concerning the choice of the basin features and boundaries condition were however not addressed in the previous methodological chapter and are justified hereafter.

7.2.1. Definition of the generic model

A. Basin shape

Comparison with other scales is done through the Froude similitude (Peakall et al., 1996). The similitude concept has been used for decades in hydraulics studies, and has proved to be "*unreasonably effective*" (Paola et al., 2009). It is particularly adapted to mountain streams that are relatively small systems with coarse material, thus imply reasonable scale reduction and maintaining turbulent rough flows (Couvert and Lefebvre, 1994). The similitude concept will not be presented here further in details (see reviews of Sharp, 1981; Peakall et al., 1996; Paola et al., 2009; Heller, 2011; Kleinhans et al., 2014; El Kadi Abderrezzak et al., 2014).

This work did not concern a specific stream as a case-study that would imply to use a classical Froude scale model with a specific and fixed geometrical scale reduction. The idea was, on the contrary, to perform a small scale version of a general geomorphic process, model defined as "*generic Froude scale model*" in Peakall et al. (1996). To design this average deposition basin, it was first necessary to define a typical geometry roughly representative of the field reality. While grain size distributions were taken from the literature (see later), typical sediment trap basin geometries are, to our knowledge, poorly available in the literature. Regarding this lack of information, field investigations were performed: we visited 31 sediment traps in the French Alps, in various contexts of slope, sediment transport process, geology, climate and land use (complete field visit report in Piton et al., 2015).

The basin shapes, sediment deposition and basin dredging slopes were measured with a laser telemeter (Truepulse 300X©). Three dimensionless parameters were defined to describe the basins' planar shapes (Fig. 7.1). We introduced the aspect ratio L^*, representing the elongation of the basin along the flow direction:

$$L^* = \frac{L_{Tot}}{W_{Tot}} \tag{7.1}$$

with the basin total length L_{Tot} (m) and the basin maximum width W_{Tot} (m). We also introduced the compactness Co^*, which inform on the effective available area, through the ratio between the trap basin area and the surface of rectangle with an equivalent L^*:

$$Co^* = \frac{Trap\ basin\ surface}{Maximum\ surface(L^*)} = \frac{\sum_i A_i}{W_{Tot} \times L_{Tot}} \tag{7.2}$$

with the surface area of the elementary subsurface A_i (Fig. 7.1a). The skewness Sk^* describes the surface distribution along the flow direction. It uses values of each subsurface areas, made dimensionless with the basin surface $A_i / \sum_i A_i$, and subsurface gravity center abscissa (Fig. 7.1as), taken from the basin inlet, L^*_{Gi}, made dimensionless with half the basin length:

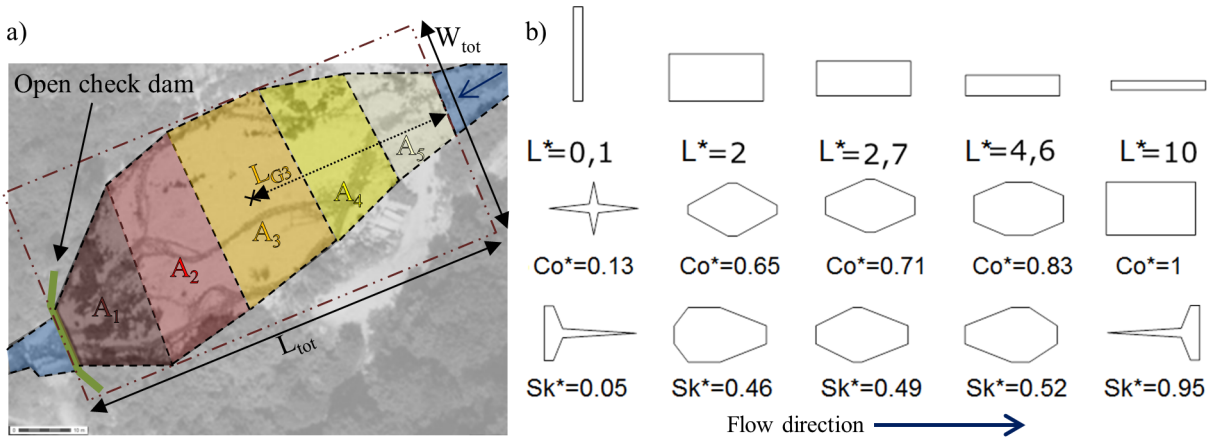

Figure 7.1 – Definition of the basin shape parameters: a) example of the Roize deposition basin (Voreppe, FRA.): L_X distance along the flow direction, W_X transversal width, A_i and Gi elementary surface area and its gravity center, respectively (aerial photo from *geoporail.fr*); and b) illustration of the shape changes depending on each dimensionless parameters on simplified shapes: extreme examples are simply illustrative, central examples are quantile 20%, the median and quantile 80% of the 31 trap sample

$$Sk^* = \sum_i \frac{L_{Gi}}{L_{Tot}/2} \times \frac{A_i}{\sum_i A_i} \tag{7.3}$$

The statistical analysis of the 31-structure sample demonstrated that:

- L^* varies significantly between traps: $L^*_{20\%} = 2$ while $L^*_{80\%} = 4.6$ highlighting that short as well as long basins exist;
- Co^* varies in a less extend with the *20%* and *80%* quantiles equal to *0.65* and *0.83* respectively; it means that $1 - Co^*_{50\%} \approx 30\%$ of the available area is lost to connect the basin to the inlet and outlet narrower sections; and
- Sk^* nearly does not vary around a centred value of *0.5*: divergent part of basins are often quite the symmetric of the convergent part.

This analysis guided the design of the shape of the investigation area built in the flume (Carbonari, 2015). On a more general perspective it demonstrates that basin shapes are not designed followings some accurate guidelines, but merely adapted to local topography and constraints.

An aspect ratio of *2* has been chosen for our experiments. This value corresponds to the quantile of probability *20%* of the 31-structure sample, *i.e.*, to a relatively short configuration. This short basin has been selected to particularly highlight the influence of the outlet structure. Conversely, longer basins would increasingly look like braided reaches submitted to intense aggradation and the outlet influence would eventually decrease. The median values of the Co^* and Sk^* were chosen for the model considering them as influencing the flows and geomorphic features at the second order, compare to basin aspect ratio.

Three sets of experiments were performed (Fig. 6.3): the first with a slit dam at the outlet (details in Carbonari, 2015); the next with a simple ground sill at the outlet on the entire basin width (details in Mejean, 2015). The basin slope was fixed for all experiments at *10%* (*i.e.*, $\approx S_{basin,50\%}$ of the 31 trap sample, Piton et al., 2015, p. 22). The basin width of the last set was reduced by a factor two, to highlight the possible effect of L^*. In the first configuration, the slit was wide enough to prevent coarse grain jamming (60-mm $= 3D_{max}$, Piton and Recking, 2016a). The deposit is thus a pure hydraulic control (*sensu.* Piton and Recking, 2016a), *i.e.*, steep submerged

deposit in the backwater area of the slit dam, prograding until establishment of sediment transfer, in the form of an aspiration cone around the slit (Zollinger, 1983).

B. Sediment mixtures

Grain size distribution (GSD) of some accurately monitored, steep slope streams were used to define an analogue GSD shape: the Rio Cordon, (ITA.) (Lenzi et al., 1999; Mao and Lenzi, 2007); the Erlenbach and the Pitzbach (CHE.) (Rickenmann and Fritschi, 2010) and the Manival (FRA.) (Theule et al., 2012; F. Liébault and A. Recking, pers. dataset). These streams are hereafter referred to as the "*reference streams*". Each GSD was made dimensionless with its D_{50} (diameter such that 50% of the mixture is finer), thus collapsing all the dimensionless curves on the median value (Fig. 7.2a). On one hand, the coarse part of the curves (>50%) are relatively homogeneous with the ratio $D_{84}/D_{50} = 3.4 \pm 1.0$; on the other hand, the fine tails pretty much differ between catchments.

Two sediments mixtures were used in our experiments, consisting in natural sediments with diameter ranging from 0.2 to 20 mm, and hereafter refer to as GSD1 & GSD2. The median grain size D_{50} of GSD1 and GSD2 are 3.8 and 2.4 mm, respectively; and the mean arithmetic diameters are of 6.4 and 4.9 mm, respectively (complete dimensionless GSDs in Fig. 7.2a to multiply by the D_{50}s to get the real GSDs). Grain size sorting being expected, different grain colors were used to easily observe it (Fig. 7.2b): blue for $D \in [14; 20mm]$, naturally brown and grey for $D \in [3; 14mm]$, naturally white for $D \in [1; 3mm]$ and naturally beige for $D \in [0.2; 1mm]$.

Comparing GSD1 and GSD2 to the field data, their fine tails correspond to relatively coarse mixtures, though they remain in the natural variability range exemplified by the reference streams. A 200-μm lower limit was actually chosen to avoid colloidal effects and other undesirable effects related to fine sands / silts in small scale models (Paola et al., 2009; Heller, 2011; Kleinhans et al., 2014).

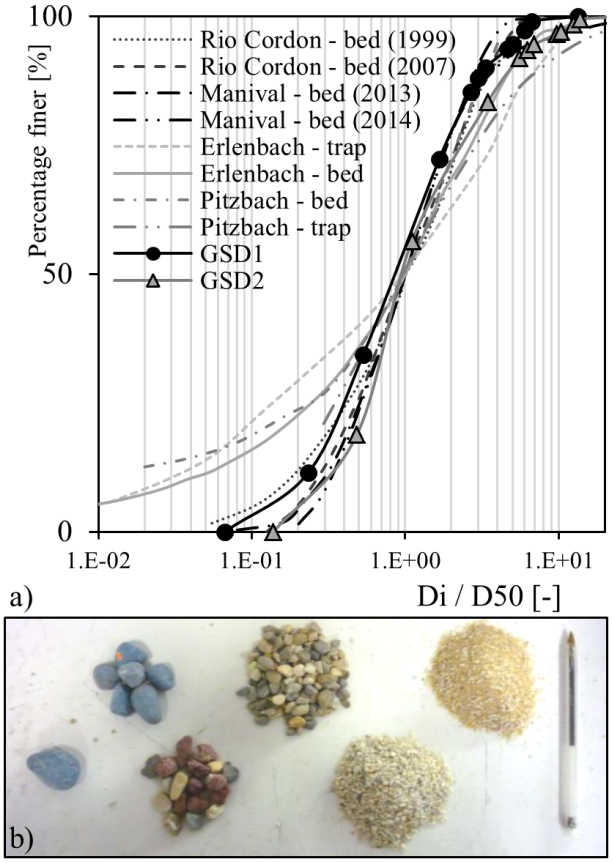

Figure 7.2 – The dimensionless GSDs of the torrents considered, GSD1 and GS2, dots correspond to the sieves used in the mixture preparation; data of the Rio Cordon after (after Lenzi et al., 1999; Mao and Lenzi, 2007); data from Erlenbach and the Pitzbach (after Rickenmann and Fritschi, 2010), and data from the Manival (persn. dataset of F. Liébault and A. Recking).

In term of geometric scale λ, here estimated by $\lambda = D_{50,prototype}/D_{50,model}$, it varies in the range $\lambda \approx [15; 50]$ with a mean value $\pm$ standard deviation of $\lambda = 25 \pm 12$ when comparing both GSD with the reference streams'. The λ mean value will regularly be taken as reference to upscale our model results, giving thus field-scale equivalents.

C. Model flood features

Sediment trap fillings in small catchments are intrinsically flashy and transient processes. It has thus been decided to use varying feeding conditions with hydrographs.

C.a. Water discharge

Hydrograph shapes and flood duration strongly vary between events (Cipriani et al., 2012). The model seeking to represent average typical floods, simple triangular hydrographs were used with a recession duration 1.7-time longer than the rising limb (Fig. 7.3, same shape as in Armanini and Larcher, 2001). This slightly longer recession limb is consistent with the typically observed hydrographs in monitored mountain catchments (*e.g.*, D'Agostino and Lenzi, 1996; D'Agostino and Lenzi, 1999; Rickenmann et al., 1998; Lenzi, 2001; Turowski et al., 2009). The peak water discharge was generally of 2.75 l/s and always >1.6 l/s (Table 1), *i.e.*, $\approx 9m^3/s$ and $\gtrsim 5m^3/s$, respectively at $\lambda = 25$. Such flood discharges are strong but not extremely high for the reference streams.

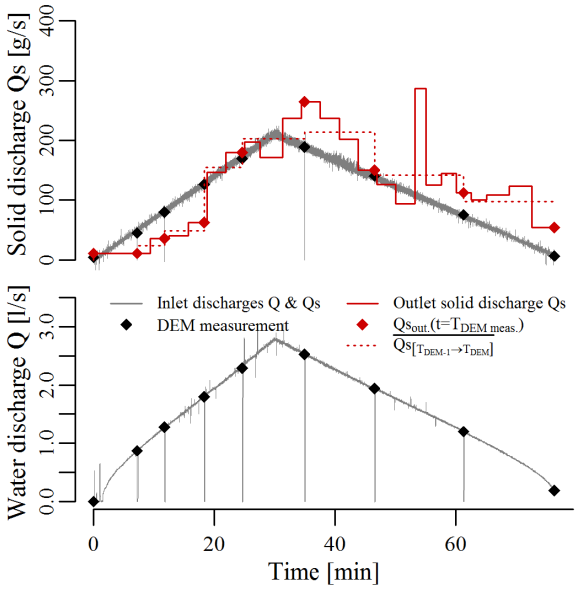

Figure 7.3 – Typical boundaries conditions: solid and water discharges at the inlet, measured outlet solid discharge and steps of DEM measurements. For each DEM measurements, the instantaneous solid discharge can be extracted as well as a mean solid discharge by difference with the previous DEM

C.b. Sediment supply

Facilities

The 10%-steep basin is fed by a 15%-steep, rough inlet pipe, figuring the upstream torrent bed. Its 0.25-m width (≈6 m at λ=25) has been selected narrow enough to prevent sediment deposit for such a steep slope. Coarse grains were glued on its floor and sides to limit flow acceleration and excessive Froude numbers at the inlet. No inlet check dam, constituting a step in the profile, has been added (field visits demonstrated that most of basins are not equipped with such a structure, Piton et al., 2015); however, a few cobbles were put at the basin inlet for energy dissipation.

Solid discharges

Computing the bedload transport related to a given flood event remains an unresolved scientific issue, particularly at the event scale (Recking et al., 2012b; Recking et al., 2016; Chap. 4). In addition to the non-linearity of the relation between water discharge and sediment discharge (Recking, 2013a), hysteresis is regularly reported (Mao, 2012), as well as varying incipient transport condition (up to one order of magnitude on the discharge, Turowski et al., 2011). For simplicity (any choice being debatable), the sediment discharge was set here proportional to the water discharge.

Various sediment concentration $C = Q_s/Q \in [0.01; 0.05]$ were used in order to observe varying deposition intensity: from near equilibrium up to nearly total deposition, with Q and Q_s water and sediment discharges, respectively (m^3/s). Conversely, to compare the various experiments the total volume injected (≈500 kg, *i.e.*, ≈8,000 t at λ=25) was kept constant between runs. Maintaining a total sediment supply while varying the instantaneous concentration imposed either i) to modify water discharge or ii) to keep the water

discharge magnitude constant while changing the flood duration. The second option was chosen whenever it was possible, to maintain the water discharge as high as possible (high but not extreme as mentioned previously). As a consequence, the experiment durations were inversely proportional to the concentration. Table 6.1 summarizes the experiment plan.

7.2.2. Measurements

A. Outlet solide discharge

The outlet flows passed by 0.1-mm-pierced boxes that, once roughly drained were weighed to measure outlet solid discharges (accuracy ±1 g/s, measurement frequency 1-5 min, depending on the outlet discharge intensity, *e.g.*, red curve on Fig. 7.3). The water content has been corrected based on dried samples weighting.

B. Deposit relief

B.a. Measurement set up

Two CANON 100D cameras took pictures from a trolley circulating over the flume. High quality digital elevation models (DEM of the elevation Z for all point X,Y) were reconstructed with the HD-pictures and a photogrammetry software (Agisoft Photoscan). The procedure is accurately detailed in Chap. 6, consequently, only complementary information is given here.

B.b. Bed elevation

For all flume point of coordinate X,Y, millimeter-accurate elevation field $Z_{X,Y}$ were built (Le Guern, 2014). De-trended elevation were also computed to represent the deposit thickness $T_{X,Y}$ ($= Z_{X,Y} - S_{flume} \times X$, with the flume slope S_{flume} and the point abscissa in the flume axis X). As several of these DEMs were available for each experiment, the sediment propagation in the model is described in several steps and deposition/erosion areas could be deduced.

C. Flow features

The high definition relief measurements have been coupled with flow surface velocity measurements using large scale particle image velocimetry (LS-PIV – Fujita et al., 1998; Muste et al., 2010). The complete procedure is described in Chap. 6. In sum, a first stage consisted in the interpolation of the flow direction at all flooded points X,Y from the LSPIV velocity measurements. The bed roughness standard deviation (σ_{Ks}) and the channel slope, hereafter referred to as "*flow slope*", were extracted from the DEM, specifically along the flow direction. In a second stage, after the validation of the Ferguson (2007) friction law in the experimental condition, the DEM and LSPIV data were used to reconstruct the water depth surface distribution from the measured velocity, flow slope and roughness of the bed.

Surface distributions of flow slope, depth and velocity, as well as bed roughness and elevation, were used to characterize the flow features (Froude number, Shields number) in the model. Measurement uncertainties are likely be quite high but are balanced by the number of measurements: the flow features were computed on regular grids with a 5-mm space between points, resulting in thousands of values per DEM-LSPIV measurement.

7.3. Results

7.3.1. Geomorphic patterns

A. Braided VS Channelized

When entering the basin, flows and sediment pass from a steep-laterally-confined to a milder-laterally-unconfined situation. In this situation, Zollinger (1983) observed both mono-channelized and braided fan-shape deposits. In our experiments also cycles of channelized flows and braided flows were systematically observed (*e.g.*, Fig. 7.4). Typical cycles begin with a steep fan shape deposit at the inlet (Fig. 7.4a top), covered by a

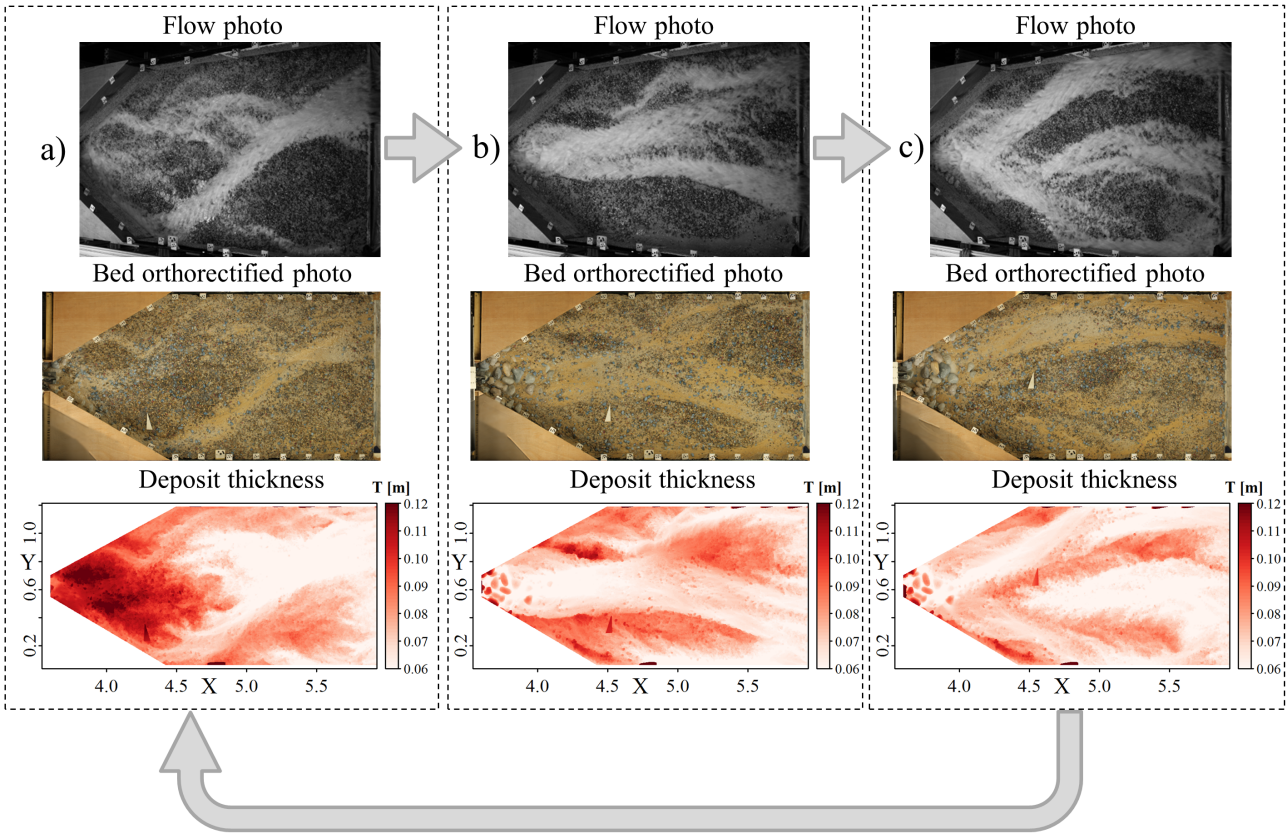

Figure 7.4 – Typical geomorphic patterns observed in cycles, illustrated by deposit thickness T and pictures of the flow just before the DEM measurement: a) massive upstream deposit drained by sheet flows, b) channelized flow eroding the inlet deposit and spreading further downstream, and c) splitting of the channel in multi-channel braided pattern, new starting of inlet deposit.

sheet flow: thin layer of water spreading over a large part of the deposit with marginal preferential paths and narrow channels (Parker et al., 1998). The flow is then very shallow with limited transport capacity, resulting in massive deposition (Fig. 7.4a bottom). The infiltration rate is quite high and subsurface flows emerge at the deposit toe (Fig. 7.4a top). An efficient grain size sorting is systematically observed (kinetic sorting, Frey and Church, 2009; 2011) with percolation of the finer grains beneath the coarsest that rapidly organized themselves to form an armour (Fig. 7.4a middle). This armour makes the deposit relatively stable, allowing the slope to increase up to a maximum before armour breaking (Bacchi et al., 2014).

Armour breakings are generally rapid and sudden. Their precise triggering process is not yet clear. Mere surface flows generally result in small armour rearrangements and additional grain deposition. In parallel, small, local, en-masse motions of water saturated material, without surface flow, were also observed on the steep deposit (for instance associated with toe erosion), looking like geomechanical failure initiation or granular flow. Sub-surface flow definitively facilitates this mechanism. Eyes observation let us think that effective failure triggering is a combined effect of surface flow shear stress and deeper geomechanical failure correlated with sub-surface flow. A section of the fan is then abruptly transported downstream, creating a preferential path in the quite regular fan shape deposit (Fig. 7.4b). This incision concentrates all flows, transforming the sheet flows or braided pattern in a deeper channelized flow. The armour breaking additionally releases the fine subsurface material that smooths the bed (Fig. 7.4b middle). The combination between flow channelization and bed smoothing thus generate a self-reinforcing feedback mechanism that enhances the flow transport capacity. The geomorphic changes during this step are consequently very fast. This dynamics stops relatively rapidly, as soon as the inlet deposit has been eroded, exhausting the main sediment source. The resulting channel slope near the inlet is then quite mild triggering a new inlet deposition cycle.

The above process transports efficiently the sediments downstream (Fig. 7.4b & c): i) at the fan toe, leading to a new deposit spread on the initially dredged basin (initial steps, similar to fan-lobes - Reitz and Jerolmack, 2012); or, ii) out of the model if the downstream channel has sufficient transport capacity (final steps). Namely, water flowed in a main channel with shallow, marginal secondary paths (Fig. 7.4b) or in braided patterns (Fig. 7.4c), depending on bar deposition dynamics and upstream flow type. These flows transported the upstream sediment supply and spread it in the basin, building lobes, terraces and wandering channels. Flows were thus gradually constrained by the terraces in construction. As soon as an active channel was built, with continuous transport capacity from the inlet to the outlet, the geomorphic cycle nearly stopped. The inlet supply was then generally continuously transported through the channel. The channel eventually wandered in the basin with lateral bank erosion and bar deposition on the other bank. This phenomenon eventually remobilized significant former deposit from the terraces (see later).

B. Deposition slope cycles

Vertical fluctuations of the deposition elevation were observed. There is thus not a unique value of deposition slope but rather a range of slope within which a dynamic-equilibrium fluctuates. Bulk longitudinal profiles of the deposits were defined by considering all bed elevations $Z_{X,Y}$ for each abscissa X along the flume (Fig. 7.5). These profiles were plotted with $Z_{X,Y}$, illustrating the deposit slopes (Fig. 7.5 bottom), but also with $T_{X,Y}$ illustrating deposit thickness (figuring its propagation in the basin - Fig. 7.5 top); or with the evolution of the deposit thickness between two DEM measurements ($dT_{X,Y} = T_{X,Y;DEM_i} - T_{X,Y;DEM_{i-1}}$), illustrating the basin part where

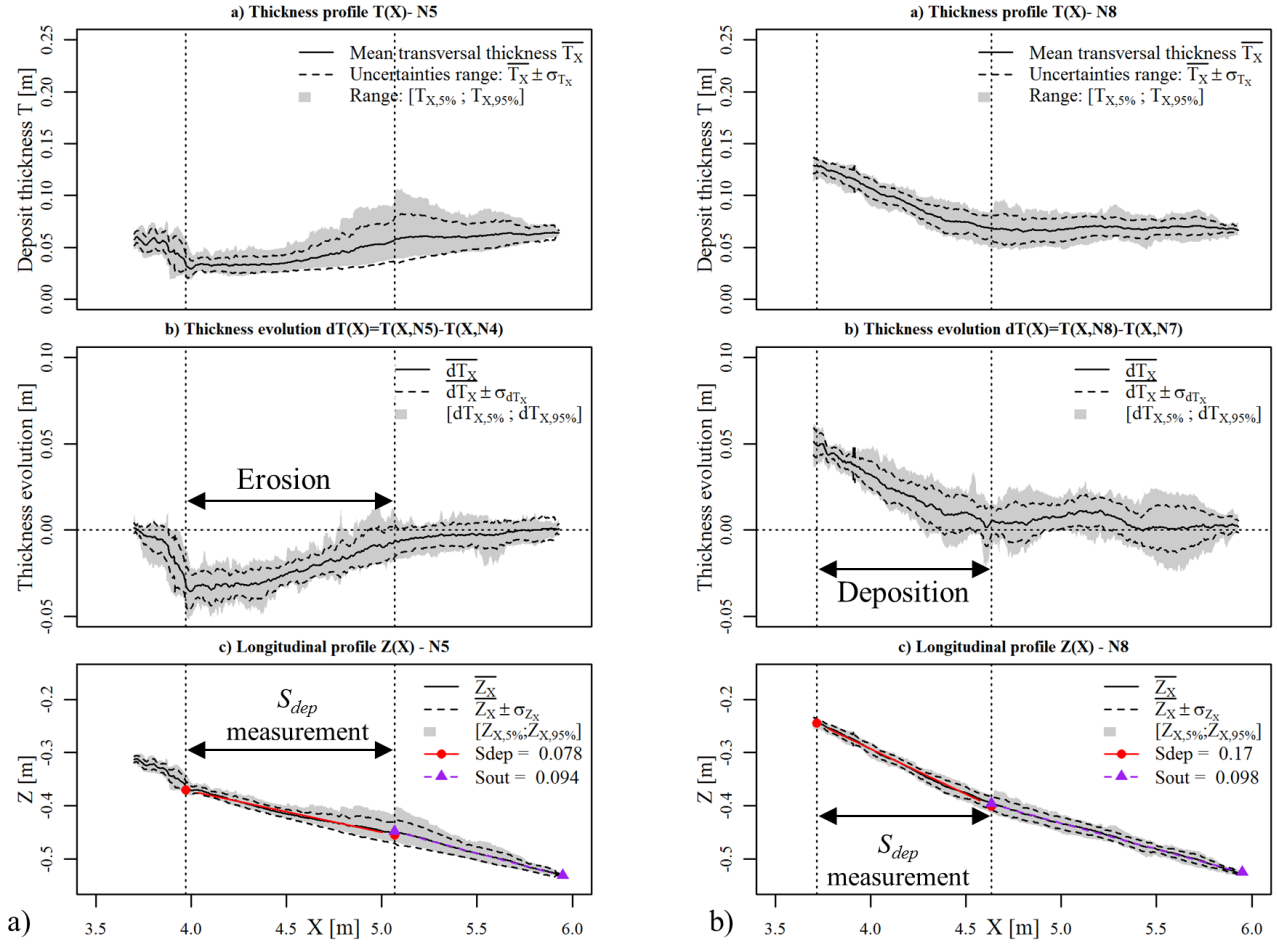

Figure 7.5 – Mean longitudinal profiles and uncertainties ranges of: the deposit thickness $T_{X,Y}(X, \forall Y)$ figuring the deposit repartition along the basin (top), the thickness evolution $dT_{X,Y}(X, \forall Y)$ (middle), showing the recently morphologically active section and the bed elevation $Z_{X,Y}(X, \forall Y)$ (down) on which the slopes S_{dep} and S_{out} are measured for a) an erosion event in the middle part of the basin and b) a deposition event in the upper part of the basin (Run nDG2/W2.3, no slit dam at the outlet)

sediment transport and geomorphic activity was the more active (Fig. 7.5 middle). In the upstream principally active section, the mean deposit slope S_{dep}, considered as representative of the recent geomorphic activity, has been measured by a linear fit between $Z_{X,Y}$ and X ($\forall$ Y) (visual selection, *e.g.*, Fig. 7.5a & b). Downstream of this section the outlet mean slope S_{out}, defined by a linear fit also, may be a driver of the outlet sediment flux.

Evidence of geomorphic cycles can be found in the three longitudinal profile types but they are more obvious in the Thickness evolution dT which is negative after armour breaking and erosion, and positive during deposition cycle (compare 7.5a & b).

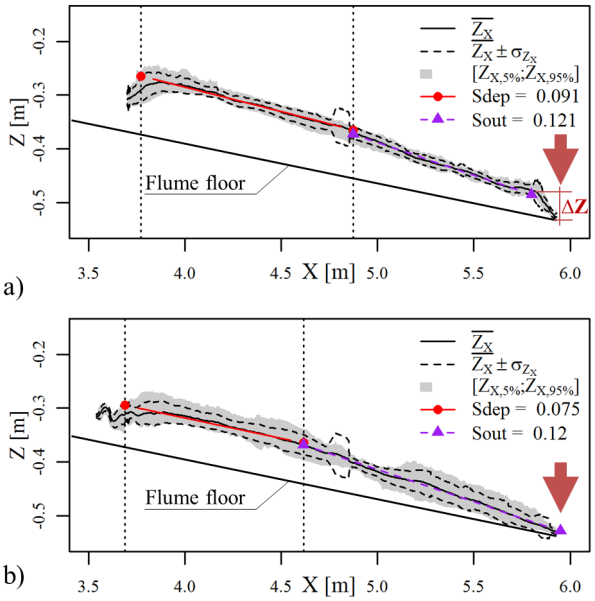

Figure 7.6 – Longitudinal for similar supply condition: a) with a slit dam at the outlet, and b) without slit dam at the outlet: quite similar deposition slopes but elevation of the downstream fulcrum at a thickness δZ related to the hydraulic control of the deposit front.

C. Fans VS deltas

From a mere longitudinal profile perspective, the process look like general aggradation of a reach submitted to an intense increase in sediment load. However, the deposit shape was definitively 3D. From, this point of view, the deposition in the basin has a strong similarity with fans creation: spreading of sediment in a laterally unconfined environment.

Conversely, the presence of the small flooded area near the slit dam generates a hydraulic trapping of the deposit front in the slit vicinity. Sediment entering this high water depth area builds a steep front with an avalanche process. Consequently, the deposition shape more looks like a delta with a submerged steep slope and atop, a milder slope. If the delta front reaches the slit dam, sediments are eventually transferred downstream and the sediment continuity is partially re-established (Zollinger, 1983).

The difference created by the hydraulic trapping is obvious on the longitudinal profile (Fig. 7.6). The additional deposition thickness at the outlet (ΔZ) elevates the fulcrum of the bulk longitudinal profile. This similar, though more elevated, deposit envelops, results in a larger trapping effect, proportional to ΔZ and to the basin surface. The bulk deposition slope upstream of the fulcrum is quite similar between experiments with similar supply condition (*e.g.*, Fig. 7.6).

In essence, the sediment deposition process in the model combines a forward dynamics of aggradation/fan creation, with an eventual backward dynamics of delta fulcrum changes when the basin outlet is equipped with a slit dam (Piton and Recking, 2016a). Both effects are most of the time coupled and the fan dynamics is basically adjusted to the downstream delta-boundary condition.

During the hydrograph recession, the delta tends to disappear. Namely, the formerly submerged steep slopes progressively emerge and are rapidly recruited by the flows reaching the slit and wandering upstream, letting few lateral perched terraces on the basin sides. The massive delta deposition occurring during the hydrograph rising is therefore considerably self-cleaned after the flood peak (Zollinger, 1983; Piton and Recking, 2016a).

7.3.2. Deposition slope analysis

The deposition and outlet slopes are analysed further in details in the following section. They are analysed jointly, S_{dep} being representative of the upstream part of a basin with a more diverse fluctuation than S_{out}, where the effect of lateral confinement relaxation has ever been buffered.

A. Influence of the grain size and solid concentration

Consistently with the theory, both slopes S_{dep} and S_{out} increase with the grain size (Fig. 7.7a & b) and inlet solid concentration (Fig. 7.7c). The fluctuation range however makes the measurement over-lapping between concentration and grain sizes. Consequently, a unique measurement of the deposition slope seems insufficient for computing the concentration by sediment transport law inversion. The inlet deposition S_{dep} fluctuates on a larger range than the downstream slope S_{out}.

B. Influence of the deposit roughness and grain size sorting

Very efficient grain size sorting has systematically been observed. The flow slope tend to adjust depending on the solid transport efficiency, which itself depends on the channel roughness (Yu et al., 2012; Recking, 2014). Slope should increase when the grain size increase. Parker et al. (1998) postulate that fan creation may settle at nearly constant dimensionless shear stress, close to the critical shear stress: higher shear stress would transport downstream the sediment while lower shear stress would make sediment settles immediately, increasing the slope:

$$\tau^* = \frac{Sd}{(s-1)D_{84}} \approx \tau^*_{cr} \tag{7.4}$$

with the dimensionless Shield stress τ^*, the slope S (m/m), the water depth d, the sediment density s (-) and the critical Shields stress for incipient motion τ^*_{cr}. Many values were proposed for τ^*_{cr} (Shields (1936) proposed 0.06, while Meyer-Peter and Müller (1948) proposed 0.047). Recent researches suggest that this parameter change with the slope (Mueller et al., 2005; Lamb et al., 2008; Recking, 2009). Recking et al. (2008b), used a dataset extending to slope up to 9% and proposed the following equation:

$$\tau^*_{cr} = 0.15 \times S^{0.275} \tag{7.5}$$

Computing the Shields stress on the deposit needs to estimate both the grain sizes and the flow depth. From our experimental data, the grain sizes of the deposit have been estimated using the deposit roughness and a calibrated relation between roughness standard deviation and grain size ($D_{84,eq.} \approx 7\sigma_{Ks}$, based on 93 Wolman (1954) surface counts, see Chap. 6). Computing the water depth is more complicated. As first approximation, Recking et al. (2016) proposed an equation to estimate the water depth:

$$d = 0.015 D_{84} \frac{q^{*2p}}{p^{2.5}} \tag{7.6}$$

where $q^* = q/\sqrt{gSD_{84}^3}$ with $p = 0.24$ if $q^* < 100$ and $p = 0.31$ otherwise, $q = Q/W$ is the water unit discharge (m^3/s.m) and g is the gravitational acceleration (m/s^2). One can introduce Equation 7.6 in the Shields stress definition (Eq. 7.4) using Equation 7.5 to estimate τ^*_{cr}:

$$\tau^*_{cr} = \frac{S \times 0.015 D_{84} q^{*2p}}{(s-1)D_{84} \times p^{2.5}} = 0.15 \times S^{0.275} \tag{7.7}$$

The equation may be rearranged to estimate the deposition slope at the critical shear stress for a given grain size and specific discharge, in our case with s=2.65, and $p = 0.24$ since $q^* < 100$ in our conditions:

$$S = 0.64 \frac{D_{84}^{1.48}}{(Q/W)^{0.99}} \cong 0.64 \frac{D_{84}^{3/2}}{Q/W} \tag{7.8}$$

This approach needs a definition of the driving channel morphology to define W. We pos-

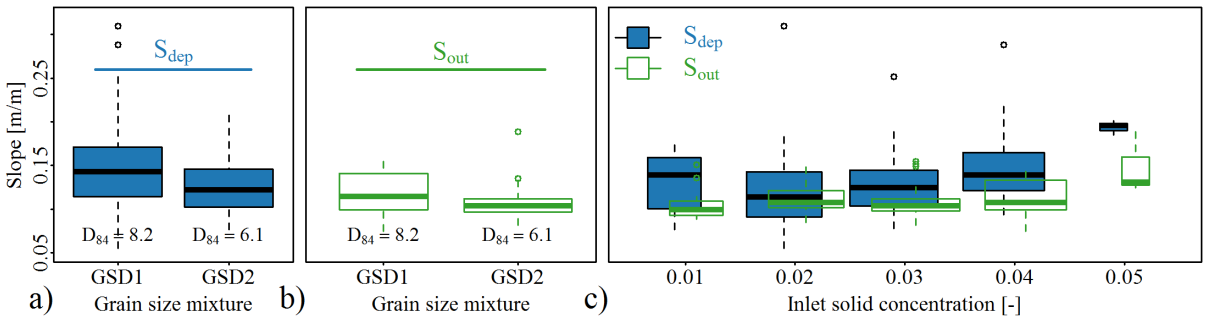

Figure 7.7 – Statistical distribution of upstream deposition and outlet deposition slopes: a) S_{dep} VS sediment mixture, b) S_{out} VS sediment mixture and c) S_{dep} and S_{out} VS solid transport concentration. S_{dep} is generally steeper than S_{out} and experiences fluctuations on a larger range. Consistent correlation with steeper, though quite variable, slopes with coarser and more concentrated supply (experiments with C=0.01 have only been carried on with the coarser GSD1, measurement are thus generally steeper than C=0.02, an artefact of the grain size influence)

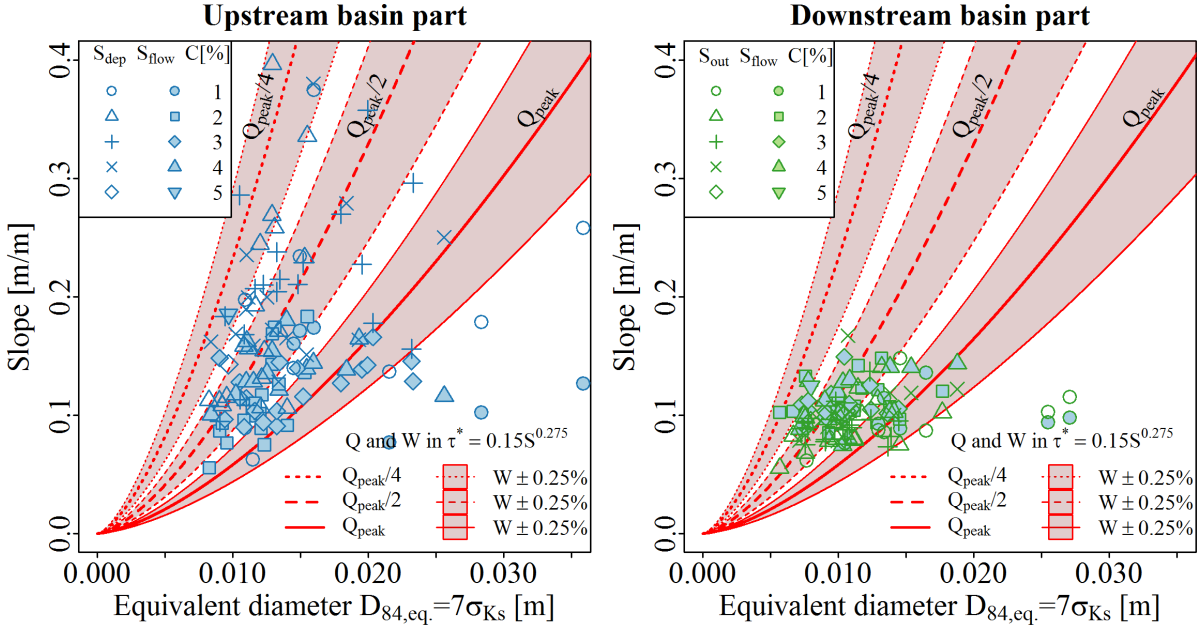

Figure 7.8 – Slope VS equivalent grain size deduced from channel roughness and comparison with a critical Shield stress hypothesis (Eq. 7.8): a) S_{dep} and S_{flow} in the upstream active section, and b) S_{out} and S_{flow} in the downstream, less active section

tulate here, that the entrance of the deposit, where the processes are the more active, is connected with the upstream channel, and that the morphodynamics width can be approximated by this upstream channel width (whose width has been selected to figure a somewhat natural width, without deposit, nor excessively energetic flows). This is consistent with our observations: the total width of the active channels was seldom narrower than ≈0.2 m and alternatively wider than ≈0.3 even further in the basin. This analysis should be pushed further using image analysis of the experiments. In the following, the condition $W = 0.25cm \pm 25\%$ is used.

Q varies between Q_{peak} and 0 during the experiment. The slope computation, using Eq. 7.8, has been performed for three discharge values: Q_{peak}, $Q_{peak}/2$ and $Q_{peak}/4$ to highlight the eventual effect of the varying hydraulic forcing (Fig. 7.8).

The slope data plotted in Figure 7.8 are mean values for the upstream and downstream sections S_{dep} and S_{out}, computed using the linear fits of the bulk elevation profiles (*e.g.*, Fig. 7.5 & Fig. 7.6). S_{flow} and $D_{84,eq.}$ were extracted from photogrammetry-LSPIV analysis (Chap. 6), on the same upstream and downstream areas.

Mean slope measurements in the upstream, very active part extend on a wider range ($S_{dep} \approx 0.1-0.4$) than in the downstream, less active part ($S_{dep} \approx 0.08-0.15$). Interestingly, their values seem consistent with the simple critical Shield stress hypothesis (red curves, Eq. 7.8). The variability in the deposition slope for a given roughness being consistent with the variable hydraulic forcing (*i.e.*, water discharge – 3 different curves). Indeed, more details analysis of the slope variations demonstrate trend of steep deposition at the beginning and at the end of the experiments, *i.e.*, for low discharge; and milder deposition slope at the peak discharge (not shown here, see details in Mejean, 2015). The difference between deposit and flow slopes is visible in the upstream basin part where channels are more regularly braided

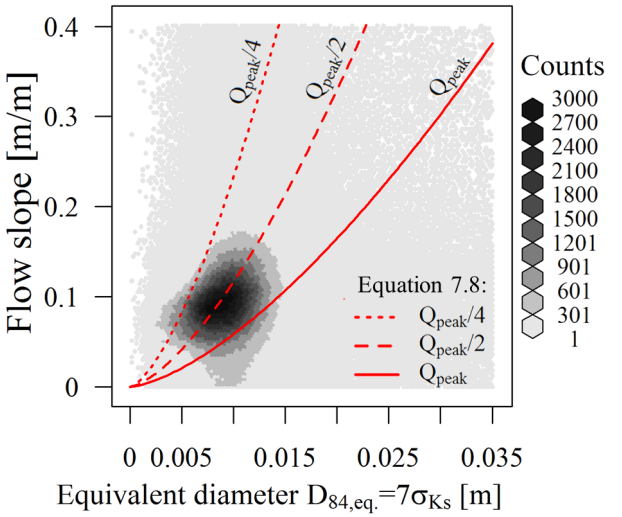

Figure 7.9 – Slope S_{flow} VS equivalent grain size deduced from channel roughness and comparison with a critical Shield stress hypothesis (Eq. 7.8) for all flow reconstruction data: widespread conditions with a significant concentration of measurements within the flow range described by the critical Shield hypothesis

and bias compare to the basin axis (compare S_{dep} and S_{flow} in Fig. 7.8a). This difference seems to disappear in the downstream basin part where the flows are more usually parallel to the basin axis (Fig. 7.8b).

These mean values are completed in Figure 7.9 by a comparison between the measured local slopes (interpolation $5mm \times 5mm$-grid on the flooded area of all experiments, *i.e.*, ≈1.7M cumulated data on the complete dataset) and the computed slope (Eq. 7.8), against the bed roughness. There is a clear concentration of data within the conditions described by the critical Shields hypothesis for the considered range of hydraulic forcing.

7.3.3. Flow features

The above analyses are mere topographical extractions that consider the LSPIV measurements only by the flow directions (flow slope and roughness σ_{Ks} being extracted along the flow direction); but that certainly not consider the flow velocity magnitudes. In a second step, we tried to

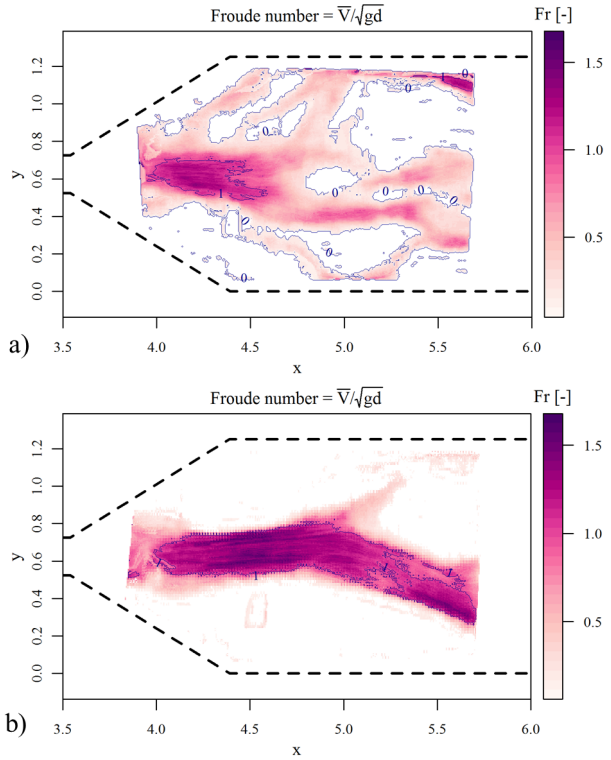

Figure 7.10 – Spatial repartition of the reconstructed Froude number in a) a braided bed with mostly subcritical flows and b) a channelized bed with mostly supercritical flows

qualify the flow features on the deposit depending on its geomorphology and slope.

A. Froude VS Geomorphology

Braided patterns were generally steeper but more paved than the armour breaking-channelized flows. Froude number was computed using the simplified equation (see Chanson, 1999, for a discussion on the Froude number estimation):

$$Fr = \frac{V}{\sqrt{gd}} \tag{7.9}$$

with V, the depth averaged velocity and d the reconstructed water depth (using the Ferguson (2007) law and the local values of slope, roughness and V; see Chap. 6 for the complete measurement and computation procedure). The flows illustrated in Figure 7.10 exemplify typical flow conditions with multichannel and channelized flows. The braided patterns were generally steeper but their rougher beds induced lower, subcritical flow conditions (Fig. 7.10a). On the contrary, transient incisions and massive sediment export generally occurred under supercritical flows on smoother beds (Fig. 7.10b). Secondary flows paths, on the sides of the main channels usually occurred in subcritical conditions due to their shallowness.

B. Froude VS Slope

The flow slope, Froude and Shield numbers of the reconstructed flows were extracted. Froude numbers are plotted against flow slope in Figure 7.11. Most data are in the range $0 < S_{flow} < 0.2$. Froude number seems to increase with slope, if the latter is milder than ≈ 0.1. On the contrary a superior envelop, inversely correlated with the slope, seems to appear for $S \gtrsim 0.1$: it is the consequence of increasing roughness and flow spreading with increasing slope, a feedback mechanism of geomorphology on the hydraulics.

Various critical Shields values were used to evaluate the changing Froude number with transport stage (τ^*/τ^*_{cr}). Indeed, most our flow data correspond to shallow flows spread over terraces experiencing low τ^*/τ^*_{cr} values, and are subcritical. On the contrary, flows experiencing high transport stage were systematically observed with a higher Froude number when filtering the data where $\tau^*/\tau^*_{cr} > 1$, the range being obviously τ^*_{cr}-dependent (see later). Since the critical Shields parameter is computed for D_{84}, there is still some possible, though less intense, sediment transport and morphological adjustments for $\tau^*/\tau^*_{cr}<1$ (Bacchi et al., 2014). There is consequently a continuous transition rather than a clear threshold between morphologically active and inactive flows, whose Froude consistently tend to decrease.

The Froude numbers for the complete dataset, as well as for flows experiencing high transport stage for diverse τ^*_{cr} definition are illustrated in Figure 7.12. The flows are generally subcritical but high transport stage flows definitively have higher Froude numbers. Since Froude, Shields and slope are correlated (Lenzi, 2001), this result

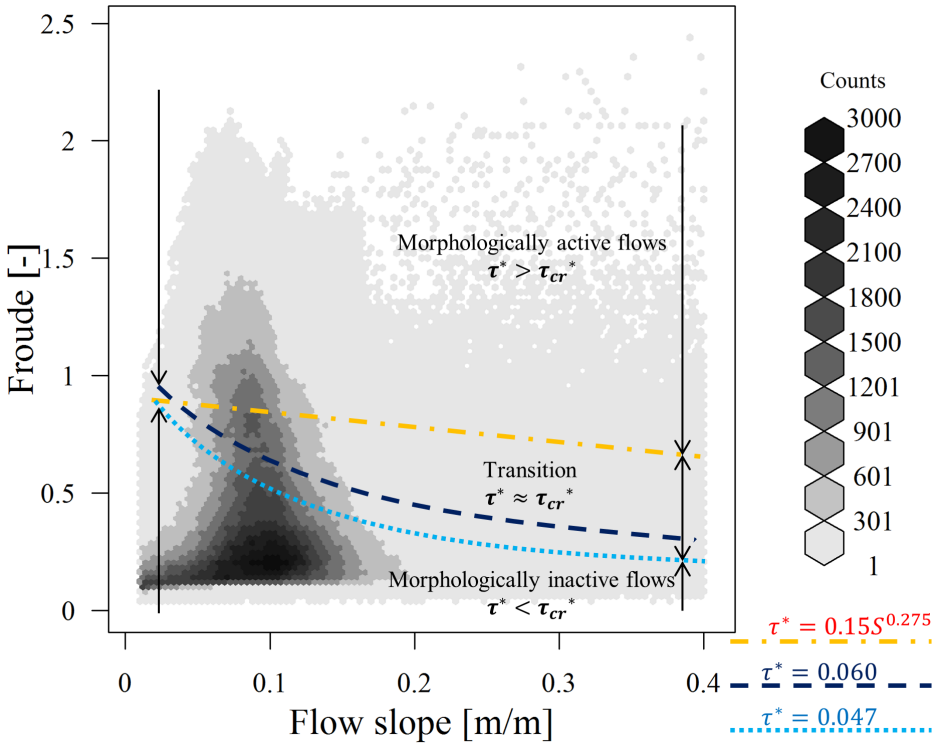

Figure 7.11 – Froude number VS flow slope and indicative limits of transport stage (τ^*/τ_{cr}^*), based on complementary filtering computations: most flows are subcritical, though the morphologically active flows tend to have Froude number approaching the critical value of 1. An superior envelop inversely correlated with the slope seems to appear: it is the print of increasing roughness and flow spreading with increasing slope, a feedback of geomorphology on hydraulics

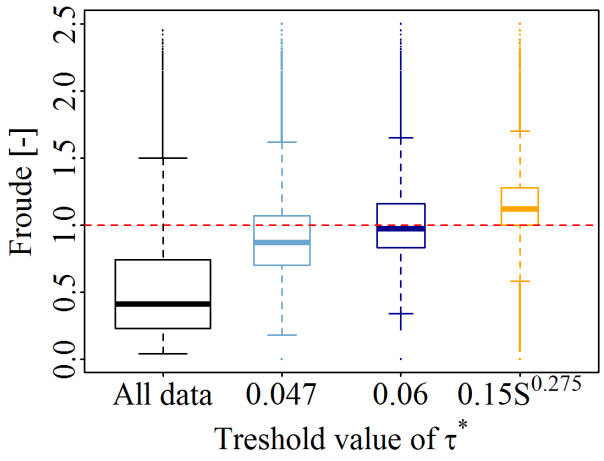

Figure 7.12 – Froude number statistics of the complete data set ($\approx 1.7M$ *data*) and filtered with varied threshold value of Shields number highlighting that morphologically active flows approach a critical Froude number

could be expected. More interestingly, the highest Froude values seldom overpass $\approx 1.5-2$ and there is a clear concentration around $Fr \approx 1$, *i.e.*, critical flows. The flow energy being minimal for critical flows (Grant, 1997), it seems that, the system adapts its channel morphology to approach this optimum, providing that the flows have a sufficient transport capacity to adjust it the bed morphology.

7.3.4. Sediment transport

The outlet sediment flux encompasses all sediment transport processes occurring in the basin and may change depending on the type of structure (slit dam or ground sill).

A. Outlet structure effect

In all experiments armour breakings produced intense sediment pulses inside the trap, but different exports were measured at the outlet, depending on the basin configuration (with and without slit dam). Without outlet structure constraining the transport dynamics (ground sill configurations, Fig. 6.3b &c), peak solid discharge could propagate at the outlet (Fig. 7.13a). Conversely, the hydraulic trapping induced by the slit dam (Fig. 6.3a) tended to buffer these pulses (Figure 7.13b), confirming the theoretical capacity of hydraulic control structure to dose instantaneous high peak of the upstream sediment transport (Armanini et al., 1991; Hübl et al., 2005; D'Agostino, 2013b; Piton and Recking, 2016a).

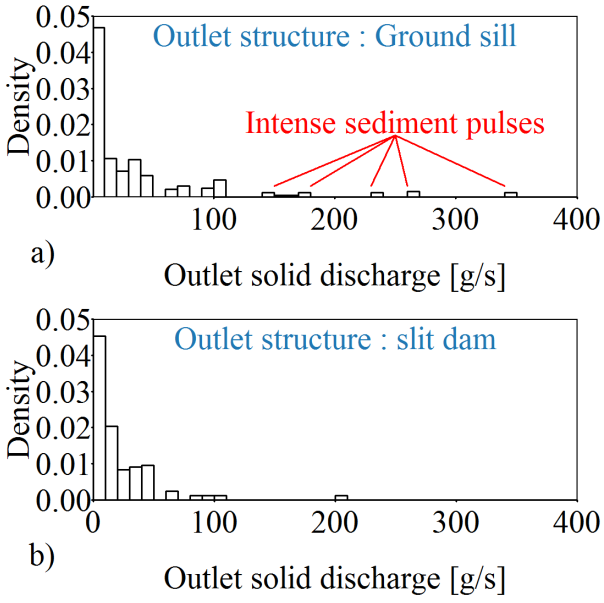

Figure 7.13 – Probability density function of outlet sediment transport of the 8 GSD1-experiments, a) 4 experiments with a mere ground sill at the outlet experiencing erratic intense sediment pulses, and b) similar 4 experiments with a slit dam at the outlet: structure inducing hydraulic trapping and dosing the upstream basin sediment transport

B. Hydrograph effects

In absence of hydraulic control or mechanical blockages, the outlet sediment discharge is correlated with the water discharge, with a maximum export nearly coinciding with the peak discharge (Fig. 7.14a). A slight hysteresis could however be observed with peak solid discharge usually occurring a bit later than the water discharge. This hysteresis can be explained by the terrace construction and accumulation necessary to create a continuous active channel.

Conversely, the dynamics changed in the slit dam configuration. The slit dam hydraulic trapping was maximal at the flood peak, increasing the trap storage (Fig. 7.6). Subsequently, self-cleaning produced a peak sediment export during the hydrograph recession (Fig. 7.14b). It was related to the efficient erosion of the formerly submerged delta with decreasing water stage (and consequent upstream terraces recruitment by chan-

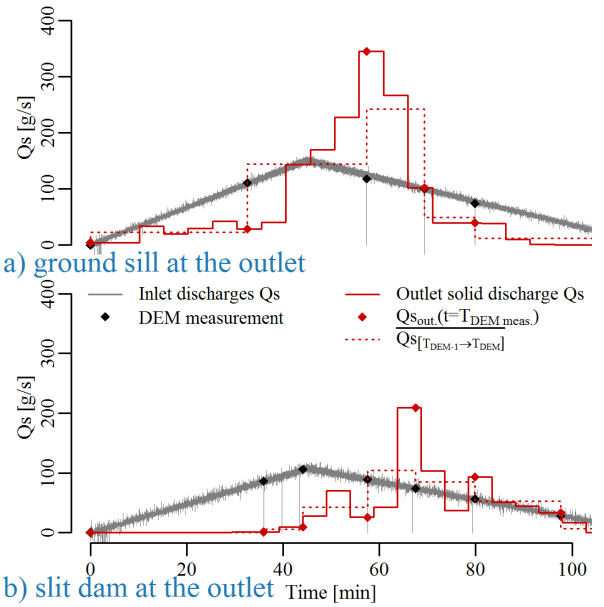

Figure 7.14 – Inlet and outlet solid discharge of similar supply with a) a simple bed sill at the outlet: after some deposit, a strong sediment release occurs near the flood peak and decreases during the end of the recession and b) a slit dam at the outlet: sediment transfer occurs mainly during the hydrograph recession (self-cleaning)

nel wandering). Nevertheless, the slit dam tended to trap more sediment than the ground sill, both at the flood peak and for the overall experiments.

7.4. Discussion

7.4.1. Evidences of scale invariance

The small scale models experiments presented in this work were built with respect to the Froude similitude, with a quite low geometrical scale reduction ($\lambda \approx 25$). However, several recent works studying the geomorphic construction of much larger landscape formations (*e.g.*, alluvial fans, fluvial delta) also show impressive similarities with our observations. Deposition and erosion dynamics are thus likely partially scale invariant justifying the interest of small scale model (Paola et al., 2009).

A. Similarity with fans creation

Parker et al. (1998) proposed a strategy for hydraulic computation of fan formation. They yet distinguished the dual channelized and sheet flow morphologies. They described that sheet flows were prone to deposition at the fan apex, as has been observed during our inlet accumulation phases. Conversely, the transport capacity of channelized flows was higher and resulted in better transfers toward the fan distal part in their analysis, consistently with our observations too. Actually, these flow patterns co-exist and occur in cycles that are autogenic, *i.e.*, self-induced, by systems experiencing total deposition (Muto and Steel, 2004; Van Dijk et al., 2009; 2012; Reitz and Jerolmack, 2012). Reitz and Jerolmack (2012) provide a particularly clear conceptual description of the coupling mechanism between fan-channel morphodynamics and lobe formation at the fan toe, which necessarily results in cycles of braided / channelized flows. Consistently with their theory, we observed that these cycles nearly totally disappear when the sediment continuity is re-established at the outlet of the trap. Higher geomorphic instability seems thus intrinsically related to total sediment deposition.

In our experiments, bed channelization was systematically associated with armour breaking, leading to very rapid bed erosion, similarly to what was described in in narrow flumes with laterally confined flows (Kuhnle and Southard, 1988; Recking et al., 2009; Bacchi et al., 2014). It is interesting to denote that geomorphic cycles on fan formation experiments have been observed even over uniform grain beds (*e.g.*, Muto and Steel, 2004; Van Dijk et al., 2009; 2012). We suppose that autogenic geomorphic cycles are exacerbated by the grain size sorting effects: i) enhancing transport capacity of channelized flows due to fine sub-surface material releases; and ii) increasing the stability of sheet and braided flows due to stronger armouring by kinetic sieving.

B. Similarity with delta dynamics

Depositions occurring in a totally flooded basin have slightly different dynamics than our experiments because mouth bars form directly at the channel outlets. Conversely flow spreading and lobe creation can expend further in slightly inclined alluvial plains (Van Dijk et al., 2012), the difference lying in the channel downstream total accumulation (delta and mouth bar formation) or partial export further (lobe formation). Fan dynamics are definitively driven by their toe deposition or erosion trends (Harvey, 2012), which shift toward delta-type dynamics in flooded area, *e.g.*, in basins equipped with slit dams.

Delta shape deposit are regularly reported in open check dams (Dodge, 1948; Armanini and Larcher, 2001; Jordan et al., 2003). The delta fulcrum, *i.e.*, inflexion point between the steep front slope and the milder top slope, classically settle near the flooded area free surface in laterally unconfined configuration (Jordan et al., 2003), and slightly below in laterally confined basin (Armanini and Larcher, 2001).

Similar pattern are reported, at an intermediate scale, for gravel deposition in dam reservoir, that classically develop delta-type dynamics (Morris et al., 2008). The remobilization and transfer in the reservoir during reservoir drawdown and flushing operations could be better understood by combining sediment trap observations with the broader literature on delta geomorphic adjustments.

Paola et al. (2009) reviewed experimental work describing delta formation. Works addressing the effect of varying sea level on delta adjustments are of particular interest for their similarities with open check dam filling and self-cleaning. Computation strategies that may be extended to open check dams have been proposed, for instance by Hotchkiss and Parker (1991) and Lorenzo-Trueba et al. (2013). Muto and Steel (2004) have described delta front shifting during sea level recession, with the upstream formerly deposited volumes being eroded and recruited by the wandering active channel, a process very similar to what we observed in our experiments during self-cleaning events. In case of massive sediment supply, Petter and Muto (2008) described possible disconnection occurring between upstream fan deposition and downstream delta dynamics, leading to steep deposition at the inlet and nearly clear water flow in the downstream part of the basin; this was also observed in our experiment with highest sediment concentration (Mejean, 2015).

7.4.2. Feedback between flow features and deposit morphology

Grant (1997) speculated that supercritical flows should be seldom encountered in the field because channel morphology tends to rapidly adjust under excessively energetic flows. This assertion has been consistently confirmed by hydraulics field measurement demonstrating generally subcritical or near critical flow conditions in mountain streams (Lenzi, 2001; Zimmermann and Church, 2001; Comiti et al., 2007; Comiti et al., 2009; Nitsche et al., 2012; Recking et al., 2012a). There is thus a non-intuitive inverse correlation between Froude number and slope. This correlation result from adjustments of the channel roughness that tend to considerably increase in the mountain stream steepest sections. This phenomenon has been thoroughly described by Schneider et al. (2015) in a stream with a one-order in magnitude increase in slope and Froude number lower in the ≈40%-steep section, compare to the milder, 3-4%-steep upstream section. Continuous field LSPIV recent measurement on a steep stream confirmed globally subcritical or near critical flows (Ran et al., 2016). These observations however generally concerned inactive or weakly morphologically active flows.

In our observation, flows were consistently naturally subcritical most of the time. The morphologically active flows shift toward a critical Froude number or only slightly higher (Fr<1.5-2 most of the time). It is consistent with a system adjusting its geometry toward a minimum of energy. The critical flow hypothesis of Grant (1997) seems to be a correct first approximation when describing massive bedload depositions that may self-adjust their channel widths.

On the contrary, in laterally confined configurations (bedrock channels or bank protection), this width adjustment cannot occur, resulting in possible much more supercritical flows. Le Boursicaud et al. (2016) for instance observed Froude number of about 2.6 (uncertainty range [2.0,3.8]) in a 6.3%-steep cut stone-protected channel during pulsatile bedload laden flows (discharge : 22 m^3/s, uncertainty range [11;33 m^3/s]), confirming the existence of quite supercritical flows in specific conditions.

7.5. Conclusions

The relative recent development of image analysis techniques make possible to study torrential flows, phenomena insufficiently known so far because fast, violent and dangerous. More particularly, the flow measurement and reconstruction method developed in Chapter 6 has been used to enrich our comprehension of massive bedload deposition.

A generic Froude scale model of a bedload deposition basin has been built. Its features were defined from a field survey of 31 structures located in diverse environments of the French Alps, and from literature data. Simplified supply conditions were used. The increasing sediment concentration resulted in increasing deposition intensities (steeper slopes). The deposition process was however far from being a continuous propagation of an aggradational profile: autogenic fluctuations emerged: deposition under sheet flows / braided pattern were periodically troubled by dramatic incision of the deposit in a singular-channel, with downstream sediment transport pulses. Such autogenic cycles are typical of depositional systems (alluvial fans, fluvial delta) and evidences of scale invariance are pointed out. Designers could therefore found complementary elements concerning the structure functioning in the literature dedicated to these larger geomorphological formations.

Our accurate photogrammetrical measurements combined with LS-PIV analysis allowed to measured the relatively high variation range of the deposition slope. Interestingly, the slope range seems to be correctly capture using a new equation (Eq. 7.8), whose development is based on the hypothesis that the depositional systems develop under nearly critical Shield stress (Parker et al., 1998) . Equation 7.8 encompasses (i) a slope-dependent critical Shields estimation, developed in experimental conditions with slope up to 9% (Recking et al., 2008b); (ii) a reformulation of the outstanding Ferguson (2007) friction law and, in our experiments, (iii) an estimation of the grain size deduced from the bed roughness (Chap. 6). Equation 7.8 deserved to be tried and tested on other datasets before to be used for structure design. We can only stress that it has the merit of (i) being based on the state of the art knowledge of the gravel threshold for motion (*i.e.*, positively slope-dependent), (ii) accounting for the importance of coarse elements (*i.e.*, use of D_{84} rather than D_{50}), and (iii) encompassing the friction law deviation from the Manning Strickler formulation typical of low submergence flows (*i.e.*, use of a reformulation of Ferguson, 2007).

In a second stage, reconstruction of flow spatial distributions highlighted that most flows were subcritical despite quite steep slopes. It once again confirms the trend of alluvial systems to adjust their roughness and channel size. More interestingly, when filtering the data that experience $\tau^*/\tau^*_{cr} > 1$, *i.e.*, when focusing on morphologically active flows, the Froude number approachs the critical value. These measurements seem to confirm the "*critical flow hypothesis*" of Grant (1997) who assumed that alluvial systems would adjust their morphology toward a minimum flow energy, and consequently, that high Froude number would not be stable in time.

Following these preliminary analysis, this dataset may be used to try and test, or to develop, more accurate models and numerical approaches of our out-of-equilibrium experiments. Ultimately, it would be possible to address numerical approaches of detailed velocity fields, geomorphic adjustments, sorting patterns and / or fluxes dynamics, with and without structures. Considering the challenge, the authors would be happy to launch collaborations on these subjects. Table 7.1 gathers a list of the available data. Analysis codes, written in the R language, are also available on demand.

Acknowledgments

This study was funded by Irstea, the INTEREG-ALCOTRA European RISBA project, and the ALPINE SPACE European SEDALP project. The authors would like to thank Hervé BELLOT, Firmin FONTAINE, Frédéric OUSSET, Christian EYMOND GRIS, Julie PELLAN and Coraline BEL for assistance in the experimental setup development.

Notation

The following symbols are used in this paper:

A_i = trap basin i^{th} subsurface area (m^2);

C = sediment concentration = Q_S/Q (-);

Co^* = dimensionless trap basin compactness (Eq. 7.2)(-);

D = sediment diameter (m);

$D_{84,eq.}$ = equivalent sediment diameter deduced from correlation with the bed roughness $7\sigma_{Ks}$ (m);

d = water depth (m);

Fr = Froude number = $V/\sqrt{gd}$ (-);

g = gravitational acceleration = 9.81 (m/s^2);

L^* = dimensionless trap basin aspect ratio (Eq. 7.1)(-);

L^*_{Gi} = trap basin i^{th} subsurface gravity center abscissa, taken from the basin inlet (m);

L_{Tot} = trap basin length, along the main flow direction (m);

K_S = local bed roughness = $Z_{X,Y} - \langle Z \rangle_{X \pm D_{MAX}/2, Y \pm D_{MAX}/2}$ (m);

p = dimensionless parameter of Eq. 4.6 (-);

Q = water discharge (m^3/s);

q = unit water discharge = Q/W ($m^3/s.m$);

q^* = dimensionless unit water discharge (Eq. 7.6) (-);

Q_S = sediment discharge (g/s);

S_{dep} = bed slope measured along the flume direction X, in the upstream part of the trap (m/m);

S_{flow} = bed slope measured along the flow direction, anywhere in flooded areas (m/m);

S_{flume} = Flume slope = 10% (m/m);

S_{out} = bed slope measured along the flume direction X, in the downtream part of the trap (m/m);

Sk^* = dimensionless trap basin skewness (Eq. 7.3)(-);

s = sediment density = 2.65 (-);

T = deposit thickness, de-trended bed elevation, *i.e.*, = $Z_{X,Y} - S_{flume} \times X$ (m);

u^* = shear velocity = $\sqrt{gdS}$ (m/s);

V *or* $\bar{V}$ = mean velocity integrated over the flow depth(m/s);

W = flow width (m);

W_{Tot} = trap basin width, transversally to the main flow direction (m);

X, Y = point spatial coordinate (m);

Z = bed elevation (m);

σ_{K_S} = standard deviation of K_S, computed along the flow direction (m);

ΔZ = delta front thicknessgrid size in the X and Y direction, respectively (m);

λ = scale reduction of the model (-);

τ^* = Shields stress (Eq. 7.4);

τ^*_{cr} = Critical Shields stress for incipient motion (Eq. 7.8);

= **Subscripts:**

$\bar{...}$ = mean value of ... ;

$...MAX$ = maximum value of ... ;

$...X,Y$ = value of ... at the coordinate X, Y;

$...X\%$ = Quantile of ... with probability $X\%$;

7.6. Available dataset

For each experiment the available data are the following (see Table 7.1 for the number of measurement per run for the varied flume width, grain size distribution and solid concentration):

- Inlet sediment and water discharge (recorded at a 10 Hz frequency),
- Outlet sediment discharge weighted each 1 to 5 minutes,
- Global flume view (*e.g.*, Fig. 6.3) taken with a CANON 450D (4272x2848 pixels), taken every 5 seconds during all experiments, allowing potential orthorectification and semi-automated flow morphology analysis,
- Variable number of flow depth (actually of the free surface elevation and of the bed elevation, measured with the point gauge with a relatively high uncertainty),
- Wolman count at each flow depth measurement in the direct vicinity of the measurement point,
- Variable number of fast-cam acquisition (more than 50 images each time), of a large part of the flume (1024x1136 pixels in grey scale),
- From which as been computed the surface flow velocity using Fudaa-LSPIV (≈20,000 calculation points on irregular grids),
- Variable number of complete picture coverage of the drained bed (taken immediately after the fast-cam acquisitions) with 2 CANON 100D (5184x3456 pixels),
- From which are computed digital elevation models and complete orthorectifed view of the flume using Agisoft Photoscan (photogrametry software).
- Interpolation of flow surface velocity and extraction of the flow slope and roughness using the procedure presented in Chap. 6 for all runs, on a $5mm \times 5mm$ regular grid.
- Complete flow depth reconstruction for all runs on the interpolation grid, even for the first uncertain tests with a slit dam and without charcoal seeding. In this case, the flow directions are quite reliable but much less the velocity magnitudes (14 measurement in the 75 acquisition dataset).
- Complete flow Froude, submersion, Shields reconstruction on the interpolated grid.

Both the LS-PIV and photogrammetry can be re-run for different accuracies or parameter values. All of the data can eventually be shared for collaboration in data re-analysis. Details in the calibration can also be directly ask to the first author[1].

[1]author personal email address: guillaume.piton[at]gmail.com

Table 7.1 – List of the available data

Code	Slit	GSD	W	Q	Qs	Tpeak	C=Qs/Q	N_{DEM}	N_{PIV}	$N_{water\ depth}$
Units	dam	code	[m]	[l/s]	[g/s]	[min]	[%]			
DaG1/C0. 1	Yes	1	1.25	2.75	73	90	1	6	3*	8*
DaG1/C0.2	-	-	-	-	146	45	2	8	6*	12*
DaG1/C0.3	-	-	-	-	219	30	3	4	2*	4*
DaG1/C0.4	-	-	-	-	292	22.5	4	5	3*	6*
nDG1/C0.1	No	-	-	-	73	90	1	7	5	10
nDG1/C0.2	-	-	-	-	146	45	2	6	4	8
nDG1/C0.3	-	-	-	-	219	30	3	4	2	4
nDG1/C0.4	-	-	-	-	292	22.5	4	5	3	6
nDG2/C0.2	-	2	-	-	146	45	2	6	2	4
nDG2/D0.2	-	-	-	-	-	-	-	6	5	10
nDG2/C0.3	-	-	-	2.69	214	30	3	4	2	4
nDG2/D0.3	-	-	-	-	-	-	-	16	14	19
nDG2/C0.4	-	-	-	2.02	-	-	4	4	2	4
nDG2/D0.4	-	-	-	-	-	-	-	9	7	11
nDG2/C0.5	-	-	-	1.62	-	-	5	4	1	2
nDG2/W2.3	-	-	0.62	2.69	-	-	3	10	7	7
nDG2/W2.4	-	-	-	2.02	-	-	4	9	7	7
Total	-	-	-	-	-	-	1-5	113	61+14*	97+30*

Note: W: basin width; Q: peak water discharge; Qs: peak solid discharge, Tpeak: duration before hydrograph peak, C: sediment concentration (assuming a sediment density of 2.65), N_{DEM}: number of DEM acquisition; N_{PIV}: number of LS-PIV acquisition; and $N_{water\ depth}$: number of reference points , *i.e.*, waterdepth measurement using the point gauge.
*The first LS-PIV measurements were done without crushed charcoal seeding; the velocity fields are thus questionable and were excluded from the dataset.

"The reward you get for digging holes is a bigger shovel."

T. Pratchett, *I Shall Wear Midnight*

Conclusions et Perspectives

All chapters of this manuscript being self-standing, they contain their own specific conclusions. This section gives thus a general perspective and reminds the essence of the thesis. Our work tries to link conceptual geomorphology perspectives with as much as possible quantitative, physically/empirically-based knowledge. This is, in addition, completed with several concisely reported cases exemplifying our explanations and conceptual descriptions.

In sum, check dams and open check dams are widely used structures in torrent hazard mitigation:

- Check dams are basically dedicated to stabilize geomorphic systems experiencing excessive erosion;
- Open check dams should trap transported solid materials that aggravate downstream flood hazards.

In general these assertions remain true. The situations are however highly divers and regularly more complicated in the details. Torrent control is thus prone to misunderstanding, possibly resulting in incorrectly designed structures and waste of public money, in the best cases.

8.1. Check dam complex duty

Check dams in Alpine streams have multiple possible effects that are far from being negligible. These effects are called functions in the risk analysis jargon. Several functions emerge from the complexity of mountain stream geomorphology, *i.e.*, form coupling and feedback loops involved in erosion and transfer processes (Keiler, 2011). Chapter 1 tried to clarify the varied expected check dam functions, and thus, implicitly details the various couplings existing in mountain stream environments:

- When armour breaking occurs, headward propagating erosion generally follows, recruiting additional material and destabilizing banks and vegetation (Zeng et al., 2009). The bed

stabilization function of check dams roughly consists in stopping this in-stream coupling between an incised point and its upstream reach (Heede, 1986). The structures also guide and constraint flows' directions, thus stabilizing the planar stream dimension, in addition to its vertical one (Deymier et al., 1995).

- Hillslope movements are partially driven by their bottom erosion, *i.e.*, by valley incision (Egholm et al., 2013). Inversing the natural incision process by elevating the valley floor with a check dam may consequently slow down the hillslope instability. Consolidation check dams take advantage of this hillslope-thalweg coupling to limit sediment production at the source.

- Mountain streams are generally paved by boulders self-organized in stable patterns (Church and Zimmermann, 2007). They are therefore generally excessively steep, though relatively stable (at least most of the time; see Chapter 4 for the possible geomorphic scenarios of bed stability / type of sediment supply and resulting transport capacities). The creation of alluvial reaches results from the conjunction between these high gradients and check dams built above the streambed level. Sediment and boulder deposit in these backfilled reaches, usually producing gentler slopes than the initial paved profile.

- These milder reaches are constituted by the actually transported material, building check dams thus results in sediment storage: a retention function. In the suitable locations, this retention capacity is eventually huge, up to several millions of cubic meters for a few giant structures (*e.g.*, Wang and Kondolf, 2014).

- Finally, by definition alluvial reaches have slope balanced with solid transport efficiency, water and sediment supply. Both supply and transport efficiency fluctuate in mountain streams (Recking et al., 2009; Jerolmack and Paola, 2010; Van De Wiel and Coulthard, 2010; Recking, 2014) resulting in successive sediment storages and releases (Fryirs, 2013). This phenomenon possibly induces a sediment transport regulation (Gras, 1857; Jaeggi, 1992) which has been studied in laboratory, in a "*reduced complexity model*" (Paola and Leeder, 2011), and is discussed in Chapter 5. This last function deserves complementary investigations since its importance in the sediment cascade is still unknown (see later).

Check dams thus control sediment transport by influencing the production (hillslope consolidation) and the in-stream recruitment (bed stabilization). By forcing alluvial reaches' creation, they eventually change the stream gradient and consequently the flows energy and transport capacity. A buffering effect may then emerge from the expression of sediment transport allogenic and autogenic fluctuations in an environment segmented by check dams. They also constitute mere sediment storage structures.

Stabilization remains the main function of check dams. We however thought important to stress that some theory existed, for quite a long time, about the other possible effects. It may explain the presence of some structure in surprising locations. It is now the role of engineers and researchers to judge on the relevance to maintain / adapt / abandon some of these structures depending on the eventual changes in the available techniques, catchment activity and related elements at risk, not a straightforward mission.

8.2. Open check dam complex duty

8.2.1. Generalities

Open check dam are expected to trap solid materials that aggravate flood hazards (sediment and woody debris). Our observation during field visits let us think; they more usually trap nearly all materials transported by the streams. This situation is not satisfying from both a local and a broader perspective because (Carladous et al., 2016c):

At the local scale (from the catchment headwaters to the open check dams):

- The material supplied by non-extreme floods partially fill the structures, diminishing their capacity to handle the hazardous events;
- Consequently, structure managers spend time and money to dredge these materials that did not threaten the downstream elements at risk;

At a broader scale (downstream of the open check dams):

- Fan channel bank protection and embankment may be naturally necessary to prevent fan flooding and avulsion (planar stabilization). Concerning the vertical dimension, examples of dramatic fan channel degradation downstream of sediment traps are numerous (*e.g.*, Chap. 2). Disrupting the catchment sediment supply results in recruitment of sediment further downstream on the fans. Fan bed sills, artificial channels, and additional structures are thus usually necessary to counterbalance effects induced by upstream works (*e.g.*, on the Roize - Chap. 4). One can think that some optimizations are possible and desirable to limit unwanted secondary effects (Heede, 1986), although they will not be straightforward to define.
- Despite being an important aggravating source of hazard on fans, sediment plays a key role in the fluvial system equilibriums (*e.g.*, geomorphology - Rinaldi et al., 2011 or biota - Wohl, 2013b). Incision trends in lowland fluvial systems had been detected in the decades following widespread reforestation and check dam building (Rinaldi and Simon, 1998; Rinaldi, 2003), though generally after a lag-time (Liébault et al., 2008). It is worth to remind that this trend has not been reported in all rivers with noticeable torrent control works in their headwaters, (*e.g.*, Ziliani and Surian, 2012). It must also be stressed that incisions related to torrent controls in rivers are generally much less intense than their equivalents related to gravel mining and dam reservoir building (Rinaldi and Simon, 1998; Liébault and Piégay, 2002; Rinaldi, 2003; Liébault et al., 2008; Ziliani and Surian, 2012).

Nonetheless, the relatively recent and better understanding of the importance of the sediment cascade and continuity results in new watershed management strategies, generally concentrating on the more active sediment sources (Liébault et al., 2010b; Rinaldi et al., 2011; Phillips et al., 2013). Torrent control works were specifically implemented in active sediment sources. These streams may therefore participate to the necessary background sediment supply if open check dams would be optimized, *i.e.*, would act mainly on high magnitude supplies.

It can even lead to study check dam removal and erosion source reactivation in some basins with severe problems of sediment starvation (Pont et al., 2009; Liébault et al., 2010b). The increasing

awareness of the continuum of river systems make necessary to extend the perspective from local risk mitigation to larger watershed management (Carladous et al., 2016c). Open check dams optimizations are thus expected to decreases the maintenance costs at the local scale (fewer dredging), while providing beneficial background sediment supply to downstream fluvial systems (Rinaldi et al., 2011; Comiti, 2012).

A precise comprehension of the functioning of a system is required in order to optimize it. Considerable works have been done to improve our comprehension of: i) sediment transport in mountain streams and, ii) water, sediment and woody debris transfer in open check dams.

8.2.2. New elements from this thesis work

A. Sediment supply

The existing structures should be used to mitigate torrential floods, but also to gain knowledge about floods. Chapter 4 exemplifies this approach. It focuses on bedload transport in steep slope streams, proposes a method taking advantage of the presence of sediment trapping structures to enhance bedload transport computation, and apply it to a few case-studies. It is a new possible way to compute boundary conditions upstream of torrent control works.

B. Design method review

A large literature compilation has been undertaken at the beginning of this work. We searched during months a general review paper explaining how sediment and woody debris interact with open check dams. After one year reading outstanding works, all of them addressing parts of the question, we decided to write this unobtainable paper. The complexity of the questions and complementarity between considerations on sediment, on one hand, and woody debris, on the other hand, rapidly make us writing two companion papers (Piton and Recking, 2016a; 2016b).

Chapter 2 thus traces the available knowledge on hydraulics and sedimentation processes in open check dams. Chapter 3 addresses the same topic, but concerning woody debris. Since design criteria related to woody debris were less advanced and numerous than hydraulics and sedimentation criteria, we had enough room to give few elements on woody debris production in Chapter 3. The question of sediment production is better known, deserved more attention and was addressed in Chapter 4 for bedload. Complementary methods dedicated to debris flows may be found in the literature. Some works published in German, Japanese, Italian, Chinese, etc. have certainly been missed. But synthetizing the available literature in only two papers has ever been frustrating (we removed so many interesting details for the sake of conciseness).

In my opinion, three main messages may be extracted from this state-of-the-art:

- Woody debris must absolutely be taken into account in hazard assessment and structure design. They have the annoying habit to be weakly present during small floods (and are thus forgotten and neglected), but to considerably increase in number during extreme events, to jam at key hydraulic structures (bridge, open check dams) and globally to strongly aggravate flood hazards. Zollinger (1984b) yet stressed it thirty years ago, we must continue to pay greater attention to this greatly stochastic and complex problem.

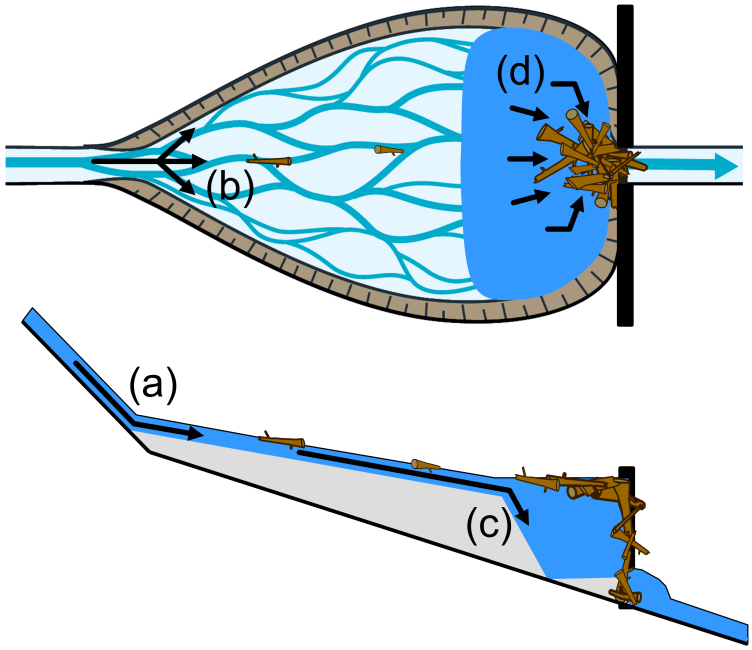

Figure 8.15 – Processes inducing material trapping: (a) slope decrease; (b) width increase; (c) delta-type hydraulic control; and (d) direct mechanical blockage

- Four processes results in deposition and trapping (Fig. 8.15). Each of them may gain in influence, or be negligible, in the highly varied cases encountered in the field. Once defined the objective of a structure, designers should make the most of each process to achieve the desirable function. Neglecting one of them may possibly result in unexpected and undesirable functioning (*e.g.*, woody debris clogging of hydraulically designed structures). The two deposition processes related to the basin shape (milder slope and wider width – Fig. 8.15a & b) are not sufficiently known. Conservative and empirical methods should thus still be used to design the lateral dikes (whose crest elevation is influenced by the deposition slope to prevent overtopping). On the contrary much more knowledge exists to design the open check dam considering hydraulic trapping and mechanical blockage (Fig. 8.15c & d).

- Mechanical blockage is a granular phenomenon: roughly the jamming of coarse elements in a narrow section (Relative Opening criteria). Conversely, the hydraulic trapping is a fluid mechanics phenomenon of deposition resulting from a shear stress collapse (the related criteria must take into account water stage – discharge equations). Regarding the literature, these two mechanisms are sometimes confused. Both approaches must be considered independently in studies of deposition / self-cleaning of open check dams.

In addition to these clarifications and some others, Chapters 2 and 3 contain sections highlighting the numerous remaining scientific gaps in open check dams and torrential hydraulics. The closure paper associated with Chapter 2 points out that the simple question of the deposition slope estimation is far from being clearly resolved, *i.e.*, the phenomena occurring during deposition in laterally unconstrained, mild slope reaches are insufficiently known. Laboratory works have therefore been carried on, while two sediment trap were equipped with monitoring cameras (see later).

C. Massive bedload deposition in open check dam basins

Several studies of massive bedload deposition in steep, wide basins were published about thirty years ago (Zollinger, 1983; 1984b; Ishikawa and Mizuyama, 1988; Mizuyama et al., 1988). These pioneering works ever contain thoughtful descriptions of the phenomena variability and complexity.

Since that time, regular publications brought new elements, while new measurement techniques appeared. Image analysis has been used for a long time in laboratory studies of mountain hydraulics: for photogrammetry acquisitions (Zollinger, 1983) and also to track transported material (Mizuyama, 1984).

We wanted to push further these works, and to compare laterally unconstrained flows with our knowledge on laterally-constrained ones (Recking et al., 2008a; 2008b; 2009; Recking, 2009; 2010; 2013a; Bacchi et al., 2014). Preliminary experiments rapidly demonstrated that intrusive measurement techniques were complicated to rigorously handle. Fast measurement techniques, mostly by image analysis, were thus installed and calibrated on the flume. We took advantage of the advent of affordable HD-cameras and user friendly photogrammetry and LSPIV software to develop a measurement and flow reconstruction procedure.

Chapter 6 describes this procedure in details to make possible its implementation by other laboratory teams. It could theoretically be used in the field, providing that one can measure the topography with marginal changes after the LSPIV measurement. It is thus not exactly applicable to a sediment trap filling (how to stop the flow?).

The method calibration additionally confirmed the relevance of the friction law developed by Ferguson (2007). It is a first step in the better description of these massive bedload deposits that were, so far, described using Chézy and Manning Strickler formulations (Armanini and Larcher, 2001; Busnelli et al., 2001; Campisano et al., 2014).

The result analysis is pushed further in Chapter 7. First of all, a geomorphic description of the sedimentation dynamics has been given. We stressed the similarities between open check dam filling and alluvial fan formation or fluvial delta progradation. Autogenic fluctuations and the general complexity of geomorphic processes again emerged, complicating our analysis. A simple deposition slope estimation criteria, based on a critical Shields stress hypothesis, has been proposed and seems able to capture the range of variation of the modelled events.

Finally, the reconstructed flows were analyzed, specifically their Froude numbers. Despite the quite steep slopes of deposition, most flows were apparently subcritical, although the most morphologically active flows seem to approach or slightly overpass the critical state (*i.e.*, Froude ≈ 1). The "*critical flow hypothesis*" developed by Grant (1997), asserting that steep alluvial systems would adjust their morphology toward a minimum flow energy thus seems, in first approximation, a reasonable description of flows during massive bedload deposition.

8.3. Perspectives

8.3.1. Proof from the field

Confrontations with field data are the ultimate validation. This work has mainly been based on laboratory approaches. Some concepts deserve to be tested / validated against field data:

A. Check dam series' monitoring

Observations of sediment storage fluctuations in check dam series exist, though, to my knowledge, not over long time period (Peteuil et al., 2008; Glassey, 2010; Astrade et al., 2011; Theule et al., 2012). Observing dynamics of bed recharge and sediment fluxes in the presence and absence of check dams would be of high interest, particularly in long lasting field monitoring, as well as, in paired-watershed experiments (see *e.g.*, Andréassian, 2004, for the effect of forest on hydrology, or Zeng et al., 2009, for general torrent control effects).

Some catchments have "*flume like configuration*", with negligible water and sediment input along a certain reach. Schneider et al. (2015) highlighted bed roughness self-adjustments along such a stream, where the slope drastically changes with marginal external input. With the same idea, it would be possible to install sediment transport and hydrology monitoring stations along an equivalent stream with a natural bed, and further downstream, a check dam series (3 stations: upstream of the natural section, downstream of the check dam series, and at the border between both sections). Such a monitoring facility would make possible to study the sediment transport dynamics for varying hydrological conditions; and possibly to highlight and quantify some regulation effect. Sediment transport occurring through relatively slow pulses, some bed recharge and transient storage are to be expected, this aspect should be monitored in addition to the fixed stations (*e.g.*, Fig. 8.16 for a short, steep check dam series or Theule et al., 2012; 2015). Small scale experiments with rigorously similar inputs may complete such a monitoring (see later).

If this sediment transport regulation is noticeable, even for quite large magnitude events, it should be taken into account in hazard studies and could modify the results of some structure efficiency assessments as presented in the discussion of chapter 1. Another lessons would be learned, if, on the contrary, check dam solid transport regulation only modify the low magnitude transport, while, as asserted by Jerolmack and Paola (2010), high magnitude inputs are weakly influenced. Such a conclusion would imply that a sort of threshold / nonlinear effect exists in sediment transfer though check dams series. In this case, it would not be relevant to extrapolate time series of cumulated sediment transport production toward extreme frequencies with a unique equation as done, for instance, by Peteuil (2010) and Peteuil et al. (2012). In such a case, the transition from regulated toward unregulated supply should be studied, possibly based on field and laboratory analysis as we have done for sediment transport over fixed or breaking amour (Chap. 4).

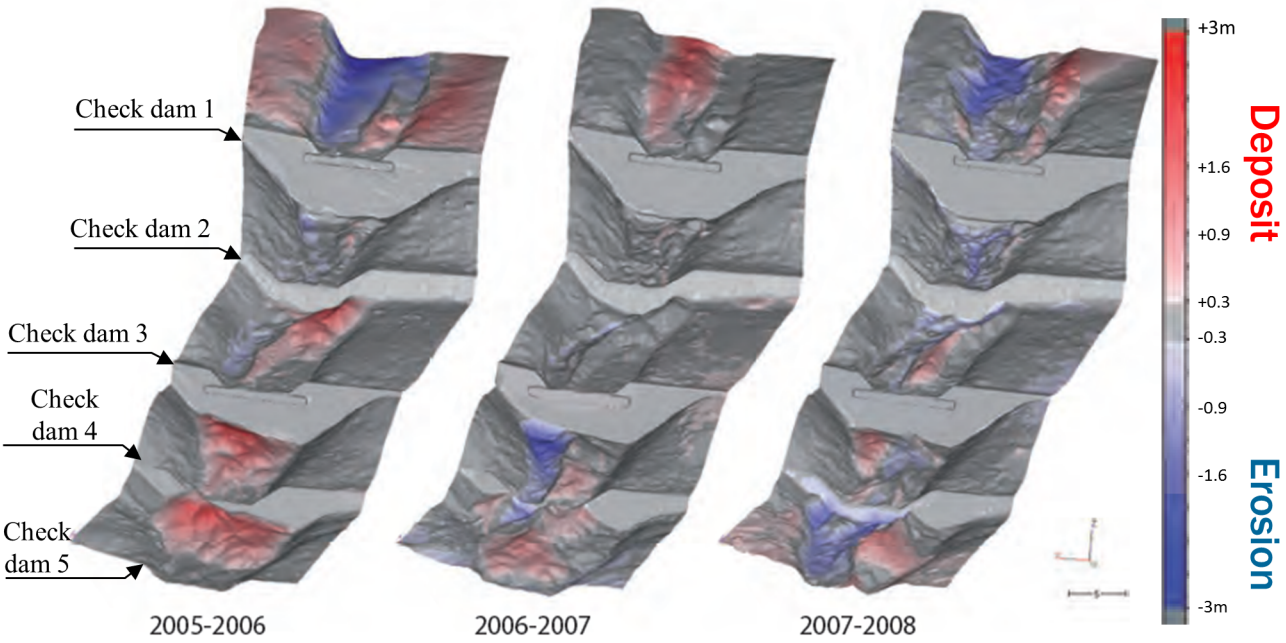

Figure 8.16 – Deposit / erosion assessment in the Lampe torrent check dam series (Saint Paul de Varces, FRA.), evidence of cycles of deposit and releases at a yearly frequency, what about the event scale? (after Astrade et al., 2011)

B. Sediment trap monitoring

We are looking for detailed observations of sediment trap filling. *Pre* and *post*-observations can be found but seldom the dynamics of the spreading in the basin, during the event. Italian colleagues of the SedAlp project[1] diffused a video of a sediment trap filling on the Gadria torrent (ITA.). To my knowledge, it is the only published equivalent.

IRSTEA has a long experience of field monitoring. It has thus been decided to launch such observations. Cameras have been installed on the Roize sediment trap (Chap. 4 – Lamand et al., 2015) and the Manival sediment trap, another well-known site (Veyrat-Charvillon and Memier, 2006; Liébault et al., 2010a; Lopez Saez et al., 2011; Theule et al., 2012; 2015). The cameras take daily pictures of the trap basins and one picture per second during floods. Flood are detected using a geophone located on the bank, with the system developed by Bel et al. (2014a; 2014b). The triggering definitely works; currently it detects even small flows without sediment transport. Further works are in progress to develop lighter and more affordable systems that would be easily diffused to facilitate mountain stream flood observations.

The Roize monitoring demonstrates that no sediment transport occurred at the sediment trap in the last 11 months (Fig. 8.17), the torrent is (sadly) dormant. The Manival experienced one small bedload-laden flood (Fig. 8.18). The pictures confirm the emergence of cycles of braided / channelized flows but the deposit was initially disturbed by a partial dredging operation. New floods are expected to confirm our laboratory observations.

[1] *http://www.sedalp.eu/*

Figure 8.17 – Pictures of the sediment trap basin of the Roize torrent (Voreppe, FRA.): (a) May 2015, b) January 2016; marginal morphic activity, perhaps even a slight self cleaning

Figure 8.18 – Small debris flood event in the Manival sediment trap on September, 17^{th} 2015, evidences of cycles of: a) braided channels, b) incision with lobe formation, and c) new braided pattern. Larger events are expected to confirm these encouraging results

C. Testing travelling bed-load and asymptotical approaches

The travelling bed-load approach for sediment transport computation(Chap. 4) should be tested on other mountain streams' datasets, eventually on both instantaneous monitoring (*e.g.*, confrontation done with the Erlenbach, Pitzbach and Diagoa streams) and cumulative production measured in sediment trap as done on the Roize. The asymptotical approach should also be tested against high magnitude bedload transport as done with previous approaches by Rickenmann (2001); Rickenmann and Koschni (2010). Cumulative transport volumes obtained from sediment traps are very interesting data for such extreme cases, optimally with a hydrological station on the stream, in order to limit the uncertainties related to water discharge estimation (possibly quite high in our Roize case-study).

8.3.2. Linking field, laboratory and numerical approaches

A. Field supply in laboratory experiments

Long lasting experiments of bedload transport are usually undertaken under steady supply[1]. The emerging solid transport autogenic fluctuations are a fascinating subject of investigation. Their physics would be much more complicated to study under the impressively transient flows of mountain streams. It is however only in such conditions that their actual field significance could be highlighted.

New experiments could be done to study the dynamics of the bedload transport under fluctuating hydrology of varied magnitude. Real time-series of both water and sediment discharges are now available on quite long durations in a few stations (Erlenbach, Rio Cordon). These field outputs could be used as direct laboratory inputs, after Froude similitude downscaling. A bed geometry could be reconstructed with coarse material, similar to the reference-stream natural bed. A series of small flood preceding an extreme event and the "relaxation" time following it could be studied in the flume. Propagation of the sediment waves in this natural reference run would constitute an interesting dataset by itself. It would also be another opportunity to test the travelling bedload and asymptotical approaches, maybe also the transition between these regimes.

The bed could then be reset and supply time series be re-run after adding check dams to the flume. The sediment transport regulation possibly emerging for small floods and for a high magnitude event would give insights on the general physics of sediment transport in paved streams. From a hazard mitigation perspective it could be a preliminary, fast test of the significance of sediment transport regulation and necessity to monitor it in the field.

B. Toward numerical modeling

The preliminary analysis presented in chapter 7 of the laboratory data acquired during this work might probably be pushed further. Complementary analysis of the roughness spatial distribution, of the self-organized flow features or of the detailed transport capacity should be studied more in details. These measurements additionally constitute a dataset that may be used for numerical model calibration and validation. Our experimental conditions would be appropriate for 2D numerical model of bedload transport that account for grain size sorting, steep slope stream specific hydraulics and sediment transport. Such numerical tool generally lack calibration and validation data. There is here

[1]though, a long lasting, cyclic experiment have recently been undertaken at the EPFL: Dhont, B., Heyman, B., Venetz, P., Ancey, C. **2014** "*Effects of successive floods on bed load transport in a steep flume*" Geophysical Research Abstracts Vol. 16, EGU2014-11194, Poster presented at the EGU General Assembly 2014

a set of about one hundred instantaneous flow measurements in varied grain size distributions, solid concentrations and water discharges.

Grain size sorting is likely partially stochastic at the flume scale. The chaos theory and resulting "sensitivity to initial conditions" of the system probably make it self-organized around a stable state but unlikely to reproduce two times identical states. Reconstitution of absolutely the same bed geometries thus cannot be expected. A preliminary analysis could help to describe the experiment evolutions using probabilistic descriptors of, for instance, the duration of braided flow and channelized flows, the flooded surface rate, the surface sorting rate, etc. The comparison with numerical model results might latter been done using these descriptor statistics, likely more adapted to this complex subject of investigation.

8.3.3. Open check dam hydraulics

It has been decided to focus on the scientific gap remaining in open check dam basin hydraulics but some complementary promising topics concern the structures themselves.

A. Optimizing outlets and basin channel

Open check dam optimizations may concern both the basin and the outlet structure. As mentioned in Chapter 2, low flood channels or parallel structures are promising designs to diminish or remove the influence of the structure on low magnitude, un-hazardous floods. This topic has regularly been investigated in Switzerland (LCH, 2011; Ghilardi et al., 2012). A few examples also exist in France (St Clément in Tours-en-Savoie; Clinel in Pontamafrey-Mont-Pascal, Piton et al., 2015), and possibly elsewhere.

Most of sediment traps are however built directly transversally to the streambed and their transformation in parallel traps seems complicated. An intermediate solution could be to dig a trench in the basin, to protect it to become a low flood channel and to design a suitable bottom outlet that would weakly influence unhazardous floods, while having a stronger influence on high flows. Defining such an outlet design, with a sort of threshold effect, is not straightforward. Experimental investigations are in progress at the EPFL-LCH on this subject (Schwindt et al., 2015).

Such a design is subtle and deserves more attention before recommending adaptations of existing structures: A well-documented case study of dramatic and unexpected sediment trap dysfunction linked to the bottom outlet design is reported by Bezzola et al. (2004) (nearly negligible sediment storage after a major flood in a 200 000 m^3 basin).

B. Driftwood and hydraulics

The clogging probability and eventual increase in trapping efficiency related to woody debris in mountain stream floods has also ever been studied (Ishikawa and Mizuyama, 1988; D'Agostino et al., 2000; Shrestha et al., 2012; Ishikawa et al., 2014). In parallel, some works have recently been done on woody debris influence and trapping in rivers (Schmocker and Hager, 2011; Schmocker et al., 2012; Schmocker and Weitbrecht, 2013; Schmocker and Hager, 2013).

It would probably be interesting to carry on quite similar experiments with measurement of head losses and clogging dynamics, though in steeper configurations, with and without sediment transport.

The implementation of detailed measurement techniques (*e.g.*, Chap. 6) would allow later numerical simulation confrontation, not only on the resulting deposit pattern but also on the hydraulics and woody debris transport. The calibration and validation of new numerical tools, and recommendations in the computation strategy for woody debris and sediment-laden flows modelling are necessary to improve natural hazard studies and more rigorous mitigation measure design.

The End

References

Aberle, J. and Smart, G. (2003). "The influence of roughness structure on flow resistance on steep slopes". English; French. *Journal of Hydraulic Research*. Vol. 41. no. 3, pp. 259–269.

Admiraal, D. M., Stansbury, J. S., and Haberman, C. J. (2004). "Case study: Particle velocimetry in a model of lake Ogallala". *Journal of Hydraulic Engineering*. Vol. 130. no. 7, pp. 599–607.

AFNOR (2001). "NF EN 13306 X 60-319 - Terminologie de la maintenance". 58p. (in French).

AFNOR (2009). "NF EN ISO 748 - Hydrométrie Mesurage du débit des liquides dans les canaux découverts au moyen de débimètres ou de flotteurs". (in French).

Agisoft LLC (2014). "Agisoft PhotoScan User Manual - Professional Edition, Version 1.1". 85p. Agisoft LLC.

Agoramoorthy, G. and Hsu, M. (2008). "Small size, big potential: Check dams for sustainable development". *Environment: Science and Policy for Sustainable Development*. Vol. 50. no. 4, pp. 22–35. DOI: 10.3200/ENVT.50.4.22-35.

Aguirre-Pe, J. and Fuentes, R. (1990). "Resistance to flow in steep rough streams". *Journal of Hydraulic Engineering*. Vol. 116. no. 11, pp. 1374–1387.

Albaba, A., Lambert, S., Nicot, F., and Chareyre, B. (2014). "Modeling the impact of granular flow against an obstacle". *Springer Series in Geomechanics and Geoengineering*. Vol. 2015, pp. 95–105. DOI: 10.1007/978-3-319-11053-0_9.

Andréassian, V. (2004). "Waters and forests: from historical controversy to scientific debate". *Journal of Hydrology*. Vol. 291. no. 1–2, pp. 1 –27. DOI: 10.1016/j.jhydrol.2003.12.015.

Armanini, A. (2014). "Closure relations for mobile bed debris flows in a wide range of slopes and concentrations". *Advances in Water Resources*. Vol. 81, 75–83. DOI: 10.1016/j.advwatres.2014.11.003.

Armanini, A. and Larcher, M. (2001). "Rational criterion for designing opening of slit-check dam". *Journal of Hydraulic Engineering*. Vol. 127. no. 2, pp. 94–104. DOI: 10.1061/(ASCE)0733-9429(2001)127:2(94).

Armanini, A., Dellagiacoma, F., and Ferrari, L. (1991). "From the check dam to the development of functional check dams". *Fluvial Hydraulics of Mountain Regions*. Vol. 37, pp. 331–344. DOI: 10.1007/BFb0011200.

Armanini, A., Dalrı, C., and Larcher, M. (2006). "Slit-Check Dams for Controlling Debris Flow and Mudflow". Disaster Mitigation of Debris Flows, Slope Failures and Landslides - INTERPRAEVENT Conference Proceedings. Ed. by U. A. Press, pp. 141–148.

Ashmore, P. (2013). "Treatise on Geomorphology". Ed. by E. E. Shroder J. (Editor in Chief) Wohl. Vol. 9. Elsevier Inc. Chap. Morphology and Dynamics of Braided Rivers, pp. 289–312. DOI: 10.1016/B978-0-12-374739-6.00242-6.

Ashmore, P., Bertoldi, W., and Tobias Gardner, J. (2011). "Active width of gravel-bed braided rivers". *Earth Surface Processes and Landforms*. Vol. 36. no. 11, pp. 1510–1521. DOI: 10.1002/esp.2182.

Astrade, L., Ployon, E., and Veyrat-Charvillon, S. (2011). "Les données laser terrestre à haute résolution pour le suivi de la charge de fond dans les tronçons torrentiels, retours d'expériences". Images et modèles 3D en milieux naturels. Ed. by S. Jaillet, E. Ployon, and T. Villemin. (In French). Coll Edytem, pp. 107–118.

Bacchi, V., Recking, A., Eckert, N., Frey, P., Piton, G., and Naaim, M. (2014). "The effects of kinetic sorting on sediment mobility on steep slopes". *Earth Surface Processes and Landforms*. Vol. 39, p. 8. DOI: 10.1002/esp.3564.

Bacchi, V. (2011). "Etude expérimentale de la dynamique sédimentaire d'un système à forte pente soumis à des conditions hydrauliques faibles". 209 p. (In french). PhD thesis. Université de Grenoble.

Badoux, A., Andres, N., and Turowski, J. (2014). "Damage costs due to bedload transport processes in Switzerland". *Natural Hazards and Earth System Sciences*. Vol. 14. no. 2, pp. 279–294. DOI: 10.5194/nhess-14-279-2014.

BAEL (1980). "Règles B.A.E.L. 80". 79-48 bis. (In French). Ministère de l'environnement et du cadre de vie et Minitère des transports.

BAFU [GHO Network] (2016). "Sediment trap monitoring dataset - Federal Office for the Environment FOEN - Swiss Confederation". http://www.bafu.admin.ch/wasser/13462/14737/15098. Accessed: 2016-05.

Beckman, N. and Wohl, E. (2014). "Effects of forest stand age on the characteristics of logjams in mountainous forest streams". *Earth Surface Processes and Landforms*. Vol. 39. no. 11, pp. 1421–1431. DOI: 10.1002/esp.3531.

Bel, C., Liébault, F., Bellot, H., Fontaine, F., Laigle, D., and Navratil, O. (2014a). "Debris flow monitoring in the French Alps". Proceedings of the 7th International Conference on Fluvial Hydraulics, RIVER FLOW 2014. Lausanne: CRC Press/Balkema, pp. 1589–1595.

Bel, C., Navratil, O., Liébault, F., Fontaine, F., Bellot, H., and Laigle, D (2014b). "Monitoring Debris Flow Propagation in Steep Erodible Channels". Engineering Geology for Society and Territory (IAEG Congress proceedings). Ed. by G. Lollino et al. Vol. 3. no. 20. ISBN: 978-3-319-09053-5. Springer International Publishing Switzerland, pp. 103–107. DOI: 10.1007/978-3-319-09054-2_20.

Benito, G., Grodek, T., and Enzel, Y. (1998). "The geomorphic and hydrologic impacts of the catastrophic failure of flood-control-dams during the 1996-Biescas flood (Central Pyrenees, Spain)". *Zeitschrift fur Geomorphologie*. Vol. 42. no. 4, pp. 417–437.

Bergmeister, K., Suda, J., Hübl, J., and Rudolf-Miklau, F. (2009). "Schutzbauwerke gegen Wildbachgefahren: Grundlagen, Entwurf und Bemessung, Beispiele [Defenses against torrent Hazards: Fundamentals, Design and calculation examples]". (In German). Ernst Sohn, pp. 1–211.

Bernard, C. (1927). "Cours de restauration des montagnes". Ed. by Ecole Nationale des Eaux et Forêt. (In French). Ecole normale des eaux et forêts, p. 788.

Bertoldi, W., Gurnell, A., and Welber, M. (2013). "Wood recruitment and retention: The fate of eroded trees on a braided river explored using a combination of field and remotely-sensed data sources". *Geomorphology*. Vol. 180-181, pp. 146–155. DOI: 10.1016/j.geomorph.2012.10.003.

Bertoldi, W., Welber, M., Mao, L., Zanella, S., and Comiti, F. (2014). "A flume experiment on wood storage and remobilization in braided river systems". *Earth Surface Processes and Landforms*. Vol. 39. no. 6, pp. 804–813. DOI: 10.1002/esp.3537.

Bezzola, G. R., Sigg, H., and Lange, D. (2004). "Driftwood retention works in Switzerland [Schwemmholzrückhalt in der Schweiz]". INTERPRAEVENT Conference Proceedings. (in German). RIVA -TRIENT.

Billi, P, D'Agostino, V, Lenzi, M., and Marchi, L (1998). "Gravel-bed Rivers in the Environment". Ed. by P. Klingeman, R. Beschya, P. Komar, and J. Bradley. Highlands Ranch, Colo: Water Resources Publications LLC. Chap. Chap. 3 Bedload, slope and channel processes in a high-altitude alpine torrent, pp. 15–38.

Bischetti, G. B., Di Fi Dio, M., and Florineth, F. (2014). "On the Origin of Soil Bioengineering". *Landscape Research*. Vol. 39. no. 5, pp. 583–595. DOI: 10.1080/01426397.2012.730139.

Blanchard, R. (1944). "Deboisement et reboisement dans les Préalpes françaises du Sud". *Revue de géographie alpine*. Vol. 32. no. 3, pp. 335–388.

Blanquart, B. (2013). "Panorama des méthodes d'estimation des incertitudes de mesure". *La Houille Blanche*. no. 6, pp. 9–15. DOI: 10.1051/lhb/2013045.

BLFUW (2009). "Kosten-Nutzen-Untersuchungen im Schutzwasserbau Richtlinie. KNU gemäß Par. 3 Abs. 2 Ziffer 3 WBFG Fassung". Tech. rep. 27 p. (in German). Vienna, Austria: Bunderministerium für Land- und Forstwirtschaft Umwelt und Wasserwirtschaft, Sektion Wasser.

Blinkov, I., Kostadinov, S., and Marinov, I. T. (2013). "Comparison of erosion and erosion control works in Macedonia, Serbia and Bulgaria". *International Soil and Water Conservation Research*. Vol. 1. no. 3, pp. 15 –28. DOI: http://dx.doi.org/10.1016/S2095-6339(15)30027-7.

Böll, A. (1997). "Wildbach- und Hangverbau". Tech. rep. no. 343. (In German). Birmendorf: Eidgenössische Forschungsanstalt für Wald Schnee und Landschaft (WSL).

Böll, A, Kienholz, H, and Romang, H (2008). "Beurteilung der Wirkung von Schutzmassnahmen gegen Naturgefahren als Grundlage für ihre Berücksichtigung in der Raumplanung TEIL E:WILDBÄCHE". Tech. rep. no. V1.02d. (in German). Bern: Swiss Confederation - National Plateform for natural Hazards.

Bombino, G., Gurnell, A., Tamburino, V., Zema, D., and Zimbone, S. (2009). "Adjustments in channel form, sediment calibre and vegetation around check-dams in the headwater reaches of mountain torrents, Calabria, Italy". *Earth Surface Processes and Landforms*. Vol. 34. no. 7, pp. 1011–1021. DOI: 10.1002/esp.1791.

Borda, J. (1769). "Histoire de l' Académie Royale des Sciences". (In French). Paris: Imp. Nationale. Chap. Mémoire sur l' écoulement des fluides par les orifices des vases [Dissertation on the fluids' flow through vases' orifices], pp. 579–606.

Bordes, J.-L. (2010). "Les barrages en France du XVIIIème à la fin du XXème siècle en France, histoire, évolution technique et transmission du savoir." *Pour Mémoire*. Vol. 9, pp. 70–120.

Bradley, J. B., Richards, D. L., and Bahner, C. D (2005). "Debris control structures: Evaluation and countermeasures". Tech. rep. no. FHWA-IF-04-016. Washington, DC.: U.S. Dept. of Transportation, Federal Highway Administration.

Brandt, S. (2000). "Classification of geomorphological effects downstream of dams". *Catena*. Vol. 40. no. 4, pp. 375–401. DOI: 10.1016/S0341-8162(00)00093-X.

Braudrick, C., Grant, G., Ishikawa, Y., and Ikeda, H. (1997). "Dynamics of wood transport in streams: A flume experiment". *Earth Surface Processes and Landforms*. Vol. 22. no. 7, pp. 669–683.

Braudrick, C. c. and Grant, G. (2001). "Transport and deposition of large woody debris in streams: A flume experiment". *Geomorphology*. Vol. 41. no. 4, pp. 263–283. DOI: 10.1016/S0169-555X(01)00058-7.

Bravard, J. (1991). "La dynamique fluviale à l'épreuve des changements environnementaux: Quels enseignements applicables à l'aménagement des rivières?" *La Houille Blanche*. no. 7-8. (In French), pp. 515–522.

Breton, P. (1867). "Mémoire sur les barrages de retenue de graviers dans les gorges des torrents". Ed. by Dunod. (In French). Paris.

Brochot, S., Duclos, P., and Bouzit, M. (2003). "L'évaluation économique des risques torrentiels: intérêts et limites pour les choix collectifs de prévention." *Ingénieries*. Vol. Spécial. (in French), pp 53–68.

Brown, J. C. (1876). "Reboisement in France: or, records of the replanting of the Alps, the Cevennes, and the Pyrenees with trees, herbage, and bush, with a view to arresting and preventing the destructive consequences and effects of torrents." London: Henry S. King Co., p. 351.

Brugnot, G. (2002). "Développement des politique forstières et naissance de la restauration des terrains en montagne". Annales des ponts et chaussées. Ed. by Elsevier. no. 103, pp 23–30. DOI: 10.1016/S0152-9668(02)80031-6.

Bründl, M., Krummenacher, B., and Merz, H. (2009). "Decision making tools for natural hazard risk management - Examples from Switzerland". Safety, reliability and risk analysis: theory, methods and applications: proceedings of the European Safety and Reliability Conference, ESREL 2008, and 17th SRA-Europe. pp 2773-2779. European Safety and Reliability Association. Valence, Spain: CRC Press/Balkema, Leiden.

Brunkal, H. and Santi, P. (2016). "Exploration of design parameters for a dewatering structure for debris flow mitigation". *Engineering Geology*. (in press), pp. –. DOI: 10.1016/j.enggeo.2016.04.011.

Bunte, K., Abt, S. R., Swingle, K. W., Cenderelli, D. A., and Schneider, J. M. (2013). "Critical Shields values in coarse-bedded steep streams". *Water Resources Research*. Vol. 49. no. 11, pp. 7427–7447. DOI: 10.1002/2012WR012672.

Busnelli, M., Stelling, G., and Larcher, M. (2001). "Numerical Morphological Modeling of Open-Check Dams". *Journal of Hydraulic Engineering*. Vol. 127. no. 2, pp. 105–114. DOI: 10.1061/(ASCE)0733-9429(2001)127:2(105).

Cadol, D., Wohl, E., Goode, J., and Jaeger, K. (2009). "Wood distribution in neotropical forested headwater streams of La Selva, Costa Rica". *Earth Surface Processes and Landforms*. Vol. 34. no. 9, pp. 1198–1215. DOI: 10.1002/esp.1800.

Campisano, A. (2009). "Laboratory investigation on the performances of baffles for the capture of sewer floatables". *Water Science and Technology*. Vol. 60. no. 1, pp. 29–36. DOI: 10.2166/wst.2009.295.

Campisano, A., Cutore, P., and Modica, C. (2013). "Modelling Sediment Deposit Evolution Upstream of Slit-Check Dams in Mountain Streams". World Environmental and Water Resources Congress. Ed. by C. L. Patterson, S. D. Struck, and J. Daniel J. Murray. Reston: ASCE, pp. 1757–1768. DOI: 10.1061/9780784412947.173.

Campisano, A., Cutore, P., and Modica, C. (2014). "Improving the Evaluation of Slit-Check Dam Trapping Efficiency by Using a 1D Unsteady Flow Numerical Model". *Journal of Hydraulic Engineering*. Vol. 140, pp. 1–10. DOI: 10.1061/(ASCE)HY.1943-7900.0000868.

Canelas, R. B., Domınguez, J. M., Crespo, A. C., Silva, M., and Ferreira, R. M. (2015). "Debris Flow Modelling With High-performance Meshless Methods". Congresso de Métodos Numéricos em Engenharia 2015. Lisboa: APMTAC, pp. 1–14.

Canovaro, F. and Solari, L. (2007). "Dissipative analogies between a schematic macro-roughness arrangement and step-pool morphology". *Earth Surface Processes and Landforms*. Vol. 32. no. 11, pp. 1628–1640.

Cao, H. H. (1985). "Résistance hydraulique d'un lit de gravier mobile à pente raide". PhD thesis. EPFL Lausanne.

Carbonari, C. (2015). "Msc. Thesis manuscripts: Experimental observations on the functioning of sediment trap basins: LSPIV measurements of low submersion flows". MA thesis. Univ. of Florence.

Carladous, S. (2013). "Analyse critique des méthodes d'évaluation de l'efficacité économique des mesures de protection contre les risques naturels en montagne." 130 p. MA thesis. Montpellier, France: Université Paul Valéry.

Carladous, S., Michaud, M.-P., Tacnet, J.-M., and Delvienne, Q. (2014a). "A survey on protection work databases used at the Alpine Space level: analysis of contents and state of the art related to protection work effectiveness assessment in START-it-uP (WP4)." Tech. rep. European Regional Development Fund - Alpine Space Progam - START-it-uP project : State-of-the-Art in Risk Management Technology: Implementation and Trial for Usability in Engineering Practive and Policy. http://www.alpine-space.eu/startitup.

Carladous, S., Tacnet, J.-M., Eckert, N., Curt, C., and Batton-Hubert, M. (2014b). "Vers une analyse intégrée de l'efficacité des ouvrages de protection contre les risques naturels en montagne : évaluation économique en complément des volets structurels et fonctionnels." 8ème Journées Fiabilité, Matériaux et Structures - analyse de risques et fiabilité des systèmes dans leur environnement. Ed. by C. Curt, L. Peyras, J. Baroth, and A. Chateauneuf. pp 61-74. France.

Carladous, S., Piton, G., Tacnet, J., Philippe, F., Nepote-Vesino, R., Quefféléan, Y, and Marco, O. (2016a). "Protection against natural hazards in French mountains: historical analysis of actions and decision contexts in public forests". 13th INTERPRAEVENT Conf. Proc..

Carladous, S., Tacnet, J.-M., and Batton-Hubert, M. (2016b). "Protection structures against natural hazards: from failure analysis to effectiveness assessment". 13th INTERPRAEVENT Conf. Proc..

Carladous, S., Piton, G., Recking, A., Liebault, F., Richard, D., Tacnet, J., Kuss, D., Philippe, F., Quefféléan, Y, and Marco, O. (2016c). "Towards a better understanding of the today French torrents management policy through a historical perspective". FLOODrisk 3rd European Conference on Flood Risk Management Conf. Proc.. (Sub.), 12p.

Castelli, B. (1628). ""della misura dell'acque correnti [traicte de la mesure des eaux courantes]". (French traduction of 1664).

Catella, M., Paris, E., and Solari, L. (2005). "Case Study: Efficiency of Slit-Check Dams in the Mountain Region of Versilia Basin". *Journal of Hydraulic Engineering*. Vol. 131. no. 3, pp. 145–152. DOI: 10.1061/(ASCE)0733-9429(2005)131:3(145).

Cazaillet, O., Guilbert, S., and Lefort, P (2008). "Management of sediment transport in the river Isère in the Grésicvaudan Valley [Gestion du transport solide en Isère dans la vallée du grésivaudan]". French. *Houille Blanche*. Vol. 5. no. 5. (In French), pp. 115–122. DOI: 10.1051/LHB:2008065.

CFBR (2013). "Recommandations pour le dimensionnement des évacuateurs de crues de barrages [recommendations for dams' spillway design]". Ed. by G. de Travail Dimensionnement des évacuateurs de crues de barrages. (In French). Le Bourget-Du-Lac: Comité Français des Barrages et Réservoirs, p. 166.

CFGB (1994). "Les crues de projet des barrages: méthode du GRADEX-Design flood determination by the GRADEX method". *Bulletin du Comité Français des Grands Barrages-18e Congrès CIGB/ICOLD*. no. 2. (in French and English), pp. 1–78.

Champion, M. (1856). "Recherche historiques sur les inondations du Rhône et de la Loire". 19 p. Typographie Panckoucke.

Chanson, H. (1999). "Comment on 'Critical flow constrains flow hydraulics in mobile-bed streams: A new hypothesis' by G. E. Grant". *Water Resources Research*. Vol. 35. no. 3, pp. 903–907. DOI: 10.1029/1998WR900054.

Chanson, H. (2004). "Sabo Check Dams - Mountain Protection Systems in Japan". *Journal of River Basin Management*. Vol. 2. no. 4, pp. 301–307.

Chatwin, S., Howes, D., Schwab, J., and Swanston, D. (1994). "A Guide for Management of Landslide-Prone Terrain in the Pacific Northwest". Vol. Land Management Handbook NUMBER 18 ISSN 0229-1622. 31 Bastion Square, Victoria, British Columbia, V8W 3E7: Ministry of Forests.

Chen, J., Chen, X., Zhao, W., and You, Y. (2016). "Discussion of "Design of Sediment Traps with Open Check Dams. I: Hydraulic and Deposition Processes" by Guillaume Piton and Alain Recking". *Journal of Hydraulic Engineering*. in press.

Chen, S.-C. and Chao, Y.-C (2010). "Locations and orientations of large woody debris in chichiawan creek". INTERPRAEVENT Conference Proceedings. Pp. 107 –113.

Chen, X., Cui, P., You, Y., Chen, J., and Li, D. (2015). "Engineering measures for debris flow hazard mitigation in the Wenchuan earthquake area". *Engineering Geology*. Vol. 194. no. Special Issue on "The Geological and Geotechnical Hazards of the 2008 Wenchuan Earthquake, China: Part II", pp. 73–85. DOI: 10.1016/j.enggeo.2014.10.002.

Choi, C. E., Ng, C. W. W., Song, D., Kwan, J. H. S., Shiu, H. Y. K., Ho, K. K. S., and Koo, R. C. H. (2014). "Flume Investigation of Landslide Debris Resisting Baffles". *Revue canadienne de géotechnique*. Vol. 51. no. 5, pp. 540–553. DOI: 10.1139/cgj-2013-0115.

Church, M and Ferguson, R. (2015). "Morphodynamics: Rivers beyond steady state". *Water Resources Research*. Vol. 51. no. 4, pp. 1883–1897. DOI: 10.1002/2014WR016862.

Church, M. and Zimmermann, A. (2007). "Form and stability of step-pool channels: Research progress". *Water Resources Research*. Vol. 43. no. 3, p. 21. DOI: 10.1029/2006WR005037.

Cipriani, T., Toilliez, T., and Sauquet, E. (2012). "Estimation régionale des débits décennaux et durées caractéristiques de crue en France". *La Houille Blanche*. no. 4–5. (in French), pp. 5–13.

Clauzel, L. and Poncet, A. (1963). "Barrages filtrants et corretion torrentielle par ségrégation des matériaux charriés". *Revue Forestière Française*. Vol. 4. (In French), pp. 280 –292. DOI: 10.4267/2042/24540.

Coeur, D. (2003). "Genesis of a public policy for flood management in France: The case of the Grenoble valley (XVIIth-XIXth centuries)". Palaeofloods, Historical Floods and Climatic Variability: Applications in Flood Risk Assessment. CSIC, Madrid (Proccedings of the PHEFRA Workshop, Barcelona, 16-19th October, 2002). Pp. 373–378.

Combes, F. (1989). "Restauration des terrains en montagne. Du rêve à la réalité". *Revue Forestière Française*. Vol. 41. no. 2. (in French), pp. 91–106. DOI: 10.4267/2042/25964.

Comiti, F., Andreoli, A., and Lenzi, M. (2005). "Morphological effects of local scouring in step-pool streams". *Earth Surface Processes and Landforms*. Vol. 30. no. 12, pp. 1567–1581. DOI: 10.1002/esp.1217.

Comiti, F., D'Agostino, V., Ferro, V., and Lenzi, M. (2006). "Fenomeni di erosione localizzata a valle di opere trasversali: integrazioni tra indagini di cam po e di laboratorio". *Quaderni di Idronomia Montana*. Vol. 26. (In Italian), pp. 285–291.

Comiti, F., Mao, L., Wilcox, A., Wohl, E., and Lenzi, M. (2007). "Field-derived relationships for flow velocity and resistance in high-gradient streams". *Journal of Hydrology*. Vol. 340. no. 1-2, pp. 48–62. DOI: 10.1016/j.jhydrol.2007.03.021.

Comiti, F., Mao, L., Preciso, E., Picco, L., Marchi, L., and Borga, M. (2008). "Large wood and flash floods: Evidence from the 2007 event in the Davča basin (Slovenia)". Monitoring, Simulation, Prevention and Remediation of Dense and Debris Flows II. Vol. 60. Southampton: WIT-Press, pp. 173–182. DOI: 10.2495/DEB080181.

Comiti, F, Cadol, D, and Wohl, E (2009). "Flow regimes, bed morphology, and flow resistance in self-formed step-pool channels". *Water Resources Research*. Vol. 45. no. 4.

Comiti, F, D'Agostino, V., Moser, M., Lenzi, M., Bettella, F., Dell'Agnese, A., Rigon, E., Gius, S., and Mazzorana, B. (2012). "Preventing wood-related hazards in mountain basins: from wood load estimation to designing retention structures". INTERPRAEVENT Conference Proceedings. Pp. 651–662.

Comiti, F., Lenzi, M., and Mao, L. (2013). "Check dams, morphological adjustments and erosion control in torrential streams". Ed. by C. Conesa-Garcia and M. Lenzi. Hauppauge, NY: Nova Science Publishers, Inc. Chap. Local scouring at check-dams in mountain rivers, pp. 263–282.

Comiti, F. (2012). "How natural are Alpine mountain rivers? Evidence from the Italian Alps". *Earth Surface Processes and Landforms*. Vol. 37. no. 7, pp. 693–707. DOI: 10.1002/esp.2267.

Conesa-Garcia, C., López-Bermudez, F., and Garcia-Lorenzo, R. (2007). "Bed stability variations after check dam construction in torrential channels (South-East Spain)". *Earth Surface Processes and Landforms*. Vol. 32. no. 14, pp. 2165–2184. DOI: 10.1002/esp.1521.

Costa, J., Cheng, R., Haeni, F., Melcher, N., Spicer, K., Hayes, E., Plant, W., Hayes, K., Teague, C., and Barrick, D. (2006). "Use of radar to monitor stream discharge by noncontact methods". *Water Resources Research*. Vol. 42, pp. 1–14.

Costa de Bastelica, M. (1874). "Les torrents : leurs lois, leurs causes, leurs effets, moyens de les réprimer et de les utiliser, leur action géologique universelle". Ed. by J. Baudry. 1 vol.-282 p. (In French). Paris: Librairie Polytechnique.

Couvert, B. and Lefebvre, B. (1994). "Contribution de modèles physiques à l'étude du charriage torrentiel". *La Houille Blanche*. Vol. 3. no. 3. (in French), pp. 81–90. DOI: 10.1051/lhb/1994046.

Couvert, B., Lefebvre, B., Lefort, P., and Morin, E. (1991). "Etude générale sur les seuils de correction torrentielle et les plages de dépôt". French. *Houille Blanche*. Vol. 46. no. 6. (In French), pp. 449–456. DOI: 10.1051/lhb/1991043.

Culman, K. (1865). "Rapport au Conseil Fédéral sur les torrents des Alpes Suisses inspectés en 1858 - 1859 - 1860 et 1863". (In French). Imprimerie L. Corbaz and Co., p. 590. DOI: 10.3931/e-rara-20090.

Cœur, D. and Lang, M. (2008). "Use of documentary sources on past flood events for flood risk management and land planning". *Comptes Rendus - Geoscience*. Vol. 340. no. 9-10, pp. 644–650. DOI: 10.1016/j.crte.2008.03.001.

D'Agostino, V. (1994). "Investigation on the scour downstream of weirs by a mobile-bed physical model [Indagine sullo scavo a valle di opere trasversali mediante modello fisico a fondo mobile]". Italian. *Energia Elettrica*. Vol. 71. no. 2, pp. 37–51.

D'Agostino, V. (2006). "Le opere di idraulica torrentizia per il controllo dei sedimenti [Sediments control works in mountain streams]". Le sistemazioni idraulico-forestali per la difesa del territorio. Vol. 26. Quaderni di Idronomia Montana. (in Italian). Cosenza: Nuova Bios, pp. 231–250.

D'Agostino, V. (2013a). "Advances in Global Change Research". Dating Torrential Processes on Fans and Cones. Ed. by M. Schneuwly-Bollschweiler, M. Stoffel, and F. Rudolf-Miklau. Vol. 47. Dordrecht: Springer Netherlands. Chap. 8-Assessment of Past Torrential Events Through Historical Sources, pp. 131–146. DOI: 10.1007/978-94-007-4336-6.

D'Agostino, V. (2013b). "Check dams, morphological adjustments and erosion control in torrential streams". Ed. by C. Conesa-Garcia and M. Lenzi. Hauppauge, NY: Nova Science Publishers, Inc. Chap. Filtering-retention check dam design in mountain torrents, pp. 185–210.

D'Agostino, V. and Ferro, V. (2004). "Scour on alluvial bed downstream of grade-control structures". *Journal of Hydraulic Engineering*. Vol. 130. no. 1, pp. 24–37. DOI: 10.1061/(ASCE)0733-9429(2004)130:1(24).

D'Agostino, V. and Lenzi, M. A. (1996). "La valutazione del trasporto solido di fondo nel bacino attrezzato del Rio Cordon". *L'acqua*. Vol. 4, pp. 23–40.

D'Agostino, V. and Lenzi, M. (1999). "Bedload transport in the instrumented catchment of the Rio Cordon. Part II: Analysis of the bedload rate". *Catena*. Vol. 36. no. 3, pp. 191–204. DOI: 10.1016/S0341-8162(99)00017-X.

D'Agostino, V., Degetto, M., and Righetti, M. (2000). "Experimental investigation on open check dam for coarse woody debris control". Dynamics of water and sediments in mountain basins. Vol. 20. Quaderni di Idronomia Montana. Cosenza: Bios, pp. 201–212.

de Crécy, L. (1983). “Evolution de la ”Restauration des terrains en montagne de 1860 à 1983”. La politique de prévention des risques naturels en montagne depuis 150 ans.” 108ème congère national des Sociétés savantes..

De Montmollin, G. and Neumann, A. (2014). “Innovative measures for management of bed load sediment transport: Case studies from alpine rivers in western Switzerland”. Special Session on Swiss Competences in River Engineering and Restoration of the 7th International Conf. on Fluvial Hydraulics, RIVER FLOW 2014. London: Taylor Francis Group, pp. 77–85.

Degetto, M. and Righetti, M. (2004). “Dynamic of wood transport in torrents”. INTERPRAEVENT Conference Proceedings. Vol. 3. no. VII, pp. 73–81.

Dell’Agnese, A., Mazzorana, B., Comiti, F., Von Maravic, P., and D’agostino, V. (2013). “Assessing the physical vulnerability of check dams through an empirical damage index”. *Journal of Agricultural Engineering*. Vol. 44. no. 1, p. 2.

Delsigne, F., Lahousse, P., Flez, C., and Guiter, G. (2001). “Le Riou Bourdoux: Un monstre alpin sous haute surveillance”. *Revue forestière française*. Vol. 53. no. 5. (in French), pp. 527–541. DOI: 10.4267/2042/5269.

Demontzey, P. (1882). “Traité pratique du reboisement et du gazonnement des montagnes”. Ed. by J. Rothschild. Second Edition (In French). Paris: Ministères de l’agriculture et du commerce et des travaux publiques, p. 528.

deWolfe, V. G., Santi, P. M., Ey, J., and Gartner, J. E. (2008). “Effective mitigation of debris flows at Lemon Dam, La Plata County, Colorado”. *Geomorphology*. Vol. 96. no. 3, pp. 366–377.

Deymier, C., Tacnet, J., and Mathys, N. (1995). “Conception et calcul de barrages de correction torrentielle [Design and computation of check dams]”. Ed. by C. Editions. Cemagref Grenoble Pegr, 287 p.

Di Stefano, C. and Ferro, V. (2013). “Experimental study of the stage-discharge relationship for an upstream inclined grid with longitudinal bars”. *Journal of Irrigation and Drainage Engineering*. Vol. 139. no. 8, pp. 691–695. DOI: 10.1061/(ASCE)IR.1943-4774.0000598.

Di Stefano, C. and Ferro, V. (2014). “Closure to Experimental Study of the Stage-Discharge Relationship for an Upstream Inclined Grid with Longitudinal Bars by C. Di Stefano and V. Ferro”. *Journal of Irrigation and Drainage Engineering*. Vol. 0. no. 0, pp. 07014028–1. DOI: 10.1061/(ASCE)IR.1943-4774.0000762.

Dìaz, V., Mongil, J., and Navarro, J. (2014). “Topographical surveying for improved assessment of sediment retention in check dams applied to a Mediterranean badlands restoration site (Central Spain)”. *Journal of Soils and Sediments*. Vol. 14. no. 12, pp. 2045–2056.

Dodge, B. H. (1948). “Design and Operation of Debris Basins”. Proceedings, Federal Inter-Agency Sedimentation Conference. Denver, CO. Washington, DC: US Department of the Interior, Bureau of Reclamation, pp. 274–301.

Doolittle, W. (2013). “Check dams, morphological adjustments and erosion control in torrential streams”. Ed. by C. Conesa-Garcia and M. Lenzi. Hauppauge, NY: Nova Science Publishers, Inc. Chap. 1-Traditional uses of check dams: Global and historical introduction, pp. 1–10.

Dramais, G., Le Coz, J., Camenen, B, and Hauet, A. (2011). “Advantages of a mobile LSPIV method for measuring flood discharges and improving stage-discharge curves”. *Journal of Hydro-environment Research*. Vol. 5/4, pp. 301–312.

Dufour, S. and Piégay, H. (2009). “From the myth of a lost paradise to targeted river restoration: forget natural references and focus on human benefits”. *River research and applications*. Vol. 25. no. 5, pp. 568–581. DOI: 10.1002/rra.1239.

Duile, J. (1826). “Über Verbauung der Wildbäche in Gebirgs-Ländern, vorzüglich in der Provinz Tirol und Vorarlberg”. (In Deutsch). Rauch, p. 180.

Duile, J. (1841). “Bericht und Anträge des Herrn J. Duile ... an Landammann und Rath des Kantons Glarus über den Untersuch der Wild- und Gebirgsbäche im Kanton Glarus”. Glarus. DOI: http://dx.doi.org/10.3931/e-rara-20165.

Eaux et Forêts (1911a). “Restauration et conservation des terrains en montagne. Deuxième partie, Description sommaire des périmetres de restauration, Région des Alpes.” Ed. by M. de l’agriculture Direction générale des Eaux et Forêts. 215p. (In French). Imprimerie Nationale.

Eaux et Forêts (1911b). "Restauration et conservation des terrains en montagne. Première partie, Renseignements généraux". Ed. by M. de l'agriculture Direction générale des Eaux et Forêts. 214 p. (In French). Imprimerie Nationale.

Eaux et Forêts (1911c). "Restauration et conservation des terrains en montagne. Troisième partie, Description sommaire des périmetres de restauration, Région des Cévennes et du Massif Central, Région des Pyrénées." Ed. by M. de l'agriculture Direction générale des Eaux et Forêts. 197p. (In French). Imprimerie Nationale.

Egashira, S. (2007). "Review of Research Related to Sediment Disaster Mitigation". *Journal of Disaster Research*. Vol. 2. no. 1, pp. 11–18.

Egholm, D., Knudsen, M., and Sandiford, M. (2013). "Lifespan of mountain ranges scaled by feedbacks between landsliding and erosion by rivers". *Nature*. Vol. 498. no. 7455, pp. 475–478. DOI: 10.1038/nature12218.

Einstein, H. A. (1950). "The bed-load function for sediment transportation in open channel flows". no. 1026. Washington: US Department of Agriculture - Soil Conservation Service, p. 71.

Eisbacher, R. (1982). "Slope stability and land use in mountain valleys". *Geoscience Canada*. Vol. 9. no. 1, pp. 14–27.

El Kadi Abderrezzak, K., Die Moran, A., Mosselman, E., Bouchard, J.-P., Habersack, H., and Aelbrecht, D. (2014). "A physical, movable-bed model for non-uniform sediment transport, fluvial erosion and bank failure in rivers". *Journal of Hydro-Environment Research*. Vol. 8. no. 2, pp. 95–114. DOI: 10.1016/j.jher.2013.09.004.

Erdlenbruch, K., Gilbert, E., Grelot, F., and Lescoulier, C. (2008). "Une analyse coût-bénéfice spatialisée de la protection contre les inondations - Application de la méthode des dommages évités à la basse vallée de l'Orb." *Ingénieries*. Vol. Vol. 53. (in French), pp 3–20.

Esmaeili Nameghi, A, Hassanli, A, and Soufi, M. (2008). "A study of the influential factors affecting the slopes of deposited sediments behind the porous check dams and model development for prediction". *Desert*. Vol. 12. no. 2, pp. 113–119.

EU (2000). "EU Water framework directive". Ed. by E. Commission. Directive 2000/60/EC. Brussels: European Union.

Evette, A., Labonne, S., Rey, F., Liebault, F., Jancke, O., and Girel, J. (2009). "History of bioengineering techniques for erosion control in rivers in western europe". *Environmental Management*. Vol. 43. no. 6, pp. 972–984. DOI: 10.1007/s00267-009-9275-y.

Fabre, J.-A. (1797). "Essai sur la théorie des torrens et des rivières". Ed. by. chez Bidault Libraire.

Ferguson, R. (2007). "Flow resistance equations for gravel-and boulder-bed streams". *Water Resources Research*. Vol. 43. no. 5, pp. 1–12. DOI: 10.1029/2006WR005422.

Ferrell, W. and Barr, W. (1965). "Criteria and methods for use of check dams in stabilizing channel banks and beds". Proceedings of the Federal Inter-Agency Sedimentation Conference, 1963. no. 970. US Department of Agriculture, p. 376.

Ferro, V. (2013). "Check dams, morphological adjustments and erosion control in torrential streams". Ed. by C. Conesa-Garcia and M. Lenzi. Hauppauge, NY: Nova Science Publishers, Inc. Chap. Modern strategies for torrent control: Slit and W-weir check dams, pp. 33–62.

Ferro, V. and Porto, P. (2011). "Predicting the equilibrium bed slope in natural streams using a stochastic model for incipient sediment motion". *Earth Surface Processes and Landforms*. Vol. 36. no. 8, pp. 1007–1022. DOI: 10.1002/esp.2128.

Fesquet, F. (1997). "Un corps quasi-militaire dans l'aménagement du territoire : le corps forestier et le reboisement des montagnes méditerranéennes en France et en Italie aux XIX et XX èmes siècles". 3 volumes - 992 p. (In French). PhD thesis. Université Paul Valéry, Montpellier III.

Fiebiger, G. (2008). "Experiences with the Chain of Functions in debris flow control". Debris Flows : Disasters, Risks, Forecast, Protection. Ed. by S. Institute. Pyatigorsk.

Fiebiger, G. (1997). "Structures of Debris Flow Countermeasures". Debris-Flow Hazards Mitigation: Mechanics, Prediction, and Assessment. Reston: ASCE, pp. 596–605.

Fourchy, P. (1966). "Déboisement et reboisement. Les débuts de la lutte contre l'érosion au XIXe siècle dans les Alpes françaises". *Revue forestière française*. pp 467–487.

Frey, P. and Church, M. (2009). "How river beds move". *Science*. Vol. 325. no. 5947, pp. 1509–1510. DOI: 10.1126/science.1178516.

Frey, P. and Church, M. (2011). "Bedload: A granular phenomenon". *Earth Surface Processes and Landforms*. Vol. 36, pp. 58–69. DOI: 10.1002/esp.2103.

Frey, P. and Tannou, S. (2000). "Experimental study on bed load control in torrents by open slit dams". Conference on water engineering and water resources planning and management Special symposium on sedimentation engineering. Minneapolis, USA: ASCE. DOI: 10.1061/40517(2000)258.

Frey, P., Tannou, S., Tacnet, J., Richard, D., and Koulinski, V. (1999). "Interactions Ecoulements torrentiels - Ouvrages terminaux de plages de dépôt [Interactions between torrential flows and open check dams]". Tech. rep. (In French). Pôle grenoblois d'Etudes et de Recherche pour la prévention des risques naturels.

Frisi, P. (1770). "A Treatise on Rivers and Torrents; with the Method of Regulating Their Course and Channels". (English traduction of 1861 by John GARSTIN). London: J. Weale, p. 226.

Fryirs, K. (2013). "(Dis)Connectivity in catchment sediment cascades: A fresh look at the sediment delivery problem". *Earth Surface Processes and Landforms*. Vol. 38. no. 1, pp. 30–46. DOI: 10.1002/esp.3242.

Fujita, I., Muste, M., and Kruger, A. (1998). "Large-scale particle image velocimetry for flow analysis in hydraulic engineering applications." *Journal of Hydraulic Research*. Vol. 36(3), pp. 397–414.

Gaffiot, F. (1934). "Dictionnaire Latin-Français". Hachette.

Galia, T., Škarpich, V., Hradeckỳ, J., and Přibyla, Z. (2016). "Effect of grade-control structures at various stages of their destruction on bed sediments and local channel parameters". *Geomorphology*. Vol. 253, pp. 305–317.

Gamper, C., Thöni, M., and Weck-Hannemann, H. (2006). "A conceptual approach to the use of Cost Benefit and Multi Criteria Analysis in natural hazard management". *Natural Hazards and Earth System Science*. Vol. Vol. 6. no. 2, pp 293–302.

Garcìa, M., MacArthur, R., French, R., Miller, J., Bradley, J., Grindeland, T., and Hadley, H. (2008). "Sedimentation engineering process measurements, modeling and practices". Sedimentation Engineering. Ed. by M. Garcia. (Manual revised in 2007). ASCE. Chap. 19 - Sedimentation Hazards, pp. 885–936. DOI: 10.1061/9780784408148.ch19.

García-Ruiz, J., Alatorre, L., Gómez-Villar, A., and Beguería, S. (2013). "Check Dams, Morphological Adjustments and Erosion Control in Torrential Streams". Ed. by C. Conesa-Garcia and M. Lenzi. Hauppauge, NY: Nova Science Publishers, Inc. Chap. Upstream and downstream effects of check dams in braided rivers, central pyrenees, pp. 307–322.

Garcia, M. (2008). "Sedimentation engineering process measurements, modeling and practices". Sedimentation Engineering. Ed. by M. Garcia. (Manual revised in 2007). ASCE. Chap. 2 - Sediment transport and Morphodynamics, pp. 21–163. DOI: 10.1061/9780784408148.ch2.

Garcìa-Ruiz, J. M., White, S., Martí Bono, C. E., Valero-Garcés, B. L., Errea, M. P., Gòmez-Villar, A., et al. (1996). "La catástrofe del barranco de Arás (Biescas, Pirineo aragonés) y su contexto espacio-temporal". I.S.B.N. 84-921842-1-3 (in Spanish). CSIC-Instituto Pirenaico de Ecologìa (IPE), p. 52.

Gaudio, R., Marion, A., and Bovolin, V. (2000). "Morphological effects of bed sills in degrading rivers". *Journal of Hydraulic Research*. Vol. 38. no. 2, pp. 89–96.

Gems, B., Wörndl, M., Gabl, R., Weber, C., and Aufleger, M. (2014). "Experimental and numerical study on the design of a deposition basin outlet structure at a mountain debris cone". *Natural Hazards and Earth System Science*. Vol. 14. no. 2, pp. 175–187. DOI: 10.5194/nhess-14-175-2014.

Gessese, A., Sellier, M., Van Houten, E., and Smart, G. (2011). "Reconstruction of river bed topography from free surface data using a direct numerical approach in one-dimensional shallow water flow". *Inverse Problems*. Vol. 27. no. 2, p. 12.

Gessese, A., Smart, G., Heining, C., and Sellier, M. (2013). "One-dimensional bathymetry based on velocity measurements". *Inverse Problems in Science and Engineering*. Vol. 21. no. 4, pp. 704–720.

Ghilardi, T., Boillat J.-L. Schleiss, A. J. D. M. G., and Bovier, S. (2012). "Gestion du risque d´inondation sur l´Avançon par rétention de sediments - optimisation sur modèle physique [Flood risk management of

the Avançon river by means of sediment retention - physical model based study]". INTERPRAEVENT Conference Proceedings. (In French), pp. 687–698.

Ghilardi, T, Franca, M., and Schleiss, A. (2014a). "Bulk velocity measurements by video analysis of dye tracer in a macro-rough channel". *Measurement Science and Technology*. Vol. 25. no. 3, pp. 1–11.

Ghilardi, T., Franca, M. J., and Schleiss, A. J. (2014b). "Bed load fluctuations in a steep channel". *Water Resources Research*. Vol. 50. no. 8, pp. 6557–6576.

Glassey, T. (2010). "EPFL Master of Advanced Studies (MAS) in Hydraulic Engineering - Edition 2007 - 2009". Ed. by P. D. A. Schleiss. (Ms Thesis abstract). Lausanne: LCH. Chap. Check dams in the debris flow context of Illgraben river (VS), pp. 111–120.

Gomez, B., Banbury, K., Marden, M., Trustrum, N., Peacock, D., and Hoskin, P. (2003). "Gully erosion and sediment production: Te Weraroa Stream, New Zealand". *Water Resources Research*. Vol. 39. no. 7, ESG31–ESG37.

Grant, G. (1997). "Critical flow constrains flow hydraulics in mobile-bed streams: A new hypothesis". *Water Resources Research*. Vol. 33. no. 2, pp. 349–358.

Gras, S. (1848). "Annales des Mines". Ed. by M. des Travaux Publiques. Vol. 14. no. 4. (In French). Administration générale des Ponts et Chaussées et des Mines. Chap. Considérations sur les anciens lits de déjection des torrents des alpes et sur leur liaison avec le phénomène erratique, p. 21. DOI: 10.3931/e-rara-16677.

Gras, S. (1850). "Exposé d'un système de défense des cours d'eau torrentiels des Alpes et application au torrent de la Romanche dans le département de l'Isère." Ed. by Carilian-Gœuri and V. Dalmont. (In French). Grenoble: Charles Vellot, 112 p. DOI: 10.3931/e-rara-16678.

Gras, S. (1857). "Etudes sur les torrents des Alpes". Ed. by V. Dalmont. (In French). Paris: F.Savy, p. 108. DOI: 10.3931/e-rara-16676.

Greminger, P. e. a. (2005). "RiskPlan LearnRisk - Pragmatisches Risikomanagement - Im Dialog zu mehr Sicherheit." Tech. rep. (in German). Bern: BABS, BUWAL, BWG.

Gruffaz, F (1996). "Etude de description et analyse des plages de dépôt torrentilles réalisées dans les Alpes et Pyrénées Françaises". Tech. rep. no. Bilan d'étape. (In French). RTM.

Hall, M. (2005). "Earth Repair: A Transatlantic History of Environmental Restoration". Charlottesville and London: University of Virginia Press.

Hampel, R. (1975). "Bedeutung wechselnder Geschiebebelastung für Geschiebebilanzen der Wildbachverbauungen." INTERPRAEVENT Conference proceedings. Vol. 2. (In German), pp. 65–71.

Harvey, A. (2012). "The coupling status of alluvial fans and debris cones: A review and synthesis". *Earth Surface Processes and Landforms*. Vol. 37. no. 1, pp. 64–76. DOI: 10.1002/esp.2213.

Hasegawa, Y., Oda, A., Mizuyama, T., Izumi, I., and Abe, H. (2004). "Evaluation of the function of slit sabo dams through hydraulic model experiments". INTERPRAEVENT Conference Proceedings.

Hasegawa, Y., Sugiura, N., Shouzawa, M., and Mizuyama, T. (2010). "An investigation of measures against woody debris through hydraulic model expriments". INTERPRAEVENT Conference Proceedings. Pp. 135 –143.

Hauet, A., Jodeau, M., Le Coz, J., Marchand, B., Die Moran, A., Le Boursicaud, R., and Dramais, G. (2014). "Application of the LSPIV method for the measurement of velocity fields and flood discharges in reduced scale model and in rivers [Application de la méthode LSPIV pour la mesure de champs de vitesse et de débits de crue sur modèle réduit et en rivière]". French. *Houille Blanche*. no. 3, pp. 16–22. DOI: 10.1051/lhb/2014024.

Hübl, J. and Fiebiger, G. (2005). "Debris-flow hazards and related phenomena". Ed. by M. Jakob and O. Hungr. Springer. Chap. 18 - Debris-flow mitigation measures, pp. 445–487. DOI: 10.1007/3-540-27129-5_18.

Hübl, J and Suda, J (2008). "Debris flow mitigation measures in Austria". Debris Flows: Disasters, Risk, Forecast, Protection. Ed. by S. Institute. Vol. Pyatigorsk, Russia, 22-29 September 2008. Pyatigorsk.

Hübl, J., Holzinger, G., Klaus, W., and Skolaut, C. (2003). "Literaturstudium und Zusammenstellung vorhandener Ansätze zu kronenoffenen Sperren". Tech. rep. no. WLS 50 / Band 1. p. 44 (In German). Universität für Bodenkultur Wien.

Hübl, J., Strauss, A., Holub, M., and Suda, J (2005). "Structural mitigation measures". Proceedings zum 3rd Probabilistic Workshop: Technical Systems + Natural Hazards, 24-25 Nov. Wien.

Heede, B. H. (1960). "A study of early gully-control structures in the Colorado Front Range." Tech. rep. no. 55. 45p. Rocky Mountain Forest and Range Experiment Station.

Heede, B. H. (1967). "Gully Development and control in the Rocky mountain of Colorado." PhD thesis. Colorado State University.

Heede, B. H. (1978). "Designing gully control systems for eroding watersheds". *Environmental Management*. Vol. 2. no. 6, pp. 509–522.

Heede, B. H. (1982). "Gully control: Determining treatment priorities for gullies in a network". *Environmental Management*. Vol. 6. no. 5, pp. 441–451. DOI: 10.1007/BF01871892.

Heede, B. H. (1986). "Designing For Dynamic Equilibrium In Streams". *Water Resources Bulletin*. Vol. 22. no. 3, pp. 351–357.

Heller, V. (2011). "Scale effects in physical hydraulic engineering models". *Journal Of Hydraulic Research*. Vol. 49. no. 3, pp. 293–306. DOI: 10.1080/00221686.2011.578914.

Heumader, J (2000). "Technical debris flow countermeasures in Austria-A review". Second International Congress on Debris Flows Hazard Mitigation: mechanics, prediction and assessment. Rotterdam: Balkema, pp. 553–564.

Heyman, J., Mettra, F., Ma, H., and Ancey, C. (2013). "Statistics of bedload transport over steep slopes: Separation of time scales and collective motion". *Geophysical Research Letters*. Vol. 40. no. 1, pp. 128–133. DOI: 10.1029/2012GL054280.

Hotchkiss, R. H. and Parker, G. (1991). "Shock fitting of aggradational profiles due to backwater". *Journal of Hydraulic Engineering*. Vol. 117. no. 9, pp. 1129–1144.

Hughes, J. D. and Thirgood, J. (1982). "Deforestation, erosion, and forest management in ancient Greece and Rome". *Journal of Forest History*. Vol. 26. no. 2, pp. 60–75.

Hungr, O., Morgan, G., and Kellerhals, R. (1984). "Quantitative analysis of debris torrent hazards for design of remedial measures." *Canadian Geotechnical Journal*. Vol. 21. no. 4, pp. 663–677.

Hungr, O. (2005). "Debris-flow hazards and related phenomena". Ed. by M. Jakob and O. Hungr. Springer. Chap. 2-Classification and terminology, pp. 9–23. DOI: 10.1007/3-540-27129-5_2.

Hungr, O., Leroueil, S., and Picarelli, L. (2014). "The Varnes classification of landslide types, an update". *Landslides*. Vol. 11. no. 2, pp. 167–194. DOI: 10.1007/s10346-013-0436-y.

Hunzinger, L. (2014). "Freeboard analysis in river engineering and flood mapping-new recommendations". Special Session on Swiss Competences in River Engineering and Restoration of the 7th International Conf. on Fluvial Hydraulics, RIVER FLOW 2014. Pp. 31–37.

Hunzinger, L. and Zarn, B. (1996). "Geschiebetransport und Ablagerungsprozesse in Wildbachschalen. [Sediment transport and aggradation processes in rigid torrent channels]". INTERPRAEVENT Conference Proceedings. Vol. 4. (In German), pp. 221 –230.

Hunzinger, L. (2004). "Flussaufweitungen: Möglichkeiten und Grenzen [River widenings: possibilities and limits]". *Wasser, Energie, Luft*. Vol. 96 (9/10). (In German), pp. 243–249.

Ikeya, H (1985). "Study on sediment control effect of open dams". International symposium on Erosion, Débris Flow and Disaster Prevention. Tokyo: Japan Erosion Control Engineering Society, pp. 401–406.

Ikeya, H. (1989). "Debris flow and its countermeasures in Japan". *Bulletin - International Association of Engineering Geology*. Vol. 40. no. 1, pp. 15–33.

IRASMOS (2008). "Recommendations for future installation and implementation of countermeasures against rapid mass movements". Tech. rep. no. D2.3. Integral Risk Management of Extremely Rapid Mass Movements project. WSL Swiss Federal Institute for Snow and Avalanche Research.

Iroume, A. and Gayoso, J. (1991). "La pendiente de los depositos en los torrentes del cerro Divisadero, Coyhaique, Chile". *Bosque*. Vol. 12. no. 1. (In Spanish), pp. 37–42.

Ishikawa, N., Fukawa, G., Katsuki, S., and T., Y. (2004). "Catch Effect of Debris Flow for the Open Type Steel Check Dam by Physical and Numerical Modeling". INTERPRAEVENT Conference Proceedings. Vol. 3. no. VII, pp. 153–163.

Ishikawa, N., Shibuya, H., Katsuki, S., and Mizuyama, T (2014). "Protective steel structures against wooden debris hazards". 6th International Conference on Protection of Structures against Hazards Conf. Proceedings. Singapore: CI-Premier, pp. 1–14.

Ishikawa, Y. and Mizuyama, T. (1988). "An Experimental study of permeable sediment control dams as a countermeasure against floating logs". 6th Congress Asian and Pacific Regional Division - IAHR. Dept. of Civil Engineering, Kyoto University. Kyoto.

Ishikawa, Y, Osanai, N, Koizumi, Y, Takezaki, S, and Matsumura, K (1996). "A method of planning and designing sediment retarding basins". INTERPRAEVENT Conference Proceedings.

Itoh, T., Horiuchi, S., Akanuma, J.-I., Kaitsuka, K., Kuraoka, S., Morita, T., Sugiyama, M., and Mizuyama, T. (2011). "Fundamental hydraulic flume tests focused on sediment control function using a grid-type high dam". Italian Journal of Engineering Geology and Environment. Sapienza Università Editrice. Roma, pp. 1051–1061. DOI: 10.4408/IJEGE.2011-03.B-114.

Itoh, T., Horiuchi, S., Mizuyama, T., and Kaitsuka, K. (2013). "Hydraulic model tests for evaluating sediment control function with a grid-type Sabo dam in mountainous torrents". *International Journal of Sediment Research*. Vol. 28. no. 4, pp. 511–522. DOI: 10.1016/S1001-6279(14)60009-3.

Jaeggi, M (2007). "Sediment transport capacity of pressure flow at bridges". Proceeding of the 32nd IAHR World Congress. Ed. by G. D. Silvio and S. Lanzoni. Vol. A.2.b linear transport. Venice: CORILA, pp. 1–7.

Jaeggi, M. N. and Pellandini, S. (1997). "Torrent check dams as a control measure for debris flows". Recent Developments on Debris Flows. Ed. by A. Armanini and M. Michiue. Vol. 64. Lecture Notes in Earth Sciences. Springer Berlin Heidelberg, pp. 186–207. DOI: 10.1007/BFb0117769.

Jaeggi, M. (1992). "Dynamics of Gravel-Bed Rivers". Ed. by P. Billi, R. Hey, C. Thorne, and P. Tacconi. Chichester: John Wiley and Sons. Chap. 30 - Effect of engineering solutions on sediment transport, pp. 593–605.

Jail, M. and Martin, N (1971). "La trombe d'eau du 5 juillet 1971 dans la basse vallée de l'Isère". *Revue de géographie alpine*. Vol. 59. no. 4. (In French), pp. 593–600. DOI: 10.3406/rga.1971.1458.

JCGM (2008). "Evaluation of measurement data — Guide to the expression of uncertainty in measurement". Tech. rep. no. JCGM 100:2008. 120p.

Jerolmack, D. and Paola, C. (2010). "Shredding of environmental signals by sediment transport". *Geophysical Research Letters*. Vol. 37. no. 19, pp. 1–5. DOI: 10.1029/2010GL044638.

Jodeau, M., Hauet, A., Paquier, A., Le Coz, J., and Dramais, G. (2008). "Application and evaluation of LS-PIV technique for the monitoring of river surface velocities in high flow conditions". *Flow Measurement and Instrumentation*. Vol. 19. no. 2, pp. 117–127. DOI: 10.1016/j.flowmeasinst.2007.11.004.

Jodeau, M., Hauet, A., and Le Coz, J. (2013). "Fudaa-LSPIV 1.3.2 - Guide d'utilisation". Tech. rep. no. v04 du 17-09-2013. 26pp. (In French). EDF R&D, EDF DTG, Irstea.

Johnson, P. A. and McCuen, R. H. (1989). "Slit dam design for debris flow mitigation". *Journal of Hydraulic Engineering*. Vol. 115. no. 9, pp. 1293–1296. DOI: 10.1061/(ASCE)0733-9429(1989)115:9(1293).

Jordan, F, Jaeggi, M, and Nigg, U (2003). "Modélisation physique d'un piège à graviers, le cas du Baltschiederbach [Small scale model of a sediment trap, the Baltschiederbach case study]". *Wasser Energie Luft*. Vol. 95. no. 9/10. (In French), pp. 283–290.

Jordan, F, Jaeggi, M, and Nigg, U (2004). "Optimisation d'un piège a graviers par modélisation physique sur le Baltschiederbach en Valais (CH) [Gravel trap Optimisation by small scale model of the Baltschiederbach in the Valais (CH)]". INTERPRAEVENT Conference Proceedings. Vol. VII. (In French), pp. 181–191.

Jouyne, Z. (1850). "Reboisement des montagnes: Reboisement, difficultés, causes des inondations et moyens de les prévenir". 169 p. Digne, France: Repos.

JSA (2003). "SABO in Japan". Brochure edited for the 2012 Interpraevent conf. (In Japanese and English). Japan Sabo Association, pp. 1–113.

JSA (2012). "SABO in Japan - Facing the challenge of National land conserve". (In Japanese and English). Japan Sabo Association, pp. 1–35.

Julien, P. (1998). "Erosion and Sedimentation". Cambridge, New York, Melbourne: Cambridge University Press.

Kaitna, R, Chiari, M., Kerschbaumer, M., Kapeller, H., Zlatic-Jugovic, J., Hengl, M., and Hübl, J. (2011). "Physical and numerical modelling of a bedload deposition area for an Alpine torrent". *Natural Hazards and Earth System Science*. Vol. 11. no. 6, pp. 1589–1597. DOI: 10.5194/nhess-11-1589-2011.

Kaitna, R. and Hübl, J. (2013). "Advances in Global Change Research". Dating Torrential Processes on Fans and Cones. Ed. by M. Schneuwly-Bollschweiler, M. Stoffel, and F. Rudolf-Miklau. Vol. 47. Springer Netherlands. Chap. 7-Silent Witnesses For Torrential Processes, pp. 111–130. DOI: 10.1007/978-94-007-4336-6.

Kalaora, B. and Savoye, A. (1986). "La forêt pacifiée. Sylviculture et sociologie au XIXe siècle." 134 p. France: L'Harmattan.

Kamibayashi, Y. (2009). "Two Dutch Engineers and Improvements of Public Works in Japan". Proceedings of the Third International Congress on Construction History. Berlin: Neunplus1, pp. 879–888.

Kantoush, S., De Cesare, G., Boillat, J., and Schleiss, A. (2008). "Flow field investigation in a rectangular shallow reservoir using UVP, LSPIV and numerical modelling". *Flow Measurement and Instrumentation*. Vol. 19, pp. 139–144.

Kantoush, S. A., Schleiss, A. J., Sumi, T., and Murasaki, M. (2011). "LSPIV implementation for environmental flow in various laboratory and field cases". *Journal of Hydro-environment Research*. Vol. 5. no. 4, pp. 263–276.

Kasai, S, Ohgi, Y, Mizoguchi, I, Matsuda, A, Aramaki, H, and Tanami, M (1996). "Structural characteristics of wood-debris entrapment facilites". INTERPRAEVENT Conference Proceedings.

Keiler, M. (2011). "Geomorphology and complexity - Inseparably connected?" *Zeitschrift fur Geomorphologie*. Vol. 55. no. SUPPL. 3, pp. 233–257. DOI: 10.1127/0372-8854/2011/0055S3-0060.

Kim, Y., Nakagawa, H., Kawaike, K., and Zhang, H. (2012). "Numerical and experimental study on Debris-flow breaker". *Annuals of Disaster Prevention Research Institute of Kyoto University*. Vol. 55 B, pp. 471–481.

King, J. G., Emmett, W. W., Whiting, P. J., Kenworthy, R. P., and Barry, J. J. (2004). "Sediment transport data and related information for selected coarse-bed streams and rivers in Idaho". Tech. rep. no. RMRS-GTR-131. 26p. Fort Collins, CO: U.S. Department of Agriculture, Forest Service, Rocky Mountain Research Station.

Kleinhans, M. G., Dijk, W. M. van, Lageweg, W. I. van de, Hoyal, D. C., Markies, H., Maarseveen, M. van, Roosendaal, C., Weesep, W. van, Breemen, D. van, Hoendervoogt, R., and Cheshier, N. (2014). "Quantifiable effectiveness of experimental scaling of river- and delta morphodynamics and stratigraphy". *Earth-Science Reviews*. Vol. 133. no. 0, pp. 43 –61. DOI: 10.1016/j.earscirev.2014.03.001.

Knauss, J (1995). "Treibholzfänge am Lainbach in Benediktbeuren und am Arzbach (ein neues Element im Wildbachausbau) [Driftwood catches on Lainbach Benediktbeuren and on Arzbach (a new element in a stream configuration)]". Tech. rep. no. 76. S. 23-66 (In German). München: Versuchsanstalt Obernach und des Lehrstuhls für Wasserbau und Wasserwirtschaft - Technical University of Munich.

Kostadinov, S. (1993). "Possibility of Assessment of the Slope of Siltation Based on the Some Hydraulic Characteristics of the Torrential Flows". *Journal of the Japan Society of Erosion Control Engineering*. Vol. 45. no. 5, pp. 28–33. DOI: 10.11475/sabo1973.45.5_28.

Kostadinov, S (2007). "Erosion and torrent control in Serbia: hundred years of experiences". International conference "Erosion and torrent control as a factor in sustainable river basin management". Key note paper, (Abstract Book, Full paper on CD). Belgrade, pp. 1–17.

Kostadinov, S. and Dragović, N. (2013). "Check dams, morphological adjustments and erosion control in torrential streams". Ed. by C. Conesa-Garcia and M. Lenzi. Hauppauge, NY: Nova Science Publishers, Inc. Chap. Check dams in the torrent control practice in small mountainous catchments, pp. 63–88.

Kostadinov, S., Dragovic, N., Zlatic, M., and Todosijevic, M. (2011). "Natural effect of classical check dams in the torrents of the river toplica drainage basin". *Fresenius Environmental Bulletin*. Vol. 20. no. 5, pp. 1102 –1108.

Koulinski, V (1993). "Etude de la formation d'un lit torrentiel par confrontation d'essais sur modèle réduit et d'observations de terrain [Study of torrent bed formation through the confrontation of small scale model

results and field survey]". Cemagref - Série Etude Num15 - 1994 - ISBN 2-853662-398-X (In french). PhD Thesis. INPG.

Koulinski, V (2010). "Etude d'optimisation de la gestion de la plage de dépôt RTM de la Ravoire de Pontamafrey". Tech. rep. 63 p. (In French). Chambéry: Service RTM de Savoie.

Koulinski, V. and Richard, P. (2008). "Apports des modéles réduits pour la gestion des sédiments et des flottants en torrents et rivières torrentielles [Small scale models contribution to sedimentation processes and floating debris transit of torrential rivers]". French. *Houille Blanche*. Vol. 4. no. 4, pp. 90–97. DOI: 10.1051/lhb:2008044.

Koulinski, V., ARTELIA, and RTM (2011). "Étude sur modèle réduit de la plage de dépôt du Chagnon". Tech. rep. (In French). Commune de Vars.

Koutsoyiannis, D. (2002). "The Hurst phenomenon and fractional Gaussian noise made easy [Le phénomène de Hurst et le bruit fractionnel gaussien rendus faciles dans leur utilisation]". English; French. *Hydrological Sciences Journal*. Vol. 47. no. 4, pp. 573–596.

Koutsoyiannis, D. and Montanari, A. (2007). "Statistical analysis of hydroclimatic time series: Uncertainty and insights". *Water Resources Research*. Vol. 43. no. 5, pp. 1–9. DOI: 10.1029/2006WR005592.

Koutsoyiannis, D., Zarkadoulas, N., Angelakis, A., and Tchobanoglous, G. (2008). "Urban water management in Ancient Greece: Legacies and lessons". *Journal of water resources planning and management*. Vol. 134. no. 1, pp. 45–54.

Kramer, N. and Wohl, E. (2014). "Estimating fluvial wood discharge using time-lapse photography with varying sampling intervals". *Earth Surface Processes and Landforms*. Vol. 39. no. 6, pp. 844–852. DOI: 10.1002/esp.3540.

Kronfellner-Kraus, G. (1983). "Torrent Erosion And Its Control In Europe And Some Research Activities In This Field In Austria". *Sabo Gakkaishi - Journal of the Japan Society of Erosion Control Engineering*. Vol. 35. no. 3, pp. 33–44. DOI: 10.11475/sabo1973.35.3_33.

Kuhnle, R. A. and Southard, J. B. (1988). "Bed load transport fluctuations in a gravel bed laboratory channel". *Water Resources Research*. Vol. 24. no. 2, pp. 247–260.

Kuss, C. (1900a). "Restauration et conservation des terrains en montagne. Éboulements, glissements et barrages". Ed. by M. de l'Agriculture. Administration des eaux et forêts. Exposition universelle internationale de 1900, à Paris. (In French). Imprimerie Nationale, p. 61.

Kuss, C. (1900b). "Restauration et conservation des terrains en montagne. Les Torrents glaciaires". Ed. by M. de l'Agriculture. Administration des eaux et forêts. Exposition universelle internationale de 1900, à Paris. (In French). Imprimerie Nationale, p. 88.

L.A. County (1979). "Debris Dams and Basins Design Manual". Ed. by J. L. Easton, C. W. Hallstrom, and K. Senzaki. 2250 Alcazar Street, Los Angeles, California: Los Angeles County Department of Public Works, p. 76.

L.A. County (2006). "Sedimentation Manual - 2nd Edition". Ed. by I. Nasseri, S. Klippel, B. Willardson, L. Soriano, M. J., and M. Gaplandzhyan. 900 South Fremont Avenue Alhambra, California 91803: Los Angeles County Department of Public Works, p. 221.

Lala Rakotoson, S. G. (1994). "Etude de l'influence de la largeur disponible à l'écoulement sur le charriage torrentiel [Study of the flow width influence on the torrential bed-load transport]". Mémoire de DEA. Université Joseph FOURIER de Grenoble / Cemagref.

Lamand, E., Piton, G., and Recking, A. (2015). "Hydrologie et hydraulique torrentielle, étude d'un cas pratique: la Roize". Tech. rep. (In French). IRSTEA.

Lamb, M. P., Dietrich, W. E., and Venditti, J. G. (2008). "Is the critical Shields stress for incipient sediment motion dependent on channel-bed slope?" *Journal of Geophysical Research: Earth Surface*. Vol. 113. no. F2. DOI: 10.1029/2007JF000831.

Lancaster, S. T., Hayes, S. K., and Grant, G. E. (2001). "Geomorphic processes and riverine habitat, (4)". Ed. by J. M. Dorava, D. R. Montgomery, B. B. Palcsak, and F. A. Fitzpatrick. Washington, DC.: American Geophysical Union. Chap. Modeling Sediment and Wood Storage and Dynamics in Small Mountainous Watersheds, pp. 85–102. DOI: 10.1029/WS004p0085.

Lane, E. W. (1955). "Importance of fluvial morphology in hydraulic engineering". *Journal of the Hydraulics Division of the American Society of Civil Engineers*. Vol. 81. paper no. 745, pp. 1–17.

Lange, D. and Bezzola, G. (2006). "Schwemmholz - Probleme und Lösungsansätze [Driftwood - Problems and solutions]". Tech. rep. no. 188. 125p. ISSN 0374-0056. ETH-Zentrum - Zürich: Versuchsanstalt für Wasserbau Hydrologie und Glaziologie der Eidgenössischen Technischen Hochschule (VAW) Zürich.

Larcher, M. and Armanini, A. (2000). "Design criteria of slit check dams and downstream channels for debris flows". Proceedings International Workshop The debris flow disaster of december 1999 in Venezuela. Caracas: Universidad Central de Venezuela.

LCH (2011). "HWS Gampel-Bratsch - Geschiebesammler Tschingelbach: Hydraulische Modellversuche". Tech. rep. no. 01/2011. p. 56+App. (In German). EPFL.

Le Boursicaud, R., Pénard, L., Hauet, A., Thollet, F., and Le Coz, J. (2016). "Gauging extreme floods on YouTube: Application of LSPIV to home movies for the post-event determination of stream discharges". *Hydrological Processes*. Vol. 30. no. 1, pp. 90–105.

Le Coz, J., Hauet, A., Pierrefeu, G., Dramais, G., and Camenen, B. (2010). "Performance of image-based velocimetry (LSPIV) applied to flash-flood discharge measurements in Mediterranean rivers". *Journal of Hydrology*. Vol. 394, pp. 42–52.

Le Coz, J., Jodeau, M., Hauet, A., Marchand, B., and Le Boursicaud, R. (2014). "Image-based velocity and discharge measurements in field and laboratory river engineering studies using the free FUDAA-LSPIV software". Proceedings of the International Conference on Fluvial Hydraulics, RIVER FLOW 2014,. Lausanne: CRC Press/Balkema, pp. 1961–1967.

Le Guern, J. (2014). "Msc. Thesis manuscripts: Modélisation physique des plages de dépôt : analyse de la dynamique de remplissage [Small scale model of sediment traps: filling dynamic analysis]". Univ. François Rablais - Tours / Laboratoire IRSTEA - Grenoble (In French). MA thesis.

Leduc, P, Ashmore, P, and Gardner, J. (2015). "Grain sorting in the morphological active layer of a braided river physical model". *Earth Surface Dynamics*. Vol. 3. no. 4, p. 577. DOI: 10.5194/esurf-3-577-2015.

Leduc, P. (2013). "Étude expérimentale de la dynamique sédimentaire des rivières en tresses". 234 p. (in French). PhD thesis. Université de Grenoble.

Lefebvre, B. and Demmerle, D. (2004). "Protection du village du Tour contre le glissement des Posettes à l'amont de la vallée de Chamonix Mont-Blanc [Protection of the Le Tour village against the Posettes landslide in the upstream part of Chamonix Valley]". French. *Houille Blanche*. Vol. 3i. no. 3. (In French), pp. 31–36. DOI: 10.1051/lhb:200403003.

Lefort, P (1996). "Transports solides dans le lit des cours d'eau [Solid transport in watercourses' beds]". Note de cours (In French). Ecole Nationale Superieure d'Hydraulique et de Mecanique de Grenoble - Institut National Polytechnique De Grenoble, 225 p.

Legout, C., Darboux, F., Nédélec, Y., Hauet, A., Esteves, M., Renaux, B., Denis, H., and Cordier, S. (2012). "High spatial resolution mapping of surface velocities and depths for shallow overland flow". *Earth Surface Processes and Landforms*. Vol. 37. no. 9, pp. 984–993. DOI: 10.1002/esp.3220.

Leitgeb, M. (2002). "Integrated Watershed Management on a large-scale base". Proceedings of the European Regional Workshop: Preparing for the next generation of watershed management programmes and projects. Ed. by M. Achouri. and L. Tennyson. Roma: FAO, pp. 101–105.

León Marín, V. M. (2011). "Evaluación de los procesos de sedimentación de las presas para el control de aludes torrenciales en las quebradas San José de Galipán, Camurí Chico, Cerro Grande, Camurí Grande y Migueleno, del estado Vargas". 171 p. (In Spanish). MA thesis. Caracas: Universidad Central de Venezuela.

Lencastre, A. (1983). "Hydraulique générale". (In French). Paris: Eyrolles, p. 633.

Lenzi, M. A., Marion, A., and Comiti, F. (2003a). "Local scouring at grade-control structures in alluvial mountain rivers". *Water Resources Research*. Vol. 39. no. 7, pp. 1–12. DOI: 10.1029/2002WR001815.

Lenzi, M. (2001). "Step-pool evolution in the Rio Cordon, Northeastern Italy". *Earth Surface Processes and Landforms*. Vol. 26. no. 9, pp. 991–1008. DOI: 10.1002/esp.239.

Lenzi, M. (2002). "Stream bed stabilization using boulder check dams that mimic step-pool morphology features in Northern Italy". *Geomorphology*. Vol. 45. no. 3-4, pp. 243–260. DOI: 10.1016/S0169-555X(01)00157-X.

Lenzi, M., D'Agostino, V., and Billi, P. (1999). "Bedload transport in the instrumented catchment of the Rio Cordon. Part I: Analysis of bedload records, conditions and threshold of bedload entrainment". *Catena*. Vol. 36. no. 3, pp. 171–190. DOI: 10.1016/S0341-8162(99)00016-8.

Lenzi, M., Marion, A., Comiti, F., and Gaudio, R. (2002). "Local scouring in low and high gradient streams at bed sills". *Journal of Hydraulic Research*. Vol. 40. no. 6, pp. 731–739.

Lenzi, M., Marion, A., and Comiti, F. (2003b). "Interference processes on scouring at bed sills". *Earth Surface Processes and Landforms*. Vol. 28. no. 1, pp. 99–110. DOI: 10.1002/esp.433.

Lenzi, M., Mao, L., and Comiti, F. (2004). "Magnitude-frequency analysis of bed load data in an Alpine boulder bed stream". *Water Resources Research*. Vol. 40. no. 7. DOI: 10.1029/2003WR002961.

Liébault, F. and Piégay, H. (2002). "Causes of 20th century channel narrowing in mountain and piedmont rivers of Southeastern France". *Earth Surface Processes and Landforms*. Vol. 27. no. 4, pp. 425–444. DOI: 10.1002/esp.328.

Liébault, F. and Zahnd, E. (2001). "La Restauration des Terrains en Montagne dans le Diois et les Baronnies". *Terres Voconces*. Vol. 3. (In French), pp. 27–48.

Liébault, F., Gomez, B., Page, M., Marden, M., Peacock, D., Richard, D., and Trotter, C. (2005). "Land-use change, sediment production and channel response in upland regions". *River Research and Applications*. Vol. 21. no. 7, pp. 739–756. DOI: 10.1002/rra.880.

Liébault, F., Piégay, H., Frey, P., and Landon, N. (2008). "Tributaries and the Management of Main-Stem Geomorphology". John Wiley Sons, Ltd, pp. 243–270. DOI: 10.1002/9780470760383.ch12.

Liébault, F., Peteuil, C, Jousse, C., Fragnol, B., Theule, J., Berger, F., Lopez Saez, J., Gotteland, A., Jaboyedoff, M., and Loye, A. (2010a). "L'utilisation des plages de dépôts pour la mesure du transport solide torrentiel : applications dans le département de l'Isère". Tech. rep. no. Programme de recherche 2008. (in French). PGRN.

Liébault, F., Clément, P., Piégay, H., and Zahnd, E. (2010b). "Risques et territoires, Interroger et comprendre la dimension locale de quelques risques contemporains." Ed. by T. Coanus, J. Comby, F. Duchêne, and E. Martinais. (in French). Lavoisier. Chap. Gestion du risque ou gestion de l'environnement? Le cas des massifs du Diois et des Baronnies, Préalpes du Sud, France, pp. 47–57.

Liebault, F., Remaître, A., and Peteuil, C (2013). "Torrents et rivières de montagne - Dynamique et aménagement". Ed. by A. Recking, D. Richard, and G. Degoutte. (In French). Antony: QUAE. Chap. 1 - Géomorphologie des rivières de montagne, pp. 15–89.

Lien, H.-P. (2003). "Design of slit dams for controlling stony debris flows". *International Journal of Sediment Research*. Vol. 18. no. 1, p. 74.

Lilin, C. (1986). "Histoire de la restauration des terrains en montagne au 19e siècle". *Cah. ORSTOM, sér. Pédol.* Vol. 32. no. 2, pp 139–145.

Lin, B.-S., Yeh, C.-H., and Lien, H.-P. (2008). "The experimental study for the allocation of ground-sills downstream of check dams". *International Journal of Sediment Research*. Vol. 23. no. 1, pp. 28–43. DOI: 10.1016/S1001-6279(08)60003-7.

Lin, Y.-L., Lu, H.-S., and Omura, H. (2010). "Low check dam in early stage of erosion control history in taiwan". *INTERPRAEVENT*. Vol. 1, pp. 850–854.

Liu, C.-M. (1992). "The effectiveness of check dams in controlling upstream channel stability in northeastern Taiwan". Proc. of the Chengdu Symposium on Erosion, Debris Flows and Environment in Mountain Regions. Vol. 209. IAHS, pp. 423–428.

Logar, J., Fifer Bizjak, K., Kočevar, M., Mikoš, M., Ribičič, M., and Majes, B. (2005). "History and present state of the Slano Blato landslide". *Natural Hazards and Earth System Science*. Vol. 5. no. 3, pp. 447–457.

Lopez Saez, J., Corona, C., Stoffel, M., Gotteland, A., Berger, F., and Liébault, F. (2011). "Debris-flow activity in abandoned channels of the Manival torrent reconstructed with LiDAR and tree-ring data". *Natural Hazards and Earth System Science*. Vol. 11. no. 5, pp. 1247–1257. DOI: 10.5194/nhess-11-1247-2011.

Lorenzo-Trueba, J., Voller, V., and Paola, C. (2013). "A geometric model for the dynamics of a fluvially dominated deltaic system under base-level change". *Computers and Geosciences*. Vol. 53, pp. 39–47. DOI: 10.1016/j.cageo.2012.02.010.

López, J. L., Hernandez-Perez, D., and Courtel, F. (2010a). "Lecciones aprendidas del desastre de Vargas. Aportes científico-tecnológico y experiencias nacionales en el campo de la prevención y mitigación de riesgos." Ed. by J. L. López. (In Spanish). Fundación Polar / Universidad Central De Venezuela, Caracas - Venezuela. Chap. Monitoreo y evaluación del comportamiento de las presas de retención de sedimentos en el estado Vargas, pp. 479–459.

López, J. L., Falcón, M, and Muñoz, Z. (2010b). "Lecciones aprendidas del desastre de Vargas. Aportes científico-tecnológico y experiencias nacionales en el campo de la prevención y mitigación de riesgos." Ed. by J. L. López. (In Spanish). Fundación Polar / Universidad Central De Venezuela, Caracas - Venezuela. Chap. Cambios altimétricos y granulométricos debido a presas de control de sedimentos en ríos de montaña, pp. 277–290.

López, J. L., Hernandez-Perez, D., and Falcón, M (2010c). "Lecciones aprendidas del desastre de Vargas. Aportes científico-tecnológico y experiencias nacionales en el campo de la prevención y mitigación de riesgos." Ed. by J. L. López. (In Spanish). Fundación Polar / Universidad Central De Venezuela, Caracas - Venezuela. Chap. Efecto de las lluvias de Febrero del 2005 en las obras construidas en el Estado Vargas, pp. 441–458.

Luzian, R., Kohl, B., Bichler, I., Kohl, J., and Bauer, W. (2002). "Wildbäche und Muren: eine Wildbachkunde mit einer Übersicht von Schutzmaßnahmen der Ära Aulitzky". Bundesministerium für Land-und Forstwirtschaft, Umwelt und Wasserwirtschaft, Forstliche Bundesversuchsanstalt Waldforschungszentrum.

Maita, H (1993). "Influence of heterogeneous sediment transport on the function of sediment control of a check dam". Sediment Problems: Strategies for Monitoring, Prediction and Control Yokohama Symp. Conf. Proc.. no. 217. IAHS, pp. 277–277.

Malavoi, J., Garnier, C., Landon, N., Recking, A., and Baran, P. (2011). "Eléments de connaissance pour la gestion du transport solide en rivière." Ed. by V. Barre. (In French). Onema, p. 216.

Mao, L. (2012). "The effect of hydrographs on bed load transport and bed sediment spatial arrangement". *Journal of Geophysical Research F: Earth Surface*. Vol. 117. no. 3, pp. 1–16. DOI: 10.1029/2012JF002428.

Mao, L. and Lenzi, M. (2007). "Sediment of mobility and bedload transport conditions in an alpine stream". *Hydrological Processes*. Vol. 21. no. 14, pp. 1882–1891. DOI: 10.1002/hyp.6372.

Marchi, L. and Cavalli, M. (2007). "Procedures for the documentation of historical debris flows: Application to the Chieppena Torrent (Italian Alps)". *Environmental Management*. Vol. 40. no. 3, pp. 493–503. DOI: 10.1007/s00267-006-0288-5.

Margreth, S. and Romang, H. (2010). "Effectiveness of mitigation measures against natural hazards". *Cold Regions Science and Technology*. Vol. 64. no. 2, pp. 199–207. DOI: 10.1016/j.coldregions.2010.04.013.

Maricar, F. and Hashimoto, H. (2014). "A comparison of wood-sediment-water mixture flows at a closed type and an open type of check dams in mountain rivers". River Flow 2014 conference proceedings. London: Taylor Francis Group, pp. 711–716.

Marion, A., Lenzi, M., and Comiti, F. (2004). "Effect of sill spacing and sediment size grading on scouring at grade-control structures". *Earth Surface Processes and Landforms*. Vol. 29. no. 8, pp. 983–993. DOI: 10.1002/esp.1081.

Marion, A., Tregnaghi, M., and Tait, S. (2006). "Sediment supply and local scouring at bed sills in high-gradient streams". *Water Resources Research*. Vol. 42. no. 6. DOI: 10.1029/2005WR004124.

Marion, D. A. and Weirich, F. (2003). "Equal-mobility bed load transport in a small, step-pool channel in the Ouachita Mountains". *Geomorphology*. Vol. 55. no. 1, pp. 139–154. DOI: 10.1016/S0169-555X(03)00137-5.

Marsh, G. P. (1864). "Man and Nature; or, Physical geography as modified by human action". New York: Charles Scribner.

Martìn-Vide, J. and Andreatta, A. (2006). "Disturbance caused by bed sills on the slopes of steep streams". *Journal of Hydraulic Engineering*. Vol. 132. no. 11, pp. 1186–1194. DOI: 10.1061/(ASCE)0733-9429(2006)132:11(1186).

Martìn-Vide, J. and Andreatta, A. (2009). "Channel degradation and slope adjustment in steep streams controlled through bed sills". *Earth Surface Processes and Landforms*. Vol. 34. no. 1, pp. 38–47. DOI: 10.1002/esp.1687.

Martson, R., Bravard, J., and Green, T. (2003). "Impacts of reforestation and gravel mining on the Malnant River, Haute-Savoie, French Alps". *Geomorphology*. Vol. 55, pp. 65–74. DOI: 10.1016/S0169-555X(03)00132-6.

Masuko, K, Ohgi, Y, and Abe, S (1996). "Surveys on the efficiency of wood-debris entrapment facilites". INTERPRAEVENT Conference Proceedings.

Mathys, N., Lang, M., Sauquet, E., Cipriani, T., and Peteuil, C. (2013). "Torrents et Rivières de Montagne: dynamique et aménagement". Ed. by A. Recking, D. Richard, and G. Degoutte. (In French). Antony: QUAE. Chap. 2 - Hydrologie, pp. 81–138.

Mazzorana, B., Zischg, A., Largiader, A., and Hübl, J. (2009). "Hazard index maps for woody material recruitment and transport in alpine catchments". *Natural Hazards and Earth System Science*. Vol. 9. no. 1, pp. 197–209.

Mazzorana, B., Hübl, J., Zischg, A., and Largiader, A. (2011). "Modelling woody material transport and deposition in alpine rivers". *Natural Hazards*. Vol. 56. no. 2, pp. 425–449. DOI: 10.1007/s11069-009-9492-y.

Mazzorana, B., Comiti, F., Scherer, C., and Fuchs, S. (2012). "Developing consistent scenarios to assess flood hazards in mountain streams". *Journal of Environmental Management*. Vol. 94. no. 1, pp. 112–124. DOI: 10.1016/j.jenvman.2011.06.030.

Mazzorana, B., Trenkwalder-Platzer, H. J., Fuchs, S., and Hübl, J. (2014). "The susceptibility of consolidation check dams as a key factor for maintenance planning". *Österreichische Wasser-und Abfallwirtschaft*. Vol. 66. no. 5-6, pp. 214–216.

Mazzorana, B., Piton, G., Picco, L., Sodnik, J., Moser, M., Jager, G., Melhorn, S., Hubl, J., Chiari, M., Martin, T., Aufleger, M., Gems, B., and Strum, M. (2015). "Work Package 6 - Interactions with structures". Ed. by J. Sodnik, S. Rusjan, M. Kogoj, and M. Mikoš. SedAlp project - Alpine Space. Chap. 3.2 Guideline for planning/designing of efficient torrent control structures with low impact on sediment continuity between upstream torrential headwaters and downstream river reaches, pp. 71–111.

McCorriston, J. and Oches, E. (2001). "Two early Holocene check dams from Southern Arabia". *Antiquity*. Vol. 75. no. 290, pp. 675–676.

Mejean, S. (2015). "Msc Thesis: Caractérisation des conditions hydrauliques du piégeage de la charge sédimentaire grossière des torrents : Synthèse bilbiographique et expérimentations sur modèle physique d'une plage de dépôt [Characterization of the hydraulic conditions for trapping coarse sediment load in torrents: literature review and experiments on a sediment trap small scale model]". (In French). MA thesis. Grenoble INP - IRSTEA.

Melton, M. A. (1965). "The geomorphic and paleoclimatic significance of alluvial deposits in southern Arizona". *The Journal of Geology*. Pp. 1–38. DOI: 10.1086/627044.

Messines du Sourbier, J. (1939a). "Les calamités publiques en Savoie au cours de l'année 1938". *Revue de géographie alpine*. Vol. 27. no. 3. (In French), pp. 647–669. DOI: 10.3406/rga.1939.4019.

Messines du Sourbier, J. (1939b). "Nécrologie. Paul Mougin - Inspecteur général des Eaux et Forêts (1866-1939)". *Revue de géographie alpine*. Vol. 27. no. 4. (In French), pp. 899–904.

Messines du Sourbier, J. (1964). "Enquête sur la conservation et la restauration des terrains de montagne". Tableau II : situation au 1/01/1964 des grands travaux effectués dans les périmètres avec récapitulation par département et régions (In French). Paris: Administration des eaux et forêts.

Meunier, M (1989). "Essai de synthèse des connaissances en érosion et hydraulique torrentielle". *La Houille Blanche*. Vol. 5. (In French), pp. 361–376. DOI: 10.1051/lhb/1989040.

Meunier, M. (1991). "Éléments d'hydraulique torrentielle." Etudes: Montagne no. 1. 278 pp. (In French). Antony: Cemagref.

Meyer-Peter, E. and Müller, R (1948). "Formulas for bed-load transport". Proceedings of the 2nd Meeting of the International Association for Hydraulic Structures Research. Delft: IAHR, pp. 39–64.

Mizuyama, T. (1984). "Mechanism of the movement of grains and logs in debris flow". INTERPRAEVENT Conference Proceedings. Vol. 3, pp. 189 –196.

Mizuyama, T (2008). "Structural Countermeasures for Debris Flow Disasters". *International Journal of Erosion Control Engineering*. Vol. 1. no. 2, pp. 38–43.

Mizuyama, T and Fujita, M. (2000). "Sediment control with slit Sabo-dam." INTERPRAEVENT Conference Proceedings. Vol. 3, pp. 251 –258.

Mizuyama, T., Abe, S., and Ido, K. (1988). "Sediment controle by Sabo Dams with Slits and/or Large Drainage Conduits". 6th Congress Asian and Pacific Regional Division - IAHR. Dept. of Civil Engineering, Kyoto University. Kyoto.

Mizuyama, T., Kobashi, S., and Mizuno, H. (1996). "Development and improvement of open dams". INTERPRAEVENT Conference Proceedings. Vol. 5, pp. 59–65.

Molnar, P., Densmore, A. L., McArdell, B. W., Turowski, J. M., and Burlando, P. (2010). "Analysis of changes in the step-pool morphology and channel profile of a steep mountain stream following a large flood". *Geomorphology*. Vol. 124. no. 1, pp. 85–94. DOI: 10.1016/j.geomorph.2010.08.014.

Montgomery, D. and Buffington, J. (1997). "Channel-reach morphology in mountain drainage basins". *Geological Society of America Bulletin*. Vol. 109. no. 5, pp. 596–611. DOI: 10.1130/0016-7606(1997)109<0596:CRMIMD>2.3.CO;2.

Morris, G. L., Annandale, G., and Hotchkiss., R. (2008). "Sedimentation engineering process measurements, modeling and practices". Ed. by M. Garcia. Amer Soc Civil Engineer (ASCE) , Reston, USA. Chap. 12 - Reservoir sedimentation, pp. 579–612. DOI: 10.1061/9780784408148.ch12.

Moser, M. and Jäger, G. (2014). "Bedload Management of Torrents Experiences, Simulation Models and Laboratory Investigations to Improve Protection Systems". Engineering Geology for Society and Territory (IAEG Congress proceedings). Ed. by G. Lollino et al. Vol. 3. Springer International Publishing Switzerland, pp. 343–345. DOI: 10.1007/978-3-319-09054-2_72.

Mougin, P. (1900). "Restauration et conservation des terrains en montagne - consolidation des berges par dérivation d'un torrent (torrent de Saint Julien)". Ed. by M. de l'Agriculture. Direction générale des eaux et forêts. Exposition universelle internationale de 1900, à Paris (In French). Imprimerie Nationale, p. 39.

Mougin, P. (1931). "La restauration des Alpes." 584 p. Paris, France: Ministère de l'Agriculture, Direction générale des eaux et des forêts, Eaux et génie rural.

Mériaux, P, Richard, D, Félix, H, Laigle, D, Bon, M, Astier, G, Boncompain, I, and Quefféléan, Y (2013). "Etude de dangers des digues de protection contre les crues torrentielles: présentation du cas de l'EDD des digues du torrent de La Salle, recommandations et perspectives [Hazard study of torrential floods protection dikes: case study of the La Salle torrent, recommendations and perspectives]". Digues maritimes et fluviales de protection contre les submersions-2e colloque national-Digues 2013. Ed. by P. Royet and S. Bonelli. Paris: Lavoisier, pp. 164–175.

Mueller, E. R. and Pitlick, J. (2005). "Morphologically based model of bed load transport capacity in a headwater stream". *Journal of Geophysical Research: Earth Surface*. Vol. 110. no. F2. DOI: 10.1029/2003JF000117.

Mueller, E. R., Pitlick, J., and Nelson, J. M. (2005). "Variation in the reference Shields stress for bed load transport in gravel-bed streams and rivers". *Water Resources Research*. Vol. 41. no. 4. DOI: 10.1029/2004WR003692.

Muste, M., Fujita, I., and Hauet, A. (2010). "Large-scale particle image velocimetry for measurements in riverine environments". *Water Resources Research*. Vol. 46. no. 4, pp. 1–14. DOI: 10.1029/2008WR006950.

Muste, M., Xiong, Z., Schöne, J., and Li, Z. (2004). "Validation and extension of image velocimetry capabilities for flow diagnostics in hydraulic modeling". *Journal of Hydraulic Engineering*. Vol. 130. no. 3, pp. 175–185.

Muto, T. and Steel, R. J. (2004). "Autogenic response of fluvial deltas to steady sea-level fall: Implications from flume-tank experiments". *Geology*. Vol. 32. no. 5, pp. 401–404.

Napoléon III (1960). "Discours, messages et proclamations de S. M. Napoléon III, empereur des Français : 1849-1860". (In French). Mirencourt: Imp. Humbert, p. 168.

Nicot, F., Tacnet, J., and Flavigny, E. (2001). "Barrages de correction torrentielle: estimation des poussées de berges". *Revue française de géotechnique*. no. 95-96. (in French), pp. 55–63.

Nishimoto, H. (2014). "Relationship between european countries and japan in the field of erosion control at the beginning of the 20th century". Proc. of the 2014 International Debris-Flow Worshop. (abstract). Tawian: National Cheng Kung University, T04–2.

Nitsche, M., Rickenmann, D., Kirchner, J., Turowski, J., and Badoux, A. (2012). "Macroroughness and variations in reach-averaged flow resistance in steep mountain streams". *Water Resources Research*. Vol. 48. no. 12, pp. 1–16. DOI: 10.1029/2012WR012091.

Nord, G., Esteves, M., Lapetite, J.-M., and Hauet, A. (2009). "Effect of particle density and inflow concentration of suspended sediment on bedload transport in rill flow". *Earth Surface Processes and Landforms*. Vol. 34. no. 2, pp. 253–263. DOI: 10.1002/esp.1710.

Nowakowski, A. and Wohl, E. (2008). "Influences on wood load in mountain streams of the Bighorn National Forest, Wyoming, USA". *Environmental Management*. Vol. 42. no. 4, pp. 557–571. DOI: 10.1007/s00267-008-9140-4.

Oda, A., Izumi, I., Abe, H., Hasegawa, Y., and Mizuyama, T. (2002). "The trend and anticipated future subject of hydraulic erosion control model experiments in Japan". INTERPRAEVENT Conference Proceedings. Pp. 175 –186.

Oda, A, Hasegawa Y Sugiura, N, and Mizuyama, T (2008). "Recent trends in Japanese Sabo model experiment technology". INTERPRAEVENT Conference Proceedings. Pp. 433–444.

Okamoto, M. (2007). "The Structure of Sabo Administration". Tokyo: Japan Sabo Association, p. 115.

Okubo, S., Ikeya, H., Ishikawa, Y., and Yamada, T. (1997). "Development of new methods for countermeasures against debris flows". Recent Developments on Debris Flows. Ed. by A. Armanini and M. Michiue. Vol. 64. Lecture Notes in Earth Sciences. Springer Berlin Heidelberg, pp. 166–185. DOI: 10.1007/BFb0117768.

Ono, G., Mizuyama, T., and Matsumura, K. (2004). "Current practices in the design and evaluation of steel SABO facilities in Japan". INTERPRAEVENT Conference Proceedings. Vol. 3. no. VII. RIVA / TRIENT, pp. 253–264.

ONR24800 (2009). "Protection works for torrent control - Terms, definitions and classification". 75p. (In German). ON Österreichisches Normungsinstitut.

ONR24801 (2013). "Protection works for torrent control - Static and dynamic actions on structures". 32p. (In German). ON Österreichisches Normungsinstitut.

ONR24802 (2010). "Protection works for torrent control - Design of structures". 94p. (In German). ON Österreichisches Normungsinstitut.

ONR24803 (2008). "Protection works for torrent control - Operation, monitoring, maintenance". 38p. (In German). ON Österreichisches Normungsinstitut.

Osanai, N, Mizuno, H, and Mizuyama, T (2010). "Design Standard of Control Structures Against Debris Flow in Japan". *Journal of Disaster Research*. Vol. Vol.5. no. 3, pp.307–314.

Osti, R. and Egashira, S. (2008). "Method to improve the mitigative effectiveness of a series of check dams against debris flows". *Hydrological Processes*. Vol. 22. no. 26, pp. 4986–4996. DOI: 10.1002/hyp.7118.

Osti, R. and Egashira, S. (2013). "Check dams, morphological adjustments and erosion control in torrential streams". Ed. by C. Conesa-Garcia and M. Lenzi. Hauppauge, NY: Nova Science Publishers, Inc. Chap. Sediment transportation from bed-load to debris-flow and its control by check dams in torrential streams, pp. 151–184.

Paola, C. and Leeder, M. (2011). "Environmental dynamics: Simplicity versus complexity." *Nature*. Vol. 469. no. 7328, pp. 38–39. DOI: 10.1038/469038a.

Paola, C., Straub, K., Mohrig, D., and Reinhardt, L. (2009). "The "unreasonable effectiveness" of stratigraphic and geomorphic experiments". *Earth-Science Reviews*. Vol. 97. no. 1-4, pp. 1–43. DOI: 10.1016/j.earscirev.2009.05.003.

Papež, J., Moser, M., Jager, G., Piton, G., Recking, A., Silvestro, C., Bodrato, G., Tresso, F., Del Vesco, R., Sodnik, J., Klabus, A., Krivograd Klemenčič, A., Lakota Jeriček, v., and Mrak, S. (2015). "Work Package 6 - Interactions with structures". Ed. by J. Sodnik, S. Rusjan, M. Kogoj, and M. Mikoš. SedAlp project -

Alpine Space. Chap. 3.1 Report on improved concepts of responses of torrent/river control structures to floods and debris flow impacts (including wood), pp. 24–70.

Parker, G. (2008). "Sedimentation engineering process measurements, modeling and practices". Sedimentation Engineering. Ed. by M. Garcia. ASCE. Chap. 3 - Transport of Gravel and Sediment Mixtures, pp. 165–251. DOI: 10.1061/9780784408148.ch03.

Parker, G. and Wilcock, P. (1993). "Sediment feed and recirculating flumes: fundamental difference". *Journal of Hydraulic Engineering - ASCE*. Vol. 119. no. 11, pp. 1192–1204.

Parker, G., Paola, C., Whipple, K., and Mohrig, D. (1998). "Alluvial fans formed by channelized fluvial and sheet flow. I: theory". *Journal of Hydraulic Engineering*. Vol. 124. no. 10, pp. 985–995. DOI: 10.1061/(ASCE)0733-9429(1998)124:10(985).

Parker, G., Wilcock, P., Paola, C., Dietrich, W., and Pitlick, J. (2007). "Physical basis for quasi-universal relations describing bankfull hydraulic geometry of single-thread gravel bed rivers". *Journal of Geophysical Research: Earth Surface*. Vol. 112. no. 4, pp. 1–21. DOI: 10.1029/2006JF000549.

Parker, G. and Klingeman, P. C. (1982). "On why gravel bed streams are paved". *Water Resources Research*. Vol. 18. no. 5, pp. 1409–1423. DOI: 10.1029/WR018i005p01409.

Patek, M. (2008). "Ist es der Sindtfluss?–Kulturelle Strategien Reflexionen zur Prävention und Bewältigung von Naturgefahren". Ed. by R. Lackner, R. Psenner, and M. Walcher. (in German). innsbruck university press. Chap. Über die Versuche die Natur zu beherrschen - Naturgefahrenmanagement im Wandel der Zeit, pp. 3–9.

Peakall, J., Ashworth, P., and Best, J. (1996). "Physical Modelling in Fluvial Geomorphology: Principles, Applications and Unresolved Issues". The Scientific Nature of Geomorphology: Proceedings of the 27th Binghamton Symposium in Geomorphology. Ed. by B. L. Rhoads and C. E. Thorn. John Wiley Sons Ltd.

Peiry, J.-L. (1990). "Les torrents de l'Arve: dynamique des sédiments et impact de l'aménagement des bassins versants sur l'activité torrentielle". *Revue de Géographie alpine*. Vol. 78. no. 1, pp. 25–58.

Peteuil, C (2010). "Synthèse des données de production sédimentaire des bassins versants torrentiels des Alpes françaises". Note technique. (In French). Grenoble: ONF-service RTM de l´Isére.

Peteuil, C., Maraval, C., Bertrand, C., and Monier, G. (2008). "TORRENT DU MANIVAL - Schéma d'aménagement et de gestion du bassin versant contre les crues". Tech. rep. OFFICE NATIONAL DES FORETS - Service départemental RTM de l'Isère.

Peteuil, C, Liébault, F., and Marco, O. (2012). "ECsTREM, a practical approach for predicting the sediment yield in torrents of the French Alps [ECsTREM, une approche pratique pour predire la production sedimentaire des torrents des Alpes Françaises]". INTERPRAEVENT Conference Proceedings. Vol. 1. (In French), pp. 293 –304.

Petter, A. L. and Muto, T. (2008). "Sustained alluvial aggradation and autogenic detachment of the alluvial river from the shoreline in response to steady fall of relative sea level". *Journal of Sedimentary Research*. Vol. 78. no. 2, pp. 98–111.

Phillips, C., Rey, F., Marden, M., and Liébault, F. (2013). "Revegetation of steeplands in France and New Zealand: Geomorphic and policy responses". *New Zealand Journal of Forestry Science*. Vol. 43, pp. 1–16. DOI: 10.1186/1179-5395-43-14.

Pitlick, J., Marr, J., and Pizzuto, J. (2013). "Width adjustment in experimental gravel-bed channels in response to overbank flows". *J. Geophys. Res. Earth Surf,*. Vol. 118. no. 2, pp. 1–18. DOI: 10.1002/jgrf.20059..

Piton, G. and Recking, A. (2014). "The dynamic of streams equipped with check dams". Proceedings of the International Conference on Fluvial Hydraulics, RIVER FLOW 2014. Pp. 1437–1445.

Piton, G. and Recking, A. (2016a). "Design of sediment traps with open check dams. I: hydraulic and deposition processes". *Journal of Hydraulic Engineering*. Vol. 142. no. 2, pp. 1–23. DOI: 10.1061/(ASCE)HY.1943-7900.0001048.

Piton, G. and Recking, A. (2016b). "Design of sediment traps with open check dams. II: woody debris". *Journal of Hydraulic Engineering*. Vol. 142. no. 2, pp. 1–17. DOI: 10.1061/(ASCE)HY.1943-7900.0001049.

Piton, G. and Recking, A. (2016c). "Effects of check dams on bed-load transport and steep slope stream morphodynamics". *Geomorphology*. Vol. (in press.) DOI: 10.1016/j.geomorph.2016.03.001.

Piton, G., Recking, A., Patrocco, D., Ropele, P., Colle, F., Le Guern, J., and Rifaï, I (2015). "Rapport final : Action 2.5 - Vulnérabilité des barrages vis-à-vis des aléas torrentiels". Tech. rep. (In French). Projet transfrontalier Italie-France ALCOTRA - RISBA - RISCHIO DEGLI SBARRAMENTI ARTIFICIALI - RISQUES DES BARRAGES.

Piton, G., Mejean, S., Bellot, H., Le Guern, J., Carbonari, C., and Recking, A. (2016a). "Bed-load trapping in open check dam basins measurments of flow velocities and depositions patterns". INTERPRAEVENT Conference proceedings. Ed. by G. Koboltschnig, pp. 808–817.

Piton, G., Vázquez-Tarrío, D., and Recking, A. (2016b). "Can bed-load help to validate hydrology studies in mountainous catchment? The case study of the Roize (Voreppe – FR)". FLOODrisk 3rd European Conference on Flood Risk Management Conf. Proc.. (Sub.), 12p.

Piton, G., Carladous, S., Recking, A., Liebault, F., Tacnet, J., Kuss, D., Quefféléan, Y, and Marco, O. (2016c). "Why do we build check dams in Alpine streams? An historical perspective from the French experience". *Earth Surface Processes and Landforms*. Vol. in press. DOI: 10.1002/esp.3967.

Polatel, C. (2006). "Large-Scale Roughness Effect On Free-Surface And Bulk Flow Characteristics In Open-channel Flows". PhD thesis. Iowa City: University of Iowa.

Poncet, A. (1968). "Cours de restauration et conservation des terrains en montagne". Paris, France: Ecole Nationale des Ingénieurs des Travaux, des Eaux et Forêts.

Poncet, A (1975). "Réflexions sur la restauration des terrains en montagne pour une meilleure programmation". *Revue Forestière Française*. Vol. XXVII. no. 5. (in French), pp. 362–370. DOI: 10.4267/2042/20957.

Poncet, A (1995). "Restauration et conservation des terrains en montagne". Ed. by Service RTM. 10 volumes (In French). Office National des Forêts, p. 1000.

Pont, D., Piégay, H., Farinetti, A., Allain, S., Landon, N., Liébault, F., Dumont, B., and Richard-Mazet, A. (2009). "Conceptual framework and interdisciplinary approach for the sustainable management of gravel-bed rivers: The case of the Drôme River basin (S.E. France)". *Aquatic Sciences*. Vol. 71. no. 3, pp. 356–370. DOI: 10.1007/s00027-009-9201-7.

Porto, P. and Gessler, J. (1999). "Ultimate bed slope in Calabrian streams upstream of check dams: Field study". *Journal of Hydraulic Engineering*. Vol. 125. no. 12, pp. 1231–1242. DOI: 10.1061/(ASCE)0733-9429(1999)125:12(1231).

Prochaska, A. B., Santi, P. M., and Higgins, J. D. (2008). "Debris basin and deflection berm design for fire-related debris-flow mitigation". *Environmental Engineering Geoscience*. Vol. 14. no. 4, pp. 297–313. DOI: 10.2113/gseegeosci.14.4.297.

Pulfer, G, Naaim, M, Thibert, E, and Soruco, A (2013). "Retrieving avalanche basal friction law from high rate positioning of avalanches". International Snow Science Workshop (ISSW). Irstea, ANENA, Meteo France, p–1418.

Ran, Q., Li, W., Liao, Q., Tang, H., and Wang, M. (2016). "Application of an Automated LSPIV System in a Mountainous Stream for Continuous Flood Flow Measurements". *Journal of Hydrology*. (in press). DOI: 10.1002/hyp.10836.

Ratomski, J (1988). "Configuration of sediment deposit in bed-load reservoirs". INTERPRAEVENT Conference Proceedings.

Recking, A. (2006). "An experimental study of grain sorting effects on bedload". PhD thesis. INSA Lyon.

Recking, A. (2009). "Theoretical development on the effects of changing flow hydraulics on incipient bed load motion". *Water Resources Research*. Vol. 45. no. 4, pp. 1–16. DOI: 10.1029/2008WR006826.

Recking, A. (2010). "A comparison between flume and field bed load transport data and consequences for surface-based bed load transport prediction". *Water Resources Research*. Vol. 46. no. 3. DOI: 10.1029/2009WR008007.

Recking, A. (2012). "Influence of sediment supply on mountain streams bedload transport". *Geomorphology*. Vol. 175-176, pp. 139–150. DOI: 10.1016/j.geomorph.2012.07.005.

Recking, A. (2013a). "An analysis of nonlinearity effects on bed load transport prediction". *Journal of Geophysical Research: Earth Surface*. Vol. 118. no. 3, pp. 1–18. DOI: 10.1002/jgrf.20090.

Recking, A. (2013b). "Simple method for calculating reach-averaged bed-load transport". *Journal of Hydraulic Engineering*. Vol. 139, pp. 70–75.

Recking, A. (2014). "Relations between bed recharge and magnitude of mountain streams erosions". *Journal of Hydro-Environment Research*. Vol. 8. no. 2, pp. 143–152. DOI: 10.1016/j.jher.2013.08.005.

Recking, A. and Pitlick, J. (2013). "Shields versus Isbash". *Journal of Hydraulic Engineering*. Vol. 139. no. 1, pp. 51–54. DOI: 10.1061/(ASCE)HY.1943-7900.0000647.

Recking, A., Frey, P., Paquier, A., Belleudy, P., and Champagne, J. (2008a). "Bed-Load transport flume experiments on steep slopes". *Journal of Hydraulic Engineering*. Vol. 134. no. 9, pp. 1302–1310. DOI: 10.1061/(ASCE)0733-9429(2008)134:9(1302).

Recking, A., Frey, P., Paquier, A., Belleudy, P., and Champagne, J. (2008b). "Feedback between bed load and flow resistance in gravel and cobble bed rivers". *Water Resources Research*. Vol. 44. no. 8, pp. 1–21. DOI: 10.1029/2008WR007272.

Recking, A., Frey, P., Paquier, A., and Belleudy, P. (2009). "An experimental investigation of mechanisms involved in bed load sheet production and migration". *Journal of Geophysical Research B: Solid Earth*. Vol. 114. no. 3, pp. 1–13. DOI: 10.1029/2008JF000990.

Recking, A., Leduc, P., Liébault, F., and Church, M. (2012a). "A field investigation of the influence of sediment supply on step-pool morphology and stability". *Geomorphology*. Vol. 139-140, pp. 53–66. DOI: 10.1016/j.geomorph.2011.09.024.

Recking, A., Liébault, F., Peteuil, C., and Jolimet, T. (2012b). "Testing bedload transport equations with consideration of time scales". *Earth Surface Processes and Landforms*. Vol. 37. no. 7, pp. 774–789. DOI: 10.1002/esp.3213.

Recking, A., Piton, G., Vázquez-Tarrío, D., and Parker, G (2016). "Quantifying the morphological print of bedload transport". *Earth Surface Processes and Landforms*. Vol. 41. no. 6, pp. 809–822.

Reid, L. M. and Dunne, T. (2003). "Sediment budgets as an organizing framework in fluvial geomorphology". *Tools in fluvial geomorphology*. Pp. 463–500.

Reitz, M. and Jerolmack, D. (2012). "Experimental alluvial fan evolution: Channel dynamics, slope controls, and shoreline growth". *Journal of Geophysical Research F: Earth Surface*. Vol. 117. no. 2, pp. 1–19. DOI: 10.1029/2011JF002261.

Remaître, A. and Malet, J.-P. (2013). "Check dams, morphological adjustments and erosion control in torrential streams". Ed. by C. Conesa-Garcia and M. Lenzi. Hauppauge, NY: Nova Science Publishers, Inc. Chap. The effectiveness of torrent check dams to control channel instability: Example of debris-flow events in clay shales, pp. 211–237.

Remaître, A., W. J. Van Asch, T., Malet, J.-P., and Maquaire, O. (2008). "Influence of check dams on debris-flow run-out intensity". *Natural Hazards and Earth System Science*. Vol. 8. no. 6, pp. 1403–1416. DOI: 10.5194/nhess-8-1403-2008.

Reneuve, P. (1955). "L'évolution de la technique de correction torrentielle". *Revue Forestière Française*. no. 9-10. (in French), pp. 689–693. DOI: 10.4267/2042/27132.

Requillard, J., Hespel, F., and Segel, V. (1997). "Evolution de la politique de protection contre les torrents au cours de ces deux derniers siecles". *Risques Infos*. Vol. 8. (In French), pp. 14–18.

Revil-Baudard, T., Chauchat, J., Hurther, D., and Barraud, P.-A. (2015). "Investigation of sheet-flow processes based on novel acoustic high-resolution velocity and concentration measurements". *Journal of Fluid Mechanics*. Vol. 767, pp. 1–30.

Rickenmann, D. (1990). "Bedload transport capacity of slurry flows at steep slopes". (Diss ETH No. 9065). PhD thesis. ETH Zurich.

Rickenmann, D. (1997a). "Sediment transport in Swiss torrents". *Earth Surface Processes and Landforms*. Vol. 22. no. 10, pp. 937–951. DOI: 10.1002/(SICI)1096-9837(199710)22:10<937::AID-ESP786>3.0.CO;2-R.

Rickenmann, D and Fritschi, B (2010). "Bedload transport measurements using piezoelectric impact sensors and geophones". Proceedings of International Bedload-Surrogate Monitoring Workshop.

Rickenmann, D. and Koschni, A. (2010). "Sediment loads due to fluvial transport and debris flows during the 2005 flood events in Switzerland". *Hydrological Processes*. Vol. 24. no. 8, pp. 993–1007. DOI: 10.1002/hyp.7536.

Rickenmann, D. and Recking, A. (2011). "Evaluation of flow resistance in gravel-bed rivers through a large field data set". *Water Resources Research*. Vol. 47. no. 7, pp. 1–22. DOI: 10.1029/2010WR009793.

Rickenmann, D., D'Agostino, V., Fontana, G., Lenzi, M., and Marchi, L. (1998). "New results from sediment transport measurements in two Alpine torrents". *IAHS-AISH Publication*. Vol. 248, pp. 283–289.

Rickenmann, D., Badoux, A., and Hunzinger, L. (2015). "Significance of sediment transport processes during piedmont floods: The 2005 flood events in Switzerland". *Earth Surface Processes and Landforms*. Article in Press. DOI: 10.1002/esp.3835.

Rickenmann, D. (1991). "Hyperconcentrated flow and sediment transport at steep slopes". *Journal of Hydraulic Engineering*. Vol. 117. no. 11, pp. 1419–1439.

Rickenmann, D. (1997b). "Schwemmholz und hochwasser [Driftwood and floods]". *Wasser Energie Luft*. Vol. 89. no. 5/6, pp. 115–119.

Rickenmann, D. (2001). "Comparison of bed load transport in torrents and gravel bed streams". *Water resources research*. Vol. 37. no. 12, pp. 3295–3305.

Rickenmann, D. and Zimmermann, M. (1993). "The 1987 debris flows in Switzerland: documentation and analysis". *Geomorphology*. Vol. 8. no. 2, pp. 175–189.

Rimböck, A (2004). "Design of rope net barriers for woody debris entrapment: introduction of a design concept". INTERPRAEVENT Conference Proceedings. Vol. 3. no. VII, pp. 265–276.

Rimböck, A. and Strobl, T. (2002). "Loads on rope net constructions for woody debris entrapment in torrents". INTERPRAEVENT Conference Proceedings. Vol. 2, pp. 797 –807.

Rinaldi, M. (2003). "Recent channel adjustments in alluvial rivers of Tuscany, Central Italy". English. *Earth Surface Processes and Landforms*. Vol. 28. no. 6, pp. 587–608. DOI: 10.1002/esp.464.

Rinaldi, M. and Simon, A. (1998). "Bed-level adjustments in the Arno River, central Italy". English. *Geomorphology*. Vol. 22. no. 1. cited By 69, pp. 57–71.

Rinaldi, M., Piégay, H., and Surian, N. (2011). "Geomorphological approaches for river management and restoration in Italian and French Rivers". *Geophysical Monograph Series*. Vol. 194, pp. 95–113. DOI: 10.1029/2010GM000984.

Roux, H. and Dartus, D. (2008). "Sensitivity Analysis and Predictive Uncertainty Using Inundation Observations for Parameter Estimation in Open-Channel Inverse Problem". *Journal of Hydraulic Engineering*. Vol. 134 (5), pp. 541–549.

RTM38 (2009). "Torrent de la Roize - Division domaniale de Voreppe / Pommiers la Placette". Tech. rep. 10p. (In French). Office National des Forêts - Service Restauration des Terrains de Montagne - Service RTM de l'Isère.

Rudolf-Miklau, F. and Hübl, J. (2010). "Managing risks related to drift wood (woody debris)". INTERPRAEVENT Conference Proceedings. Pp. 868 –878.

Rudolf-Miklau, F. and Suda, J. (2011). "Technical standards for debris flow barriers and breakers". Proceedings of the International Conference on Debris-Flow Hazards Mitigation: Mechanics, Prediction, and Assessment. Roma: Università La Sapienza, pp. 1083–1091. DOI: 10.4408/IJEGE.2011-03.B-117.

Rudolf-Miklau, F. and Suda, J. (2013). "Advances in Global Change Research". Dating Torrential Processes on Fans and Cones. Ed. by M. Schneuwly-Bollschweiler, M. Stoffel, and F. Rudolf-Miklau. Vol. 47. Springer Netherlands. Chap. 26-Design Criteria for Torrential Barriers, pp. 375–389. DOI: 10.1007/978-94-007-4336-6_26.

Sabo Department. (2000). "Sabo Methods and Facilities made of Natural Materials". Tech. rep. Ministry of Construction. Japan.

SABO Division (2000). "Guideline for driftwood countermeasures (proposal and design)". Ed. by Sediment Control (Sabo) Department. Tokyo: Ministry of Construction. Japan., p. 42.

Sasahara, K., Yamashita, S., and Subarkah (2002). "Effect of concrete slit dams to control sediment discharge in volcanic areas". INTERPRAEVENT Conference Proceedings. Vol. 1, pp. 187 –197.

Schärlig, A. (1985). "Décider sur plusieurs critères. Panorama de l'aide à la décision multicritère." Diriger l'entreprise no. 1. 304 p. (in French). Presses polytechniques et universitaires romandes.

Schmocker, L. and Hager, W. (2011). "Probability of Drift Blockage at Bridge Decks". *Journal of Hydraulic Engineering*. Vol. 137. no. 4, pp. 470–479. DOI: 10.1061/(ASCE)HY.1943-7900.0000319.

Schmocker, L. and Hager, W. (2013). "Scale modeling of wooden debris accumulation at a debris rack". *Journal of Hydraulic Engineering*. Vol. 139. no. 8, pp. 827–836. DOI: 10.1061/(ASCE)HY.1943-7900.0000714.

Schmocker, L. and Weitbrecht, V. (2013). "Driftwood: Risk analysis and engineering measures". *Journal of Hydraulic Engineering*. Vol. 139. no. 7, pp. 683–695. DOI: 10.1061/(ASCE)HY.1943-7900.0000728.

Schmocker, L., Detert, M., and Weitbrecht, V. (2012). "Schwemmholzrückhalt Sihl Standort Rütiboden". Tech. rep. no. 4293. (In German). VAW-ETH Zürich.

Schneider, J., Rickenmann, D., Turowski, J., and Kirchner, J. (2015). "Self-adjustment of stream bed roughness and flow velocity in a steep mountain channel". *Water Resources Research*. Vol. 51. no. 10, pp. 7838–7859. DOI: 10.1002/2015WR016934.

Schuerch, P., Densmore, A. L., McArdell, B. W., and Molnar, P. (2006). "The influence of landsliding on sediment supply and channel change in a steep mountain catchment". *Geomorphology*. Vol. 78. no. 3, pp. 222–235.

Schumm, S. and Harvey, M. (2008). "Sedimentation engineering process measurements, modeling and practices". Sedimentation Engineering. Ed. by M. Garcia. (Manual revised in 2007). ASCE. Chap. 18 - Engineering Geomorphology, pp. 859–883. DOI: 10.1061/9780784408148.ch18.

Schuster, R. (2000). "Outburst debris-flows from failure of natural dams". Proceedings 2nd International Conference on Debris Flow Hazard Mitigation. Pp. 16–20.

Schwindt, S., Franca, M., and Schleiss, A. (2015). "Experimental evaluation of the discharge capacity of flow constrictions by check dams in mountain rivers". E-proceedings of the 36th IAHR World Congress. IAHR. The Hague, pp. 1–4.

SedAlp (2015a). "Work Package 4 - Basin-scale Sediment Dynamics- Guidelines for assessing sediment dynamics in alpine basins and channel reaches". Tech. rep. 71p. Alpine Space European project.

SedAlp (2015b). "Work Package 6 - Interactions with structures". Tech. rep. no. WP6 Final Report. 242pp. Alpine Space European project.

Senoo, K. and Mizuyama, T (1984). "Function of structures against debris flow". INTERPRAEVENT Conference Proceedings. Vol. 3, pp. 113–120.

Sharp, J. (1981). "Hydraulic modelling". Butterworths.

Shibuya, H., Katsuki, S., Ohsumi, H., Ishikawa, N., and Mizuyama, T (2010). "Experimental study on woody debris trap performance of drift wood capturing structure". *Journal of the Japan Society of Erosion Control Engineering*. Vol. 63. no. 3. (In Japanese), pp. 34–41.

Shields, A. (1936). "Application of similarity principles and turbulence research to bed load movement." Ed. by S. C. S. C. Laboratory. California Institute of Technology, Pasadena, CA.: U.S. Dept. of Agriculture.

Shrestha, B., Nakagawa, H., Kawaike, K., Baba, Y., and Zhang, H. (2012). "Driftwood deposition from debris flows at slit-check dams and fans". *Natural Hazards*. Vol. 61. no. 2, pp. 577–602. DOI: 10.1007/s11069-011-9939-9.

Silva, M, Costa, S, Canelas, R., Pinheiro, A., and Cardoso, A. (2016). "Experimental And Numerical Study Of Slit-check Dams". *International Journal of Sustainable Development and Planning*. Vol. 11. no. 2, pp. 107–118.

Skermer, N. A. and VanDine, D. F. (2005). "Debris-flow Hazards and Related Phenomena". Ed. by M. Jakob and O. Hungr. Springer, pp. 25–51.

Sklar, L. and Dietrich, W. (2008). "Implications of the saltation-abrasion bedrock incision model for steady-state river longitudinal profile relief and concavity". *Earth Surface Processes and Landforms*. Vol. 33. no. 7, pp. 1129–1151. DOI: 10.1002/esp.1689.

Sklar, L., Fadde, J., Venditti, J., Nelson, P., Aleksandra Wydzga, M., Cui, Y., and Dietrich, W. (2009). "Translation and dispersion of sediment pulses in flume experiments simulating gravel augmentation below dams". *Water Resources Research*. Vol. 45. no. 8, pp. 1–14. DOI: 10.1029/2008WR007346.

Smart, G. and Jaeggi, M. (1983). "Sediment Transport on Steep Slopes". Mitteilung der Versuchsanstalt für Wasserbau, Hydrologie und Glaziologie der ETH Zürich, Nr. 64.

Smart, G., Duncan, M., and Walsh, J. (2002). "Relatively rough flow resistance equations". *Journal of Hydraulic Engineering*. Vol. 128. no. 6, pp. 568–578. DOI: 10.1061/(ASCE)0733-9429(2002)128:6(568).

Smart, G., Bind, J., and Duncan, M. (2009). "River bathymetry from conventional LiDAR using water surface returns". 18th World IMACS / MODSIM Congress Conf. Proc.. Pp. 2521–2527.

Sodnik, J., Martinčič, M., Mikoš, M., and Kryžanowski, A. (2014). "Are Torrent Check-Dams Potential Debris-Flow Sources?" Engineering Geology for Society and Territory (IAEG Congress proceedings). Ed. by G. L. et al. Vol. 2. Springer International Publishing Switzerland, pp. 485–488. DOI: 10.1007/978-3-319-09057-3_79.

SOGREAH (1992). "Etude préliminaire à une recherche expérimentale sur les plages de dépôts torrentiels". Tech. rep. no. 6 0172 R3. 32p.+ App. (In French). CEMAGREF de Grenoble and Services RTM.

SOGREAH (1994). "Etude de l'écoulement et du dépôt des laves torrentielle - Second volet: étude expérimentale". Tech. rep. no. 30 0151 R1. 33p.+ App. (In French). Pôle Grenoblois d'étude et de recherches - risques naturels.

Solari, L. and Parker, G. (2000). "The curious case of mobility reversal in sediment mixtures". *Journal of Hydraulic Engineering*. Vol. 126. no. 3, pp. 185–197. DOI: 10.1061/(ASCE)0733-9429(2000)126:3(185).

Suda, J., Hübl, J., and Bergmeister, K. (2010). "Design and construction of high stressed concrete structures as protection works for torrent control in the Austrian alps". Proceedings of the third international fib congress, 29 May–2 June. Washington DC. Chicago: Precast Prestressed Concrete Institute (PCI), pp. 1–12.

Surell, A. (1841). "Etude sur les torrents des Hautes Alpes (1st edition)". Ed. by Carilian-Gœury and V. Dalmont. (In French). Paris: Librairie des corps impériaux des ponts et chaussées et des mines, p. 280.

Tacnet, J., Piton, G., and Carladous, S. (2014a). "Torrent du Saint-Antoine, événement du 31 juillet 2014 - CR visite du 6 août 2014 [Saint Antoine torrent, July, 31 2014 event - August, 6 2014 visit report]". Tech. rep. no. 0.4 - 140814. 27p. (In French). IRSTEA.

Tacnet, J.-M., Dezert, J., Curt, C., Batton-Hubert, M., and Chojnacki, E. (2014b). "How to manage natural risks in mountain areas in a context of imperfect information? New frameworks and paradigms for expert assessments and decision-making". *Environment Systems and Decisions*. Vol. Vol. 34. no. 2, pp 288–311.

Tacnet, J.-M., Curt, C., Rey, B., and Richard, D. (2012). "Efficiency assessment for torrent protection works: an approach based on safety and reliability analysis". Proceedings of the 12th international conference Interpraevent. pp 821-831. Grenoble, France.

Tacnet, M. and Degoutte, G. (2013). "Torrents et rivières de montagne - Dynamique et aménagement". Ed. by A. Recking, D. Richard, and G. Degoutte. (In French). Antony: QUAE. Chap. 5 - Principes de conception des ouvrages de protection contre les risques torrentiels [Design principles of torrential hazard mitigation structures], pp. 267–331.

Takahashi, T. (2014). "Debris flow: mechanics, prediction and countermeasures". 2nd edition. London: CRC Press, p. 551.

Theule, J., Liébault, F., Laigle, D., Loye, A., and Jaboyedoff, M. (2015). "Channel scour and fill by debris flows and bedload transport". *Geomorphology*. Vol. 243, pp. 92–105. DOI: 10.1016/j.geomorph.2015.05.003.

Theule, J., Liébault, F., Loye, A., Laigle, D., and Jaboyedoff, M. (2012). "Sediment budget monitoring of debris-flow and bedload transport in the Manival Torrent, SE France". *Natural Hazards and Earth System Science*. Vol. 12. no. 3, pp. 731–749. DOI: 10.5194/nhess-12-731-2012.

Thiéry, E. (1891). "Restauration des montagnes, correction des torrents, reboisement". Ed. by Baudry et Cie. (In French). Paris: Librairie Polytechnique, p. 443.

Todosijević, M. and Kostadinov, S. (2006). "Effects of Transversal Structures in the Torrents of the River Drina Catchment". BALWOIS Conf. Water Observation and Information System for Decision Support. Skopje: Ministry of Environment and Physical Planning of Republic of Macedonia, pp. 23–26.

Tétreau, A. (1883). "Commentaire de la loi du 4 avril 1882 sur la restauration et la conservation des terrains en montagne". 209 p. Société d'imprimerie et librairie administratives et classiques.

Turowski, J. M. and Rickenmann, D. (2009). "Tools and cover effects in bedload transport observations in the Pitzbach, Austria". *Earth Surface Processes and Landforms*. Vol. 34. no. 1, pp. 26–37. DOI: 10.1002/esp.1686.

Turowski, J. M., Yager, E. M., Badoux, A., Rickenmann, D., and Molnar, P. (2009). "The impact of exceptional events on erosion, bedload transport and channel stability in a step-pool channel". *Earth Surface Processes and Landforms*. Vol. 34. no. 12, pp. 1661–1673. DOI: 10.1002/esp.1855.

Turowski, J. M., Badoux, A., and Rickenmann, D. (2011). "Start and end of bedload transport in gravel-bed streams". *Geophysical Research Letters*. Vol. 38. no. 4.

Uchiogi, T, Shima, J, Tajima, H, and Ishikawa, Y (1996). "Design methodes for woody-debris entrapment". INTERPRAEVENT Conference Proceedings. Pp. 279–288.

USACE (1994). "Channel stability assessment for flood control projects". Engineer Manual N˚1110-2-1418. U.S. Army Corps of Engineers. Washington, DC 20314-1000.

Van Andel, T. H., Runnels, C. N., and Pope, K. O. (1986). "Five Thousands Years of Land Use and Abuse in the Southern Argolid, Greece". *Hesperia: The Journal of the American School of Classical Studies at Athens*. Vol. 55. no. 1, pp. 103–128.

Van De Wiel, M. and Coulthard, T. (2010). "Self-organized criticality in river basins: Challenging sedimentary records of environmental change". *Geology*. Vol. 38. no. 1, pp. 87–90. DOI: 10.1130/G30490.1.

Van Dijk, M., Kleinhans, M., Postma, G., and Kraal, E. (2012). "Contrasting morphodynamics in alluvial fans and fan deltas: Effect of the downstream boundary". *Sedimentology*. Vol. 59. no. 7, pp. 2125–2145. DOI: 10.1111/j.1365-3091.2012.01337.x.

Van Dijk, M., Postma, G., and Kleinhans, M. (2009). "Autocyclic behaviour of fan deltas: An analogue experimental study". *Sedimentology*. Vol. 56. no. 5, pp. 1569–1589. DOI: 10.1111/j.1365-3091.2008.01047.x.

Van Effenterre, C (1982). "Les barrage perméables de sédimentation". *Revue Forestière Française*. Vol. 5. (In French), pp. 87–93.

VanDine, D. (1996). "Debris Flow Control Structures for Forest Engineering". no. 68. Victoria, BC: Res. Br., B.C. Min. For.,

Vatankhah, A. R. (2014). "Discussion of Experimental Study of the Stage-Discharge Relationship for an Upstream Inclined Grid with Longitudinal Bars by C. Di Stefano and V. Ferro". *Journal of Irrigation and Drainage Engineering*. Vol. 07014027, pp. 1–3. DOI: 10.1061/(ASCE)IR.1943-4774.0000761.

Venditti, J., Dietrich, W., Nelson, P., Wydzga, M., Fadde, J., and Sklar, L. (2010). "Effect of sediment pulse grain size on sediment transport rates and bed mobility in gravel bed rivers". *Journal of Geophysical Research F: Earth Surface*. Vol. 115. no. 3, pp. 1–19. DOI: 10.1029/2009JF001418.

Vericat, D., Batalla, R., and Garcia, C. (2006). "Breakup and reestablishment of the armour layer in a large gravel-bed river below dams: The lower Ebro". *Geomorphology*. Vol. 76. no. 1-2, pp. 122–136. DOI: 10.1016/j.geomorph.2005.10.005.

Veronese, A (1937). "Erosion de fond en aval d'une decharge". IAHR, meeting for hydraulic works, Berlin.

Verrier, M. (1980). "Coûts et avantages des travaux RTM - Cas des voies de communication." 143 p. (in French). MA thesis. Grenoble, France: UER de Géographie.

Veyrat-Charvillon, S. and Memier, M (2006). "Stereophotogrammetry of archive data and topographic approaches to debris-flow torrent measurements: calculation of channel-sediment states and a partial sediment budget for Manival torrent (Isère, France)". *Earth Surface Processes and Landforms*. Vol. 31. no. 2, pp. 201–219.

Vischer, D. L. (2003). "Histoire de la protection contre les crues en Suisse, Des origines jusqu au 19e siècle". (In French or German). OFEG, Série Eaux.

Vogl, A., Luxner, M. H., and Agerer, H. (2016). "Controlled and efficient bed load management by means of variable drain locks embedded in a crownclosed large drain sediment control dam [Aktive und effiziente Geschiebebewirtschaftung mit Hilfe variabler Dolenverschlüsse an einer kronengeschlossenen großdoligen Bogensperre]". INTERPRAEVENT Conference proceedings. Ed. by G. Koboltschnig. (in German), pp. 853–861.

Volkwein, A., Wendeler, C., and Guasti, G. (2011). "Design of flexible debris flow barriers". Proceedings of the International Conference on Debris-Flow Hazards Mitigation: Mechanics, Prediction, and Assessment. Roma: Università La Sapienza, pp. 1093–1100. DOI: 10.4408/IJEGE.2011-03.B-118.

von Aretin, J. G. (1808). "Über Bergfalle und die mittel, denfelben vorzubeugen, oder wenigftens ihre Schädlichkeit zu vermindern mit vorzüglicher Rücksicht auf Tirol". (in German). Innsbruck: Fifcherifchen Buchhabdlung.

von Zallinger, F. S. (1779). "Abhandlung von den Ueberschwemmungen in Tyrol". (in German). kk Hofbuchdr.

Vuillet, M. (2012). "Elaboration d'un modèle d'aide à la décision basé sur une approche probabiliste pour l'évaluation de la performance des digues fluviales." 201 p. + Annexes (in French). PhD thesis. Paris, France: Université Paris-Est.

Wallerstein, N., Arthur, S., and Blanc, J. (2013). "Culvert designand operation guide supplementary technical note on Understanding blockage risks." Tech. rep. no. CIRIA-C720. London: Heriot-Watt University.

Wang, F. (1901). "Grundriss der wildbachverbauung". (in German). Leipzig: S. Hirzel.

Wang, G. (2013). "Lessons learned from protective measures associated with the 2010 Zhouqu debris flow disaster in China". *Natural Hazards*. Vol. 69. no. 3, pp. 1835–1847. DOI: 10.1007/s11069-013-0772-1.

Wang, H.-W. and Kondolf, G. (2014). "Upstream sediment-control dams: Five decades of experience in the rapidly eroding dahan river basin, Taiwan". *Journal of the American Water Resources Association*. Vol. 50. no. 3, pp. 735–747. DOI: 10.1111/jawr.12141.

Warburton, J. (1992). "Observations of bed load transport and channel bed changes in a proglacial mountain stream". *Arctic Alpine Research*. Vol. 24. no. 3, pp. 195–203. DOI: 10.2307/1551657.

Watanabe, M, Mizuyama, T, and Uehara, S (1980). "Review of debris flow countermeasure facilities". *Journal of the Japan Erosion Control Engineering Society*. Vol. 115. (in Japanese), pp. 40–45.

Wehrmann, H., Hübl, J., and Holzinger, G. (2006). "Classification of Dams in Torrential Watersheds". INTERPRAEVENT Conference Proceedings. Universal Academy Press, Inc. Tokyo, Japan, pp. 829 –838.

Weitbrecht, V, Kühn, G, and Jirka, G. (2002). "Large scale PIV-measurements at the surface of shallow water flows". *Flow Measurement and Instrumentation*. Vol. 13. no. 5, pp. 237–245.

Welber, M., Bertoldi, W., and Tubino, M. (2013). "Wood dispersal in braided streams: Results from physical modeling". *Water Resources Research*. Vol. 49. no. 11, pp. 7388–7400. DOI: 10.1002/2013WR014046.

Welber, M., Le Coz, J., Laronne, J., Zolezzi, G., Zamler, D., Dramais, G., Hauet, A., and Salvaro, M. (2016). "Field assessment of non-contact stream gauging using portable surface velocity radars (SVR)". *Water Resources Research*. DOI: 10.1002/2015WR017906.

Whitaker, A. and Potts, D. (2007). "Analysis of flow competence in an alluvial gravel bed stream, Dupuyer Creek, Montana". *Water Resources Research*. Vol. 43. no. 7, pp. 1–16.

White, S., García-Ruiz, J. M., Martí, C., Valero, B., Errea, M. P., and Gòmez-Villar, A. (1997). "The 1996 Biescas campsite disaster in the Central Spanish Pyrenees, and its temporal and spatial context". *Hydrological Processes*. Vol. 11. no. 14, pp. 1797–1812.

Whittaker, J. (1987). "Sediment Transport in Gravel-Bed Rivers". Ed. by J. Thorne C.R. Bathurst and R. Hey. John Wiley and Sons, New York. Chap. Sediment transport in step-pool streams, pp. 545–579.

Wilcock, P. and Crowe, J. (2003). "Surface-based transport model for mixed-size sediment". *Journal of Hydraulic Engineering*. Vol. 129. no. 2, pp. 120–128. DOI: 10.1061/(ASCE)0733-9429(2003)129:2(120).

Woeikof, A. (1901). "Annales de géographie". Ed. by P. Vidal de la Blache, L. Gallois, and E. de Margerie. Vol. X. (In French). Paris: Librairie Armand Colin. Chap. I - Geographie générale - De l'influence de l'homme sur la terre, pp. 97–114.

Wohl, E. (2006). "Human impacts to mountain streams". *Geomorphology*. Vol. 79. no. 3-4, pp. 217–248. DOI: 10.1016/j.geomorph.2006.06.020.

Wohl, E. and Goode, J. (2008). "Wood dynamics in headwater streams of the Colorado Rocky Mountains". *Water Resources Research*. Vol. 44. no. 9, pp. 1–14. DOI: 10.1029/2007WR006522.

Wohl, E. and Jaeger, K. (2009). "A conceptual model for the longitudinal distribution of wood in mountain streams". *Earth Surface Processes and Landforms*. Vol. 34. no. 3, pp. 329–344. DOI: 10.1002/esp.1722.

Wohl, E., Ogden, F., and Goode, J. (2009). "Episodic wood loading in a mountainous neotropical watershed". *Geomorphology*. Vol. 111. no. 3-4, pp. 149–159. DOI: 10.1016/j.geomorph.2009.04.013.

Wohl, E., Cenderelli, D., Dwire, K., Ryan-Burkett, S., Young, M., and Fausch, K. (2010). "Large in-stream wood studies: A call for common metrics". *Earth Surface Processes and Landforms*. Vol. 35. no. 5, pp. 618–625. DOI: 10.1002/esp.1966.

Wohl, E., Bolton, S., Cadol, D., Comiti, F., Goode, J., and Mao, L. (2012). "A two end-member model of wood dynamics in headwater neotropical rivers". *Journal of Hydrology*. Vol. 462-463, pp. 67–76. DOI: 10.1016/j.jhydrol.2011.01.061.

Wohl, E. (2013a). "Mountain Rivers Revisited". Rev. ed. Water Resources Monograph 19. Washington, DC: American Geophysical Union, p. 573. DOI: 10.1029/WM019.

Wohl, E. (2013b). "Mountain Rivers Revisited". Mountain Rivers Revisited. American Geophysical Union. Chap. Mountain River Biota, pp. 259–293. DOI: 10.1002/9781118665572.ch5.

Wolman, M. G. (1954). "A method of sampling coarse bed material". *Transactions of American Geophysical Union*. Vol. 35, pp. 951–956.

Wolman, M. G. and Miller, J. P. (1960). "Magnitude and frequency of forces in geomorphic processes". *The Journal of Geology*. Pp. 54–74.

Wu, C.-C. and Chang, Y.-R. (2003). "Debris-trapping efficiency of crossing-truss open-type check dams". 3rd International Conference on Debris-Flow Hazards Mitigation: Mechanics, Prediction, and Assessment, Proceedings. Ed. by C. Rickenmann D. Chen. Vol. 2. Amsterdam: IOS Press, pp. 1315–1325.

Xu, X.-Z., Zhang, H.-W., Wang, G.-Q., Xu, Y., and Zhang, O.-Y. (2013). "Check dams, morphological adjustments and erosion control in torrential streams". Ed. by C. Conesa-Garcia and M. Lenzi. Hauppauge, NY: Nova Science Publishers, Inc. Chap. Induced morphological changes affecting the stability of check dam systems, pp. 239–262.

Yager, E., Dietrich, W., Kirchner, J., and McArdell, B. (2012a). "Prediction of sediment transport in step-pool channels". *Water Resources Research*. Vol. 48. no. 1, pp. 1–20. DOI: 10.1029/2011WR010829.

Yager, E., Turowski, J., Rickenman, D., and McArdell, B. (2012b). "Sediment supply, grain protrusion, and bedload transport in mountain streams". *Geophysical Research Letters*. Vol. 39. no. 10, pp. 1–5. DOI: 10.1029/2012GL051654.

Yalin, M. (1992). "River mechanics". Pergamon Press Oxford.

Yu, G.-A., Wang, Z.-Y., Huang, H., Liu, H.-X., Blue, B., and Zhang, K. (2012). "Bed load transport under different streambed conditions - a field experimental study in a mountain stream". *International Journal of Sediment Research*. Vol. 27. no. 4, pp. 426–438. DOI: 10.1016/S1001-6279(13)60002-5.

Yu, G., Wang, Z., Zhang, K., Chang, T., and Liu, H. (2009). "Effect of incoming sediment on the transport rate of bed load in mountain streams". *International Journal of Sediment Research*. Vol. 24. no. 3, pp. 260–273. DOI: 10.1016/S1001-6279(10)60002-9.

Yu, G.-A., Wang, Z.-Y., Zhang, K., Duan, X., and Chang, T.-C. (2010). "Restoration of an incised mountain stream using artificial step-pool system". *Journal of Hydraulic Research*. Vol. 48. no. 2, pp. 178–187. DOI: 10.1080/00221681003704186.

Zaheer, I., Cui, G.-B., and Zhang, L.-Q. (2003). "Sedimentation retention basin utilization for best management practice". *Journal of Environmental Sciences*. Vol. 15. no. 5, pp. 662–668.

Zeng, Q., Yue, Z., Yang, Z., and Zhang, X. (2009). "A case study of long-term field performance of check-dams in mitigation of soil erosion in Jiangjia stream, China". *Environmental Geology*. Vol. 58. no. 4, pp. 897–911. DOI: 10.1007/s00254-008-1570-z.

Ziliani, L. and Surian, N. (2012). "Evolutionary trajectory of channel morphology and controlling factors in a large gravel-bed river". *Geomorphology*. Vol. 173-174, pp. 104–117. DOI: 10.1016/j.geomorph.2012.06.001.

Zimmermann, A. (2009). "Experimental Investigation of step-pool channel formation and stability". PhD thesis. University of British Columbia.

Zimmermann, A. and Church, M. (2001). "Channel morphology, gradient profiles and bed stresses during flood in a step-pool channel". *Geomorphology.* Vol. 40. no. 3-4, pp. 311–327. DOI: 10.1016/S0169-555X(01)00057-5.

Zollinger, F. (1983). "Die Vorgänge in einem Geschiebeablagerungsplatz (ihre Morphologie und die Möglichkeiten einer Steuerung)". (In German). PhD thesis. ETH Zürich. DOI: 10.3929/ethz-a-000318964.

Zollinger, F. (1984a). "100 Jahre Wildbachverbauung in Österreich". *Vermessung, Photogrammetrie, Kulturtechnik.* Vol. 82. (in German), pp. 394–399.

Zollinger, F. (1984b). "Die verschiedenen Funktionen von Geschieberückhaltebauwerken [The different functions of Debris detention dams]". *INTERPRAEVENT Conference Proceedings.* Vol. 1. (In German), pp. 147–160.

Zollinger, F. (1985). "Debris detention basins in the European Alps". International symposium on Erosion, Débris Flow and Disaster Prevention. Vol. 1. Tokyo: Japan Erosion Control Engineering Society, pp. 433–438.

Zou, Y., Hu, K., Chen, X., and Zhong, W. (2014). "Efficiency of Slot-Check Dam Group on Debris Flow Control in Shengou Basin, Kunming, China". Landslide Science for a Safer Geoenvironment. Springer, pp. 37–43.

APPENDIX A

Error propagation analysis

This appendix rapidly explains how error analysis and propagation had been done for laboratory experiments presented in Chap. 5, Chap. 6 and Chap. 7.

It report how is combined the uncertainties of same physical parameters X and their own specific uncertainties $u(X)$.

There is several ways to estimate uncertainties in measurements, two are mainly used in laboratory experiments and especially in hydraulics (JCGM, 2008; Blanquart, 2013): variance analysis and error propagation.

A.1. Direct measurement

A.1.1. Variance analysis

The first method consists in performing several time the measurement of the same physical parameter X and to analyse the mean ($\langle X \rangle$) and the variance or more usually, its square root,

the standard deviation (σ_X) of the results. It naturally leads to the so-called standard error ($se(X)$) that is usually plotted with error bars around the data points. It is computed by:

$$se(X) = \frac{\sigma_X}{\sqrt{N}} \tag{A.1}$$

with, N the number of measurements of the data of interest X in the sample; the standard error of the sample $se(X)$ and the standard deviation of the sample σ_X. Their is not a general consensus on this point and in some community, the error bars usually more refer to the standard deviation σ_X.

It is possible to use the standard error as a proxy of the uncertainty on X, *i.e.*$u(X) = se(X)$; few remarks about that:

- Measuring $se(X)$ is possible if a measurement technique works fast enough to perform several measurements in a period of time short enough to assume that the system did not evolve unreasonably, *i.e.*, such that the physical quantity measured by X did not changed significantly.
- The standard error is not the envelop of all possible values taken by the measurement. If the uncertainties are normally distributed, 68% of the values of X should be measured within the range $\langle X \rangle \pm se(X)$. If a given confidence interval is sought, a coefficient multiply the value of $se(X)$ (see later).

The standard error approach has been used, for instance, in Chap. 6 on LS-PIV measurements to determine the uncertainties of the resulting velocities. We assume that the fifty to several hundreds of images taken in less than few seconds were all measurements of the same velocity field. The uncertainty on the result decreases when the number of image increases ($\propto \sqrt{N}$, N number of image couple) because, to determine the velocity, velocity fields deduced from dozens of image couples, each of them giving one velocity field, were averaged. Using only one couple of image would have been much more uncertain.

A.1.2. Expert assessment

In several cases (*e.g.*, technical limits, excessively fast changes in the system, sensor limitation), it is not possible to do several accurate measurement of the parameter. In these cases, an expert assessment is done to estimate a reasonable value of the uncertainty range. This assessment is then detailed in the text.

A.2. Compound (indirect) measurement: Error propagation

Error propagation is basically a rigorous framework helping to determine how a primary variable uncertainty influence a compound variable uncertainty. To do so, it is necessary:

- to determine what are the influencing factors,called y, on the physical quantity measured by X;
- to construct a model $X = f(y_1, y_2, \cdots, y_n)$;
- to determine the standard uncertainties $u(y_i)$ of each variable y_i (taken as their own standard error: $u(y_i) = se(y_i)$), and

- to propagate them through the model.

The standard uncertainty on X, called $u(X)$ is computed at the first order by Blanquart, 2013:

$$u^2(X) = \sum_{i=1}^{n} \left(\frac{\partial f(y_i)}{\partial y_i} \right)^2 u^2(y_i) + 2 \sum_{i=1}^{n-1} \sum_{j=i+1}^{n} \frac{\partial f(y_i)}{\partial y_i} \frac{\partial f(y_j)}{\partial y_j} u(y_i, y_j) \tag{A.2}$$

The second term is neglected if the variables y_i are assumed independent, which lead to the more generally used equation:

$$u(X) = \sqrt{\sum_{i=1}^{n} \left(\frac{\partial f(y_i)}{\partial y_i} \right)^2 u^2(y_i)} \tag{A.3}$$

The standard uncertainty value $u(X)$ is then generally multiplied by a constant k to determine the uncertainty range $U(X)$. Assuming a normal distribution of the uncertainties, k is taken as 2 (more exactly 1.96) for a confidence interval at 95% (k=3 at 99.7% - Blanquart, 2013). Within all this manuscript, the multiply factor is not consider, *i.e.*, $k = 1$, which correspond to an implicitly considered confidence interval of 68% (assuming a normal distribution of the error).

THÈSE DE DOCTORAT DE L'UNIVERSITÉ DE GRENOBLE

Sediment transport control by check dams and open check dams in Alpine torrents

Guillaume PITON

Résumé: Barrages de corrections torrentielles et plages de dépôts jouent un rôle clés dans la protection contre les crues des torrents. Leurs gestionnaires ont pour mission de réduire les risques d'inondations, mais doivent désormais aussi minimiser les impacts environnementaux liés aux ouvrages de protection. Ceci nécessite une meilleure compréhension des effets des barrages de corrections torrentielles et des plages de dépôts sur le transport sédimentaire des torrents. Cette thèse s'inscrit dans cet objectif et se décompose en deux parties. Sa section sur l'état de l'art présente: i) les différents effets des barrages de correction torrentielle sur la production et le transfert sédimentaire; ii) des descriptions des processus hydrauliques et de sédimentation ayant lieu dans les plages de dépôts; et iii) les processus liés à la production et au transfert de bois d'embâcle. Une nouvelle méthode de quantification de la production sédimentaire des torrents complète cet état de l'art. La seconde partie de cette thèse présente le travail réalisé en banc d'essai expérimental. Une première série d'expérience a permis de mettre en évidence un transport par charriage plus régulier lorsque des barrages de correction torrentielle sont ajoutés à un bief alluvial. Une seconde série d'essais a été réalisée sur un modèle générique de plage de dépôt dans l'objectif d'en caractériser les écoulements. Pour cela, une nouvelle procédure de mesure et de reconstruction par approche inverse a été développée. Il en résulte une description des caractéristiques d'un écoulement proche du régime critique, ainsi que des mécanismes de rétrocontrôle entre morphologie et hydraulique pendant la phase de dépôt.

Mots clés: Torrents, Transport Sédimentaire, Risques Torrentiels, Protection Contre Les Inondations Et L'Erosion, Modélisation Physique

---

Abstract: Check dams and open check dams are key structures in torrent hazard protection. Their managers must mitigate flood hazards, but now must also minimize the environmental impacts of these protection structures. This requires to improve the knowledge on the effects of check dams and open check dams on the sediment transport, and this thesis forms a contribution towards this end. The section on the current state of research reviews i) the diverse effects of check dams on sediment production and transfer; ii) descriptions of the hydraulics and sedimentation processes occurring in open check dams; and iii) woody debris production and trapping processes. This state of the art is completed with proposition of new bedload transport estimation methods, specifically developed for paved streams experiencing external supply or armour breaking. Experimental results are then provided. Firstly, flume experiments highlight the emergence of a more regular bedload transport when check dams are built in alluvial reaches. In a second stage, experiments were performed on a generic Froude scale model of an open check dam basin in order to capture the features of laterally-unconstrained, highly mobile flows. A new flow measurement and inverse-reconstruction procedure has been developed. A preliminary analysis of the results describes flows that tend toward a critical regime and the occurrence of feedback mechanisms between geomorphology and hydraulics during massive bedload deposition.

Keywords: Steep Slope Streams, Sediment Transport, Torrential Hazards, Flood Hazard Mitigation and Erosion Control, Small Scale Modelling.